Advancing Biofloc Aquaponics: Effects of Hydraulic Configuration and Light Exposure on Microbial Dynamics, Nutrient Cycling, and System Productivity

by

Shima Rezaei

A dissertation submitted to the Graduate Faculty of
Auburn University
in partial fulfillment of the
requirements for the Degree of
Doctor of Philosophy

Auburn, Alabama
May 2, 2026

Keywords: biofloc aquaponics, nutrient cycling,
microbial community, food security

Approved by

Brendan Higgins, Chair, Professor of Biosystems Engineering
David Cline, Associate Extension Professor of Fisheries, Aquaculture, and Aquatic Sciences
Tanzeel Rehman, Assistant Professor of Biosystems Engineering
Daniel Wells, Associate Professor of Horticulture
Neha Potnis, Associate Professor of Entomology and Plant Pathology

Abstract

Growing demand for food, water scarcity, and the need for circular and resource-efficient production systems have increased interest in aquaponics as a sustainable method for simultaneous fish and crop production. By integrating aquaculture and hydroponics, aquaponics can recover nutrients from fish waste while reducing water use and fertilizer inputs. However, commercial adoption remains limited due to unstable productivity, incomplete understanding of nutrient use efficiency, and limited knowledge of how system design influences microbial ecology and long-term performance. In particular, critical knowledge gaps remain regarding how design decisions, such as hydraulic configuration and fish-tank light exposure, affect nutrient cycling, microbial community structure, fish productivity, plant performance, root-zone health, and overall system reliability in media-based biofloc aquaponic systems. This dissertation addressed these gaps through a series of replicated, long-term studies conducted over a three-year experimental campaign evaluating the effects of system coupling versus decoupling and photoautotrophic versus heterotrophic conditions on fish, plants, microbial communities, and nutrient dynamics in aquaponic systems producing tilapia and cherry tomato.

The first component evaluated the combined effects of fish-tank illumination and hydraulic configuration on aquaponic productivity in the first year of the experiment (2023). Illumination increased fish yield by 21%, while hydraulic coupling increased fish yield by 22%, largely due to the contribution of algal biofloc as a supplemental food source and improved water clarity in coupled systems. Plant performance showed a tradeoff between nutrient availability and solids accumulation. In one production cycle, coupled systems produced 44.5% higher yields due to higher nutrient availability, whereas in a subsequent cycle, decoupled systems outperformed

coupled systems by 26%, yielding 1711 g per plant, due to reduced sludge accumulation and improved root-zone conditions. Importantly, illumination did not negatively affect plant growth and, in some cases, improved yield. These results highlight that while coupling enhances nutrient retention, excessive solids accumulation can limit plant performance.

The second component examined how system design shaped microbial communities and their functional roles in the second year of the experiment (2024). Coupled systems retained higher nutrient concentrations but supported less diverse microbial communities, whereas decoupled systems promoted greater microbial diversity and higher abundance of plant growth-promoting bacteria. For example, putative siderophore-producing *Streptomyce*s reached 1.16% relative abundance in decoupled systems compared to 0.068% in coupled systems, corresponding to increased iron and zinc availability in plants. However, decoupled systems also exhibited unstable nitrification, with ammonium-N concentrations reaching 20 mg L^{-1}, which likely negatively affected plant productivity. Putative pathogens such as *Pythium graminicola* and *Xiphinema rivesi* were associated with plant stress and wilting under certain conditions. These findings demonstrate that system design influences not only microbial composition but also the balance between beneficial and harmful organisms, directly affecting plant health and system performance.

The third component focused on long-term system reliability and root-zone disorders. Plant wilt in media-based systems was primarily driven by sludge accumulation and poor drainage, which created hypoxic root-zone conditions and reduced yields by 21% in affected systems. System modifications, including improved solids removal and controlled irrigation, significantly enhanced performance; however, some failures persisted. Root-zone analysis showed that wilted plants exhibited lower dissolved oxygen levels (65% lower) and trends toward higher relative abundance

of putative pathogens and parasitic organisms (*Pythium graminicola* and *Xiphinema rives*). These results indicate that long-term aquaponic stability depends on both effective solids management and maintaining a balanced root-zone microbiome.

The fourth component evaluated tilapia production and biofloc quality under different design conditions over a two-year production. Illuminated systems developed photoautotrophic biofloc communities dominated by algae, which improved nutritional quality, including higher protein, lipid content, and essential fatty acids. These changes enhanced fish growth, with light-coupled systems achieving the highest biomass (up to 581 g) and improved feed conversion ratios. Importantly, illumination did not promote off-flavor compounds, as cyanobacteria remained below 0.03% and geosmin/MIB concentrations remained below sensory detection thresholds. These findings demonstrate that light exposure can be used strategically to enhance fish productivity without compromising product quality.

The final component quantified the fate of feed-derived nitrogen and phosphorus across two fish growth stages and experimental treatments. Nutrient partitioning was strongly influenced by fish size, with 30.0–34.4% of feed nitrogen recovered in fish biomass in 2025 compared to 10.2–15.6% in 2024, along with approximately 50% lower nitrogen loss in 2025. Photoautotrophic systems retained a greater fraction of nitrogen and phosphorus in measurable pools (solids and water) and exhibited reduced loss, indicating improved internal recycling. Plant uptake remained relatively consistent across treatments, accounting for approximately 6–11% of nitrogen and 7–12% of phosphorus, with the highest recovery observed in heterotrophic-coupled systems. These results highlight that while aquaponics is often described as a circular system, nutrient recovery efficiency depends strongly on fish growth stage, microbial regime and hydraulic configuration.

Overall, this dissertation demonstrates that aquaponic system performance is governed by interactions among hydraulic design, fish-tank illumination, microbial community structure, and solids management. Photoautotrophic conditions and hydraulic coupling enhance fish productivity and nutrient recovery, while plant performance is more strongly influenced by root-zone conditions and microbial balance. By linking system design to microbial processes, nutrient cycling, and biological performance, this work provides a mechanistic foundation for improving the stability, productivity, and resource efficiency of aquaponic systems and supports their advancement within controlled-environment agriculture and circular food production systems.

Artificial Intelligence (AI) Use Disclosure Statement

In the preparation of this dissertation, the following Artificial Intelligence (AI) tools were used: ChatGPT and Gemini. These tools were used primarily to assist with grammar refinement, improve writing clarity, support literature searches, and compare sequencing data with reference databases (the latter applied specifically in Chapters 3 and 4). The author acknowledges full responsibility for the intellectual content of this work and has ensured that all AI-assisted sections have been reviewed and revised for accuracy and appropriate academic style. All AI-generated content was reviewed and validated for relevance, appropriateness, and accuracy before incorporation into the final document to maintain the scholarly integrity of this research.

Digital Accessibility Use Disclosure Statement

In the preparation of this dissertation, the following digital accessibility tools were used to ensure this document complies with federal requirements: Microsoft Word Accessibility Checker. The author acknowledges full responsibility for the intellectual content of this work and has made a good faith effort to comply with digital accessibility requirements in publishing, wherein the nature of the content does not significantly change in order to do so. Furthermore, all content has been reviewed and revised to meet these requirements prior to final publication.

Acknowledgments

I would first like to express my sincere gratitude to my advisor, Dr. Brendan Higgins, for his continuous support, guidance, and mentorship throughout my doctoral studies. Through his mentorship, I have learned not only how to approach scientific problems with critical thinking and creativity, but also how to manage research projects, mentor students, and communicate scientific ideas effectively. I am deeply grateful for his encouragement, thoughtful discussions, and unwavering support throughout every stage of this work.

I would also like to thank Dr. David Cline for his invaluable support throughout this project. His expertise in designing, building, and operating the aquaponics systems was essential to this work. I am especially grateful for his dedication to the school outreach component and his efforts to educate students and teachers about aquaculture and sustainable food production.

I would like to thank my committee members, Dr. Daniel Wells, Dr. Tanzeel Rehman, and Dr. Cline, for their valuable guidance, feedback, and support throughout my doctoral program. Their insights and perspectives greatly improved the quality of this research. I am also grateful to Dr. Neha Potnis for serving as the university reader and for her time and thoughtful evaluation of this dissertation.

This work was made possible through the generous support of funding agencies, including the National Science Foundation (NSF) and the United States Department of Agriculture (USDA). Their support enabled the research, outreach, and educational components that were integral to this project.

I would also like to thank the Department of Biosystems Engineering at Auburn University for providing an environment that supported both my academic and professional development. I am

particularly grateful to Dr. Oladiran Fasina for his leadership and for fostering opportunities that allowed students to grow not only academically but also professionally and personally.

I am thankful to my colleagues at the E. W. Shell Fisheries Station, including Gift Bender, Mollie Smith, Leticia Fantini Hoag, Larry Lawson, and Jory Garnto, for their assistance with system operation, greenhouse maintenance, and sample collection. I would also like to express my sincere appreciation to my undergraduate research team, including Sarah Hensless, Mary Beth Hall, Madeline Spoor, Kelly Sullivan, Rachel Schorer, Grace Hohn, and Ellie Malkemus, for their dedication and hard work in assisting with data collection, sampling, laboratory analyses, and system operation.

I am also grateful to my fellow graduate students and undergraduate lab members for creating a supportive and collaborative research environment. I would like to especially thank Dr. Qichen Wang, Dr. Saravanan Ramiah Shanmugam, and Margaret Otto for their constant support, insightful discussions, and generous contributions to this work.

Finally, I would like to express my deepest gratitude to my family in Iran. Their unwavering encouragement, sacrifices, and belief in me made it possible for me to pursue my education abroad and complete this journey. Their support has been the foundation that made this achievement possible.

Table of Contents

List of Tables

List of Figures

List of Abbreviations

CAS	Chrome Azurol S
CEA	Controlled-environment agriculture
COD	Chemical oxygen demand
CV	Coefficient of variation
DC	Dark-coupled
DD	Dark-decoupled
DO	Dissolved oxygen
DNA	Deoxyribonucleic acid
FCRa	Apparent feed conversion ratio
FASTQ	FastQ sequence format
HC	Heterotrophic-coupled
HD	Heterotrophic-decoupled
HPLC	High-performance liquid chromatography
HRT	Hydraulic retention time
IACUC	Institutional Animal Care and Use Committee
IBC	Intermediate bulk container
ICP	Inductively coupled plasma
ICP-OES	Inductively coupled plasma optical emission spectroscopy
K	Potassium
LC	Light-coupled
LD	Light-decoupled
MLSS	Mixed liquor suspended solids
MRDNA	Molecular Research DNA Laboratory
NCBI	National Center for Biotechnology Information
NOB	Nitrite-oxidizing bacteria
NO2-N	Nitrite-nitrogen

NO3-N	Nitrate-nitrogen
NH3-N	Ammonia-nitrogen
NH4-N	Ammonium-nitrogen
N	Nitrogen
OD	Optical density
P	Phosphorus
PAR	Photosynthetically active radiation
PC	Photoautotrophic-coupled
PD	Photoautotrophic-decoupled
PGPB	Plant growth-promoting bacteria
PO4-P	Phosphate-phosphorus
PPFD	Photosynthetic photon flux density
RAS	Recirculating aquaculture system
RFS	Radial flow settler
rRNA	Ribosomal ribonucleic acid
SR	Survival rate
SRA	Sequence Read Archive
SRT	Solids retention time
TGC	Thermal growth coefficient
TSS	Total suspended solids
ZOTU	Zero-radius operational taxonomic unit

Chapter 1: Introduction

1.1 Background

Global population growth, urbanization, freshwater scarcity, and increasing pressure on fertilizer and energy resources have intensified the need for more resource-efficient food production systems. Controlled-environment agriculture (CEA) and other circular production approaches are gaining attention for their potential to improve water use efficiency and reduce nutrient waste. Among these, aquaponics integrates aquaculture and hydroponics by using nutrient-rich fish wastewater to fertilize crops while recirculating water within the system, enabling simultaneous production of fish and plants (1).

Despite its promise and rapid growth over the past decade, aquaponics still faces major barriers to commercialization (2, 3). These challenges largely stem from the biological complexity of the system, which must simultaneously sustain fish, plants, and microbial communities that interact through water, solids, and nutrient transformations (4). As a result, many systems experience unstable production, inefficient nutrient use, inconsistent yields, and difficulties maintaining water quality and biological balance (5, 6). Improving aquaponics, therefore, requires a deeper understanding of how system design influences nutrient cycling, microbial ecology, and overall performance.

Microorganisms play a central role in aquaponics by transforming fish waste into plant-available nutrients and maintaining water quality (7). Because much of the nutrient input from fish feed enters the system as dissolved or particulate waste, microbial processes are essential for nutrient mineralization and recycling (8). Microbial sludge that accumulates throughout the system acts as both a nutrient reservoir and a habitat for key microbial groups (9). Beneficial microbes such as

nitrifying bacteria and plant growth-promoting bacteria support nutrient cycling and plant development, while sludge-rich and oxygen-limited zones may also promote pathogens, linking microbial dynamics to nutrient recovery, plant health, and overall system stability (10, 11).

Because these microbial processes are highly sensitive to environmental conditions, aquaponic performance is strongly shaped by system design. Hydraulic retention time, solids retention time, water flow patterns, oxygen availability, pH, and light exposure can all influence microbial colonization and nutrient transformations (12-14). One major design distinction is the difference between coupled and decoupled aquaponics. In coupled systems, water continuously recirculates between fish and plant units in a single loop, which is the most common design in aquaponics (15). However, maintaining optimal conditions for both fish and plants can be difficult because the two components often have different environmental requirements, particularly with respect to pH and nutrient conditions (16). In decoupled systems, water moves one-way from the aquaculture unit to the hydroponic unit, allowing greater control over plant-side conditions (17). These two modes differ in solids retention, nutrient accumulation, water exchange, and habitat stability, and therefore likely support different microbial communities and nutrient cycling patterns.

Fish-tank illumination represents another important but underexplored design factor. Many aquaponic producers cover fish tanks to prevent algae growth, assuming that algae will compete with plants for nutrients or destabilize water quality. However, natural light exposure can shift fish-tank microbial communities toward photoautotrophic conditions by promoting algae and other light-responsive organisms (18, 19). This shift may benefit the system in several ways. Algal biofloc can serve as a supplemental food source for fish because of its protein, lipid, and bioactive compound content (20) (21, 22). Algae can also influence nutrient dynamics through direct uptake of inorganic nitrogen and oxygen production during photosynthesis, which may support

nitrification and reduce nitrogen loss (23, 24). In addition, algal compounds have shown plant biostimulant effects in other cultivation systems (25, 26). At the same time, light exposure may also promote cyanobacteria and other organisms associated with geosmin and 2-methylisoborneol formation, raising concern about off-flavor development in fish flesh (27, 28). The overall effects of fish-tank illumination, therefore, remain uncertain, particularly when combined with different hydraulic configurations.

These questions are especially relevant in biofloc aquaponics, where dense microbial aggregates and limited water exchange make system performance highly dependent on microbial structure and solids dynamics. Traditional biofloc systems are typically operated under low-light conditions that favor heterotrophic bacteria, whereas illuminated systems may shift toward photoautotrophic communities dominated by algae. Such changes may alter nutrient partitioning, nitrification, solids quality, and the nutritional value of biofloc for fish. The interaction between fish-tank illumination and hydraulic configuration is also likely important. Higher solids retention in decoupled biofloc systems may support denser microbial flocs and stronger microbial transformations, while the continuous recirculation and more frequent filtration typical of coupled systems may promote clearer water and different microbial niches. Because these factors are interconnected, system productivity likely depends on the interaction between hydraulic design and microbial metabolic regime rather than on either factor alone.

Plant performance in aquaponics is also strongly influenced by physical and microbial conditions in the root zone, especially in long-term media-based systems. One of the most persistent problems is root stress caused by waterlogging, insufficient oxygenation, and sludge accumulation (29, 30). As fine solids and organic matter build up in grow beds, pore spaces can become clogged, reducing drainage and gas exchange. Root-zone hypoxia impairs respiration, restricts nutrient uptake,

weakens plant defenses, and can shift the rhizosphere microbiome toward opportunistic pathogens (31). Under moist, warm, and organic-rich conditions, pathogens such as Pythium, Phytophthora, Fusarium, and plant-parasitic nematodes can proliferate and spread through recirculating water, leading to root rot, wilting, and yield loss (32-34). These risks are particularly important in long-term tomato production, where crops remain in the system long enough for solids and microbial imbalances to accumulate (35-37). Although aquaponic growers frequently report plant wilt and declining root health, few long-term studies have examined the combined physical and microbial causes of these failures or evaluated how design changes can improve reliability.

Another key but unresolved issue is nutrient recovery efficiency. Aquaponics is widely described as a circular food production system, yet the whole-system fate of feed-derived nutrients is rarely quantified (38). This is important because nitrogen and phosphorus behave differently in aquaponic systems. Nitrogen can be incorporated into fish, plants, microbes, dissolved pools, or lost through gaseous pathways following microbial transformations (39, 40). Phosphorus, in contrast, lacks a major gaseous loss pathway and tends to accumulate in solids or become chemically immobilized (41, 42). As a result, water chemistry data alone cannot show whether nutrients are effectively recovered into harvestable biomass or retained in less useful pools. Mass-balance analysis provides a more complete framework for evaluating nutrient use efficiency because it quantifies nutrient partitioning across fish, plants, water, and solids. However, few studies have examined how biofloc metabolic regime and hydraulic configuration together influence whole-system nitrogen and phosphorus recovery.

Although previous studies have investigated aquaponic microbiomes, water chemistry, and production performance, most have focused on short-term trials, single system designs, or isolated compartments rather than long-term replicated comparisons. Important questions therefore remain

unresolved. It is still unclear how design decisions such as hydraulic configuration and fish-tank light exposure jointly shape microbial communities involved in nitrification, plant growth promotion, and disease risk. The role of these design factors in fish productivity, biofloc quality, off-flavor formation, plant reliability, and nutrient recovery also remains insufficiently understood. Likewise, the extent to which solids retention, root-zone oxygenation, and microbial balance determine chronic problems such as wilt and root rot in media-based aquaponics has not been well characterized.

This dissertation addresses these knowledge gaps through a series of replicated, long-term studies conducted over a three-year experimental campaign using media-based biofloc aquaponic systems producing Nile tilapia (*Oreochromis niloticus*) and cherry tomato. Tilapia is widely used in aquaponics because of its tolerance to variable water conditions and compatibility with biofloc systems, while cherry tomato is a high-value greenhouse crop that is both nutritionally demanding and sensitive to root-zone disorders. Across this dissertation, particular emphasis was placed on two practical design factors with strong but poorly understood biological implications: hydraulic configuration (coupled versus decoupled) and fish-tank light exposure (light versus dark). By examining how these factors influence microbial ecology, nutrient cycling, solids dynamics, fish performance, plant productivity, and root-zone health, this work aims to provide a more mechanistic understanding of why aquaponic systems succeed or fail over time. Such knowledge is needed to support the design of more stable, productive, and nutrient-efficient aquaponic systems and to advance aquaponics as a viable component of controlled-environment agriculture and the circular bioeconomy.

1.2 Research objectives

This dissertation aimed to evaluate how system configuration (coupling/decoupling) and fish tank illumination influence productivity, microbial community structure, nutrient cycling, and long-term reliability in biofloc aquaponics systems. The goal was to identify system designs that improve fish and plant performance while enhancing nutrient utilization and system stability. The specific objectives are as follows:

Objective 1: Evaluate the effects of fish tank illumination and system configuration (coupled vs. decoupled) on fish growth, tomato yield, nutrient availability, and nitrification performance in biofloc aquaponics systems. (Chapter 2)

Objective 2: Determine how system configuration and illumination shape the functional microbiome associated with aquaponic water and plant roots, with emphasis on nitrifiers, plant growth–promoting bacteria, and potential pathogens involved in nutrient cycling and plant health. (Chapter 3)

Objective 3: Investigate the development of root rot and wilt under different aquaponic configurations by examining sludge accumulation, microbial community dynamics, and root-zone conditions affecting plant health and system reliability. (Chapter 4)

Objective 4: Assess the effects of fish tank illumination on biofloc composition, fatty acid profiles, and fish growth performance to evaluate the nutritional and functional role of light-driven biofloc communities. (Chapter 5)

Objective 5: Quantify nitrogen and phosphorus flows in biofloc aquaponics systems using a mass balance approach to determine how system configuration and microbial regimes influence nutrient recovery, storage, and losses. (Chapter 6)

1.3 Dissertation Outline

This dissertation is organized into six chapters with additional supporting appendices. Chapter 1 introduces the research background and outlines the motivation for examining how aquaponic system configuration and fish tank illumination affect productivity, microbial processes, and nutrient dynamics in biofloc-based aquaponics systems. The final chapter (Chapter 6) summarizes the main findings of the study and discusses broader implications and directions for future research. Chapters 2 through 5 present the primary research components of this work and are written in the format of journal articles derived from long-term greenhouse experiments conducted over two production cycles. Each chapter addresses a specific research question and is structured so it can be read independently as a stand-alone study. At the same time, the chapters are connected conceptually and collectively contribute to a comprehensive understanding of how design choices impact biofloc aquaponics performance.

1.4 Dissertation Output

The research presented in this dissertation forms the basis for several manuscripts that have been published or are currently being prepared for submission. The chapters corresponding to these manuscripts are listed below.

Chapter 2: Rezaei S, Spoor M, Hohn G, Schorer R, Bender G, Cline D, Wells DE, de-Bashan L, Higgins B. Enhancing yields: The role of fish tank illumination and coupling/decoupling in biofloc aquaponics performance. Aquaculture. 2026;613:743286.

https://doi.org/10.1016/j.aquaculture.2025.743286

Chapter 3 Rezaei S, Otto M, Hohn G, Wang Q, Arthur W, Hensless S, Hall MB, Spoor M, Potnis N, Cline D, Higgins B. Coupling, decoupling, and fish tank illumination shape the functional

microbiome and nutrient cycling in aquaponics. Bioresource Technology Reports. 2025;32:102439. https://doi.org/10.1016/j.biteb.2025.102439

Chapter 4: Rezaei S, Otto M, Wang Q, Arthur W, Shantharaj D, Sullivan K, Wells D, Potnis N, Higgins B. Root rot and wilt development in aquaponics: the role of sludge accumulation, microbial dynamics, and root-zone conditions. (Under review)

Chapter 5 Rezaei S, Hohn G, Hawkins S, Farahmandzad N, Shanmugam SR, Sullivan K, Hensless S, Hall MB, de-Bashan L, Cline D, Higgins B. Effects of fish tank illumination on biofloc composition, fatty acid profiles, and fish performance in aquaponics systems. (Ready for submission)

Chapter 6: Rezaei S, Wang Q, Spoor M, Hensless S, Sullivan K, Hall MB, Malkemus E, Hohn G, Adhikari S, Cline D, Higgins B. Nitrogen and phosphorus mass balance in biofloc aquaponics systems under different microbial regimes and system configurations. (Article in preparation)

Chapter 2: Enhancing Yields: The Role of Fish Tank Illumination and Coupling/Decoupling in Biofloc Aquaponics Performance

Enhancing Yields: The Role of Fish Tank Illumination and Coupling/Decoupling in Biofloc Aquaponics Performance

Authors: Shima Rezaei[1], Madeline Spoor[1], Grace Hohn[1], Rachel Schorer[1], Gift Bender[2], David Cline[3], Daniel E. Wells[2], Luz de-Bashan[4,5], Brendan Higgins[1]*

[1]Biosystems Engineering, Auburn University, Auburn, AL 36849, USA

[2]Horticulture, Auburn University, Auburn, AL 36849, USA

[3]School of Fisheries, Aquaculture and Aquatic Sciences, Auburn University, Auburn, AL 36849, USA

[4]Bashan Institute of Science, Dadeville, AL, 36853, USA

[5]Department of Entomology and Plant Pathology, Auburn University, Auburn, AL 36849, USA

*Corresponding author:

Brendan T. Higgins

Department of Biosystems Engineering, 203 Corley Building, Auburn, AL 36849, USA

Phone: 334-844-3532

e-mail: bth0023@auburn.edu

Abstract

Despite the sustainable potential of aquaponics, its commercialization remains limited due to technical and socio-economic challenges, including unstable production. This study aimed to evaluate the impact of exposing fish tanks to sunlight and system configuration (coupled vs. decoupled) in aquaponics. Four replicated system types (light-coupled, dark-coupled, light-decoupled, and dark-decoupled) were monitored over ten months, encompassing two cherry tomato production trials using inert substrate cultivation. Illumination and coupling increased fish yield by 21% ($p = 0.02$) and 22% ($p < 0.001$), respectively. This was attributed partly to the availability of algal biofloc as an additional food source in illuminated systems and improved water clarity from continuous filtration in coupled systems. Tomato production varied between the two trials. In the first trial, coupled systems outperformed decoupled ones, achieving 44.5% higher yields due to elevated nutrient concentrations and more frequent irrigation. In the second trial, decoupled systems produced 1711 g per plant, surpassing coupled systems by 26%, owing largely to poor drainage caused by excess microbial sludge accumulation in the latter. Notably, illumination and the algal-dominated microbial community had no adverse effects on plant growth and even enhanced tomato yield in the second trial ($p = 0.011$). Analysis of nitrifying bacteria revealed that decoupled systems fostered higher nitrifier abundance in fish tanks than coupled systems, likely due to differences in solids retention and hydraulic retention time. These findings underscore the potential of fish tank illumination to boost system productivity and highlight the importance of solids management in optimizing overall system performance.

Keywords: Aquaculture wastewater; Hydroponics; Microalgae; Nitrification; Nutrient dynamics

Graphical Abstract

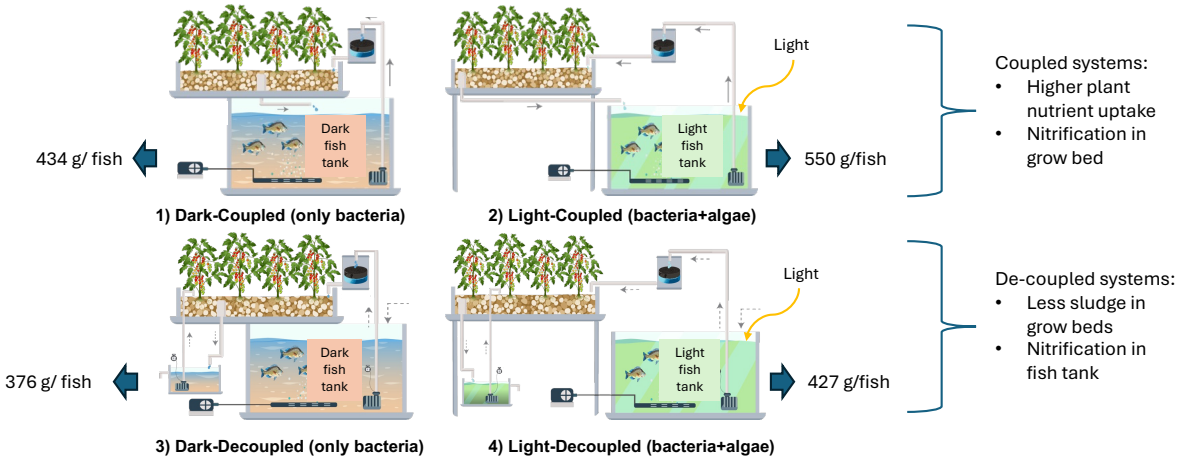

Highlights

- Fish tank illumination increased fish growth by 21%
- Coupled aquaponics increased fish growth and tomato nutrient uptake
- Fish tank illumination and algae growth did not harm tomato growth
- Nitrification is predominant in the fish tank of decoupled, grow-bed of coupled systems

2.1 Introduction

Aquaponics is a promising sustainable food production system that uses nutrient-rich fish wastewater to irrigate and fertilize plants (1). Although aquaponics has expanded considerably over the past decade, it still faces significant challenges on the path to full commercialization (2, 3). Key issues include system complexity caused by the need to sustain three biological components: fish, plants, and microbes (4), inefficient nutrient management (5), and low yields (6). All of these challenges hurt the economic viability and risk associated with aquaponics. Microorganisms in aquaponics systems play a crucial role in maintaining the health of both fish and plants by breaking down organic matter and converting them into essential nutrients that are readily available for plant uptake (7). Therefore, effective management of nutrient and microbial interactions between fish and plants is key for enhancing system stability and optimizing yields.

Illuminating fish tanks with sunlight can significantly affect the microbial community and potentially impact nutrient levels (18). Light exposure promotes the growth of photoautotrophic microorganisms, resulting in a higher abundance of microalgae in illuminated tanks compared to those kept in the dark (19). This integration of algae into biofloc aquaculture can positively affect fish growth, as algae, rich in lipids and protein, can provide a complementary food source for filter-feeding fish, improving their yield (20). Using nutrients from fish waste to grow algal biofloc, and subsequently feeding fish with algal biomass, offers a sustainable and efficient approach to enhancing system performance (21, 22). Beyond their effects on fish, microalgal extracts have demonstrated potential in both hydroponic and soil-based cultivation, enhancing plant resistance to abiotic stress (25). Additionally, they contribute to improved crop growth and yield by releasing beneficial hormones and amino acids (26). However, many aquaponics producers shield their fish production systems from light in the belief that algae growth will deprive the downstream plants

of critical nutrients. While microalgae extracts have been studied as plant biostimulants in soil, there is much less known about how their growth within aquaponics systems impacts plant performance. Moreover, algae have the potential to improve nitrification and reduce excess ammonia (23, 24), both of which are critical for fish and plant health. While studies have shown algae's ability to promote nitrification in other types of wastewater, there remains a knowledge gap regarding its impact on nitrification and nutrient dynamics (particularly nitrogen and phosphorus) in aquaponics.

The connection between the fish tank and hydroponic bed can influence microbial communities and nutrient availability. Coupled aquaponics, where water recirculates between the fish tank and grow bed, is the most common design (15), but maintaining optimal conditions for both fish and plants can be challenging due to differing environmental needs, such as pH preferences (16). In contrast, decoupled systems function as semi-continuous reactors with a one-way water flow from fish tanks to grow beds, offering more flexibility to adjust water chemistry for plants (17). The operational mode can impact the microbial structure and nutrient dynamics within the system (16). Coupled systems often accumulate nutrients and solids due to limited water exchange (43), while decoupled systems rely on regular make-up water and tend to maintain lower nutrient concentrations. Moreover, due to the one-way flow in these systems, nitrification relies solely on biofloc in the fish tank unless an additional biological filter is present (14), whereas coupled systems benefit from nitrification in both the fish tank and grow bed as water recirculates back to the fish tank (44), potentially improving stability. Understanding differences in nitrification and nutrient dynamics between coupled and decoupled systems can help producers optimize system performance. Yet, no prior study has systematically investigated the combined effects of fish tank illumination and coupling versus decoupling in aquaponics.

This study addresses a key knowledge gap by using a full-factorial experiment to evaluate the effects of two practical strategies, fish tank sunlight exposure and system coupling/decoupling, on aquaponics performance. Four treatments (dark-coupled, light-coupled, dark-decoupled, and light-decoupled) were tested, each with three replicates. The systems were operated for ten months, tracking Nile tilapia (*Oreochromis niloticus*) growth from 20 g fingerlings to 500 g market size. Unlike most prior studies, which focus on short-term (<4 months) system behavior with limited replication, this study adopts a longer-term approach to capture dynamic changes in performance. We hypothesized that algae growth in illuminated fish tanks would enhance tilapia growth, particularly in the biofloc conditions expected in decoupled systems given past findings that biofloc serves as supplemental feed (45). We also expected green algae to support nitrifying bacteria based on previous studies (23, 24), while potentially reducing soluble nutrient levels. Improving yield and stability without added material inputs could make aquaponics more environmentally and economically sustainable.

2.2 Materials and Method

2.2.1 Experimental design

Figure 2.1 illustrates the four treatment groups in this study: 1) dark-coupled (DC), 2) light-coupled (LC), 3) dark-decoupled (DD), and 4) light-decoupled (LD). Each treatment was replicated three times in a randomized complete block design in a heated and ventilated greenhouse with a 268 m^2 area (built by Atlas Greenhouse, USA) at the E.W. Shell Fisheries Station in Auburn, Alabama. The greenhouse used three fans and a cooling wall for staged cooling and a propane heater set to keep the greenhouse from falling below 20 °C. The systems were operated over 10 months, comprising 2 months for inoculation and biofloc development followed by 8 months of fish growth (Figure S2.1). System performance was monitored throughout, with a focus on fish

and plant growth, nutrient dynamics, and microbial community analysis. In late January 2023, the aquaponic systems were established by introducing biofloc from existing tilapia raceways at the E.W. Shell Fisheries Station. To support the development of nitrifying bacterial flocs, molasses was added as a carbon source and ammonia as a nitrogen source, maintaining concentrations of 72 mg/L and 20 mg/L, respectively (46). pH levels were consistently maintained around 7 to optimize conditions for nitrification (47), with daily additions of hydrochloric acid (3 M) or calcium carbonate as needed for pH adjustments. Once a stable nitrifying population was established, each fish tank was stocked with 40 all-male Nile tilapia fingerlings (20 g each, stocking density of 1.2 kg/m^3 on average), sourced from existing raceways at the E.W. Shell Fisheries Station, and raised to a marketable size of ~500 g over 8 months (density of 28.5 kg/m^3). During this period, two cherry tomato production trials were conducted: the first (March 30–June 21, Spring) with six *Washington* seedlings per grow bed, and the second (September 17–December 11, Fall) with five *Favorita F1* seedlings per bed. Tomato seeds were sourced from Johnny's Selected Seeds (48). The switch to a more productive and flavorful tomato varietal (*Favorita F1*) in the fall trial prevents direct comparisons between trials, limiting tomato analysis to within-trial trends. No experiments were conducted from June 22–September 17 due to high greenhouse temperatures and suboptimal tomato plant growth, but systems remained operational to sustain fish growth and microbial communities since our goal was to study the full fish grow-out period. For nutrient absorption during the summer, two cherry tomato plants, four lettuce plants, and one basil plant were added per grow bed, though their growth was not monitored for data collection.

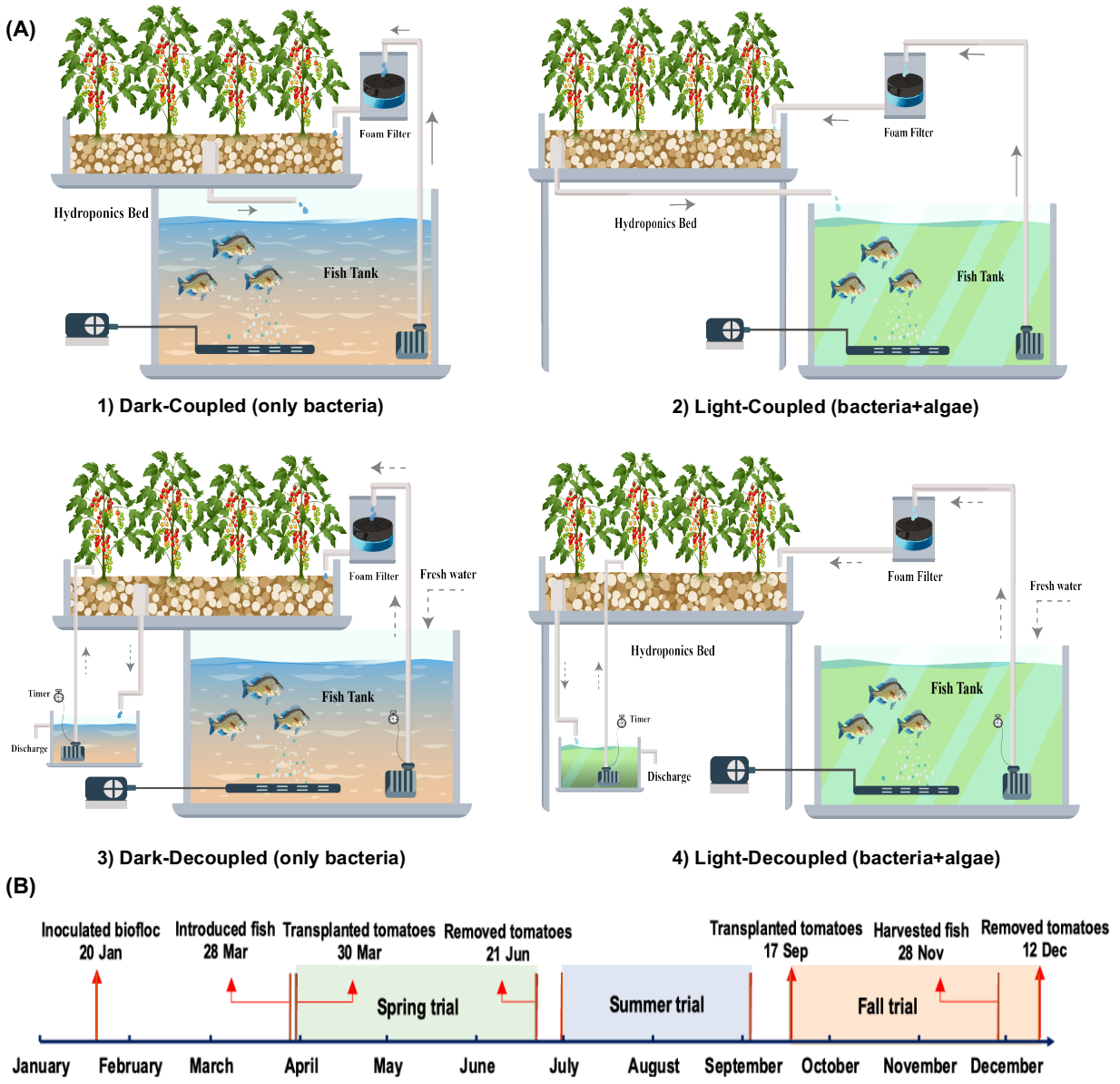

Figure 2.1 (A) Schematic of the four aquaponic system types: (1) Dark-coupled (bacteria-dominant community), (2) Light-coupled (algae-dominant community), (3) Dark-decoupled (bacteria-dominant community), and (4) Light-decoupled (algae-dominant community). (B) Timeline of major events during the ten-month experiment period, including biofloc inoculation, fish introduction, tomato production trials, and fish harvest.

2.2.2 System setup

Each aquaponics system was constructed from an intermediate bulk container (IBC tote) with a 700 L fish tank (working volume) and a 1 m² media-based hydroponics bed using pea gravel as

the substrate (particle size: 0.5–1.5 cm) with 20 cm depth (49). In coupled systems, water continuously circulated from the fish tank to the hydroponics bed at a flow rate of 9 L/min (HRT: 80 minutes) via a pump, passing through foam filters to remove solids. A bell siphon created an ebb and flow cycle for root aeration, and an aerator (40 L/min) maintained a dissolved oxygen (50) level of ~7 mg/L in the fish tank.

In the decoupled systems, water pumps operated twice daily for 3 minutes (25 L per cycle), resulting in a fish tank HRT of 14 days. To maintain a 700 L volume, about 50 L of fresh water was added daily, consistent with water exchange rates in previous studies (51). This extended HRT allowed the systems to function as biofloc systems, relying on the fish tanks for mineralization and nitrification. This decision was intentional and based in part on previous findings that biofloc systems are compatible with decoupled aquaponics and can provide tilapia with supplemental feed (45). Irrigation water drained into a 70 L sump (HRT: 1.5 hours), where a secondary pump recirculated water to the hydroponics bed eight times daily (5 minutes per cycle at 9 L/min). This setup ensured adequate hydration of plant roots and extended the contact time between the plants and fish water, allowing for more complete nutrient utilization before the water was discharged from the system. Decoupled systems used a higher-capacity aerator (80 L/min) to maintain adequate DO levels. In the systems with "dark" fish tanks, the tanks were painted and covered with dark fabric to block light.

2.2.3 System maintenance

Fish were fed twice daily, in the morning (7–8 am) and afternoon (1–2 pm). During the first four months, they were fed Cargill Triton-4512 feed (45% crude protein, 12% crude fat, 3% crude fiber, 1% phosphorus). Once the fish averaged 100 g, they were transitioned to a larger pellet, Cargill Triton-3603 (36% crude protein, 6% crude fat, 4% crude fiber, and 1% phosphorus)

(52). Feeding rates, initially set at 3% of body mass, were adjusted monthly based on fish growth (determined by sampling), water temperature, and consumption patterns, and were reduced to 2% after two months and 1.5% for the final two months (53). Foam filters were cleaned daily during the first five months and twice daily in the final three months as feeding rates increased. Because potassium is typically deficient in aquaculture water (54), it was supplemented using potassium chloride (potash) to reach 100 mg/L in the first trial, a level safe for fish and beneficial for plants (55). In the second trial, based on earlier trends, potassium was added daily to the make-up water to maintain this concentration. Fish production adhered to Auburn University's Institutional Animal Care and Use Committee protocol (#22-4099), with standards of care upheld throughout the study.

2.2.4 Water quality assessment

Total suspended solids (TSS) in fish tanks across the four treatments were monitored every other day by measuring optical density at 550 nm and 680 nm. To correlate the optical density readings with solids concentrations, a calibration curve was established following the method of Bertrand et al. (56). Soluble chemical oxygen demand (COD) was periodically measured using a HACH assay kit. pH was recorded daily with a Bluelab Metcombo meter, with hydrochloric acid (3 M) or calcium carbonate added as needed to maintain a target of ~7. Dissolved oxygen and temperature were measured every other day using a Milwaukee MW600 portable DO meter. Daily temperature and photosynthetically active radiation (PAR) data were obtained from the NASA POWER database (Figure 2.2A) (57).

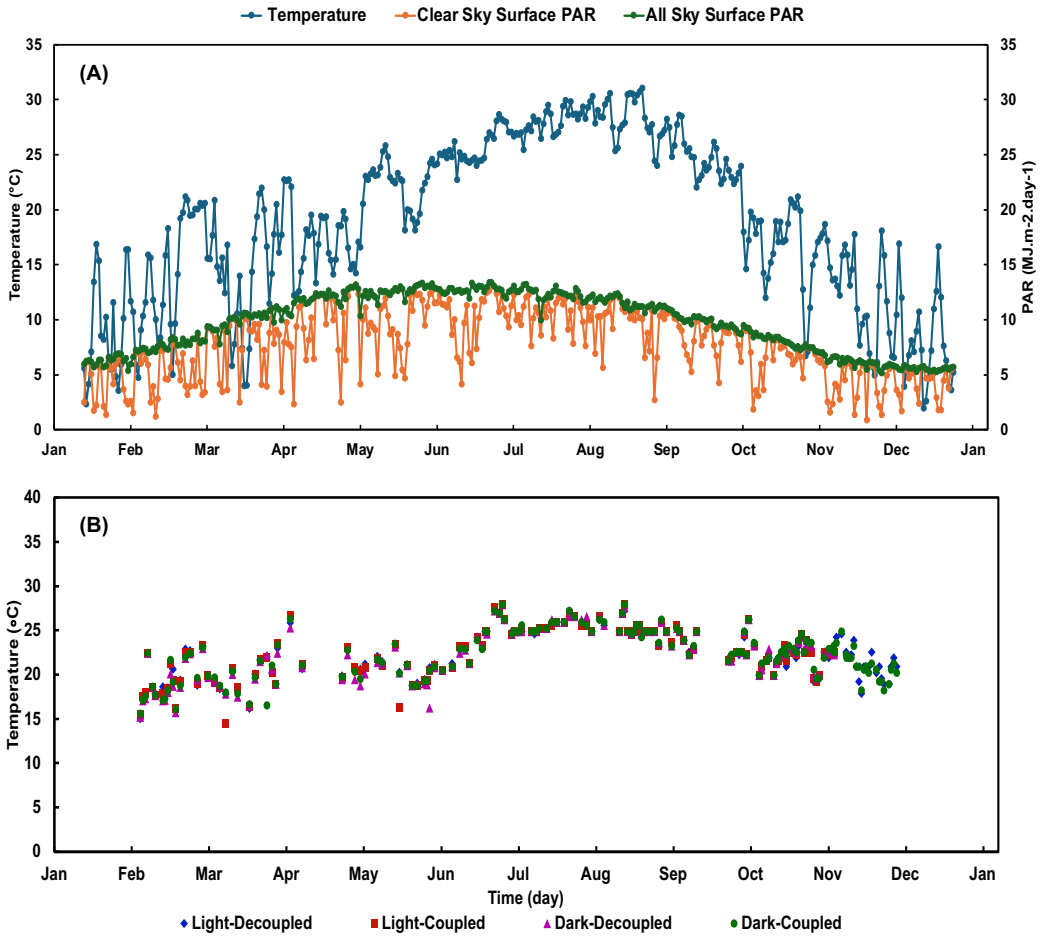

Figure 2.2 A) Time-course plot of site weather temperature (°C) and all sky and clear sky surface photosynthetically active radiation (PAR, MJ.m-2.day-1). B) Time-course plot of the temperature of the fish tank water. The greenhouse roof was covered with white shade cloth, providing a 30% PAR reduction, from June 28th to October 1st.

2.2.5 Nutrient analyses

Water samples were collected every other day from fish tanks and decoupled sumps to analyze soluble nutrients and essential plant minerals. Samples were filtered (0.2 µm glass microfiber filter 696, VWR, USA) and stored at -20°C for later analysis. Soluble ions, including nitrate, nitrite, phosphate, and sulfate were measured via high-pressure liquid chromatography (HPLC) using a Prominence LC System (Shimadzu) with an anion exchange column (Dionex AS22, ThermoFisher Scientific, USA) and ion suppressor (Dionex AERS 500, ThermoFisher Scientific, USA). Cations,

such as ammonium, potassium, magnesium, and calcium, were analyzed using cation chromatography with the Dionex CS16 column (ThermoFisher Scientific, USA) in conjunction with an ion suppressor (Dionex CERS500, ThermoFisher Scientific, USA).

To assess plant nutrient sufficiency, middle leaflets from recently matured leaves were collected at the end of the second trial and analyzed for mineral content using Inductively Coupled Plasma (ICP) spectroscopy at the Soil, Plant, and Water Laboratory (University of Georgia) The leaf samples were oven-dried at 60°C and digested with nitric acid before ICP analysis, following the method described by Chaump et al. (58). Measured nutrients included total nitrogen, sulfur, phosphorus, potassium, calcium, magnesium, manganese, iron, aluminum, boron, copper, zinc, sodium, and molybdenum. Results were compared against sufficiency ranges from the Plant Analysis Handbook (version 3) to identify potential nutrient deficiencies (59). In addition, micronutrient concentrations in fish tank water were measured once per plant production trial via ICP spectroscopy.

2.2.6 Fish and plant yield measurements

Ripe tomatoes were harvested from all plants in each system, weighed, and summed over time to calculate the cumulative yield for each trial. Each grow bed, with six plants (spring trial) or five plants (fall trial), served as an experimental unit (n=3). Yields were normalized per plant by dividing system yield by the number of plants in the bed. Fish biomass was monitored monthly by sampling 10 fish per system and weighing them in their wet state to calculate the average fish mass. At the trial's conclusion, the total harvested fish biomass was recorded. Additional metrics, including apparent feed conversion ratio (FCRa, Eq. 1), survival rate (SR, Eq. 2), and thermal growth coefficient (TGC, Eq. 3), were calculated as follows:

FCRa = feed offered (g, dry basis) / biomass increase (g, wet basis) Eq. 1

SR (%) = (final number of fish / initial number of fish) × 100 Eq. 2

TGC = ((final fish weight)$^{1/3}$ – (initial fish weight)$^{1/3}$) × 1000 / $\sum_{i=1}^{n} T_i$ Eq. 3

where n is the number of growth-period days and T_I is the mean daily water temperature (°C). Survival rates were calculated and reported for each two months due to the trial's extended duration.

2.2.7 Nitrifying microbial analysis

To analyze nitrifying microbial communities, DNA was extracted from microbial biomass pellets collected from fish tank water at four sampling points (March 29th, May 15th, September 24th, and October 8th) and from grow bed water at one sampling point (May 24th). The extraction was carried out using the FastDNA Spin Kit (MP Biomedicals, USA). DNA concentrations were determined with the QuantiFluor dsDNA Quantification Kit (Promega, USA) to ensure sufficient yield for downstream analysis. The samples were then sent to the Molecular Research Laboratory (MRDNA Lab, Texas, USA) for sequencing of the 16S rRNA gene (primers 515F-806R) on an Illumina MiSeq platform. The sequencing center's data analysis pipeline was employed to demultiplex, de-noise, and assign the reads to zero-radius taxonomic units using an in-house curated database. The FASTQ files have been uploaded to the NCBI's Sequence Read Archive (SRA) under BioProject PRJNA1193631.

2.2.8 Statistical analyses

Each experimental treatment was replicated over three independent aquaponics systems to ensure the reliability of the results (12 systems in total). Fish growth and tomato yield data were analyzed using multiple regression in R, with a significance level of 0.05. Fish tank illumination and coupling/decoupling were each treated as fixed factors and time was a random factor in the model. To assess temporal variations in nitrogen and phosphorus levels among treatments, time-course

ANOVA was conducted ($p < 0.05$) with the "agricolae" and "car" packages in R. Averages, standard deviations, and coefficient of variation for FCRa, shoot wet biomass, leaf tissue elements, and nutrient composition were calculated using Microsoft Excel.

2.3 Results

2.3.1 Fish growth yield

The fish grow-out from April to December demonstrated that illuminating fish tanks and system coupling significantly enhanced tilapia growth (Figure 2.3A). By the end of the experiment, fish in the light systems weighed on average 492 ± 65 g (CV = 13%), 87 g more than those in the dark systems ($p = 0.02$). The FCRa was also lower in the light systems (1.23 ± 0.09, CV = 7%) compared to the dark systems (1.4 ± 0.05, CV = 4%), indicating more efficient weight gain per unit of food, though with slightly greater variability among systems (Figure 2.3B). This enhanced growth in light systems can be attributed to the shift in the aquatic environment from a heterotrophic system, dominated by bacteria and protozoa, to a partially photoautotrophic system under sunlight exposure (60). The presence of algae can increase the overall biomass of bioflocs through photosynthesis and serve as an additional food source for tilapia (61, 62). In our study, a noticeable difference in biofilm thickness was observed visually before and after introducing fish into the systems (Figure S2.2, Video S2.1), providing further evidence of algae consumption by fish. Interestingly, in addition to biofilm, the fish also consumed suspended algae, which enhanced water clarity (Figure S2.2). Tilapia typically prefer pellet-sized food for consumption (63), yet they adapted to eating the small suspended flocs in the systems.

There was also a significant difference between the fish biomass in the coupled and decoupled systems. In the coupled systems, fish weighed on average 493 g ± 68 g (CV = 14%), 87 g more than those in the decoupled systems ($p < 0.001$). Continuous water recirculation and

filtration in the coupled systems led to the reduction of TSS and clearer water in the fish tanks (Figure S2.3), which may have enhanced fish growth. However, less frequent filtration in the decoupled systems led to dense biofloc accumulation, with TSS levels reaching 600 mg/L, compared to just 16 mg/L in the coupled systems.

The combined impact of light exposure and system coupling was evident in the light-coupled treatment, where fish achieved an average weight of 551 ± 15 g (CV = 3%), 174 g more than those in the dark-decoupled system. Fish in this system benefited from both the algae-rich environment promoted by illumination and the enhanced water quality due to better filtration provided by system coupling. Differences in fish performance among the systems were not linked to differences in fish tank temperature, pH, or DO, which remained remarkably similar across all system types (Figure 2.2B and S4). It was clear that the intensive aeration used in the systems muted any effects of DO production by photosynthesis in light systems.

Survival rates for each two-month growth period and TGC are shown in Tables S1 and S2. Light-coupled systems maintained 100% survival and the highest TGC of 1.83 ± 0.03 (CV = 1.4%) throughout the experiment. Minor mortalities occurred in the dark-decoupled and dark-coupled systems between June and October and August and October, resulting in survival rates of 99% and 98%, respectively. In the final month, two mass mortality events occurred in two replicates of the light-decoupled system, approximately three weeks apart. Critical parameters, including ammonia, chlorine, nitrite, DO, pH, temperature, and water pump functionality, were assessed after each event and found to be within safe ranges. Given that each event occurred over a short period (<18 hours), the likelihood of an infectious pathogen being the cause was considered low. Nevertheless, autopsies conducted by trained pathologists immediately after each mortality event found no pathogenic evidence. Another possible cause that was considered (but was not tested due to

restrictions of the IACUC protocol) was the possibility of fish poisoning from consumption of tomato leaves. It was noticed that in these two systems, tomato vines had a few lower branches that had come into contact with the water and that the leaves were stripped from these branches, possibly due to fish attempting to eat them. Tomatoes are known to produce solanine in their leaves which is toxic to many animals (64) but few studies exist on its toxicity to fish. One such study showed little toxicity of potato-derived solanine to adult fish but toxic effects in embryos (65). Future work should be conducted on this matter given its relevance to aquaponics systems, but in the present study, action was immediately taken to ensure no trailing branches were within reach of the fish on any system for the remainder of the study.

Throughout the experiment, pH was monitored daily and maintained between 6.5 and 7, optimal for aquaponics (Figure S2.5A)(66). After fish introduction, pH gradually declined, requiring regular lime additions to restore it to 7. Temperature and DO were monitored every other day, with DO consistently around 7 mg/L, suitable for tilapia and nitrifying bacteria (Figure S2.5B) (67). Water temperature ranged from 20°C to 25°C, which is considered acceptable for tilapia health (Figure S2.5C)(68).

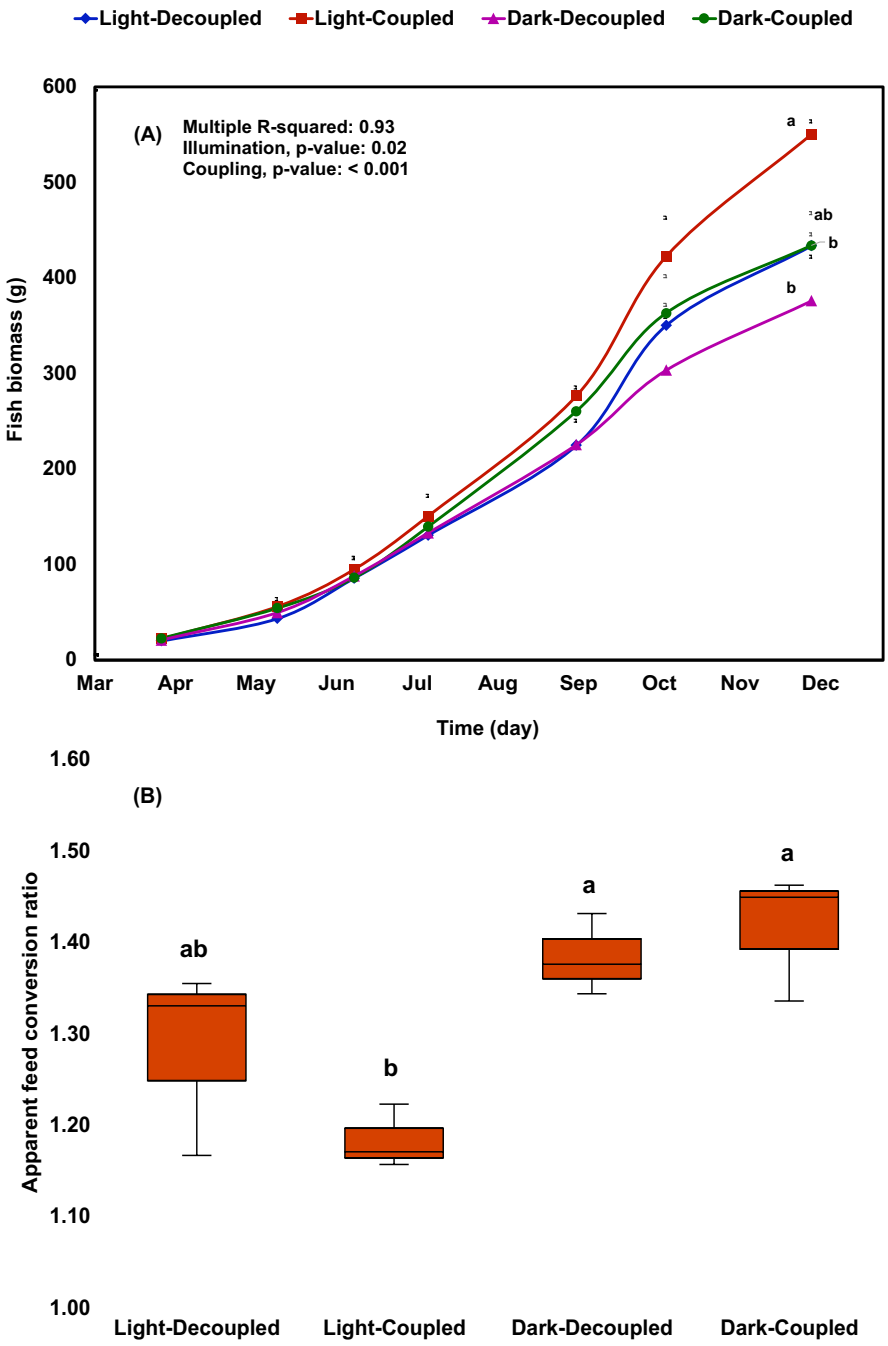

Figure 2.3 (A) Fish biomass growth monitored over eight months (April to December) and (B) final apparent feed conversion ratio (FCRa) for the four aquaponic system types. Error bars are standard deviations based on n = 3 system replicates. Treatments with the same letter are not significantly different (alpha > 0.05) based on Tukey's HSD test. Fixed factor p-values from the multiple regression model are shown in panel A.

2.3.2 Plant growth yield

In the first tomato trial (March 30–June 22), coupling the systems significantly enhanced plant growth ($p < 0.0001$). Coupled systems produced 694 ± 172 g (CV = 24%) of tomatoes per plant, compared to 481 ± 57 g (CV = 12%) per plant in decoupled systems (Figure 4A). While the coupled systems achieved higher yields on average, the larger CV indicates greater variability among replicates, suggesting that plant performance was less consistent than in the decoupled systems. In contrast, the lower CV in decoupled systems reflects more uniform growth despite their lower yield. During this period, organic and nutrient input was low since fish grew from 20 g to 130 g, and daily feed increased from 20 g to 70 g per system to match biomass growth. Limited water exchange in the coupled systems led to nutrient buildup, while decoupled systems, with daily water discharges of ~50 L, sustained lower nutrient concentrations. Key macronutrients (nitrate-nitrogen (NO3-N), potassium, calcium, and magnesium) were consistently higher in the coupled systems, averaging 73, 80, 130, and 20 mg/L, respectively, compared to 22, 72, 23, and 5.3 mg/L in the decoupled systems at the midpoint of the fruiting stage (May 22) (Figure 2.5A, Figure S2.5A, Table 2.1).

Coupled systems also provided nutrients more frequently through continuous irrigation, compared to 10 cycles per day in the decoupled systems. The combination of higher nutrient concentrations and frequent irrigation contributed to improved plant growth and larger plant size ($p = 0.002$), with an average shoot wet biomass of 1147 ± 204 g per plant in coupled systems (CV = 17%, indicating more uniform growth) compared to 691 ± 166 g in decoupled systems (CV = 24%, reflecting greater variability) (Figure 2.4B). Illumination of the fish tanks did not significantly affect plant growth during the first trial ($p = 0.55$).

Despite the positive effects of coupling on plant growth and yield in the first trial (Spring), the second trial (Fall) showed the opposite trend, with decoupling and illumination significantly improving fruit yield. In the fall trial, fish were now larger, and feeding rates were therefore higher. Decoupled systems produced an average of 1712 ± 257 g (CV = 15%) of fruit per plant, compared to 1356 ± 183 g (CV = 13%) in coupled systems ($p < 0.001$) (Figure 2.4C). While fruit yield was higher in the decoupled systems, the slightly greater CV indicates more variability among replicates compared to the coupled systems, where fruit production was more consistent. Note that direct numerical comparisons between spring and fall trials yield cannot be undertaken due to the switch to a more productive cultivar. The poorer performance of the coupled systems in the second trial was linked to continuous water recirculation, which, combined with higher fish densities and increased feeding, caused excessive sludge buildup in the grow beds despite the filtration system. Some of the sludge made it past the filter, but soluble organics in the water (soluble COD levels: 119 mg/L in coupled vs. 44 mg/L in decoupled systems) also contributed to sludge growth in the grow bed media. This resulted in waterlogged roots and likely reduced oxygen levels in the root zone, ultimately leading to root asphyxiation and stunted plant growth (29). By the end of the trial, many plants in the coupled systems were wilting despite sufficient water supply (Figure S2.6).

In the fall trial, the plants grown in the illuminated systems yielded significantly more fruit compared to those in the dark systems ($p = 0.011$), with yields of 1569 ± 321 g (CV = 20%, indicating greater variability) and 1499 ± 264 g (CV = 17%, indicating more uniform growth) per plant, respectively.

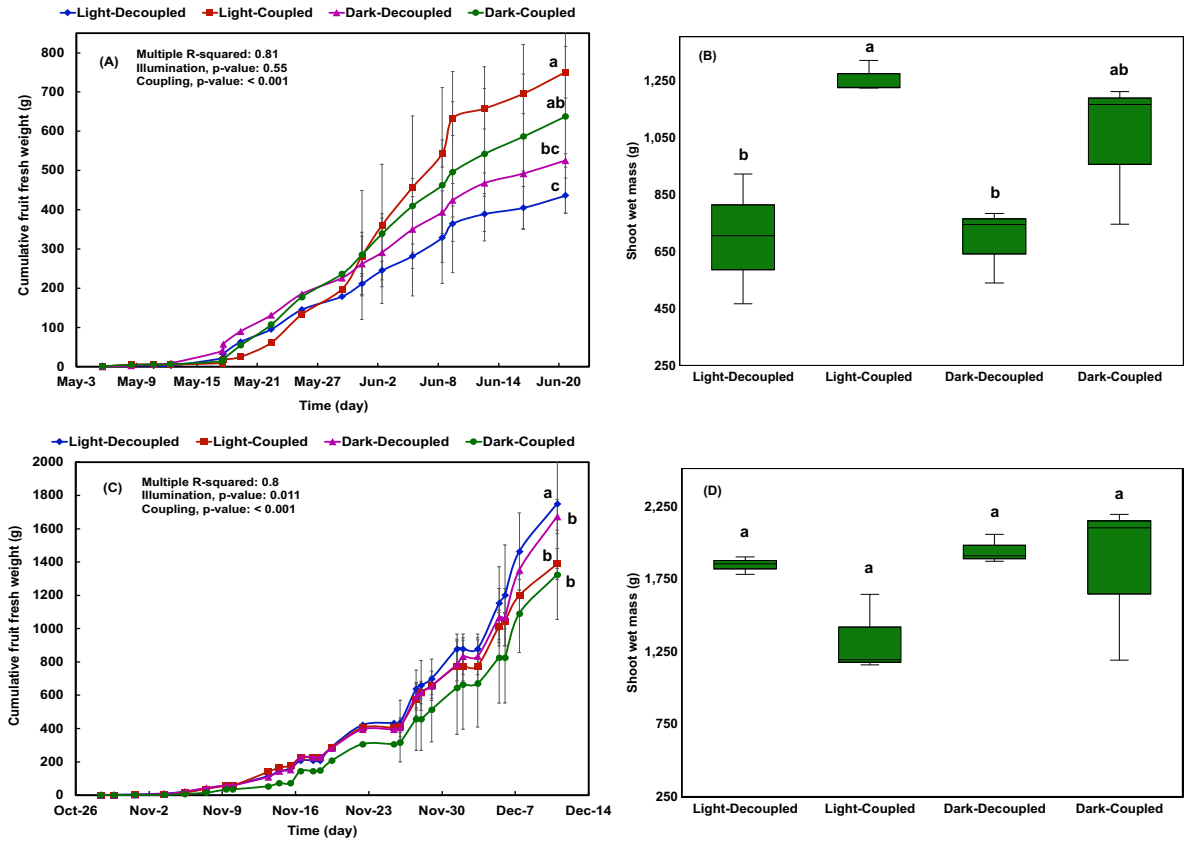

Figure 2.4 Cherry tomato plant productivity across treatment: (A) cumulative fresh fruit weight during the first trial (Spring: April 1st to June 22nd), (B) shoot wet mass from the first trial, (C) cumulative fresh fruit weight during the second trial (Fall: September 17th to December 11th), and (D) shoot wet mass from the second trial.

2.3.3 Nutrient dynamics

The coupled systems consistently exhibited higher NO_3-N levels compared to the decoupled systems ($p < 0.001$), primarily due to nutrient accumulation resulting from limited water exchange (Figure 2.5A). During the first trial, NO_3-N levels in the coupled systems were adequate for tomato growth, reaching approximately 150 mg/L in the dark-coupled system and 100 mg/L in the light-coupled system by the end of the trial. The recommended nitrogen concentration for hydroponic tomatoes across different growth stages ranges from 70 to 150 mg/L (69). In contrast, the NO_3-N levels in both decoupled systems were significantly lower, averaging around 40 mg/L. During the

initial phase, when fish feeding ranged between 20 to 70 g/day, the coupled systems effectively provided sufficient nitrogen for plant growth. However, as the experiment progressed and the fish biomass increased, NO_3-N continued to accumulate in the coupled systems, ultimately reaching concentrations far exceeding plant requirements: 610 mg/L in the dark-coupled system and 350 mg/L in the light-coupled system. Compared to spring, the decoupled systems better met plant nitrogen demands in the fall trial, with NO_3-N concentrations ranging from 70 to 90 mg/L. This higher nutrient balance in the fall is attributable to the higher feeding rates to support the higher fish densities.

No significant differences in ammonium (NH_3-N) or nitrite (NO_2-N) levels were observed among treatments, aside from occasional spikes in decoupled systems during the first four months (Figure 2.5B, C), particularly at the fish introduction and increased feeding. However, as the systems matured, nitrification stabilized, and fluctuations declined. Conversely, coupled systems showed better nitrification early on but experienced ammonia spikes later, likely due to increased organic input, poor drainage, and anoxic zones in the grow beds where most nitrifiers were located (see Section 2.3.4).

Leaf tissue analysis in the second trial indicated sufficient nitrogen in both coupled and decoupled systems, though the coupled systems displayed higher leaf nitrogen content (Figure 2.6A). These levels were close to the upper limit of the sufficiency range, aligning with the higher nitrate concentrations in the fish tanks of coupled systems. Although algae did apparently consume nutrients in the light systems as hypothesized, no significant impact was observed on plant nutrient status: as shown in Figure 6, there were no significant differences in leaf tissue nutrient content between light and dark systems, whereas decoupled systems exhibited significantly higher levels

of nitrogen, phosphorus, potassium, manganese, and copper. Thus, coupling versus decoupling was the more important factor influencing plant nutrient status.

Phosphate-phosphorus (PO_4-P) levels, unlike other nutrients such as nitrogen, potassium, calcium, magnesium, and sulfate, showed no significant differences across treatments, except for dark-coupled systems in the fall trial (Figure 2.5D). Leaf tissue analysis during the second trial showed sufficient phosphate availability in all system types, with concentrations near or exceeding optimal levels (Figure 2.6B).

Potassium, unlike nitrogen and phosphorus, is not sufficiently replenished through feed in aquaponic systems (55) and was supplemented during the experiment. Its accumulation was more pronounced in the coupled systems, resulting in higher water concentrations and sufficient levels in plant tissue (Figure 2.6C, Figure S2.5A). However, plants in decoupled systems also maintained sufficient potassium. Calcium and magnesium, typically deficient in aquaponics due to their low abundance in fish feed (Figure S2.7) (1, 54), were similarly lacking in this study. Despite daily lime additions for pH regulation, plant tissue analysis revealed deficiencies in both nutrients (Figure S2.8A, B), likely due to precipitation and the low solubility of lime, which limited calcium availability. Therefore, to supplement calcium and magnesium more effectively in aquaponics, lowering the pH in the grow beds or using targeted methods such as foliar application may provide better solutions. Such applications are best suited for decoupled aquaponics. Among micronutrients, zinc and copper were sufficient across all systems during the second trial, while manganese sufficiency was observed only in the coupled systems (Figure 2.6D, E, F). These results suggest that most micronutrients can be supplied organically through fish feed without additional fertilization. However, leaf tissue analysis indicated deficiencies in boron, molybdenum, and iron across all systems, suggesting the need for supplementation in future studies (Figure S2.8D, E, F).

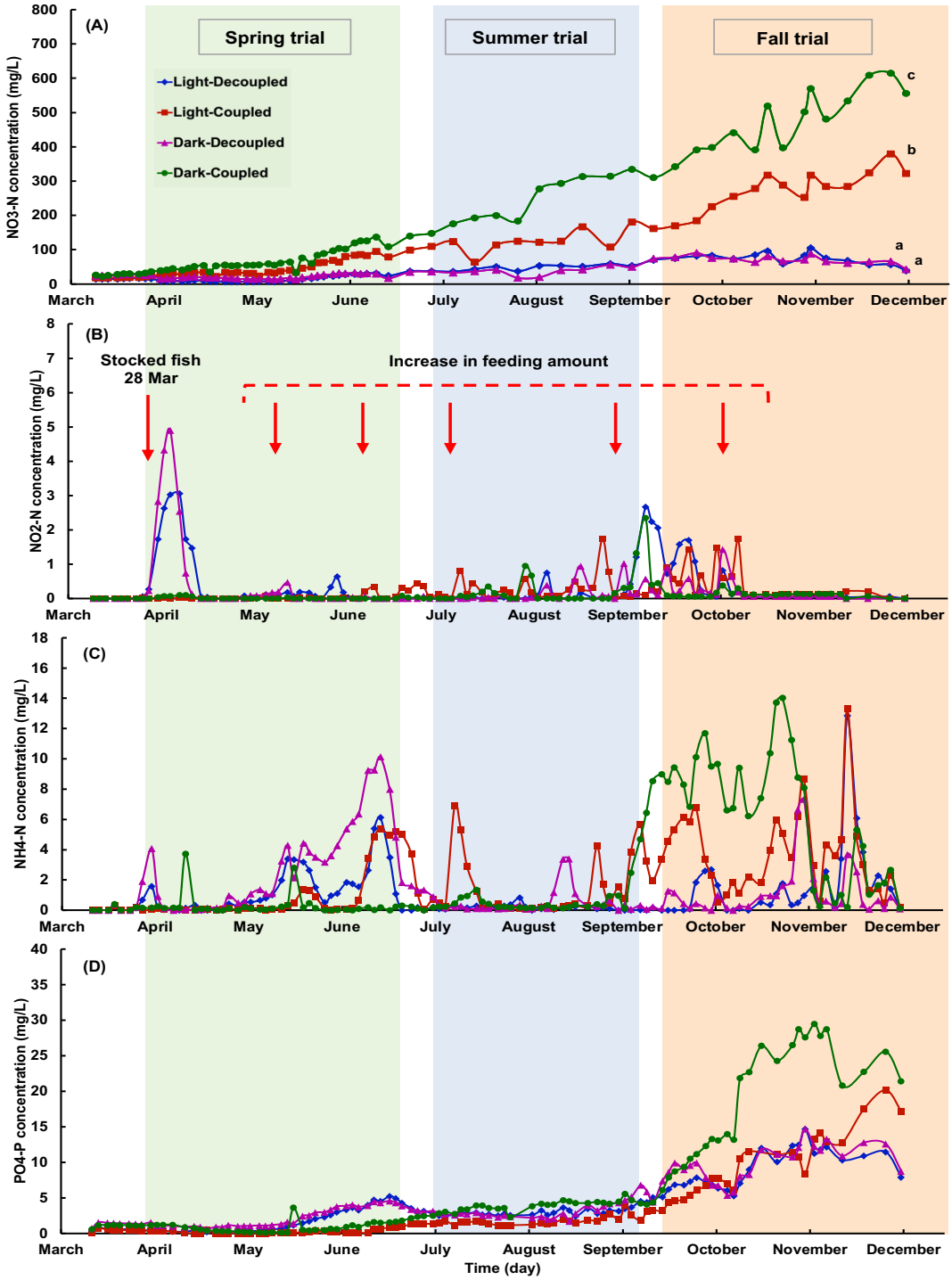

Figure 2.5 Time-course plots of nutrient concentrations in the fish tanks across the four treatments: (A) NO3-N, (B) NO2-N, (C) NH4-N, and (D) PO4-P.

Table 2.1 Nutrient concentrations in fish tank water analyzed once during each trial across the four treatments.

Tomato production trials	Treatments	Calcium (mg/L)	Magnesium (mg/L)	Potassium (mg/L)	Phosporus (mg/L)	Boron (mg/L)	Zinc (mg/L)	Manganese (mg/L)	Molybdenum (mg/L)	Sodium (mg/L)
First trial (Spring)	Light-Decoupled	24.04 ± 8.78	5.7 ± 2.33	73.91 ± 3.56	1.48 ± 0.54	0.02 ± 0.01	0 ± 0	0 ± 0	0.03 ± 0.02	21.08 ± 0.4
	Light-Coupled	125.89 ± 26.98	19.97 ± 6.09	80.48 ± 7.03	0.18 ± 0.19	0.01 ± 0	0.09 ± 0.02	0.1 ± 0.01	0.03 ± 0	41.48 ± 1.58
	Dark-Decoupled	21.91 ± 4.29	4.86 ± 0.44	70.33 ± 4.26	2.53 ± 0.57	0.02 ± 0	0.02 ± 0.03	0 ± 0	0.02 ± 0	20.52 ± 0.86
	Dark-Coupled	134.46 ± 16.11	19.37 ± 1.81	79.83 ± 4.08	0.45 ± 0.15	0.01 ± 0.01	0.07 ± 0.06	0.1 ± 0.08	0.02 ± 0	44.63 ± 4.22
Second trial (Fall)	Light-Decoupled	100.67 ± 14.59	14.14 ± 2.12	130.05 ± 8.81	7.68 ± 1.24	0.05 ± 0.01	0 ± 0	0.02 ± 0.03	0 ± 0.01	25.3 ± 1.06
	Light-Coupled	302.8 ± 12.58	54.56 ± 2.94	333.56 ± 1.89	9.35 ± 2.13	0.17 ± 0.01	0.04 ± 0.04	0.17 ± 0.11	0.01 ± 0.01	69.18 ± 3.91
	Dark-Decoupled	85.48 ± 10.5	12.1 ± 0.39	120.82 ± 1.62	7.8 ± 0.54	0.04 ± 0	0 ± 0	0 ± 0	0 ± 0	23.33 ± 0.16
	Dark-Coupled	522.47 ± 100.42	70.08 ± 10.35	342.86 ± 26.04	17.28 ± 1.57	0.17 ± 0.01	0.08 ± 0.02	0.33 ± 0.13	0.01 ± 0	76.71 ± 9.57

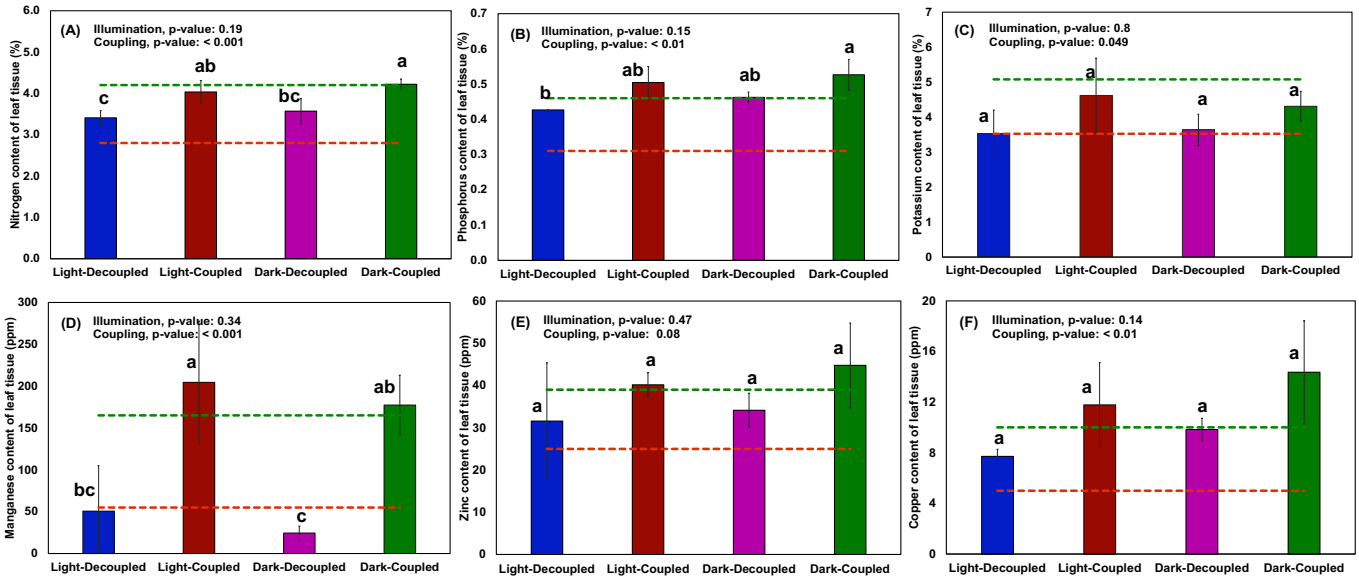

Figure 2.6 Nutrient contents of leaf tissue measured during the second trial across the four treatments: (A) nitrogen, (B) phosphorus, (C) potassium, (D) manganese, (E) zinc, and (F) copper. The orange and green lines represent the minimum and maximum thresholds of the sufficiency range, respectively.

2.3.4 Nitrifying microbial community

The nitrifying microbial community was analyzed by 16S rRNA sequencing at four time points for fish tanks and one time point for grow beds (Figure 2.7A). The grow beds exhibited a higher relative abundance of nitrifying bacteria compared to the fish tanks, likely due to the large surface area provided by the gravel substrate, which supports bacterial growth (70). Within the grow beds, the coupled systems showed greater nominal nitrifier abundance, but the difference was not statistically significant. After fish introduction, however, the decoupled systems supported a higher nitrifier population in the fish tanks, compared to the coupled systems.

Relative abundance can be misleading when comparing across systems with different TSS levels in the fish tank. We, therefore, also report nitrifier relative abundance scaled to the level of TSS (Figure 2.7B). Although imperfect and not a representation of the absolute abundance of

nitrifiers in the system, the scaled values showed little difference in nitrifier abundance between light and dark systems, except for the October time point where light systems had a significantly higher nitrifying population ($p < 0.005$, Tukey HSD).

The trend in the fish tank nitrifier populations aligned with patterns of nitrification instability initially observed in decoupled systems. In the initial six months when organic input was lower, *Nitrospira* relative abundance was <0.05% of prokaryotes in the decoupled fish tanks and coincided with disruptions in nitrification performance. As nutrient inputs increased in the fall trial, the *Nitrospira* relative abundance in decoupled fish tanks increased to ~0.2% of the prokaryotic community.

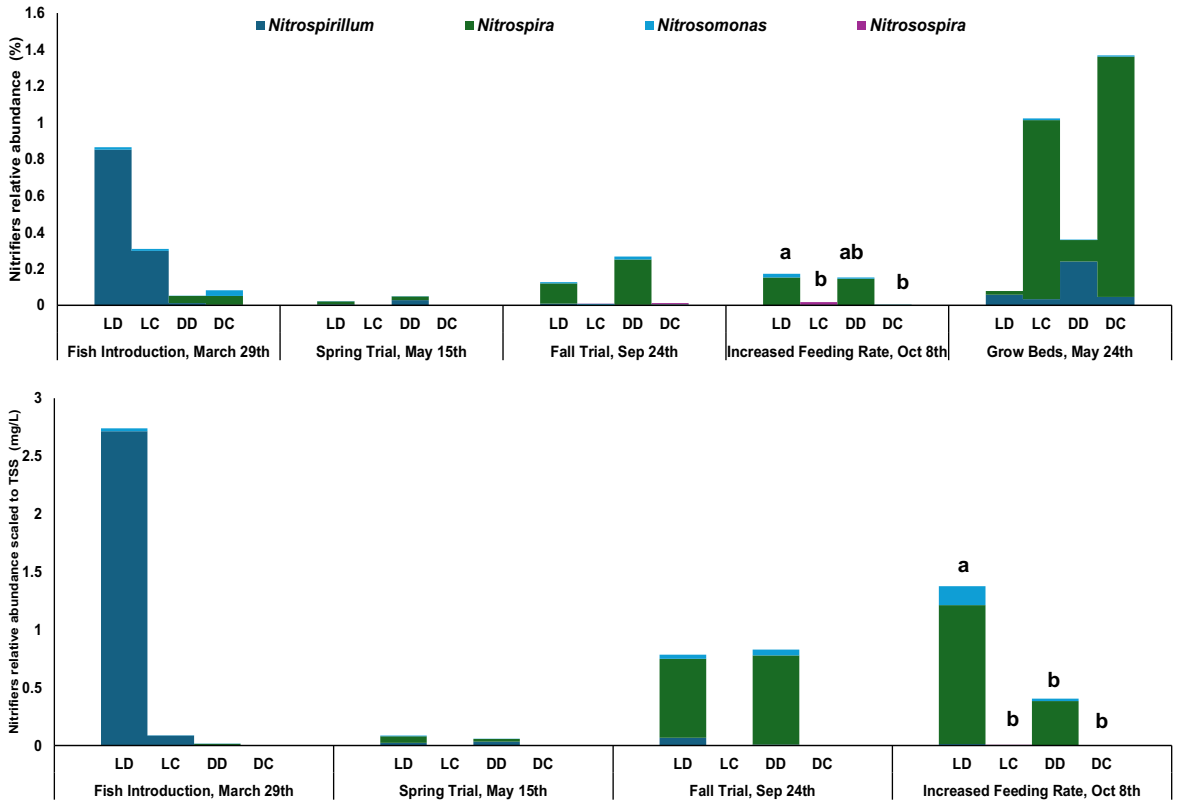

Figure 2.7 (A) Relative abundance of nitrifying bacteria at four time points for fish tank samples and one time point for grow bed samples, and (B) TSS-scaled nitrifying bacteria abundance in the fish tanks. Lowercase letters (a, b, c, etc.) indicate statistically significant differences between treatments ($p < 0.05$). Figures without letters were not statistically different from the others.

2.4 Discussion

2.4.1 Fish growth enhanced by coupling and light penetration into tanks

Biofloc is widely recognized as a sustainable and nutritious supplement in aquafeeds (71) and several studies have reported enhanced performance of tilapia reared in biofloc systems (72-74). To the authors' knowledge, however, this is the first study to systematically compare coupled and biofloc-decoupled aquaponics systems under both dark and light fish tank conditions. Despite its wide practice in stand-alone aquaculture systems, many practitioners of aquaponics have been reluctant to allow light penetration into fish tanks. Extension documents published in the US describing best practices in aquaponics advocate for covering fish tanks, largely to prevent algae growth (75, 76). These documents are important because many producers rely on them for system design information, yet these claims appear to be unsupported by a rigorous study. The present study appears to contradict this advice, at least for systems rearing tilapia and cherry tomatoes. Here, a significant 21% increase in fish mass was observed in tanks exposed to natural sunlight versus fish from covered tanks. Studies in stand-alone aquaculture systems confirm these results with a study on Nile tilapia by Khanjani and Sharifinia (20) showing the highest body weight gain and lowest FCRa when fish tanks were exposed to light. They attributed this in part to the abundance of photoautotrophic organisms in illuminated systems (20). Our results clearly showed tilapia eating both suspended biofloc and algal biofilms that grew on the walls of the light-exposed fish tanks. Additionally, the findings by Reis et al. confirmed this, demonstrating that natural photoperiod conditions led to increased concentrations of proteins and lipids in the biofloc system, which improved the zootechnical performance of Pacific white shrimp (60).

Similar to the findings in our study, (77) showed that "green water" biofloc systems that relied on algae growth yielded higher total fish mass and lower apparent FCR in tilapia than

traditional molasses-fed biofloc systems. However, the apparent FCRs of 1.27-1.46 in green water systems and 1.35-1.61 in molasses biofloc systems were higher than those observed in our study, possibly due to the use of higher feeding rates. All of the systems studied by Suarez-Puerto et al. were outdoors and exposed to sunlight, which also contrasts with our study conditions (greenhouse environment with some tanks systems covered to limit light).

In addition to algal feed effects, photoperiod and light intensity can also affect fish's biological rhythms, metabolic rates, and feed intake (78, 79). Thus, higher light intensity and exposure to natural photoperiod could also contribute to the enhanced growth observed in the light systems. In contrast, the reduced light levels and continuous darkness in the covered systems may have disrupted the fish's biological clock and natural rhythms, negatively impacting their growth (78, 79). Regardless of the multiple mechanisms (supplemental food from algae, direct effects of light on fish biology), the findings from the present study support the benefit of allowing natural sunlight into tilapia production systems, similar to findings from stand-alone aquaculture systems.

Although they did not specifically study algal biofloc systems, Pinho et al. reported that microbial biofloc systems improved juvenile tilapia growth and FCRa compared to RAS, attributing the benefits to supplemental microbial food (45). Another study reported that tilapia raised in a Bio-RAS system (a biofloc system integrated with an external anaerobic bioreactor) exhibited significantly higher growth, feed intake, and protein efficiency compared to those reared in a conventional RAS (80). Beyond improving fish growth, biofloc technology has also been shown to increase crude lipid content, enhance digestive enzyme activity, and strengthen the immune response in tilapia (81). For these reasons, we initially hypothesized that illuminated fish tanks in decoupled biofloc aquaponics would produce the highest fish yields.

In reality, the decoupled biofloc systems resulted in 17% lower fish production than the coupled systems. Decoupled systems had higher suspended biomass (algae and bacteria, TSS = 600 mg L^{-1}) than the recirculating coupled systems (TSS = 16 mg L^{-1}). Although biofloc can serve as supplemental feed for tilapia, studies have shown that high settleable solids in zero-exchange biofloc systems impaired growth and altered clinical biochemistry (43, 82). Their study reported that an optimal density of 13 kg/m³ was optimal for tilapia reared in grow-out biofloc systems, while excessively high solids (≥74 mL/L) were associated with reduced growth and lower carcass crude protein at higher densities. Similarly, Pai et al. reported that maximum tilapia production was achieved at a stocking density of 13.2 kg/m³ without compromising growth, immunity, or survival in a hybrid biofloc system equipped with an additional biofiltration unit. They also observed greater weight gain in tilapia reared in the hybrid system compared to a stand-alone biofloc setup, owing to improved water quality (83). In our study, the coupled systems effectively functioned as a hybrid biofloc design, since water recirculated through gravel-media grow beds that served as both physical and biological filters, thereby enhancing water clarity. Furthermore, Ekasari et al. reported that incorporating a settling tank into biofloc systems to reduce excess biofloc biomass improved gill health and enhanced production performance in red tilapia (84). The results contrast with those reported by Pinho, Lima (45), who achieved strong growth of juvenile tilapia in decoupled flocponics compared to recirculating systems. Their shorter growth period (56 days), lower stocking density (from 0.43 kg/m^3 to ~5 kg/m^3), and clearer water (settleable solids of 30 mg/L) may explain the differing outcomes from the present study. These findings highlight that biofloc can enhance fish growth, but once TSS becomes excessive, the negative impacts outweigh the nutritional benefits.

2.4.2 Tomato production impacted by system coupling more than by algae

One of the main concerns about algal growth in aquaponics systems is that algae compete with plants for nutrients. This is a view widely held within the hydroponics community (85) and there is a great deal of advice from companies on how to eliminate or prevent algae. The results from the present study do suggest lower levels of aqueous calcium and nitrate in systems with algae but similar levels of potassium, sulfate, phosphate, and micronutrients when compared to dark systems. However, the nitrate levels in the coupled systems exceeded the needs of the plants in coupled systems, particularly in the fall trial when feeding rates were higher. Such high nitrate levels can increase the risk of nitrate accumulation in tomatoes, which can pose health concerns for humans if consumed in excess (86). These differences in NO_3-N between dark-coupled and light-coupled systems are due partly to nitrate assimilation by algae in the light-exposed systems, which contributed to enhanced fish growth and yield, as discussed previously.

More importantly, however, there were not statistically significant differences among light and dark systems regarding plant nutrient status as measured by leaf tissue sampling. The upshot of these results is that fish tank illumination had either no effect or a small positive effect on tomato production. These results were somewhat surprising given a general paradigm in the field that algae growth in aquaponics deprives plants of nutrients. Algal photosynthesis may have contributed to the improvement in tomato yield observed in light systems during the fall trial by supplying dissolved oxygen and preventing root anaerobiosis (87). Additionally, biostimulants and allelochemicals released by microalgae, such as vitamins, amino acids, and proteins, have been shown to enhance plant resistance to stress conditions like root suffocation (88, 89). Barone et al. similarly found that co-cultivation of tomatoes with *Chlorella vulgaris* and *Scenedesmus quadricauda* resulted in higher fresh shoot and root biomass in hydroponic systems (90). In our

study, these factors may have helped mitigate the root asphyxia that likely occurred in the light-coupled system, leading to 5% higher tomato production compared to the dark-coupled system. Interestingly, light-coupled tomato plants had the lowest fresh shoot biomass despite higher fruit yields than dark coupled systems.

In terms of nutrient availability and uptake in tomatoes, it was coupling versus decoupling that was a significant factor. Coupled operation resulted in significantly higher leaf tissue concentrations of multiple critical macro and micronutrients, as shown in Figure 2.6. Coupled systems resulted in greater fruit production in the spring trial but lower production in the fall trial. Part of this difference could be attributed to the distinct responses of the two tomato cultivars tested and their varying sensitivities to environmental conditions. Each cultivar can differ in its optimal temperature, light, and nutrient requirements, which may help explain the seasonal variation observed in treatment responses. For example, seed producer guidelines indicate that the Washington cultivar has a lower optimal temperature range (16–21 °C) compared to Favorita F1 (23–25 °C). Beyond differences across plant types, as shown in studies on nitrogen and phosphorus retention and growth performance in biofloc aquaponics (91), even cultivars within the same species can display different responses. This has been demonstrated in cherry tomato, where different cultivars exhibited significant variation in growth and yield outcomes under similar conditions (92).

However, there was also evidence of wilt and waterlogging of roots in the coupled systems in the fall trial that likely suppressed yields. Cantore et al. similarly found that waterlogging and root hypoxia reduced tomato production in loam soil (93). Gravel, while inexpensive, is prone to clogging from suspended solids, microbial growth, and roots, leading to reduced water circulation and anaerobic zones that damage or kill plant roots (54). However, intermittent irrigation in the

decoupled systems may have promoted better air circulation around roots, resulting in significantly higher fruit yields and ~315 g more fresh shoot biomass per plant, though this difference was not statistically significant ($p = 0.12$, Figure 2.4D). The poor drainage in coupled systems negated their nutrient uptake advantages. Coupled systems still maintained higher aqeuous macronutrient concentrations, including nitrate, potassium, sulfate, calcium, and magnesium, throughout the fall trial (Figure 2.5A, Figure S2.5, Table 2.1). The exception to this was aqueous phosphate which was very similar among the systems for most of the trial, except for dark-coupled systems in the fall. Factors affecting PO_4-P levels include feed input, plant uptake, water discharge, and precipitation with cations. Higher calcium and magnesium concentrations in the coupled systems (Table 2.1) promoted greater calcium and magnesium phosphate precipitation (94). These precipitates were filtered through grow beds due to continuous water recirculation, resulting in visible white crystals in the beds. Precipitation explains why phosphate patterns differed from other nutrients. Plant tissue analysis confirmed that coupled systems maintained higher levels of nitrogen, phosphate, potassium, zinc, manganese, and copper within optimal ranges (Figure 2.6). However, the superior nutrient availability was offset by growth limitations caused by poor drainage. These findings highlight the need to adjust plant bed sizing based on fish density and system configuration.

In the fall trial, fish densities exceeded 20 kg/m³, a level commonly used in high-density production systems (95), highlighting the need for improved solids management and larger grow beds in coupled systems. While moderate to low solids benefited plant growth in the first trial, excess sludge in the second trial negatively impacted tomato production. In practical settings, maintaining consistent stocking densities is feasible because there is no need to create experimentally replicated aquaponics systems, and fish can be grown in rotation to support a single

large plant production system. Our study revealed that the “best” system for tomato production depends in part on fish density.

2.4.3 Nitrification minimally affected by the presence of algae

Nitrification is one of the most important microbial processes in aquaponics because insufficient nitrification is harmful to both fish and plants. Incomplete nitrification results in the accumulation of ammonia and nitrite, both of which are harmful to tilapia (77) and tomatoes (96). Although the levels of ammonium and nitrite observed in our study are unlikely to be problematic for fish and plants, differences in nitrogen species were observed among the experimental treatments as previously described. We initially hypothesized that the presence of algae in the illuminated fish tanks of aquaponics systems would increase the abundance of nitrifying bacteria based on results from past lab-scale trials (23, 24). Only weak evidence exists from the present study to support this hypothesis: higher nitrifier abundance was observed in the light-decoupled biofloc system compared to the corresponding dark system. Otherwise, meaningful differences in nitrifying populations were not observed between light and dark systems. More importantly, no significant differences were observed between light and dark systems with regard to ammonium and nitrite levels in the fish tanks. In the decoupled biofloc systems, light versus dark systems also had no effect on nitrate levels, suggesting that any difference in nitrifier abundance did not translate to tangible performance differences. Suarez-Puerto, Delgadillo-Díaz (77) likewise showed no significant differences in ammonia-N or nitrite-N levels between traditional brown biofloc and green biofloc stand-alone aquaculture systems. Evidence from the aquatic ecology literature suggests that algae primarily benefit nitrifying bacteria in conditions with high N loading and sub-saturation DO conditions (97). In such an environment, algal photosynthesis supplies oxygen to nitrifying organisms but does not induce competition for ammonia-N. Although aquaculture

systems supply a high flux of reduced N into the system (in the form of feed), the intensive aeration rates used in the present study did not allow for sub-saturation DO conditions to develop. As such no DO benefit from the presence of algae was observed. This is a contrast between the intensive aquaculture systems used for aquaponics and pond-based aquaculture systems where algae are a widely recognized DO source and sink (62).

Past research has shown that grow beds of coupled systems are the dominant aquaponics compartment for nitrification (98) and our results generally confirmed this finding. However, there was no significant difference in total nitrifier relative abundance in grow beds of coupled versus decoupled systems despite higher nominal levels in the former. In contrast, the decoupled biofloc systems had much higher nitrifier relative abundance in the fish tanks than the coupled systems. This difference can be attributed to the higher HRT and solids retention time (SRT) in the decoupled fish tanks, which allowed a larger population of nitrifying bacteria to establish and remain within the system (13). Similar findings were reported by Liu et al., who demonstrated that higher SRT significantly enhanced the growth of nitrifying bacteria, particularly *Nitrospira*-like nitrite-oxidizing bacteria (NOB), in a complete-mix activated sludge process (99). They attributed this to the slower decay rates of *Nitrospira* compared to other nitrifiers, allowing them to dominate at higher SRTs, thereby improving the nitrification process. In our systems, the initial nitrifying community converged to a *Nitrospira*-dominated community for the duration of the study. This bacterium, is capable of complete nitrification, conducting both ammonia and nitrite oxidation (100). This unique capability allows *Nitrospira* to enhance nitrogen cycling in aquaponics systems. Despite this capability, the decoupled biofloc systems suffered from occasional spikes in ammonia-N and nitrite-N following system disturbances including fish stocking and feed rate increases. In these cases, elevated organic matter and reduced DO likely favored heterotrophs,

which may have temporarily outcompeted nitrifiers for oxygen, resulting in ammonia accumulation (101, 102).

2.5 Conclusion

This study compared coupled and decoupled biofloc operation of aquaponics under both dark and light fish tank environments for the first time. Over ten months, the full-factorial experiment demonstrated fish tank illumination boosted fish yield by providing a protein-rich algal biofloc, while coupling improved water quality through continuous filtration. The combined effect of light and coupling was most evident in light-coupled systems, which achieved the highest fish biomass of 550 g per fish compared to 376 g in dark-decoupled systems. Importantly, algal-dominant communities and fish tank illumination did not negatively affect plant growth, further supporting the viability of their integration into aquaponics. Coupling significantly influenced plant yields, with coupled systems producing 44.5% higher tomato yields in the spring due to superior nutrient availability but 21% lower yields in the fall compared to decoupled systems. This latter result was likely due to excessive sludge accumulation in grow beds that restricted water and airflow, leading to root asphyxiation. However, moderate sludge levels were likely beneficial, as this material was shown to be a reservoir for nitrifying bacteria. Coupled grow beds had a higher relative abundance of nitrifiers, while decoupled systems favored nitrifier growth in fish tanks due to longer solids and hydraulic retention times. This study provides data over the entire fish grow-out and demonstrates the benefits of fish tank illumination and system coupling, so long as grow bed sludge is well-managed.

Chapter 3: Coupling, Decoupling, and Fish Tank Illumination Shape the Functional Microbiome and Nutrient Cycling in Aquaponics

Coupling, Decoupling, and Fish Tank Illumination Shape the Functional Microbiome and Nutrient Cycling in Aquaponics

Authors: Shima Rezaei[1], Margaret Otto[1], Grace Hohn[1], Qichen Wang[1], Wellington Arthur[1], Sarah Hensless[1], Mary Beth Hall[1], Madeline Spoor[1], Neha Potnis[2], David Cline[3], Brendan Higgins[1]*

[1]Biosystems Engineering, Auburn University, Auburn, AL 36849, USA

[2]Entomology and Plant Pathology, Auburn University, Auburn, AL 36849, USA

[3]Fisheries and Aquatic Sciences, Auburn University, Auburn, AL 36849, USA

*Corresponding author:

Brendan T. Higgins

Department of Biosystems Engineering, 203 Corley Building, Auburn, AL 36849, USA

Phone: 334-844-3532

e-mail: bth0023@auburn.edu

Abstract

This study examined how aquaponics system configuration (coupled vs. decoupled) and natural light penetration into the fish tank (light vs. dark) influence key microbial groups (algae, nitrifiers, plant growth-promoting bacteria (PGPBs), and phytopathogens) and their impact on cherry tomato production across two seasons. In coupled systems, water was continuously recirculated between the fish and plant units with minimal water exchange. Coupled systems retained higher nutrient concentrations in the grow bed sludge, leading to 1.15-fold higher tomato yield in the spring trial and >2-fold higher yield in the fall trial compared to the decoupled systems, which involved one-way flow and regular water discharge and replenishment. Decoupled systems supported more diverse microbiomes and higher putative PGPB abundance in the hydroponics beds, including beneficial genera such as *Bradyrhizobium*, *Ensifer*, and *Streptomyces*. Of particular interest, *Streptomyces* associated with siderophore production had a relative abundance of 1.16% in the decoupled systems compared to 0.068% in coupled systems, which coincided with over 50% greater siderophore activity and elevated iron content in plant leaf tissue. Despite the higher abundance of PGPBs, unstable nitrification in the decoupled systems led to ammonia buildup (up to 1 mg L^{-1}), nutrient deficiencies, and reduced yields. Putative pathogen analysis revealed potential threats from *Pythium graminicola* in the dark-decoupled system and from the parasitic nematode *Xiphinema rivesi* in the light-coupled system during the fall, both of which coincided with plant wilting and stunted growth in these systems. This study showed how system design shaped microbiome structure and function, affecting nutrient dynamics and plant health.

Keywords: Bioponics; Cherry tomato; Microbial community; Nitrification; Pathogens; Siderophore

Graphical Abstract

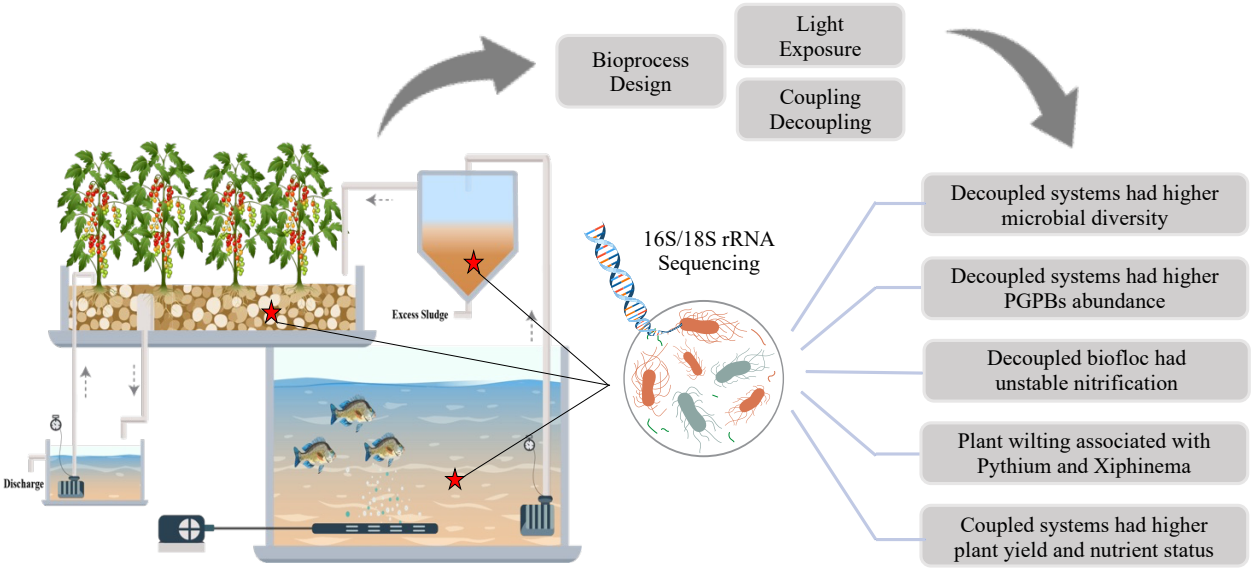

Highlights

- Aquaponics system coupling vs. decoupling and light vs. dark fish tank tested
- Coupled systems had 15-104% higher tomato yield and plant macronutrient levels
- Decoupled systems had >50% higher siderophore activity and plant Fe content in the fall
- Weak nitrification in decoupled systems led to reduced feeding and nutrient levels
- Plant wilting in fall trial associated with abundance of *Pythium graminicola* and *Xiphinema rivesi*

3.1 Introduction

Biofloc aquaponics is a bioregenerative food production system that integrates aquaculture and hydroponics, relying heavily on complex microbial processes to maintain water quality and support plant and fish growth (103). Microbial processes are particularly important because bioregenerative food systems have limited reliance on the biogeochemical cycles of the natural environment. Consequently, nutrient cycling processes must be embedded within the engineered system. Within aquaponics systems, microbial sludge accumulates in various compartments, such as fish tanks, clarifiers, and hydroponics beds, and plays a critical role in nutrient recycling and microbial regulation (11). This sludge not only acts as a nutrient reservoir but also harbors diverse microbial populations that significantly influence the biological functioning of the system (9). Among these microorganisms, nitrifiers, plant growth-promoting bacteria (PGPBs), and plant pathogens have particularly notable effects on plant productivity and health (10). As such, microorganisms create critical linkages within circular biological systems.

Stable populations of nitrifying bacteria are essential for both fish and plant growth, as they convert toxic ammonia into plant-available nitrate, a process primarily carried out by ammonia-oxidizing bacteria (e.g., *Nitrosomonas*) and nitrite-oxidizing bacteria (e.g., *Nitrobacter*) (104). Their abundance is closely tied to environmental conditions such as pH, light, and solids retention (12), making system configuration crucial for sustaining their populations. In parallel, PGPBs contribute to plant growth through a range of mechanisms, including nitrogen fixation, phytohormone production (e.g., indole-3-acetic acid), siderophore release to improve micronutrient availability, and antagonism against plant pathogens (105). Several genera commonly found in aquaponics, such as *Bacillus*, *Azospirillium*, *Rhizobium*, and *Pseudomonas*, are well-documented for their PGPB traits (106). The effectiveness of PGPB depends on their

adaptability to environmental changes and competitiveness within diverse microbial communities (107). Factors such as plant traits, nutrient levels, flow regime, hydroponics type, and light intensity influence their colonization (108). Conversely, the accumulation of microbial sludge can create favorable conditions for the proliferation of plant pathogens, including bacteria, fungi, and parasitic nematodes (109). Pathogenic fungi such as *Pythium* spp. and *Fusarium* spp., as well as nematodes like *Pratylenchus* and *Xiphinema*, are known to thrive in moist, organic-rich environments, conditions commonly found in aquaponic sludge zones (110). These organisms can spread rapidly through recirculating water, increasing the risk of root rot, stem cankers, and wilt diseases across the system (111). Moreover, the presence of sludge, organic matter, and low oxygen can lead to waterborne pathogens, such as *Ralstonia*, *Phytophthora*, and *Pythium* (112). Therefore, characterizing the functional microbiome within sludge and identifying the environmental and operational factors that shape its composition is critical for mitigating disease risk and promoting beneficial microbial activity. Among these factors, process design plays a pivotal role in determining microbial structure and distribution within biofloc and recirculating aquaponic systems.

Key parameters such as hydraulic retention time (HRT), solids retention time (SRT), and water flow patterns directly influence microbial colonization and community dynamics (13, 14). Common system arrangements in aquaponics include coupled operation and decoupled operation (45) which influence HRT and SRT in aquaponics compartments. In coupled systems, where water circulates continuously between the fish and hydroponic units, the SRT in the fish tank is typically lower due to more frequent solid filtration (113). Such systems undergo near-continuous biological filtration and have higher water clarity. In contrast, decoupled biofloc systems, which involve linear flow from the fish tank to the hydroponics bed and typically feature less frequent water

transfer to the grow bed, tend to exhibit higher SRT and greater mixed liquor suspended solids (MLSS) in the fish tank (113). These differences can significantly alter the microbial loading and accumulation patterns across compartments, including fish tanks, clarifiers, and grow beds, potentially fostering distinct microbial consortia between coupled and decoupled systems (16). Light exposure represents another important variable influencing microbial community composition, with past work showing benefits to fish production (113). Illuminated environments can favor the proliferation of photoautotrophic organisms, such as algae and cyanobacteria, which can shift nutrient dynamics and potentially outcompete or suppress other microbial groups (20).

Several studies have explored microbial community dynamics in aquaponic systems, but these studies focused on comparisons among compartments within a single aquaponics configuration. For instance, Schmautz et al. examined microbial diversity across system compartments at the phylum level and found that the aerobic and anaerobic loops influenced bacterial composition in distinct areas of the system (114). Similarly, Ruiz et al. investigated the microbiome in a coupled aquaponic system and reported that biofilms in the hydroponic bed and biofilter formed distinct clusters compared to suspended bacteria in the water column (9). However, the role of system design in shaping microbial communities remains poorly understood. No study has systematically compared how coupled recirculating aquaponics and decoupled biofloc aquaponics system configurations influence the composition of beneficial and harmful microbes and their downstream effects on plant performance. Moreover, no study has simultaneously investigated the impact of allowing natural light penetration into fish tanks (versus covering them to block light) on microbial community structure in aquaponics. This is noteworthy because all of the above techniques have been employed in aquaponics systems in past work (45) but without comparative assessment of microbiomes and associated impact on performance.

Understanding how system configuration and light exposure influence functional microbial groups, such as nitrifiers, PGPBs, and pathogens, is critical for optimizing system productivity and stability. Design choices alter habitat conditions that shape microbial dynamics, affecting nutrient cycling, plant–microbe interactions, and disease risk. These insights can guide producers in selecting configurations that support beneficial microbes, reduce disease risk, and enable microbiome engineering for more resilient bioponic systems. Therefore, the objective of this study was to investigate functional microbial communities associated with plant growth in four aquaponic system configurations: dark-coupled (DC), light-coupled (LC), dark-decoupled biofloc (DD), and light-decoupled biofloc (LD). The decoupled system operation bears many similarities to bioponic systems in general, broadening the implications of this work. It was hypothesized that system configuration would significantly alter the microbial community structure in the plant grow beds and fish tanks. Focus was given to functional microbial groups pertinent to plant health and yield. While fish production performance was monitored, those results are not included here and are available in a previous publication (113).

3.2 Materials and Methods

3.2.1 Experimental design

This study was designed to evaluate how aquaponic system configuration, specifically, the interaction between water flow regime and light exposure, affects the structure of microbial communities critical to plant health. A full-factorial experimental design was employed, incorporating two main factors: (1) system type (coupled vs. decoupled) and fish tank light exposure (light vs. dark). This resulted in four treatment combinations: the previously defined DC, LC, DD, and LD conditions. Each treatment was replicated three times in a randomized complete block design at the E.W. Shell Fisheries Station in Auburn, Alabama. Tanks in the “dark”

treatments (DC, DD) were painted and covered with black fabric to block light. In the "light" treatments, tanks were uncovered and their semi-transparent plastic walls allowed for sunlight penetration. A summary of outdoor and greenhouse environmental conditions, including temperature, humidity, and photosynthetic photon flux density (PPFD), is presented in the supplementary information (Figure S3.1). Additional details on greenhouse operation are described in a prior study (115). The photoperiod in Auburn, Alabama, during the experimental period (March–December) ranged from approximately 10 hours in spring and fall to about 14 hours in summer. Figure 3.1 illustrates the layout and flow of coupled (LC, DC) and decoupled (LD, DD) aquaponics systems.

3.2.1.1 Coupled aquaponics configuration

In the coupled systems, wastewater from the 700 L fish tank was pumped to the grow bed on a 30-minute interval cycle (30 min on, 30 min off) at a flow rate of 9 $L \cdot min^{-1}$, resulting in a HRT of 2.5 hours. Each system featured a 1 m^2 media-based hydroponic grow bed filled with pea gravel (particle size: 0.5–1.5 cm) as the root-zone substrate. The water depth in the grow beds was maintained at 12 cm, and an ebb-and-flow irrigation configuration was implemented using a timer to control drainage and re-flooding cycles. Before entering the grow bed, water passed through a 110-L radial flow settler (RFS) with an HRT of around 25 min to separate solids. Clarified water exited from the top, while sludge was discharged from the bottom twice per week. To compensate for water loss due to evaporation and sludge removal, fresh water was replenished twice weekly. Freshwater was sourced from the Auburn municipal supply, held in an open-top reservoir for 24 hours to allow dechlorination, and tested using on-site strips to ensure chlorine was undetectable before use. An aerator (40 $L \cdot min^{-1}$) maintained dissolved oxygen (50) levels near 7 $mg \cdot L^{-1}$ in the fish tank.

3.2.1.2 Decoupled aquaponics configuration

The decoupled aquaponics systems were operated as biofloc systems in light of a recent publication pointing to the benefits of this approach (45). Water was pumped from the fish tank to the RFS and then into the grow bed twice daily for 3 minutes, with each cycle moving 25 L. This resulted in a prolonged HRT of 14 days in the fish tank, which supported the development of dense bioflocs necessary for sustaining nitrification. Freshwater was added daily to maintain the 700-L tank volume. Water drained from the grow bed into a 70-L sump (HRT = 1.5 h), where a secondary pump recirculated it to the hydroponic bed eight times daily (10 minutes per cycle at 9 $L \cdot min^{-1}$) to hydrate plant roots and improve nutrient uptake (113). In the decoupled systems, lack of water recirculation necessitated the use of a higher-capacity aerator (80 $L \cdot min^{-1}$) to maintain adequate dissolved oxygen levels (7.0 $mg \cdot L^{-1}$) in the fish tanks. Sludge was discharged from the clarifiers in the same manner as in the coupled systems, twice per week from the bottom outlet.

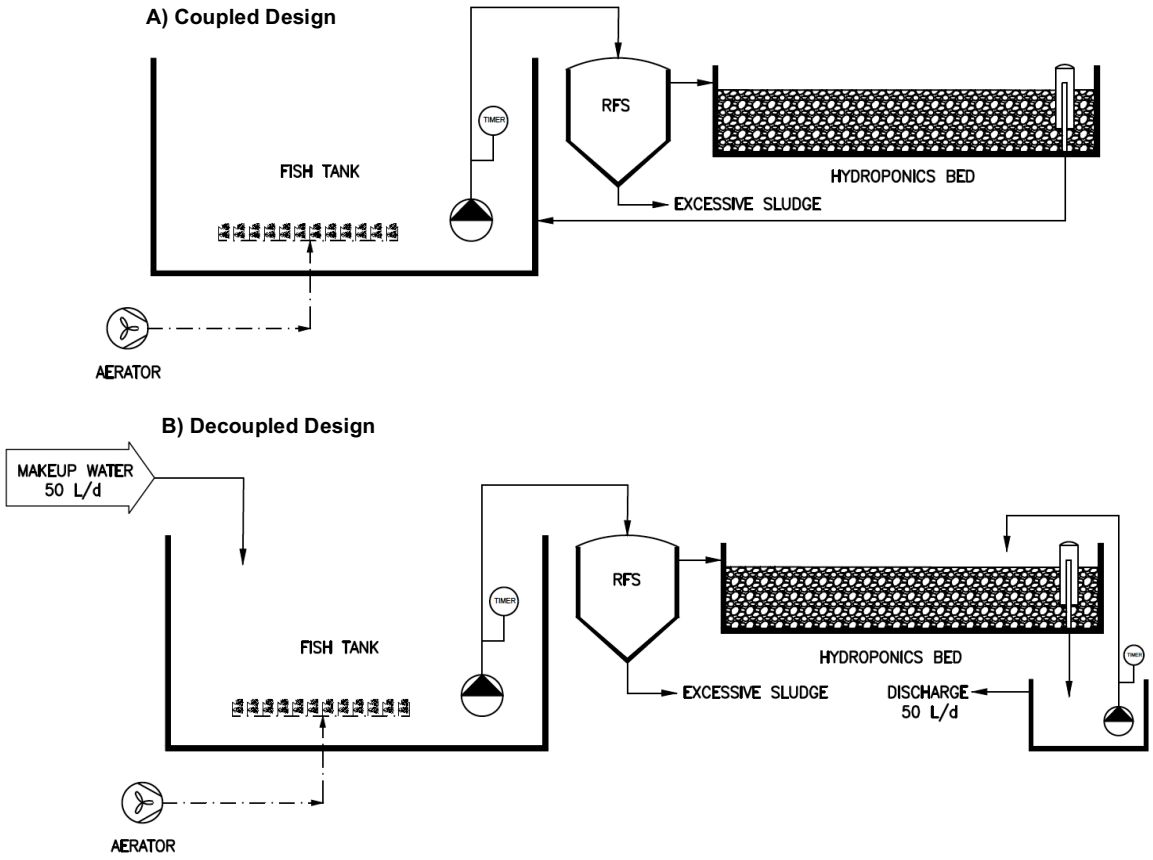

Figure 0.1 Process flow diagram of A) coupled and B) decoupled biofloc aquaponics operation.

3.2.2 System operation

The systems were operated from March to December, enabling a Nile tilapia grow-out from 130 g to over 400 g weight. The systems were inoculated with microorganisms sourced from the station's existing tilapia raceway, followed by eight months of grow-out for fish production. The pH was maintained near 7 through daily additions of 3 M hydrochloric acid or calcium carbonate (113). Tilapia were fed Cargill Triton-3603 feed (36% protein, 6% fat, 4% fiber, 1% phosphorus) twice daily with feed offered at a rate of 1.5% of body mass. However, in some systems, fish had low feeding enthusiasm, resulting in lower amounts of feed consumed as described in the results. Potassium, which is commonly deficient in aquaculture systems, was supplemented daily through

the make-up water to maintain a target concentration of 100 mg L^{-1} in the fish tanks. Each fish tank was stocked on March 11th with 40 Nile tilapia fingerlings (~130 g), sourced from the station's raceways, at an initial average stocking density of 8 kg m^{-3}. Fish were grown to market size (~430 g), reaching an average density of 17 kg m^{-3}, and harvested on November 20th. In September, when stocking density exceeded 20 kg m^{-3}, a portion of the fish was removed to lower the density to ~14 kg m^{-3}. This adjustment was based on reports suggesting an optimal stocking density of ~13 kg m^{-3} for biofloc aquaponics and to reduce potential health risks from elevated biomass and total solids, particularly in the LD systems where a mass mortality event occurred during the final month of the first year, as reported previously (113). All animal work complied with Auburn University's Institutional Animal Care and Use Committee (IACUC protocol #22-4099).

Two cherry tomato production trials were conducted over the 9 month period: Spring (March 15–June 27) and Fall (July 25–November 14), using *Favorita F1* seedlings (Johnny's Selected Seeds, USA), with five *Favorita F1* plants per bed. Cherry tomato seeds were sown in seedling trays and germinated under controlled greenhouse conditions. After approximately five weeks, when seedlings reached the 4–5 true leaf stage, they were transplanted into the hydroponic grow beds. Plants were spaced evenly to ensure uniform light exposure and root zone space. Throughout the cultivation period, plants were manually pruned every week to remove axillary suckers and maintain a single-stem growth habit, which improves airflow and fruit quality. Ripe fruits were harvested twice weekly, and fresh weight was recorded at each harvest to monitor total fruit yield.

Microbial profiles were analyzed in fish tanks, clarifiers, and hydroponics beds over this timeframe, with a focus on three functional groups essential to plant health: nitrifiers, PGPBs, and

plant pathogens/parasites. Understanding the dynamics of these groups is critical for microbial management and the development of resilient bioregenerative food systems.

3.2.3 Water quality and solid measurements

Total suspended solids (TSS) in fish tanks were measured every other day using optical density (OD) at 550 and 680 nm. Suspended solids were centrifuged (4696 × g, 10 min), oven-dried, and weighed to develop a TSS–OD calibration curve following Bertrand-Krajewski (116). At the end of each tomato trial, sludge accumulation in grow beds was measured by collecting three gravel sample columns per bed, rinsing and drying them to quantify total solids. Daily pH readings were taken in the fish tank with a Bluelab Metcombo meter, and pH was adjusted as needed. DO and temperature were recorded every other day using a Milwaukee MW600 portable DO meter.

3.2.4 Nutrient analyses

To monitor nutrient trends over time, water samples were collected from fish tanks every other day across all treatments, filtered through 0.2 μm nylon microfiber filters (VWR, USA), and stored at –20°C. Nitrate, nitrite, and phosphate were measured via HPLC (Shimadzu Prominence, Kyoto, Japan) using an anion exchange column (Dionex AS22) and ion suppressor (Dionex AERS 500). Ammonium and potassium were measured using cation exchange chromatography (Dionex CS16 column with CERS 500 suppressor) as described previously (113). To assess nutrient sufficiency, middle leaflets from mature tomato leaves were collected at the end of each trial, oven-dried at 60°C, digested in nitric acid, and analyzed via ICP-OES spectroscopy. The analysis included sulfur (S), phosphorus (P), potassium (K), calcium (Ca), magnesium, manganese (Mn), iron (117), boron (B), copper (118), zinc (Zn), sodium (119), and molybdenum (Mo). Total nitrogen (120) was analyzed separately at the same laboratory using an Elementar Vario Max total combustion analyzer. Results were compared to sufficiency ranges from the Plant Analysis Handbook v3

(121). Grow bed sludge and water nutrient concentrations were also analyzed once per trial by ICP.

3.2.5 Plant yield measurements

Ripe tomatoes were harvested regularly throughout each trial, and their weights were recorded to calculate the cumulative yield for each growing season. Each grow bed, planted with five tomato plants, was treated as an experimental unit (n=3 per treatment). At the conclusion of each trial, all plants were removed, and their fresh shoot mass was measured. Both total yield and shoot mass were normalized on a per-plant basis by dividing the values by the number of plants in each grow bed.

3.2.6 Siderophore activity detection

Water samples from hydroponic beds were centrifuged (4696 × g, 10 min), filtered (0.22 μm), and stored at –80°C. Siderophore activity was quantified using the Chrome Azurol S assay (122) by mixing 1:1 with CAS reagent and measuring absorbance at 630 nm. A 15 μM deferoxamine mesylate (Sigma) standard was used as the positive control.

3.2.7 Microbial sampling

Biomass pellets for microbial community analysis were collected from the fish tanks at three time points (May 13 (spring trial), June 20 (summer), and October 23 (fall trial)), from the hydroponics grow beds at two time points (May 13 and October 23). Sampling time points were selected to capture microbial community shifts across two tomato production trials (spring and fall). An additional sampling of the clarifier (RFS) was conducted in the fall when microbial communities had stabilized to provide insight into sludge-associated populations. To further investigate the cause of elevated ammonia levels in the decoupled systems, an intermediate fish tank sample was

collected during the summer to assess potential disruptions in nitrifier abundance. Fish tank solid samples were collected by filtering 13 mL of water from each tank, followed by centrifugation at 4696 × g for 10 minutes. The supernatant was decanted, and the resulting biomass pellet was stored at −20 °C. Clarifier sludge samples were collected from the bottom outlet of the RFS during routine sludge discharge. Grow bed sludge samples were obtained by excavating the gravel media to access the accumulated sludge around the roots, mixing it with grow bed water, and collecting the resulting slurry. All clarifier and grow bed samples were processed using the same centrifugation and storage method as described for the fish tank samples.

3.2.8 Microbial analyses

Microbial community analysis was conducted by extracting DNA from biomass pellets collected from the fish tanks, hydroponics grow beds, and from the RFS. DNA extraction was performed using the FastDNA Spin Kit (MP Biomedicals, USA), and concentrations were quantified using the QuantiFluor dsDNA Quantification Kit (Promega, USA) to ensure sufficient yield for sequencing. Samples were submitted to the Molecular Research Laboratory (MRDNA Lab, Texas, USA) for high-throughput sequencing of the 16S rRNA gene (primers 515F–806R) and 18S rRNA gene (primers 1391F and EukBr) on an Illumina MiSeq platform. Sequencing data were processed using the facility's bioinformatics pipeline, which included demultiplexing, denoising, and taxonomic assignment to zero-radius operational taxonomic units (ZOTUs) based on an in-house curated database. The resulting FASTQ files have been deposited in the NCBI Sequence Read Archive (SRA) under BioProject accession numbers PRJNA1333965 and PRJNA1335545. To identify functionally relevant microorganisms, species-level data from the 16S and 18S rRNA sequencing were annotated for putative plant growth-promoting bacteria (PGPBs), putative fungal and bacterial pathogens, and parasitic nematodes. For identification of putative PGPBs, a two-step

strategy was used: species were first matched against curated databases, including PLaBAse (123) and an internal Auburn University database (124), using automated text comparison tools to assist in word matching. Genera known to contain PGPBs were then screened, and all detected species within those genera were manually reviewed through targeted literature searches. Only species with peer-reviewed evidence of PGPB activity were retained. A similar strategy was used to identify potential pathogens, using multiple reference sources including BacDive, Phytopath, HealthyHydroponics, Nemaplex, and the EPPO Global Database (125-130). Species present in the dataset were cross-referenced at both the genus and species levels to confirm their relevance to plant health. Given the inherent uncertainty in species-level assignments, representative sequences of critical microbial taxa were re-evaluated using the NCBI BLASTn database to validate their taxonomic identity based on percent similarity and e-value.

3.2.9 Statistical analyses

Each treatment was replicated across three independent aquaponics systems (n = 3), resulting in a total of 12 independent systems. Data on tomato yield and microbial abundance were analyzed using multiple regression in R (v4.3.1), with fish tank light penetration and system configuration (coupled vs. decoupled) treated as fixed factors, and sampling time treated as a random factor (for time course measurements). Microbial abundance data were log-transformed to reduce variance and improve the normality of residuals prior to analysis. Non-metric multidimensional scaling (NMDS) based on Bray–Curtis dissimilarity was used to visualize microbial community structure across compartments, while permutational multivariate analysis of variance (PERMANOVA) was performed to statistically evaluate differences in microbial composition across treatments and compartments. Time-course ANOVA and Tukey's HSD test were conducted using the "car" and "agricolae" packages to evaluate treatment effects on tomato yield, nutrient concentrations, and

microbial abundance ($p < 0.05$). Descriptive statistics, including averages and standard deviations, were calculated in Microsoft Excel.

3.3 Results and Discussion

3.3.1 System coupling supported tomato growth and plant nutrient status

Tomato growth appeared to be influenced not only by nutrient concentrations in the water but also by differences in sludge nutrient content, particularly the higher availability of micronutrients in the grow bed sludge. As illustrated in Figures 3.2A and 3.2B, the coupled systems consistently outperformed the decoupled systems in both tomato yield and shoot biomass during the spring trial, with increases of 15% and 30%, respectively ($p = 0.039$ and $p < 0.001$). Leaf tissue analysis and nutrient profiling of the water during the spring season indicated that nitrate, phosphate, potassium, and calcium were generally at sufficient levels across all treatments, suggesting that major macronutrients were not growth-limiting (Figure 3.3 and Figure S3.3). In contrast, while boron, iron, manganese, and copper levels were within sufficiency ranges in the coupled systems, iron and manganese were deficient in the decoupled systems due to reduced concentrations in the sludge, as shown in Figure 3.4C, F. This micronutrient imbalance likely contributed to the reduced shoot biomass and fruit yield observed in the decoupled configurations, as both iron and manganese are essential for chlorophyll biosynthesis, photosynthesis, and enzyme activation (131). Although the performance gap between systems was modest in the spring, it became more pronounced in the fall. During this period, the decoupled biofloc systems, particularly the LD treatment, exhibited noticeably poorer plant growth (Figure 3.2C, D). At the early stage of the fall trial, decoupled systems faced additional stress from elevated ammonia levels and unstable nitrification, as shown by ammonium spikes and reduced nitrate levels in Figure S3.2B, C (see also Section 3.3.4 for more detail). These conditions likely imposed physiological stress on the

plants, resulting in apical bud necrosis and plant mortality in the decoupled systems (Figure S3.6). Tomato plants are particularly sensitive to ammonium, especially under alkaline conditions, and several studies have emphasized that ammonium toxicity is closely linked to the balance between ammonium and nitrate concentrations in hydroponic nutrient solutions (132). The affected plants were subsequently replaced with new transplants.

On the other hand, macronutrient availability (nitrate, phosphate) was significantly higher ($p < 0.001$) in the coupled systems than in the decoupled systems due to accumulation of these nutrients in the recirculating systems over time (Figure S3.2) (113). Although LC and DC systems performed similarly in the spring trial, the DC systems performed exceptionally well in the fall trial, producing nearly 3,500 g of fruit per plant, exceeding the performance of all other systems ($p < 0.01$). There is a paradigm that algal growth in aquaponics (supported by light penetration into fish tanks) deprives plants of nutrients. However, the data do not support this explanation for the exceptional tomato growth observed in the DC systems during the fall trial. Nitrate and phosphate levels in the LC and DC systems were nearly identical (Figure S3.2). Moreover, leaf tissue analysis of plants shows that the LC system tomato plants had equivalent or higher levels of nearly every major nutrient when compared to the DC systems (Figure 3.3 and Figure S3.3). This suggests that other factors are at play and will be further discussed along with the microbial community data in section 3.3.3.

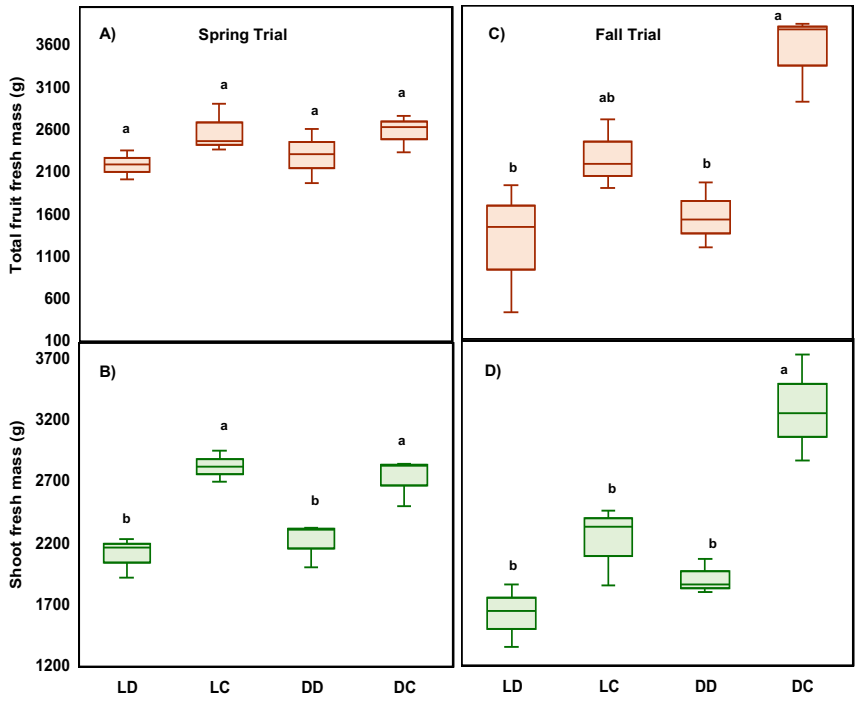

Figure 0.2 Cherry tomato plant productivity across the four treatments: (A) cumulative fresh fruit mass, (B) shoot wet mass during the spring trial (Spring: March 15th to June 27th), (C) cumulative fresh fruit mass, (D) shoot wet mass averages per plant during the fall trial (Spring: July 25th to November 14th). Lowercase letters (a, b, c, etc.) indicate statistically significant differences between treatments ($p < 0.05$). Figures without letters were not statistically different from the others.

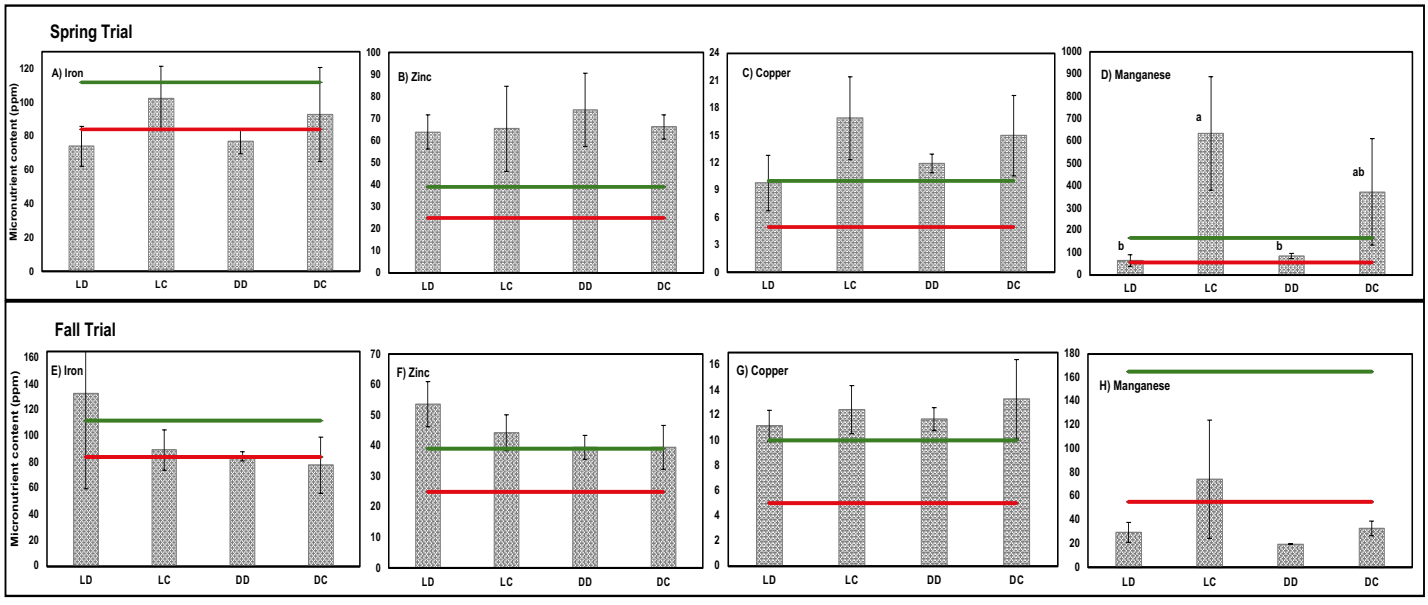

Figure 0.3 Micronutrient contents of leaf tissue measured during the spring and fall trials across the four treatments: (A), (E) iron, (B), (F) zinc, (C), (G) copper, and (D), (H) manganese. The red and green lines represent the minimum and maximum thresholds of the sufficiency range, respectively. Error bars represent standard deviation (n = 3).

Lowercase letters (a, b, c, etc.) indicate statistically significant differences between treatments ($p < 0.05$). Figures without letters did not have treatments that were statistically different from each other.

3.3.2 Aquaponic sludge serves as a key nutrient reservoir supporting higher yields

Nutrient analysis of the grow bed sludge and water revealed that the sludge consistently contained higher concentrations of both macronutrients and micronutrients compared to the water column across both growing seasons (Figure 3.4). This trend was observed for nearly all measured elements, including calcium, magnesium, iron, zinc, copper, and manganese. Among the treatments, the coupled systems retained higher nutrient concentrations in the sludge than the decoupled systems. This can be attributed to two primary factors: (1) the coupled systems maintained overall higher nutrient levels in the fish tank water (113), and they exhibited greater sludge accumulation in the grow beds (Figure S3.4). The porous structure of the sludge, along with its high cation exchange capacity, enables it to retain substantial amounts of nutrients (133). These findings emphasize that nutrient availability in aquaponics is not solely dictated by the nutrient content of the water column but is also strongly influenced by the nutrient reservoir stored within the sludge. In particular, the sludge serves as a critical sink for micronutrients, such as boron, iron, and manganese, which are typically limited in aquaponic systems (134). However, these nutrients may not be readily available to plants, and microbial processes (such as siderophore and metallophore production) can enhance the bioavailability of iron and other trace elements within the sludge matrix. Interestingly, despite having some of the lowest sludge concentrations of iron, zinc, and copper, the LD system showed no signs of deficiency in these micronutrients during the fall trial (Figure 3.3E, F). In contrast, it accumulated high levels of zinc and iron in plant tissues, which may be attributed to elevated siderophore activity, enhancing their bioavailability.

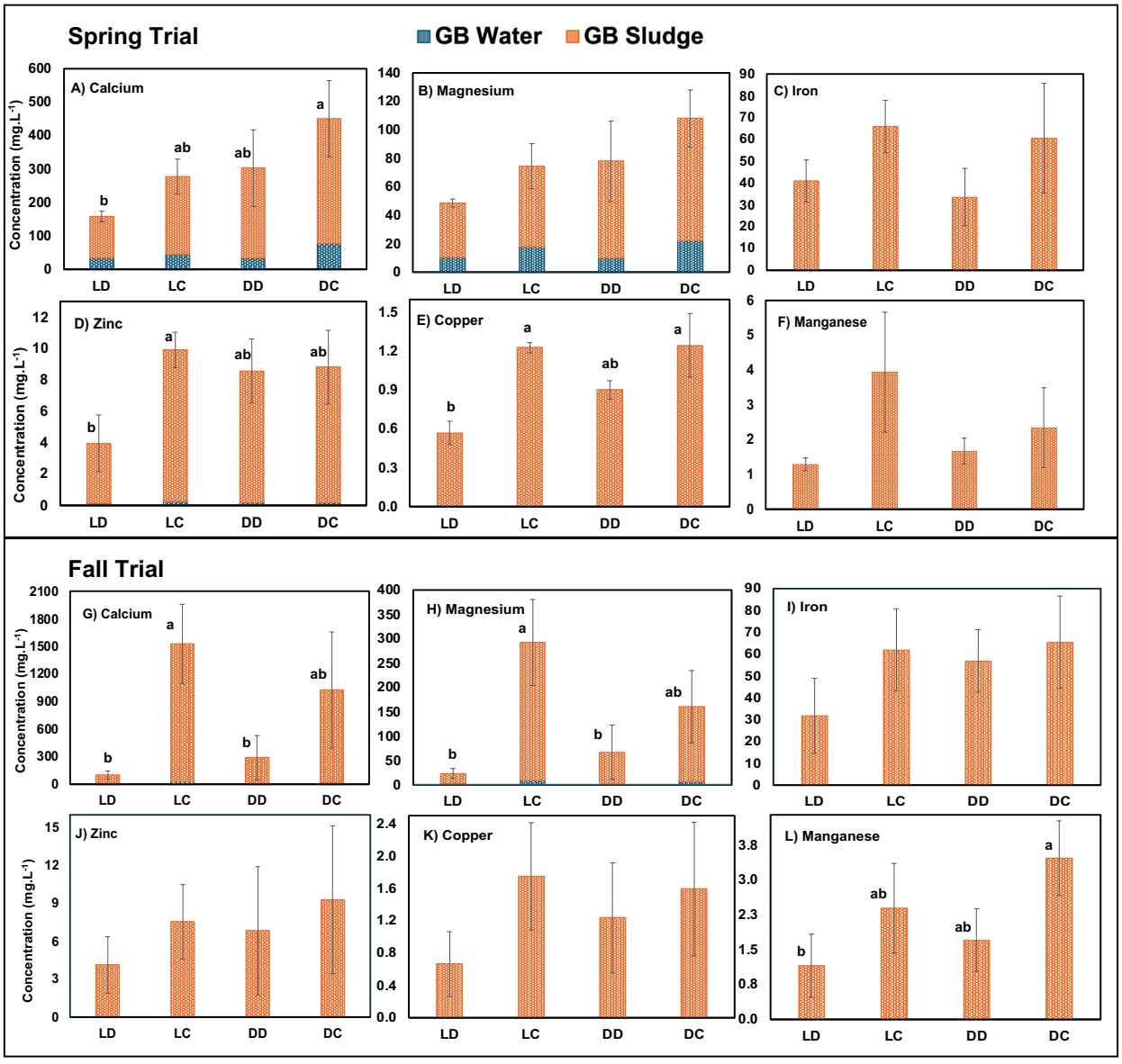

Figure 0.4 Nutrient contents of sludge and water in the grow beds during the spring and fall trial across the four treatments: 1) Light-decoupled (LD), 2) Light-coupled, 3) Dark-decoupled (DD), and 4) Dark-coupled (DC). Error bars represent standard deviation (n = 3). Lowercase letters (a, b, c, etc.) indicate statistically significant differences between treatments ($p < 0.05$). Figures without letters did not have treatments that were statistically different from each other.

3.3.3 System configuration impacted functional microorganisms abundance

Microbial communities play an important role in the transformation and availability of nutrients for plants. They can also cause harm in the form of pathogens. Consequently, analysis of major prokaryotic and eukaryotic communities was carried out. NMDS plots showed that prokaryotic

communities in the aquaponic system were shaped by both compartment and system configuration ($p < 0.001$ for both factors in PERMANOVA, Figure 3.5A, B). Microbial communities in grow beds were distinct from those in clarifiers and fish tanks, which showed more similar profiles, highlighting the influence of compartment-specific environments on community structure. Within each compartment, a clear separation was observed between coupled and decoupled systems. This separation became more pronounced by the fall trial, suggesting that microbial divergence increases over time as the systems mature. Across all compartments, grow beds harbored more diverse and richer prokaryote communities than clarifiers and fish tanks ($p < 0.001$), and the decoupled systems consistently exhibited greater diversity than the coupled systems ($p < 0.01$, Figure S3.5). Decoupled grow beds were dominated by Pseudomonadota (Proteobacteria), Acidobacteriota, and Planctomycetes, with higher relative abundance compared to the coupled systems (Figure 3.5C). Fish tanks and clarifiers were dominated by Fusobacteria and Pseudomonadota, with Pseudomonadota again more abundant in the decoupled systems. Members of Pseudomonadota are central to aquaponic microbial ecology. They include key nitrifiers such as *Nitrosomonas* and *Nitrobacter*, and plant growth-promoting rhizobacteria (PGPR) such as *Pseudomonas spp*., which can produce siderophores and antibiotics that protect tomato roots from pathogens (103). However, this group also includes potential plant pathogens, including *Ralstonia* and *Xanthomonas* (103). Planctomycetes, often found in low-oxygen niches such as sludge and biofilms, can contribute to nitrogen removal through anaerobic ammonium oxidation (anammox). However, there is no evidence of pathogenicity or direct symbiotic interactions with plants (114).

Eukaryotic community analysis showed that light-exposed systems, especially the LD system, had high relative abundances of Chlorophyta and Ascomycota across all compartments (Figure 3.5D). While the LC fish tanks had high levels of Chlorophyta (green algae) and

Ascomycota in the spring trial, these two phyla declined dramatically in the fall trial, such that the LC system more closely resembled the DC system with high levels of Ciliophora and Eukaryota. Decoupled grow beds had elevated levels of Chlorophyta, Ascomycota, and Streptophyta, whereas coupled systems had higher abundances of Nematoda, Rotifera, and Tardigrada. Chlorophyta commonly proliferate under high light and nutrient conditions and can contribute positively to aquaponic systems by assimilating excess nutrients or serving as fish feed or biofertilizer (135). Ascomycota include both beneficial and harmful fungi. Beneficial genera such as *Trichoderma* can promote tomato root growth and suppress disease through antibiotic and enzyme production (136).

In contrast, pathogenic Ascomycetes like *Fusarium oxysporum*, the causative agent of Fusarium wilt, and *Botrytis cinerea*, responsible for gray mold, can cause significant damage to tomato plants in warm, humid conditions (137). Nematodes also play diverse roles. Free-living (non-parasitic) nematodes enhance nitrogen availability by feeding on bacteria and fungi, promoting nutrient cycling. However, plant-parasitic species such as *Meloidogyne* (root-knot), *Xiphinema* (root rot), and *Pratylenchus* (lesion) can damage tomato roots, leading to galls, lesions, stunted growth, and chlorosis (109). While only a small subset of nematodes are parasitic, their presence poses a potential threat under conducive conditions. *Rotifers*, found in higher abundance in coupled grow beds, are beneficial microfauna that graze on excess bacteria and organic particulates. They help maintain microbial balance and water quality and are considered indicators of a stable, well-oxygenated system. In wastewater biology, they are also known to stabilize organic waste and reduce sludge volume by preying on filamentous bacteria (138). Tardigrades (water bears), although present, pose no risk to plant health. These micro-animals feed on algae, bacteria, and occasionally plant fluids but do not target roots or cause damage, as they lack the

mass attack behavior seen in parasitic nematodes (139). Given that genera and species within the same phylum can have contrasting functions (ranging from beneficial to harmful effects on plant health), their abundance was further analyzed at the genus and species level (where possible) in subsequent sections to better assess their potential impact on plant growth.

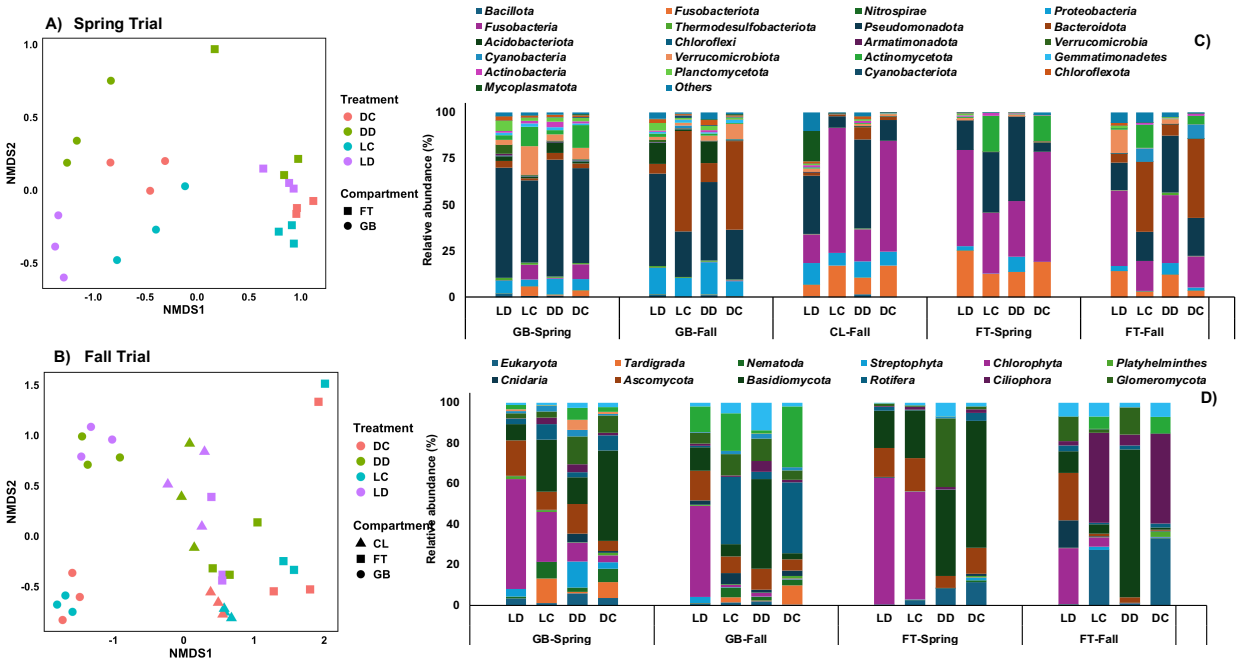

Figure 0.5 Microbial community structure across compartments and treatments. Non-metric multidimensional scaling (NMDS) plots illustrate microbial community composition in grow beds, fish tanks, and clarifiers (CL) across four treatments (light-decoupled (LD), light-coupled, dark-decoupled (DD), and dark-coupled (DC)) during (A) the spring and (B) fall trials. Relative abundance of dominant microbial taxa is shown at the phylum level for (C) 16S rRNA and (D) 18S rRNA gene datasets; phyla with less than 1% relative abundance are grouped as "Others."

3.3.4 Nitrifying bacteria

Nitrifying bacteria play a critical role in supporting plant growth by converting ammonia, a toxic byproduct of fish metabolism, into nitrate, a more beneficial form of nitrogen for tomato plants. In this study, nitrifier abundance (predominantly from the genus *Nitrospira*) was consistently higher in the grow beds than in the fish tanks across both coupled and decoupled systems (Figure 3.6A), highlighting the potential of media-bed hydroponics to function as effective biological

filters. In the coupled systems, recycling water from the grow beds allowed nitrification to occur within the grow bed media, extending the biological filtration beyond the fish tank. This distributed nitrification capacity enhanced ammonia removal and supported a more stable nitrogen cycle. In contrast, decoupled biofloc systems lacked this feedback loop, and nitrification activity in the plant bed did not provide benefits to fish (113). This made the systems more susceptible to ammonia accumulation in the fish tank, even though decoupled systems exhibited higher nitrifier abundance in the fish tanks ($p < 0.001$). Water in the decoupled biofloc fish tanks had significantly higher concentrations of ammonia-N compared to fish tank water in the coupled systems (Figure S3.2, $p < 0.001$). Moreover, pH in the decoupled systems was higher (6.8 ± 0.2) between June and September than in the coupled ones (6.5 ± 0.1, $p < 0.001$), increasing the concentration of free ammonia to detectable levels (0.2 $mg \cdot L^{-1}$). As a result, elevated ammonia concentrations were recorded between June and September, necessitating a reduction in fish feeding to prevent toxicity. This reduction negatively impacted fish growth and further limited the supply of nitrogen to plants. The LD system exhibited the most pronounced symptoms. Several tomato plants showed apical bud necrosis (main growing point) during early growth stages, with four plants in one replicate dying before fruiting (Figure S3.6A). In another replicate, one plant showed similar symptoms. Visual inspections of the roots and stems revealed no signs of disease, suggesting that the damage was likely caused by elevated ammonia toxicity and nitrogen deficiencies rather than pathogen infection. Similar symptoms, though milder and delayed, appeared during the fruiting stage in the DD systems, affecting two plants in one replicate (Figure S3.6B).

A seasonal decline in nitrifier abundance, especially during the summer months, likely contributed to the instability. Although a downward trend in nitrifier populations was observed in Figure 3.6B, the differences were not statistically significant, likely due to variability among

replicates. Interestingly, a concurrent decline in TSS concentration was observed during this period, which may have further contributed to the reduced nitrifier population (Figure S3.4). To mitigate the decline, a one-time re-inoculation was carried out in mid-September using fresh sludge from clarifiers, a method akin to activated sludge practice in wastewater treatment. This intervention improved nitrifier abundance and successfully reduced ammonia concentrations (Figure S3.2). Ultimately, the limited and unstable nitrification capacity in the decoupled systems necessitated reduced feed inputs as an operational strategy to prevent ammonia accumulation. The cumulative feed addition was lowest in the LD system (15,871 ± 2,020 g), followed by the DD (19,600 ± 527 g), LC (26,200 ± 1,207 g), and DC systems (26,550 ± 3,457 g). These differences were also driven in part by fish demand for food. This resulted in smaller fish and, consequently, poorer plant performance in the decoupled systems, with fruit yield and shoot biomass approximately half of those observed in the coupled systems ($p < 0.0001$) (Figure 3.2C, D). These findings underscore a key challenge in decoupled biofloc aquaponic systems, as challenges with nitrification in the fish tank have spillover effects on plants, even if robust nitrification (and nitrifying populations) are available in the plant grow bed.

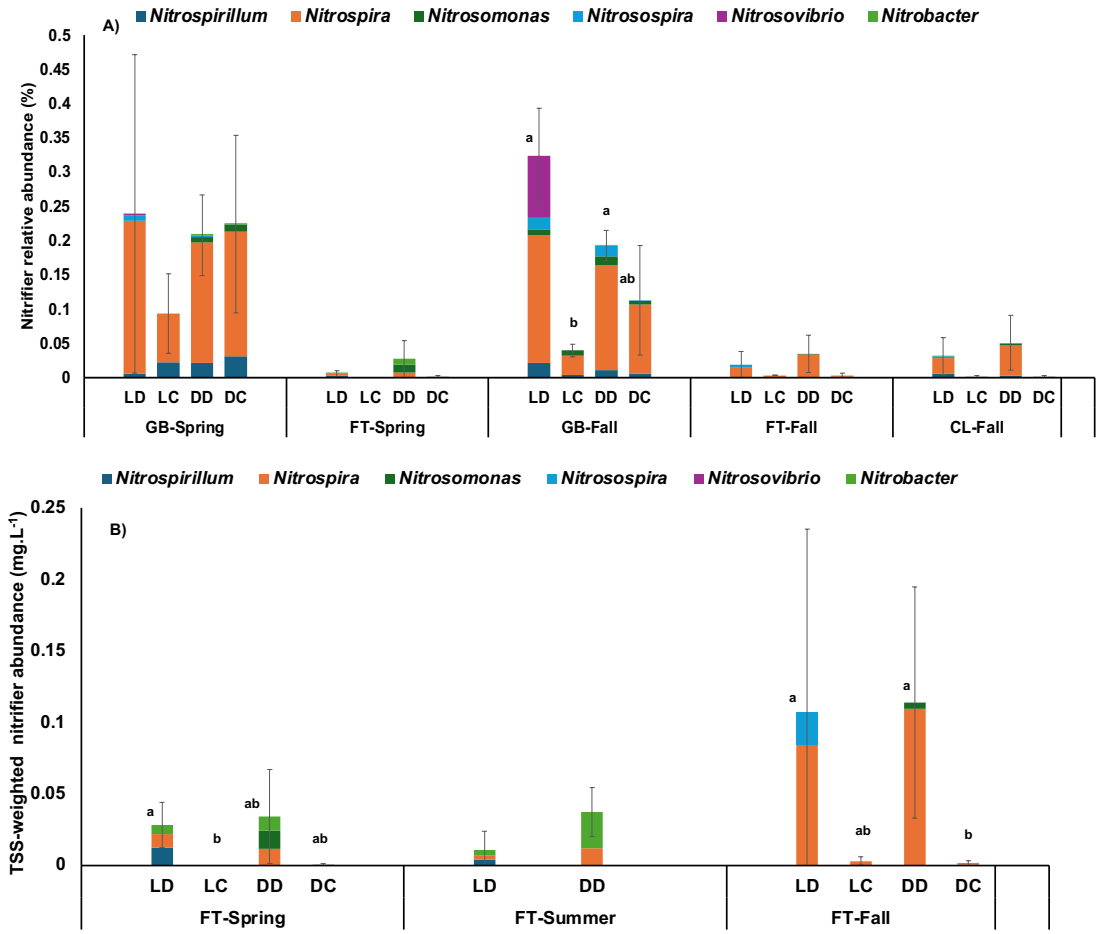

Figure 0.6 Relative abundance of nitrifying bacteria across treatments during the spring and fall trials. (A) The relative abundance of key nitrifying genera within compartments (fish tank (FT), grow bed, and clarifier (CL)) under the four system configurations: light-decoupled (LD), light-coupled, dark-decoupled (DD), and dark-coupled (DC). (B) Nitrifier abundance scaled to total suspended solids (TSS) levels in the fish tanks across three sampling time points: spring, summer, and fall. Error bars represent standard deviation (n = 3). Lowercase letters (a, b, c, etc.) indicate statistically significant differences between treatments ($p < 0.05$). Figures without letters did not have treatments that were statistically different from each other.

3.3.5 Plant growth-promoting bacteria

The distribution of putative PGPBs across treatments and compartments highlights the critical role of system design in shaping microbial communities. Media-based grow beds consistently supported higher putative PGPB abundance and diversity compared to the fish tanks, underscoring their favorable conditions for sustaining beneficial microbes (Figure 3.7A). *Bradyrhizobium guangdongense*, *Sinorhizobium americanum*, *Ensifer adhaerens*, and *Novosphingobium*

arabidopsis were among the most dominant PGPB across all treatments and compartments. Decoupling resulted in significantly higher putative PGPB levels compared to the coupled operation ($p < 0.0001$), with the LD system appearing to support the highest abundance. This trend was particularly evident in the fish tanks and clarifiers, suggesting that decoupled configurations provided more favorable conditions for the development of these taxa. Notably, decoupled systems exhibited higher abundances of *Bradyrhizobium guangdongense* and *Ensifer adhaerens*. *Ensifer adhaerens*, in particular, has been identified as a beneficial PGPB for tomato, enhancing crop vigor and resilience under various environmental conditions. Nevertheless, any potential benefits of these putative PGPBs in the decoupled systems were clearly outweighed by the higher ammonia levels, lower nitrogen inputs, and lower nutrient concentrations in both the water and the grow bed sludge (Figure 3.4) that limited plant growth. Still, it is possible that some of these putative PGPB organisms were recruited by plants to help mitigate some of the stress induced by lower nutrient levels in the decoupled systems (140).

Decoupled systems had higher abundance of potentially siderophore-producing bacteria ($p < 0.001$) in almost all compartments (with LD being the highest), dominated by *Streptomyces* (141) (Figure 3.7B), especially during the fall trial (>10x higher). Significantly higher abundance of these bacteria resulted in over 50% higher siderophore production in the decoupled versus coupled systems in the fall trial, based on a siderophore assay ($p = 0.043$) (Figure 3.7C, D). This microbially mediated siderophore activity may have had real benefits toward enhancing micronutrient availability to the tomato plants. Of particular interest, the leaf tissue analysis of tomatoes in the LD system had the highest nominal level of iron and zinc (Figure 3.3E, F) despite these same systems having the lowest levels of iron and zinc in the grow bed root zone (Figure 3.4 I, J).

Additionally, several other PGPBs with known biocontrol and growth-promoting properties for tomato were detected. *Bacillus mycoides* and *Bradyrhizobium japonicum* have demonstrated biocontrol activity against bacterial wilt and root-knot nematodes for tomato seedlings (142). *Delftia acidovorans* exhibits nematicidal activity against *Meloidogyne incognita*, a common tomato root-knot nematode (143). *Rhizobium etli* strain G12 has shown the ability to reduce nematode infection in tomato plants (144). *Paenibacillus graminis* is recognized for its plant growth-promoting traits, including phosphate solubilization and production of growth hormones, which can benefit tomato cultivation. *Pseudomonas gessardii* has been identified as a PGPB that supports tomato growth under biotic stress conditions (145). *Pseudomonas oryzihabitans* is known to promote tomato growth and acts as a biocontrol agent against root-knot nematodes, enhancing root immune responses (146). These findings suggest that sludge accumulated in grow beds or fish tanks of aquaponics systems can serve as a rich source of beneficial microbes, especially grow bed sludge from decoupled systems, and that this sludge may have commercial applications as biofertilizers. However, the high abundance of PGPBs in the decoupled systems did not translate into higher tomato yields, likely due to the influence of other limiting factors such as nutrient availability, nitrifier instability, and pathogen pressure (sections 3.3.1, 3.3.4, and 3.3.6).

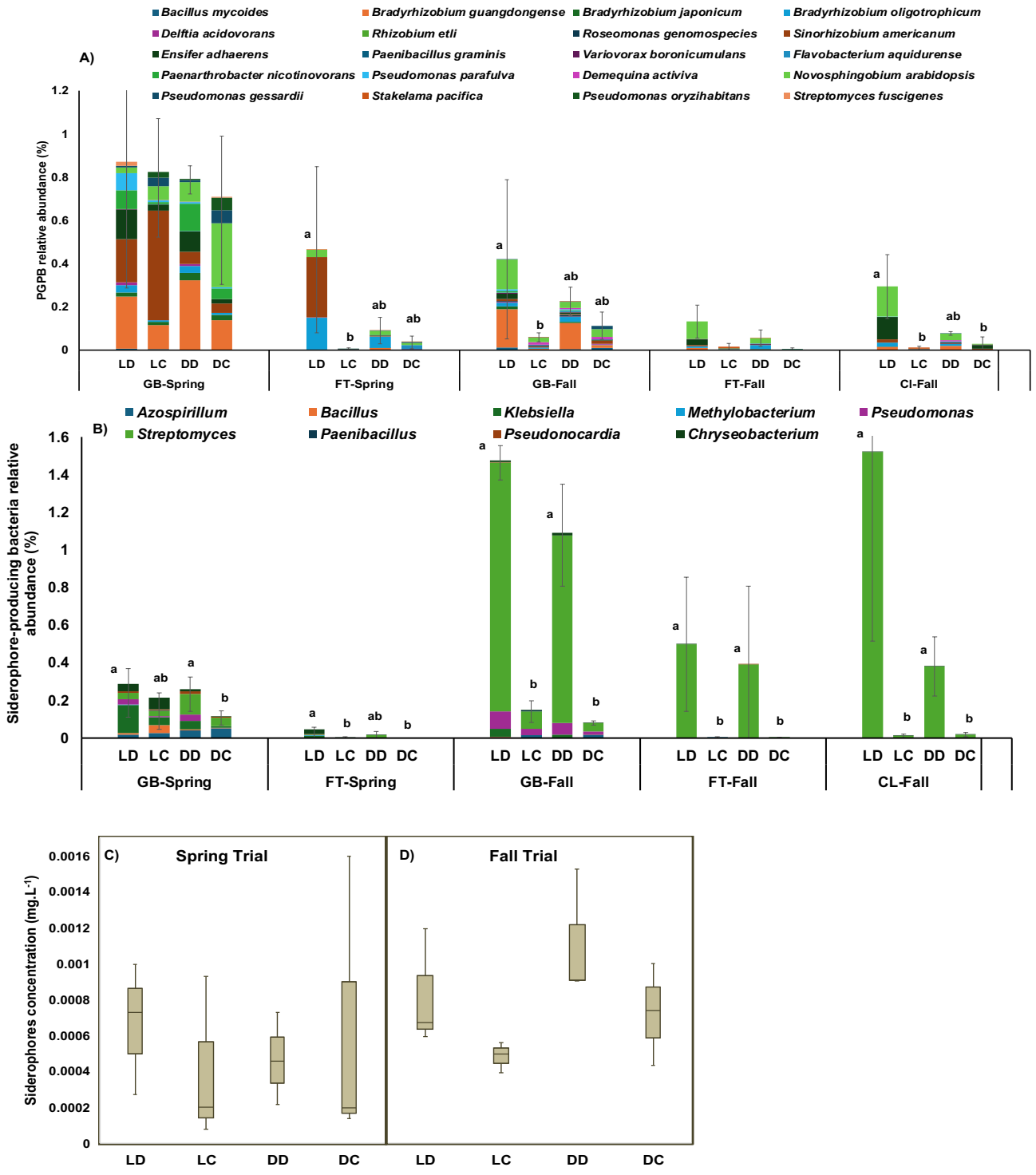

Figure 0.7 Relative abundance of (A) plant growth-promoting bacteria (PGPBs) at the species level and (B) siderophore-producing bacteria at the genus level across system configurations and compartments. (C), (D) Siderophore activity in the grow beds across the treatments during the spring and fall trials is shown in deferoxamine equivalents. Error bars represent standard deviation (n = 3). Lowercase letters (a, b, c, etc.) indicate statistically significant differences between treatments ($p < 0.05$). Figures without letters did not have treatments that were statistically different from each other.

3.3.6 Plant pathogens and parasites

The analysis of putative pathogenic microorganisms across treatments and seasons revealed a complex interplay of factors influencing tomato health in aquaponic systems. Among the potential bacterial pathogens, *Robbsia andropogonis*, *Burkholderia andropogonis*, *Xanthomonas oryzae*, and *Burkholderia dolosa* were predominant (Figure 3.8A). *Xanthomonas oryzae* is not recognized as a tomato pathogen and is primarily known as the causative agent of bacterial blight in rice (147). In contrast, *Robbsia andropogonis* (formerly *Burkholderia andropogonis*) is a foliar plant pathogen with a broad host range, causing leaf spots, streaks, and stripe diseases in various crops. While no reports currently confirm its pathogenicity in tomato, its demonstrated ability to infect new hosts warrants attention to its presence. Despite the presence of these putative pathogens, no statistically significant differences in bacterial pathogen abundance were observed across treatments, except during the fall, when coupled systems exhibited higher loads of putative bacterial pathogens ($p < 0.01$). As these same systems yielded better tomato plant growth and yield, this suggests that these organisms were either not harmful to the tomato or mitigated by other factors such as beneficial microbial populations, nutrient dynamics, and overall plant immunity.

Among the fungal pathogens, *Pythium graminicola*, *Synchytrium endobioticum*, *Didymella prosopidis*, and *Ustilago maydis* were the most abundant pathogenic fungi (Figure 3.8B). *Pythium graminicola* poses the most direct risk to tomato plants. To verify the species-level annotation, the representative sequence was subjected to BLASTn analysis against the NCBI database, yielding an e-value of 2×10^{-55} and 98.5% sequence identity. This indicates a close match to *Pythium graminicola*, though the sequence could potentially represent other *Pythium* species that are pathogenic to plants (148). This soil-borne oomycete is a known causal agent of damping-off and

root rot in tomato seedlings, especially under water-saturated conditions (148). Its high relative abundance in the DD system during the fall trial coincided with symptoms such as wilting, stunted growth, and low yield (Figure 3.2C, D, and Figure S3.6C), indicating a possible pathogenic impact. *Didymella prosopidis*, although not confirmed as a tomato pathogen, is taxonomically related to *Didymella lycopersici*, which may pose a risk of leaf, stem, and root disease in tomato (149). However, *D. prosopidis* was present at a very low relative abundance (<0.01%) in the systems, and this very low abundance was less likely to harm plants. *Synchytrium endobioticum* and *Ustilago maydis*, known pathogens of potato and corn, respectively, are not considered relevant to tomato pathology.

Nematode analysis revealed that *Plectus murrayi* was the dominant species in the grow beds, accounting for an average of 81% of the total nematode population across all systems. As a non-parasitic nematode, it is known to contribute positively to microbial balance and soil ecosystem health. Among parasitic nematodes, *Xiphinema rivesi*, *Xiphinema macroacanthum,* and *Pratylenchus crenatus* are of concern. *X. rivesi*, a dagger nematode, is capable of transmitting plant viruses and causing root damage in a variety of crops, including tomato (150) (Figure 3.8C). *P. crenatus is* often found alongside *P. penetrans* and belongs to the genus of root-lesion nematodes. It penetrates roots and disrupts nutrient and water uptake, infecting a broad host range that includes blueberry, carrot, potato, and tomato, which can lead to stunting and reduced yields (151). *Xiphinema macroacanthum*, though not specifically linked to tomato, belongs to a genus with several known tomato pathogens and may present a risk due to genetic similarity. Notably, coupled systems showed a significantly higher abundance of *X. rivesi* during the fall trial (p = 0.018). BLAST analysis of the representative sequence annotated as *Xiphinema rivesi* yielded 90.7% identity (e-value = 8×10^{-39}), indicating insufficient similarity for confident species-level

identification. Despite the high abundance of the parasitic nematodes in the coupled systems, only one replicate of the light-coupled system exhibited visible disease symptoms, including yellowing, wilting, and stunted growth (Figure S3.6 D), symptoms consistent with dagger nematode damage previously reported in tomato (152). This may have partially contributed to the lower tomato yields seen in the light-coupled system relative to the dark-coupled system. Notably, similar wilting was observed in the previous year's tomato trial in the light-coupled system as reported in a previous study (113). In that study, it was postulated that excess sludge accumulation in the grow bed led to oversaturation with water, resulting in root asphyxiation. Such an environment may have also been favorable to *Pythium* and *Xiphinema* pathogens, which may have exacerbated the wilting issue. As wilting issues have now been observed over two consecutive years of aquaponics tomato production, further research is being carried out to investigate the root cause of this issue in more detail.

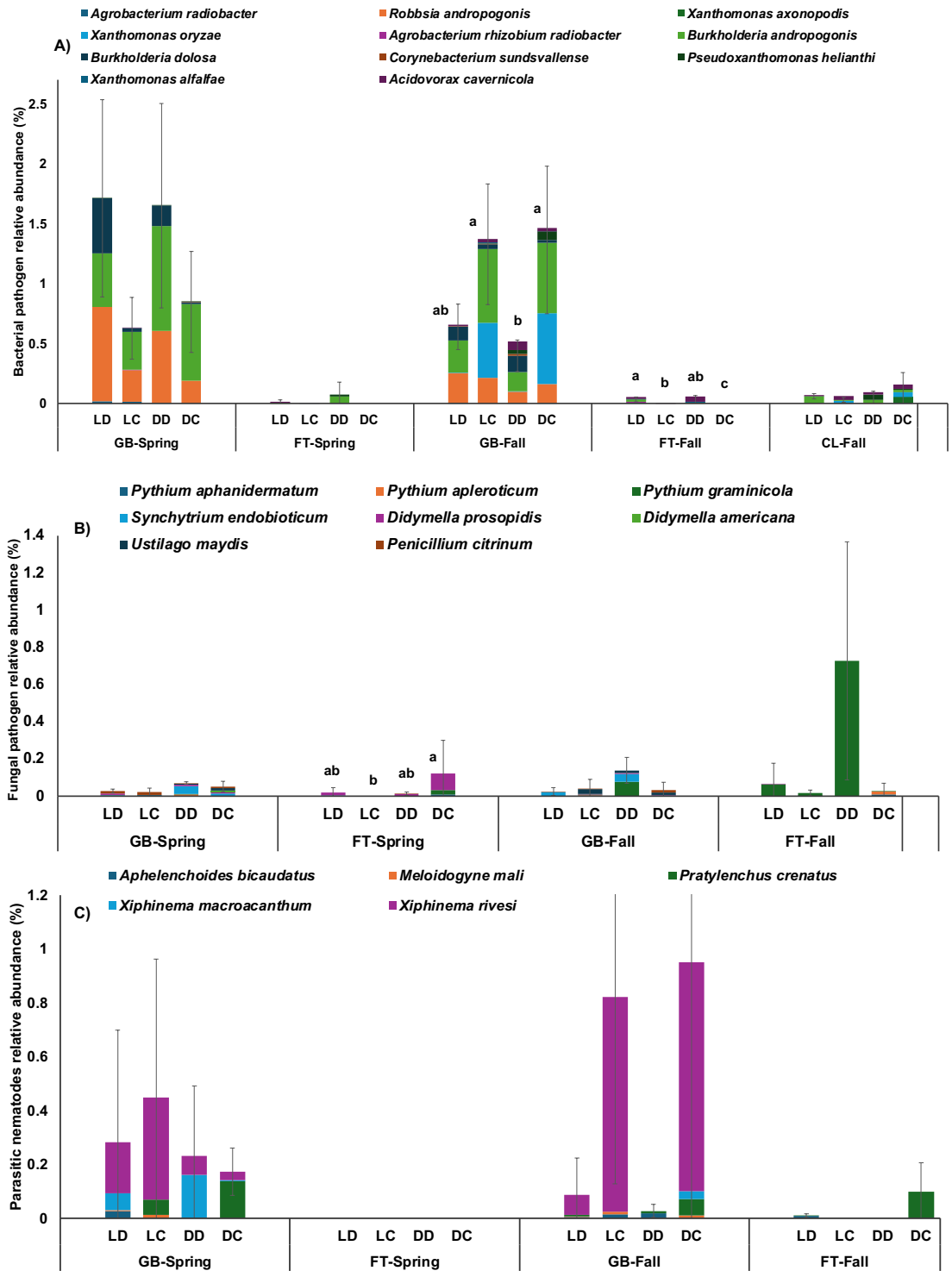

Figure 0.8 Relative abundance of key (A) plant-pathogenic bacteria, (B) plant-pathogenic fungi, and (C) parasitic nematodes at the species level across fish tank, grow bed, and clarifier (CL) compartments for each system design: light-decoupled (LD), light-coupled, dark-decoupled (DD), and dark-coupled (DC). Error bars represent standard deviation (n = 3). Lowercase letters (a, b, c, etc.) indicate statistically significant differences between treatments ($p < 0.05$). Figures without letters did not have treatments that were statistically different from each other.

3.3.7 Broader implications of the work

Decoupled aquaponics systems suffered from nutrient deficiencies in tomato plant tissue when compared to the coupled systems. That said, they offered higher abundance of putative PGPB including higher siderophore production than coupled systems. One of the advantages of decoupled systems is that their water can be augmented with nutrients with no effect on fish. Consequently, a targeted supplementation strategy for deficient nutrients like copper, manganese, and zinc could be undertaken. This can also enable operators to protect plants from upstream problems in the fish tank such as the situation that emerged in light decoupled systems in this experiment. Poor nitrification necessitated temporary feed reductions to protect fish, reducing nutrient availability to plants. Exogenous nutrient dosing could be used to overcome this issue.

The microbial processes that are essential to the function of aquaponics systems also extend to bioponics systems in general. With the exception of "tea methods" for producing bioponic solutions, all bioponic system types rely extensively on microorganisms to mineralize nutrients from organic wastes and oxidize nitrogen (153). Similar to the findings in this study, bioponic systems have been shown to harbor microorganisms with plant growth-promoting properties, including biocontrol of disease-causing organisms like *Pythium* (154). Like aquaponics, bioponics frequently suffers from nutrient deficiencies and imbalances (153), wherein nutrient-solubilizing microorganisms (e.g., siderophore producers) investigated in the present study could improve plant nutrient availability. Bioprocess design choices have likewise been shown to alter microbial activity, nitrification, and downstream plant health in bioponics systems (155). In the context of the present work, decoupled aquaponics is a true parallel to these other bioponic systems: waste enters, it is converted into forms suitable for hydroponic production, and then effluent exits the system. On the other hand, coupled aquaponics is unique among bioponic systems in that effluent

from hydroponics is recycled back into the aquaculture system. Nevertheless, this provides a unique case study for microbial dynamics in a self-contained circular biosystem with no direct environmental discharge.

3.4 Conclusion

This study demonstrated that bioprocess design significantly influenced the abundance and distribution of nitrifiers, PGPBs, and plant pathogens across aquaponic compartments. Microbial profiling revealed that hydroponic sludge hosted the most diverse communities and served as a key reservoir for both beneficial and harmful microorganisms, as well as essential nutrients. Coupled systems consistently exhibited higher nutrient concentrations in water and sludge across both growing seasons. Despite higher nitrifier abundance in the fish tanks of the decoupled systems, the lack of water recirculation led to elevated ammonia levels, lower fish growth, and consequently lower feed (nutrient) inputs to the system. In contrast, the closed-loop design of coupled systems maintained more stable nitrification and higher nutrient retention in the system. Possibly in response to the lower-nutrient environment, decoupled grow beds supported greater abundances of PGPBs and siderophore-producing bacteria, with the light-decoupled system showing the highest level (though not significantly higher than the dark decoupled system). However, these potential microbial benefits could not fully compensate for the nutrient deficiencies and ammonia stress of decoupled systems, resulting in significantly lower tomato yields. Eukaryotic pathogens such as *Pythium* and *Xiphinema* likely contributed to the wilting, yellowing, and stunted growth observed in the fall trial, particularly in the dark-decoupled and light-coupled system, possibly due to excessive sludge buildup. Long-term system monitoring showed that plant growth and yield in aquaponics are shaped by a complex interplay of microbial

and operational factors. Further research is needed to refine bioreactor designs that favor PGPB enrichment while suppressing pathogens and parasitic organisms.

Chapter 4: Physical and Microbial Root-Zone Factors Underlying Tomato Wilt in Long-Term Biofloc Aquaponic Systems

Physical and Microbial Root-Zone Factors Underlying Tomato Wilt in Long-Term Biofloc Aquaponics Systems

Authors: Shima Rezaei[1], Margaret Otto[1], Qichen Wang[1], Wellington Arthur[1], Deepak Shantharaj[2], Kelly Sullivan[1], Daniel Wells[3], Neha Potnis[2], Brendan Higgins[1]*

[1]Biosystems Engineering, Auburn University, Auburn, AL 36849, USA

[2]Entomology and Plant Pathology, Auburn University, Auburn, AL 36849, USA

[3]Horticulture, Auburn University, Auburn, AL 36849, USA

*Corresponding author:

Brendan T. Higgins

Department of Biosystems Engineering, 203 Corley Building, Auburn, AL 36849, USA

Phone: 334-844-3532

e-mail: bth0023@auburn.edu

Abstract

Biofloc aquaponics presents a sustainable approach to soilless crop production, but its long-term reliability is often compromised by root-zone disorders such as root rot and wilt. This study evaluated four media-based biofloc aquaponic designs over two years (encompassing two full fish production cycles and four tomato growing seasons) to investigate system failures, including plant wilting, necrosis, and the underlying physical and microbial stressors. In the first year, plant wilt was primarily linked to poor drainage and sludge accumulation in coupled systems, resulting in root-zone hypoxia and a 21% reduction in yield compared to decoupled systems. In response, system modifications were implemented in the second year, including the implementation of radial flow settlers upstream of filters and timer-controlled pumps, which improved oxygenation and solids management. These interventions reversed previous trends, significantly boosting yields in the coupled systems. However, wilting still occurred in a subset of plants during the second year. Root-zone analysis showed that wilted plants exhibited lower dissolved oxygen levels (65% lower) and trends toward higher relative abundance of potential pathogens and parasitic organisms (*Pythium graminicola* and *Xiphinema rives*). In contrast, healthy root zones were associated with greater abundance of plant growth-promoting bacteria (PGPB), particularly taxa with known biocontrol potential. These findings highlight the importance of maintaining oxygen-rich root environments and effective solids management to support long-term aquaponic productivity.

Keywords: Asphyxiation, Cherry tomato, Soilless production, Pathogen, PGPB

Graphical abstract

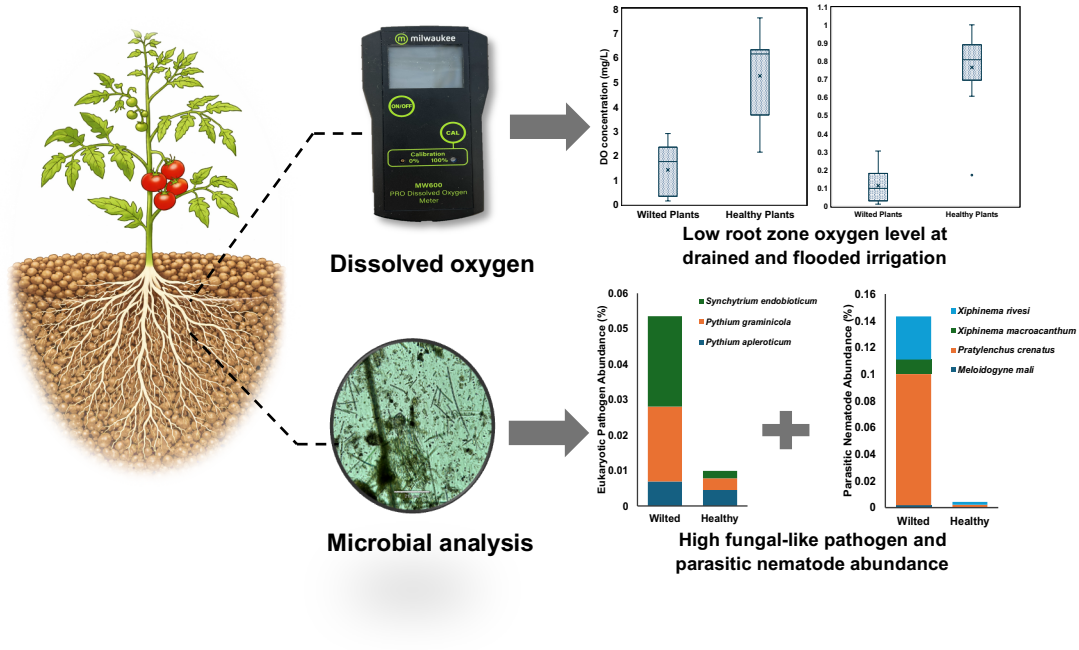

Highlights

- Tomato plant wilt and high biosolids were observed in the aquaponics grow beds
- Wilting plants had low stomatal conductance and root zone dissolved oxygen
- Wilting plants had a higher abundance of oomycetes and parasitic nematodes
- Use of radial flow separator helped coupled but harmed decoupled biofloc aquaponics

4.1 Introduction

For thousands of years, soil has supported agriculture by providing structural stability and hosting a rich microbial ecosystem essential for plant growth. However, rising global populations and increasing pressure on freshwater resources have driven the need for more sustainable and space-efficient food production systems. Soilless cultivation technologies, particularly hydroponics and aquaponics, have emerged as promising alternatives that reduce water use, recycle nutrients, and enable high-yield production in urban and land-constrained settings (5). Despite their environmental benefits and growing adoption, aquaponic systems continue to face challenges that limit their long-term reliability and scalability (156).

One of the most persistent issues is root stress, especially asphyxiation caused by prolonged waterlogging, insufficient oxygenation, and sludge accumulation in the root zone (29). Unlike soil, which provides aerated pore spaces for gas exchange, aquaponic grow beds can become oxygen-depleted over time, especially in media-based systems with high organic matter buildup. This can severely impair root respiration, limit nutrient uptake, and weaken plant immune responses (30). As reviewed by Garcia et al., hypoxia suppresses the expression of key defense-related genes, interferes with oxidative burst and structural barrier formation, and also disrupts the rhizosphere microbiome (31). Intermittent irrigation strategies such as ebb-and-flow cycles have been employed to enhance oxygen availability in the root zone, but their effectiveness remains highly dependent on substrate maintenance and the efficiency of solid waste removal (157). Maintenance of media-based grow systems is challenging in long-term crops such as the production of indeterminate tomatoes. Beyond direct physiological stress, high moisture and hypoxic conditions can shift root-zone microbial communities toward opportunistic pathogens, including Fusarium,

Pythium, Phytophthora, and other oomycetes and fungi, while also enabling parasitic nematodes to exploit stressed roots, further impairing water and nutrient uptake (158, 159). Infections by Pythium spp. are commonly associated with root browning, soft rot, and cortical degradation, leading to wilting and plant death, particularly under conditions of high moisture, organic loading, and elevated temperatures (32-34). Several aggressive species, such as P. graminicola, P. myriotylum, and P. aphanidermatum, have been frequently reported in hydroponic systems lacking optimal environmental control (35-37). Despite these challenges, the mechanisms underlying root-zone dysfunction in aquaponics remain poorly understood. Previous studies have reported inconsistent disease suppression outcomes, with aquaponic systems showing variable performance compared to hydroponics (110). Surveys of commercial operations in the United States and Europe further highlight persistent challenges in disease diagnosis and management, compounded by the dual-host nature of aquaponic systems (112, 137, 160, 161). Therefore, a clearer understanding of root-zone physical and microbial dynamics is needed to improve system reliability and long-term productivity.

To address these gaps, this study examined four media-based biofloc aquaponic system designs over two years, encompassing two full fish production cycles and four cherry tomato growing seasons. During system operation, wilting symptoms were observed in the fall trial of the first year, particularly in systems with higher fish densities and visible solid waste accumulation. These observations motivated a targeted investigation into the physical and microbial conditions of the root zone. In the second year, the system design was modified to improve solid waste removal and enhance root-zone oxygenation, including the installation of radial flow settlers for sludge separation and the use of timer-controlled pumps to maintain consistent ebb-and-flow cycles. This study aimed to identify the root-zone conditions contributing to plant wilt and reduced

yields in media-based aquaponics by monitoring dissolved oxygen levels and characterizing microbial communities in the rhizosphere of symptomatic and asymptomatic plants.

4.2 Materials and Methods

4.2.1 Experimental design

Figure S4.1 presents the four media-based biofloc aquaponic designs tested in this study: (1) dark-coupled (DC), (2) light-coupled (LC), (3) dark-decoupled biofloc (DD), and (4) light-decoupled biofloc (162). The specific nature of these treatments has been described previously (113); in brief, the coupled systems (DC and LC) operated with continuous water recirculation from the fish tank to the hydroponic grow bed at a flow rate of 9 L/min, corresponding to a hydraulic retention time (HRT) of approximately 80 minutes in the fish tank. This continuous flow mimicked recirculating aquaculture systems (161), with the media-filled grow bed serving as both a solids trap and a biofilter for nitrification and organic matter breakdown. In contrast, the decoupled systems (DD and LD) operated in a semi-continuous mode. Water was pumped from the fish tanks to the hydroponic beds twice per day for 3 minutes per cycle (25 L per cycle), resulting in a fish tank HRT of around 14 days. To maintain a stable volume of 700 L, fresh water was added daily at a rate of ~50 L, consistent with biofloc system water exchange rates reported in previous studies (163). The extended HRT in these systems enabled the fish tanks to function as primary biofloc reactors, where internal microbial activity facilitated nitrogen mineralization and organic matter degradation, while also contributing supplemental nutrition for tilapia (45). In the ‘dark’ treatments, fish tanks were painted and covered with dark fabric to prevent light exposure.

Each treatment was replicated three times in a randomized complete block design and operated in a greenhouse at the E.W. Shell Fisheries Station, Auburn, Alabama. Details of the

greenhouse setup and weather conditions have been described previously (113, 164). During the first year, solids removal was achieved using two-layer foam filters (coarse and fine), and water was pumped continuously to the grow beds in the coupled systems. In contrast, the decoupled systems pumped water from the fish tank to the grow beds using timer-controlled pumps set to operate twice daily for three minutes per cycle (9 $L \cdot min^{-1}$). In addition, the decoupled systems recovered grow bed drainage water in a sump which recirculated water to the. grow bed 8 times per day (10 minutes per cycle at 9 $L \cdot min^{-1}$). Each grow bed employed a media-based hydroponic configuration using pea gravel (0.5–1.5 cm diameter) and featured a bell siphon to facilitate intermittent flooding and draining, promoting root zone aeration (165). In the second year, solids management was upgraded by placing a 110-L radial flow settler (RFS) upstream of the foam filter, and integrating 30-minute on/off pump cycles in the coupled systems to maintain consistent ebb-and-flow irrigation. The pump cycling was used because the bell siphon became unreliable for maintaining ebb and flow once solids accumulated in the pore space of the media bed. A full description of the system layout, equipment, and modifications can be found in our earlier work (113, 120).

4.2.2 Aquaponics system operation and maintenance

All systems were operated for around 10 months each year, covering two cherry tomato (cv. *Favorita F1*) production cycles (spring and fall) and one full Nile tilapia grow-out cycle per year. Because wilt symptoms occurred only during the fall seasons, the present study focuses on the fall trial of each year. The fall tomato trials were conducted from September 17 to December 11 (Year 1) and from July 25 to November 14 (Year 2). After each tomato production cycle, grow beds were manually cleaned to remove accumulated sludge. Potassium, a nutrient commonly deficient in aquaponic and aquaculture systems (54), was supplemented daily through the make-up water to

maintain a target concentration of 100 mg/L in the fish tanks (55). In Year 1, each fish tank was stocked in March with 40 all-male Nile tilapia fingerlings (~20 g), sourced from existing raceways at the E.W. Shell Fisheries Station. Fish were grown to market size (~500 g) over eight months and harvested in November. In Year 2, tanks were stocked with 40 tilapia fingerlings (~130 g) and harvested at ~430 g. Fish were fed twice daily, once in the morning (7–8 am) and once in the afternoon (1–2 pm). During the fall tomato trials, fish received Cargill Triton-3603 feed (36% crude protein, 6% crude fat, 4% crude fiber, 1% phosphorus) at a rate of 1.5–2% of body weight, adjusted based on water temperature, observed consumption, and growth determined by monthly fish sampling (52, 53). Water quality was monitored regularly. pH readings were taken daily from the fish tanks using a Bluelab MetCombo meter, and pH was adjusted as needed to maintain values near 7.0 using either 3 M hydrochloric acid or calcium carbonate (47, 166). Dissolved oxygen (50) and temperature were recorded every other day using a Milwaukee MW600 portable DO meter. System operation protocols have been described in further detail in our previous publications (113, 120).

4.2.3 Sludge measurements

Sludge was discharged from the bottom of each RFS unit twice weekly. The discharge volume was recorded on site, and representative samples were collected after thorough mixing. Total suspended solids (TSS) concentrations in the collected RFS sludge and in the fish tank were estimated via optical density (OD) at 550 and 680 nm. Calibration curves relating OD to TSS concentration were generated seasonally by centrifuging solids (3,000 g, 10 min), drying at 105 °C, and weighing, following the protocol by Bertrand-Krajewski (56). To quantify biosolids accumulation within the grow beds, three gravel sample columns were taken per bed at the end of each tomato trial. Samples were rinsed and oven-dried to determine total solids.

4.2.4 Plant yield measurements

Ripe tomatoes were harvested throughout each growing cycle, and total fresh fruit weight was recorded per plant to determine cumulative seasonal yield. Each grow bed, containing five tomato plants, was considered an experimental unit (n = 3 per treatment). At the conclusion of each trial, shoot biomass was also harvested and weighed. Both yield and shoot mass were normalized per plant by dividing totals by the number of plants in each bed.

4.2.5 Root zone oxygen and stomatal conductance

A subset of plants from the Year 2 trial was further investigated to understand the underlying causes of wilting in certain tomato plants. Six wilting plants were identified in one LC and two DD systems. For each wilting plant, a healthy companion plant was identified in each grow bed for comparison of root zone conditions. For the following analyses, individual plants, rather than entire systems, were considered as the experimental unit. Dissolved oxygen (50) levels near the root zone were measured using a Milwaukee MW600 portable DO meter, which was carefully positioned directly in the grow bed media near plant roots. The sensor remained in place for several days to capture representative DO levels under both drained and flooded conditions in symptomatic and asymptomatic plants. After each measuring period, the probe tip was cleaned (and membrane replaced if damaged). Stomatal conductance (gsw) was measured separately on upper and lower leaves using a LICOR LI-600 porometer, which employs a steady-state, open flow-through design. The device was clamped onto each leaf until stable readings were logged, then unclamped and moved to the next sample.

4.2.6 Microbial analyses

DNA was extracted from biomass pellets collected from various system compartments, including grow beds, root zones of symptomatic and asymptomatic plants, and RFS sludge. Root zone sludge included attached microbes but not root tissues; therefore, endophytes were not included in this analysis, which may limit the interpretation of plant–microbe interactions. Extractions were performed using the FastDNA Spin Kit (MP Biomedicals, USA), and DNA concentrations were verified using the QuantiFluor dsDNA Quantification Kit (Promega, USA). Samples were submitted to MR DNA Laboratory (Texas, USA) for high-throughput sequencing. The 16S rRNA gene (primers 515F–806R) and 18S rRNA gene (primers 1391F and EukBr) were amplified and sequenced using the Illumina MiSeq platform. Reads were processed using the facility's in-house bioinformatics pipeline, which included demultiplexing, denoising, and zero-radius operational taxonomic unit (ZOTU) classification based on a curated reference database. Sequencing data have been deposited in the NCBI Sequence Read Archive (SRA) under BioProject accession numbers PRJNA1333965 and PRJNA1335545.

To identify functionally relevant taxa associated with root rot and wilt, species-level annotations from the 16S and 18S rRNA datasets were screened for putative bacterial and fungal pathogens, plant-parasitic nematodes, and potentially beneficial microorganisms. Species detected in the dataset were cross-referenced against several authoritative databases, including BacDive, Phytopath, HealthyHydroponics, Nemaplex, and the EPPO Global Database, to determine their relevance to plant disease (125-130). Automated text-matching tools were used to compare species lists with these databases to efficiently extract overlapping entries. Candidate pathogens were then manually verified through a targeted literature review to confirm host range, pathogenicity, and ecological traits. Representative sequences from critical taxa were re-evaluated through NCBI

BLASTn to validate species identity based on percent similarity and statistical support. A similar two-stage strategy was applied to identify putitive plant growth promoting bacteria (PGPBs). Species were first matched to curated PGPB repositories, including PLaBAse (123) and the Auburn University rhizobacteria database (124). Genera commonly associated with plant growth promotion, such as Bacillus, Streptomyces, Pseudomonas, and Bradyrhizobium, were screened, and species detected in those genera were subjected to a manual literature review to confirm documented roles in biocontrol, nutrient solubilization, or growth stimulation. Only taxa with peer-reviewed evidence supporting pathogenic or beneficial activity were included in the final analyses.

4.2.7 Statistical analyses

Each treatment was replicated across three independent aquaponic systems (n = 3), resulting in a total of 12 system-level experimental units. For system-level analyses (e.g., yield and RFS solids), the aquaponic system was treated as the experimental unit. For within-system comparisons (e.g., wilted vs. healthy plants), individual plants were treated as the experimental unit. For stomatal conductance measurements, 6 wilting plants were identified across 4 different aquaponics systems. All non-wilting plants in these same beds were also assessed for comparison (14 plants). For root-zone DO and microbial community analyses, four wilting plants (n = 4) and four non-wilting companion plants (from the same grow bed) were assessed. Although these sample sizes are limited, particularly for root-zone DO and microbial analyses, they reflect the number of observable wilt events within the system; therefore, statistically significant differences should be interpreted with appropriate caution. Differences in root-zone dissolved oxygen (DO), stomatal conductance, and microbial abundance between wilted and healthy plants were evaluated using a two-tailed independent groups *t*-test. RFS solids amount data were analyzed using multiple regression in R (v4.3.1), treating fish tank light exposure and system configuration (coupled vs.

decoupled) as fixed effects, and sampling time as a random effect to account for repeated measures over time. Time-course ANOVA followed by Tukey's HSD post hoc tests were conducted using the "car" and "agricolae" R packages to control for multiple comparisons among treatments, including RFS solids concentration, fruit and shoot mass, and microbial abundance ($p < 0.05$). Descriptive statistics (means and standard deviations) were calculated using Microsoft Excel.

4.3 Results and Discussion

4.3.1 Sludge in the root zone environment can cause root asphyxiation

Although sludge can serve as a reservoir of nutrients and beneficial microbes, excessive accumulation in hydroponic beds was a major contributor to root zone degradation, leading to oxygen depletion and plant wilting across treatments, as observed throughout this study and previously reported in our earlier work (113, 120). Over the two-year study, four aquaponics system types were operated, encompassing one fish production cycle (from 50 g to 500 g on average) and two tomato growing seasons (spring and fall) per year. In both years, wilt, chlorosis, and stunted growth were observed primarily during the second tomato trial (fall), when larger fish, higher feed input, and increased organic loading placed greater stress on system hydraulics and solids management. In the fall trial of the first year, continuous recirculation in the coupled systems filtered suspended solids through the gravel media, and poor drainage and sludge buildup in the grow beds likely created anaerobic microzones around the root zone, which may have contributed to root asphyxiation and the observed wilting and stunted growth. Consequently, the coupled systems produced cumulative tomato yields that were 21% lower than those of the decoupled systems (Table 4.1), despite having higher nutrient levels and more nutrients falling within sufficient ranges for tomatoes (113).

Table 4.1 Fruit production and wet shoot mass in the fall trial of the first and second year across the four aquaponics designs.

Treatments	Fruit production in year 1 (g)	Fruit production in year 2 (g)	Wet shoot mass in year 1 (g)	Wet shoot mass in year 2 (g)
LD	1749.92 ± 388.86 [a]	1253.07 ± 762.05 [b]	1840.73 ± 59.47 [a]	1596.6 ± 251.63 [b]
LC	1388.79 ± 92.87 [a]	2239.47 ± 411.02 [ab]	1327.17 ± 270.67 [a]	2189.13 ± 316.91 [b]
DD	1673.7 ± 102.05 [a]	1543.27 ± 384.69 [b]	1940.83 ± 98.03 [a]	1887.43 ± 141.83 [b]
DC	1323.85 ± 268.95 [a]	3471.47 ± 510.68 [a]	1824.57 ± 554.9 [a]	3248.93 ± 428.28 [a]

*Values are the means ± standard deviation of 3 treatment replicates. Means with the same letters were not statistically significant based on Tukey HSD on final points.

To address these issues, RFS and timer-controlled pumps were introduced in the second year to improve solid removal and maintain consistent ebb-and-flow irrigation, enhancing air exchange in the grow beds. These interventions reversed the trends caused by excessive sludge buildup observed in the first year. In the second-year fall trial, wilting symptoms in the coupled systems were minimal (observed only in one replicate of the LC system) and these systems significantly outperformed the decoupled ones in both growth and yield, producing 1,457 g more fruit mass ($p < 0.0001$) and 977 g more shoot mass ($p < 0.001$), respectively (Table 4.1). This was expected given the higher nutrient flows afforded by coupled operation as previously documented (113).

Despite these improvements in the coupled systems, root rot and wilting were observed in several decoupled systems, particularly the DD treatment. A total of 6 wilting plants were observed across DD and LC systems. Companion plants that were not wilting were selected from these same systems for comparison resulting in two groups of 6 plants each. Stomatal conductance

measurements provided insight into the physiological stress of the wilted plants. Conductance values were significantly lower in both upper and lower leaves of wilted plants (0.77 and 0.58 mol $m^{-2}s^{-1}$, respectively) compared to healthy plants (1.11 and 1.10 mol $m^{-2}s^{-1}$, respectively) (Figure 1), indicating impaired water uptake. This observation was consistent with DO measurements taken from the root zones. In wilted plants, DO levels averaged 1.4 mg/L under drained conditions, respectively, compared to 5.3 mg/L in healthy plants (Figure 4.2). The grow bed's drained period is the key time to enable root zone oxygenation but even in the flooded state, wilting plants had significantly lower DO. Low oxygen availability around the roots likely reduced their ability to absorb water, which in turn may have contributed to partial stomatal closure (167). While this response helps conserve water, it also limits photosynthetic activity and biomass accumulation, ultimately reducing plant productivity. Similar physiological responses to root hypoxia have been reported in other studies, where low DO levels led to reduced stomatal conductance and impaired growth (29, 168).

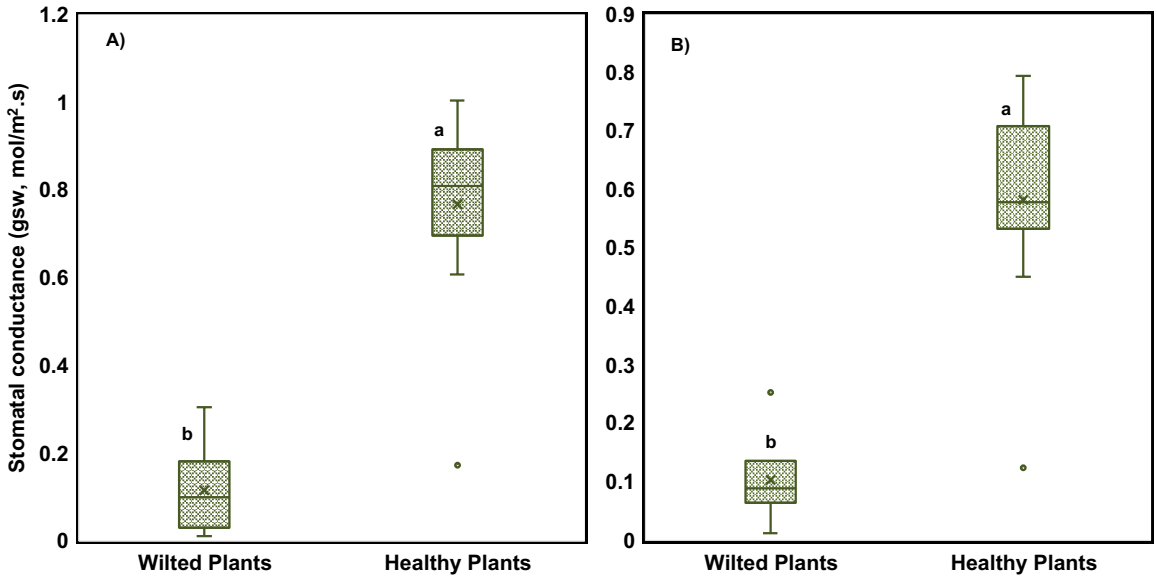

Figure 4.1 Stomatal conductance (gsw) for A) upper and B) lower leaves of wilted and healthy plants. Lowercase letters (a, b, c, etc.) indicate statistically significant differences between treatments ($p < 0.05$), n=6 plants for each group.

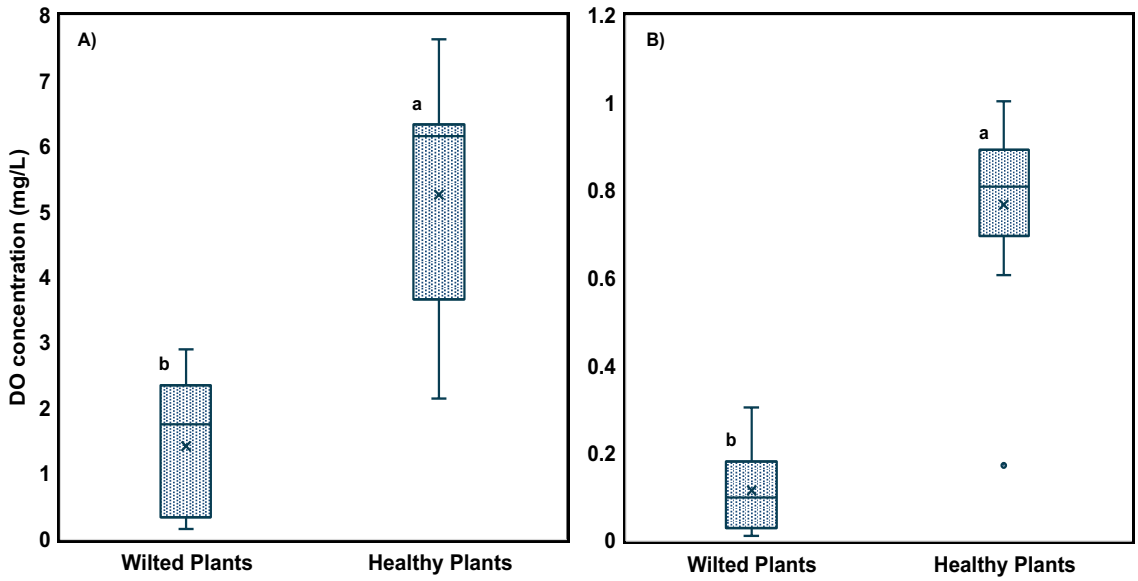

Figure 4.2 Root zone dissolved oxygen (50) of wilted and healthy plants at A) drained and B) flooded irrigation intervals/levels. Lowercase letters (a, b, c, etc.) indicate statistically significant differences between treatments ($p < 0.05$), n=6 plants for each group.

It was initially believed that improving sludge removal through the incorporation of an RFS would universally improve the performance of aquaponic tomato production (and ideally eliminate problems with wilt). This was not the case. The performance of the RFS units varied among treatments (Figure 4.3A). Coupled systems, which circulated water through the clarifiers for 12 hours per day, achieved significantly greater solid removal compared to the biofloc-based decoupled systems, which operated their RFS units for only 6 minutes per day during irrigation cycles. Nevertheless, the coupled systems accumulated more sludge in the grow beds overall (Figure 4.3B), likely due to higher nutrient concentrations (no discharge system) and microbial growth (113, 120). Interestingly, although the decoupled systems maintained lower average sludge levels in their grow beds, some plants still experienced localized oxygen-deficient zones. This indicates that the spatial distribution of sludge, rather than total sludge accumulation alone, may play a critical role in driving root-zone hypoxia and plant stress. This was particularly evident near

the clarifier outlets, where floating sludge occasionally escaped the RFS and settled on the grow bed surface. These sporadic sludge deposits created pockets of severe oxygen depletion, likely leading to localized root suffocation and wilting. Microbial community analysis further revealed differences between the clarifiers (Figure 4.3C). The decoupled systems, particularly the DD treatment, had a higher relative abundance of methanogens, strict anaerobes that thrive in low-oxygen environments and produce gases such as CO_2 and CH_4. Gas production may have contributed to sludge flotation and overflow, reducing settling efficiency in the DD clarifiers, which had the poorest solid removal performance among all treatments (Figure 4.3A). The floating sludge often settled near the hydroponic bed inlets, where it negatively affected the roots of nearby plants, causing localized oxygen depletion and wilting. As shown in Figure S4.2, wilted plants had visibly brown, decayed roots, whereas healthy plants exhibited intact, well-developed root structures. These results underscore the critical role of consistent, well-timed, and spatially informed solid management strategies in aquaponic systems (not only to minimize total sludge accumulation but also to prevent uneven sludge distribution within grow beds) to prevent root rot and wilt and maintain a healthy rhizosphere. These findings suggest that total solids in the grow bed were not necessarily problematic (it was high in the most productive coupled system). Rather, it is the quality of the solids material that appears to be important. Long periods of stagnation in the clarifiers of the decoupled system, while theoretically good for solids settling, created undesirable anaerobic conditions. Thus inclusion of the RFS, while helpful in the coupled systems, may have had unintended negative consequences for decoupled system performance. In support of this conclusion, fruit yields and shoot mass were higher in the decoupled systems of year 1 (no RFS) than they were in year 2 (with RFS).

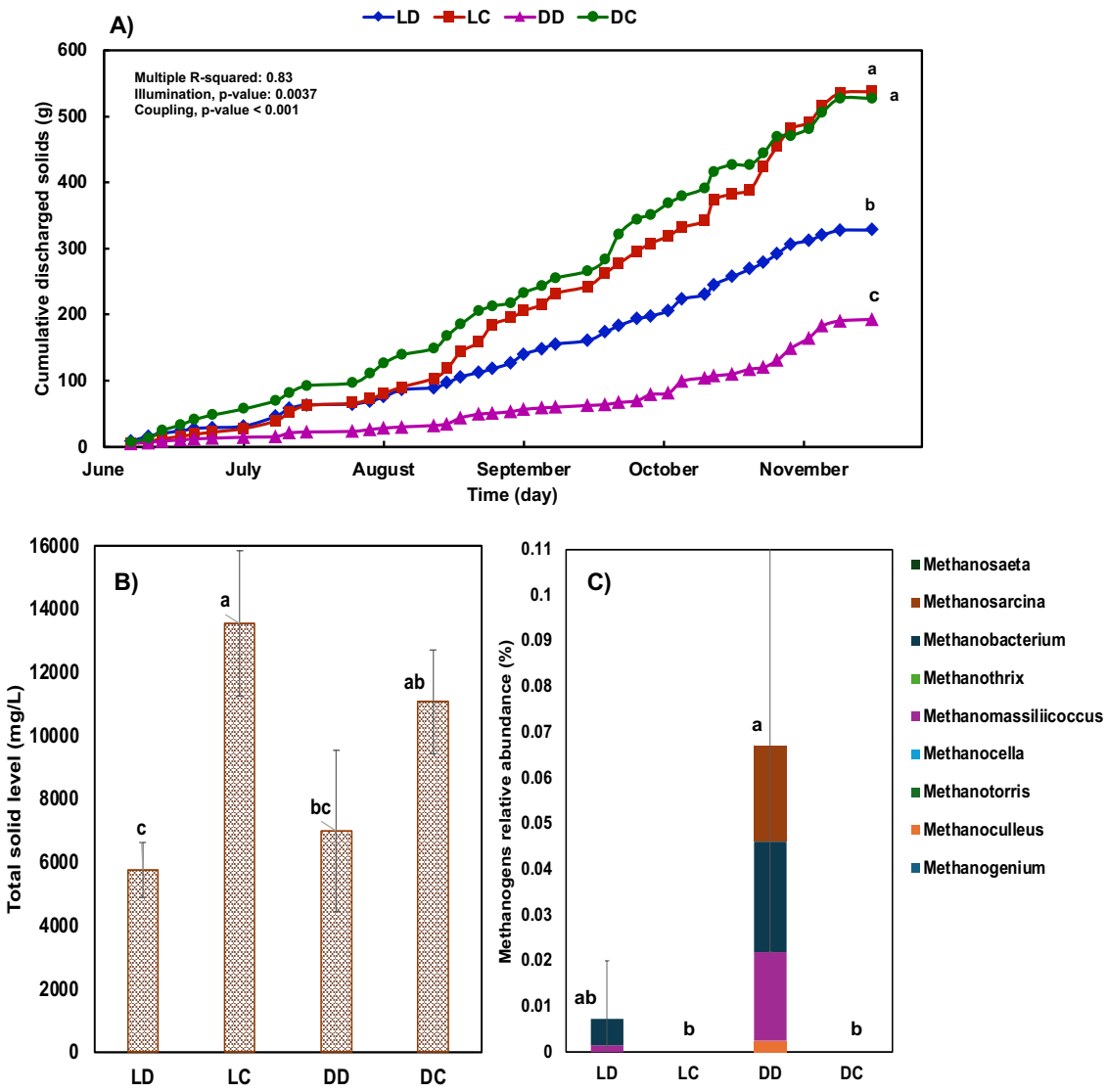

Figure 4.3 A) Cumulative dried solids discharged from the radial flow settler (RFS) units over time across the four aquaponics designs: dark-coupled (DC), (2) light-coupled (LC), (3) dark-decoupled (DD), and (4) light-decoupled (162). B) Total solids accumulated in the grow beds in the fall trial. C) Relative abundance of methanogens in the RFS unit. Error bars represent standard deviation (n = 3). Lowercase letters (a, b, c, etc.) indicate statistically significant differences between treatments ($p < 0.05$).

4.3.2 Sludge containing plant pathogens can damage roots and cause wilt

As shown in Section 4.3.1, root-zone hypoxia associated with sludge accumulation was linked to reduced stomatal conductance and plant wilting, indicating that oxygen limitation was the primary driver of plant stress in this study. Waterlogged and oxygen-deficient conditions in aquaponic

systems can also promote the proliferation of plant pathogens. Several microbial taxa known to include species that infect plant roots and vascular tissues were detected at higher relative abundances in the root zones of wilted tomato plants compared to healthy ones. These included fungal-like organisms (oomycetes and chytrids), plant-parasitic nematodes, and bacterial taxa with potential pathogenic traits (Table 4.2). Taken together, these observations suggest that microbial dynamics acted as contributing or interacting factors within an already stressed root-zone environment, rather than as the primary cause of wilting.

4.3.2.1 Fungal-like pathogens

Wilted plants showed a higher cumulative relative abundance of putative fungal-like pathogens, most notably *Synchytrium endobioticum*, *Pythium graminicola*, and *Pythium apleroticum*, though the difference was not statistically significant ($p = 0.12$). *S. endobioticum*, the causal agent of potato wart disease, is a quarantine-listed chytrid fungus capable of producing persistent soil-borne sporangia that remain viable for 30–50 years (169). While potato is its primary host, studies show it can infect other solanaceous crops, including tomato roots, potentially forming galls or subclinical infections (170). Its elevated relative abundance in the wilted tomato roots (0.0255%) compared to the healthy ones (0.0021%) suggests a potential association with root stress under unfavorable conditions, although its direct role in tomato pathology remains uncertain. However, the difference was not statistically significant ($p = 0.19$).

Pythium graminicola, an oomycete widely associated with root rot and damping-off in cereals and solanaceous crops (171), was also more abundant in wilted roots (0.0211%) versus healthy roots (0.0033%), particularly in the DD system (not statistically significant, $p = 0.11$). This species produces motile zoospores that readily disperse in water, making it particularly well adapted to aquaponic environments. It infects fine roots and root hairs, causing water-soaked

lesions, sloughing of the root cortex, and eventual necrosis. Infected tomato plants typically exhibit wilting, chlorosis, and reduced vigor, despite an intact shoot system (35, 172), which is consistent with the symptoms observed in this study. Notably, *P. graminicola* was also detected at high levels (0.73 % of relative abundance) in the fish tanks of DD systems, where it may have spread systemically and colonized the grow beds via circulating water. *Pythium apleroticum*, though less studied, belongs to the same clade and has been reported to cause fruit rot in tomato under laboratory conditions. It is considered weakly or opportunistically pathogenic but may contribute to disease in conjunction with other stressors (173, 174). Its detection exclusively in wilted root zones suggests a potential secondary or opportunistic role in exacerbating root decay, especially in systems with already compromised root health.

Interestingly, several potential PGPBs known for suppressing *Pythium* species were found at higher relative abundance in the root zones of healthy plants. While the differences were not statistically significant, the consistent presence of beneficial microbes in healthier root zones suggests an association with improved root conditions. However, this pattern may also reflect a response to favorable environmental conditions rather than a direct causal effect, as healthier roots may support or select for beneficial microbial communities. Notably, *Bacillus mycoides*, a spore-forming rhizobacterium recognized for producing phytohormones (e.g., IAA), solubilizing phosphates, and secreting antimicrobial metabolites (175), had a higher relative abundance in healthy roots (0.3016%) compared to wilted roots (0.0024%) (not statistically significant, p = 0.42). This species has shown antagonistic effects against soilborne pathogens, including *Pythium*, with some strains capable of inducing systemic resistance and emitting volatile compounds that inhibit oomycete growth (176). For instance, strain SU-23 of *B. mycoides* has demonstrated complete suppression of *Pythium*-induced damping-off in cucumber (177). Similarly,

Streptomyces spp., which were also more abundant in healthy roots (e.g., *S. glaucescens* at 0.0438% and *S. scopuliridis* at 0.0286%) (not statistically significant, $p = 0.31$ and $p = 0.5$, respectively), are known for their broad-spectrum biocontrol properties. These filamentous bacteria produce antibiotics, lytic enzymes, and antifungal compounds that disrupt pathogen cell walls and are widely documented to protect tomato plants from root rot and damping-off (162). Commercially used strains, such as *Streptomyces lydicus* WYEC108 (marketed as Actinovate), have been especially effective against *Pythium* species (178, 179). However, these interpretations are based on relative abundance patterns and do not confirm active pathogen suppression within the system.

4.3.2.2 Parasitic nematodes

Putative parasitic nematodes showed a trend toward higher relative abundance in wilted root zones, particularly *Pratylenchus crenatus*, *Xiphinema rivesi*, and *Xiphinema macroacanthum* ($p = 0.09$). *P. crenatus*, a root-lesion nematode, had a relative abundance of 0.0983% in wilted roots compared to 0.0021% in healthy roots (not statistically significant, $p = 0.24$). It penetrates cortical tissues and feeds endoparasitically, creating dark necrotic lesions and cavities that impair water and nutrient uptake. In tomato, infestation by *P. crenatus* is associated with pruned-back roots, reduced fine root density, and stunted, chlorotic shoots (180, 181), which is consistent with the symptoms observed in the wilted LC and DD tomatoes. While lesion nematodes typically prefer soil environments, *P. crenatus* can persist in moist substrates as eggs or juveniles and may thrive in periodically drained aquaponic media. Its role in tomato yield losses has been documented, with studies showing up to 44% reduction under heavy infestations (182, 183).

X. rivesi, a dagger nematode, is an ectoparasite that feeds on root tips using a long stylet and is known to vector nepoviruses such as Tomato ringspot virus (TomRSV) (184). Although

viral symptoms were not observed in this study, the feeding activity of *X. rivesi* alone can cause necrotic root lesions, tip swelling, and pruning of feeder roots, ultimately reducing water uptake and causing aboveground stunting (185). Its relative abundance was 0.0323% in wilted roots and nearly absent in healthy ones (0.0021%) (not statistically significant, $p = 0.41$). *X. macroacanthum*, a genetically related species, shares similar feeding behavior and may contribute to root damage despite being less well studied. Parasitic nematodes were found in greater relative abundance in grow beds than in fish tanks ($p = 0.047$), and the coupled grow beds had higher levels of *X. rivesi* ($p = 0.038$), which could have contributed to wilt symptoms observed in the LC systems. Interestingly, the DC systems also exhibited elevated levels of *Xiphinema*, yet no disease symptoms were observed, possibly due to the absence of additional stressors such as root-zone oxygen deprivation, as observed by higher stomatal conductance of these plants (Figure 4.1). Thus, while potentially interacting with the tomato root systems, the presence of *Xiphinema* alone does not explain the wilting symptoms observed in these aquaponic systems.

Several of the putative PGPB genera detected, particularly *Bacillus*, *Pseudomonas*, and *Streptomyces,* are known to suppress plant-parasitic nematodes through both direct and indirect mechanisms (Figure S4.3). These genera are among the most frequently reported nematode-antagonistic rhizobacteria in agricultural systems. *Bacillus* species, for instance, produce a variety of nematotoxic compounds, including crystal (Cry) proteins from *B. thuringiensis* that specifically disrupt nematode gut integrity. In addition, *Bacillus* spp. secrete extracellular enzymes such as chitinases and proteases that degrade nematode egg shells and cuticles, thereby inhibiting development and reproduction (186). The *Bacillus* genus was detected at 0.3 % relative abundance in the root zones of healthy plants, while its abundance in the root zones of wilted plants was 0.0013 % (not statistically different, $p = 0.42$) (Figure S4.3 and Table 3). Additionally, certain

Streptomyces strains have been shown to suppress populations of parasitic nematodes in tomato (187), which were also more prevalent in healthy root zones (not statistically different, $p = 0.41$) (Figure S4.3 and Table 4.3). As with other microbial observations, these patterns should be interpreted as associative and do not establish direct biocontrol activity within the system.

4.3.2.3 Bacterial pathogens

Several putative bacterial pathogens were also detected at higher relative abundances in the root zones of wilted plants, although the differences were not statistically significant. *Burkholderia andropogonis*, recently reclassified as *Robbsia andropogonis*, is a known foliar pathogen that causes leaf stripe, spot, and blight diseases in a range of hosts, including sorghum, areca palm, and ornamental plants. It carries a suite of virulence factors that enable aggressive colonization, particularly in wet environments where it can enter through stomata or wounds (188, 189). In this study, *B. andropogonis* and *R. andropogonis* were the most abundant pathogenic bacterial taxa, and were more prevalent in grow beds than in fish tanks ($p < 0.0001$) (Figure 4.4C), suggesting that the rhizosphere provided a favorable niche for their proliferation. with relative abundance of 0.439% and 0.315% in wilted and healthy roots, respectively. These taxa have not previously been confirmed as pathogens of tomato, but their broad host range and strong adaptation to moist conditions suggest the possibility that they may act as secondary or opportunistic colonizers, exacerbating root decay in already compromised plants or interfering with host defense responses. Despite less evidence of plant disease, nominally higher levels of putative bacterial pathogens were present in the highly productive coupled systems compared to the decoupled systems ($p = 0.14$). As with the parasitic nematodes, this fact suggests that bacterial pathogens were unlikely to be the primary drivers behind poor tomato growth performance in decoupled systems.

Table 4.2 Relative abundance of fungal and oomycete pathogens, parasitic nematodes, and bacterial pathogens in the root zones of the wilted and healthy plants. Values are the means ± standard deviation of 3 treatment replicates.

Fungal-like pathogens	**Wilted Plants**	**Healthy Plants**
Pythium aphanidermatum	0 %	0 %
Pythium apleroticum	0.0069 %	0.0045 %
Pythium graminicola	0.0211 %	0.0033 %
Synchytrium endobioticum	0.0255 %	0.0021 %
Fusarium oxysporum	0 %	0 %
Didymella prosopidis	0 %	0 %
Didymella americana	0 %	0 %
Ustilago maydis	0 %	0 %
Total	0.054% ± 0.041 a	0.01% ± 0.01 a
Parasitic nematodes		
Radopholus similis	0 %	0 %
Meloidogyne mali	0.0018 %	0 %
Pratylenchus crenatus	0.0983 %	0.0021 %
Xiphinema macroacanthum	0.0109 %	0 %
Xiphinema rivesi	0.0323 %	0.0021 %
Total	0.143% ± 0.113 a	0.004% ± 0.007 a
Bacterial pathogens		
Agrobacterium radiobacter	0.0013 %	0.0017 %
Robbsia andropogonis	0.153 %	0.1015 %
Xanthomonas axonopodis	0 %	0 %
Xanthomonas oryzae	0.023 %	0.0969 %
Agrobacterium rhizobium radiobacter	0.0026 %	0 %
Burkholderia andropogonis	0.2864 %	0.2131 %
Corynebacterium sundsvallense	0.0079 %	0.0134 %
Pseudoxanthomonas helianthi	0.0393 %	0.0319 %
Xanthomonas alfalfae	0.001 %	0 %
Acidovorax cavernicola	0.0364 %	0.0239 %
Total	0.55% ± 0.22 a	0.48% ± 0.18 a

Scale
0%
< 0.005%
> 0.005%
> 0.02%
> 0.05 %
> 0.1 %
> 0.5 %

Table 4.3 Relative abundance of putative plant-growth-promoting bacteria in the root zones of the wilted and healthy plants. Values are the means ± standard deviation of 3 treatment replicates.

Plant growth-promoting bacteria	Wilted Plants	Healthy Plants
Bacillus mycoides	0.0024 %	0.3016 %
Bradyrhizobium guangdongense	0.0922 %	0.0637 %
Bradyrhizobium japonicum	0.008 %	0.0017 %
Bradyrhizobium oligotrophicum	0.0312 %	0.01 %
Delftia acidovorans	0.0067 %	0.005 %
Roseomonas genomospecies	0.0149 %	0.0317 %
Sinorhizobium americanum	0.0243 %	0.0131 %
Ensifer adhaerens	0.0123 %	0.0034 %
Paenibacillus graminis	0.0096 %	0.0159 %
Variovorax boronicumulans	0.0028 %	0 %
Flavobacterium aquidurense	0.0111 %	0 %
Paenarthrobacter nicotinovorans	0 %	0.0067 %
Pseudomonas parafulva	0.0039 %	0.0017 %
Demequina activiva	0.0048 %	0.0088 %
Novosphingobium arabidopsis	0.0186 %	0.0115 %
Pseudomonas gessardii	0.0069 %	0 %
Stakelama pacifica	0.0028 %	0.0016 %
Streptomyces glaucescens	0.024 %	0.0438 %
Streptomyces scopuliridis	0.0054 %	0.0286 %
Pseudomonas mosselii	0.0237 %	0.0248 %
Total	0.32% ± 0.18	0.6% ± 0.49

Scale
0%
> 0.001%
> 0.01%
> 0.05%
> 0.2 %
> 0.3 %

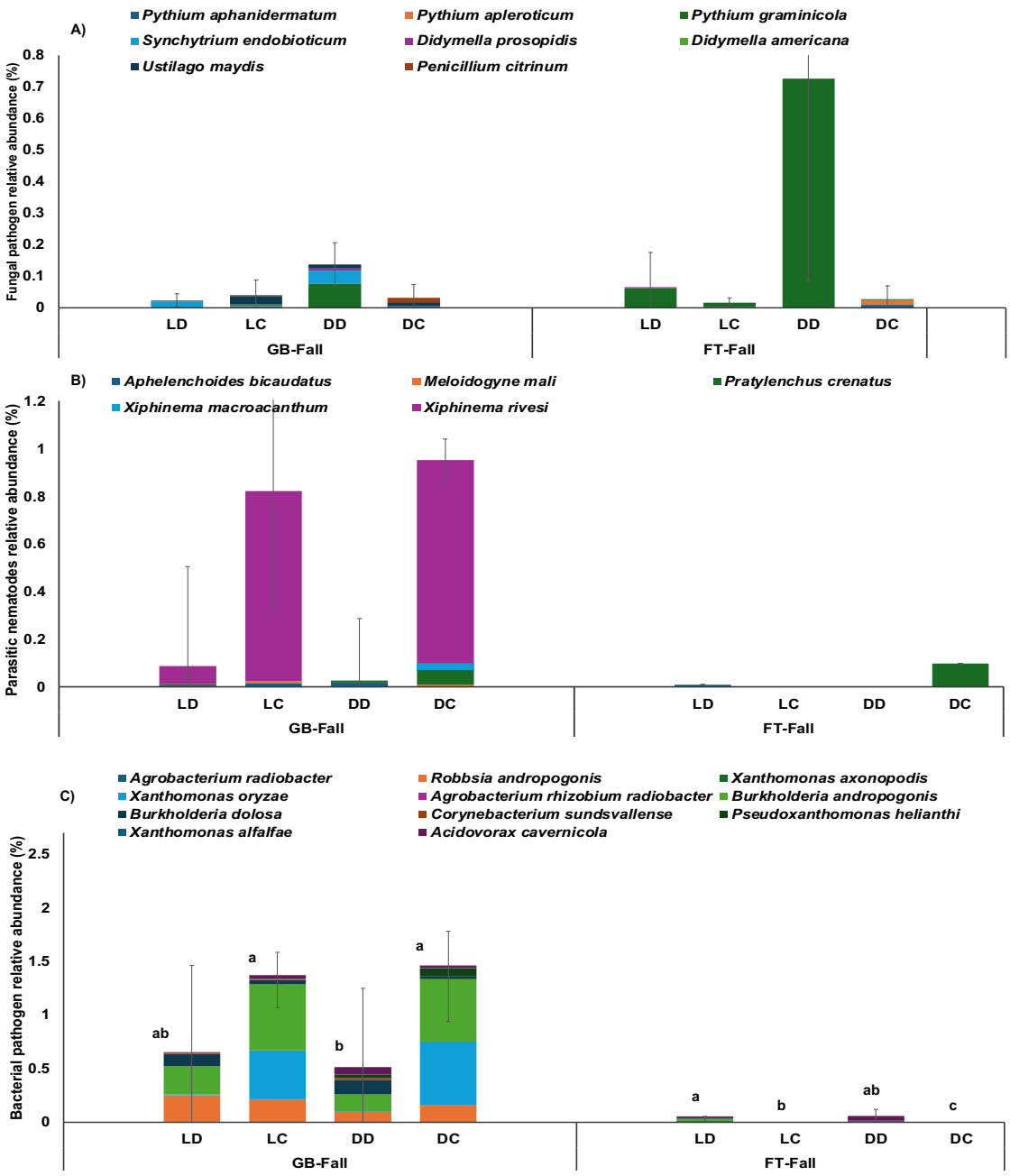

Figure 4.4 Relative abundance of (A) plant-pathogenic fungi and oomycetes, (B) parasitic nematodes, and (C) plant-pathogenic bacteria at the species level across fish tank (113) and grow bed (190) compartments for each system design: light-decoupled (162), light-coupled (LC), dark-decoupled (DD), and dark-coupled (DC). Error bars represent standard deviation (n = 3). Lowercase letters (a, b, c, etc.) indicate statistically significant differences between treatments ($p < 0.05$). Figures without letters were not statistically different from the others.

4.4 Conclusion

This study highlights the critical role of biosolids management in sustaining plant health and productivity in media-based aquaponic systems. Across two years of continuous operation, wilting and yield losses were primarily associated with oxygen-deficient root zones linked to poor drainage, sludge accumulation, and uneven solids distribution. Efforts to improve solids removal from fish tank water using an RFS were effective, but their downstream impact on tomato performance varied by system configuration. Solids removal clearly benefited the coupled systems, which produced substantially higher yields in the second year and exhibited minimal wilting. However, this intervention was associated with reduced yields and increased wilting in decoupled systems. The RFS units in decoupled systems exhibited characteristics consistent with anaerobic conditions, including elevated methanogen abundance, which may have contributed to localized root-zone stress, particularly near the water inlet. Low root-zone DO (as low as 1.4 mg L^{-1}) and reduced stomatal conductance (0.77 and 0.58 mol m^{-2} s^{-1}) in wilting plants indicate impaired water uptake and physiological stress. These conditions likely created an environment favorable for opportunistic microbial colonization. Although not statistically significant, microbial analyses showed trends toward higher relative abundance of fungal-like pathogens and parasitic nematodes in wilted plants, while healthy root zones were associated with greater relative abundance of plant growth-promoting bacteria with known biocontrol potential. However, these observations are based on relative abundance data and should be interpreted as associations rather than evidence of direct functional activity. Overall, these findings indicate that physical root-zone conditions, particularly oxygen availability and sludge distribution, are primary drivers of plant performance, while microbial dynamics likely reflect secondary or interacting responses. As aquaponics systems scale toward commercial adoption, management strategies that maintain

oxygen-rich root environments and minimize localized sludge accumulation will be critical. Importantly, increasing solids removal alone is not sufficient; system-specific design and operation must be considered. In this study, RFS implementation improved performance in coupled systems but was less effective in decoupled biofloc systems under the conditions tested.

Chapter 5: Photoautotrophic Conditions and Coupled Configuration Improve Aquaponics Fish Productivity Without Increased Off-Flavor

Photoautotrophic Conditions and Coupled Configuration Improve Aquaponics Fish Productivity Without Increased Off-Flavor

Authors: Shima Rezaei[1], Grace Hohn[1], Sonya Hawkins[2], Navid Farahmandzad[1], Saravanan Ramiah Shanmugam[1], Kelly Sullivan[1], Sarah Hensless[1], Mary Beth Hall[1], Luz de-Bashan[2,3], David Cline[4], Brendan Higgins[1]*

[1]Biosystems Engineering, Auburn University, Auburn, AL 36849, USA

[2]Bashan Institute of Science, Dadeville, AL, 36853, USA

[3]Department of Entomology and Plant Pathology, Auburn University, Auburn, AL 36849, USA

[4]School of Fisheries, Aquaculture and Aquatic Sciences, Auburn University, Auburn, AL 36849, USA

*Corresponding author:

Brendan T. Higgins

Department of Biosystems Engineering, 203 Corley Building, Auburn, AL 36849, USA

Phone: 334-844-3532

e-mail: bth0023@auburn.edu

Abstract

Over two consecutive production years, we evaluated the interplay between fish tank light exposure and system configuration (coupled vs. decoupled) as key design factors influencing tilapia production in aquaponic systems. A full factorial design with twelve independent aquaponics systems was tested for two fish production cycles (fingerling to market weight)) along with cherry tomato production. Sunlight-exposed systems developed photoautotrophic Chlorophyta-dominated communities, comprising up to 78% of biofilm biomass and 63% of suspended biofloc. Tilapia were directly observed eating these materials along with their diet of pelletized feed. Fish tanks were covered in dark systems and Chlorophyta levels were negligible. Green bioflocs contained higher protein (up to 27%) and lipid (up to 9.2%) levels than brown bioflocs in dark systems (21.4% protein, 5.4% lipid), along with enriched unsaturated fatty acids, including 0.97% polyunsaturated fatty acids and 0.64% monounsaturated fatty acids. Essential omega-3 and omega-6 precursors (18:2n-6 and 18:3n-3) were more than twice the concentrations found in dark-system flocs. Illumination improved overall yield, with the light-coupled systems producing the highest biomass in both years (551 g and 581 g) and the lowest feed conversion ratios, although fish fillet composition (proteins and fatty acids) remained unaffected. Despite potential concerns about cyanobacteria, light exposure did not promote the growth of off-flavor-producing microbes; cyanobacteria levels remained below 0.03% in green biofloc, and geosmin/MIB concentrations in fillets remained under 200 ng/kg on average, which is below the human sensory detection threshold. Together, light exposure and system coupling synergistically enhanced fish productivity by improving microbial community structure and functional resilience without compromising water quality or off flavor compounds.

Keywords: Green Biofloc, Brown Biofloc, Algae, Fatty Acid Profile, Geosmin/MIB,

Graphical Abstract

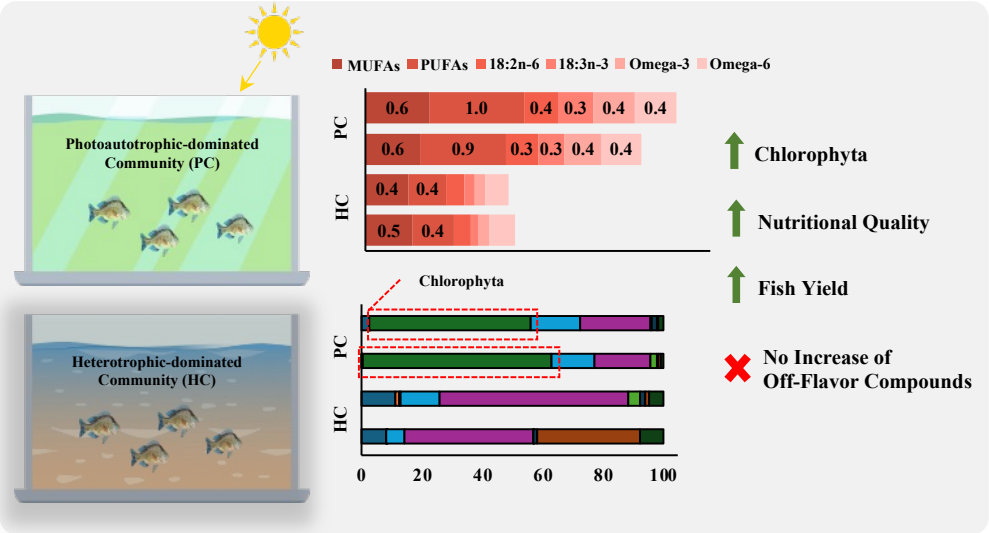

Highlights:

- Sunlight exposure promoted Chlorophyta-dominant bioflocs in fish tanks
- Green biofloc exhibited higher protein and lipid content than dark-grown floc
- Essential omega-3 and omega-6 fatty acids were enriched in light-exposed bioflocs
- Geosmin and MIB remained below sensory thresholds in all systems
- Light and coupling enhanced fish productivity without altering fillet quality

5.1 Introduction

Aquaponics offers a sustainable aquaculture model by recycling nutrients, reusing water, and supporting fish growth. The high nutrient environment of aquaponics systems can result in the growth of microbial flocs and biofilms in fish tanks. These materials are composed of bacteria, algae, and detritus. They help assimilate nitrogen and organic waste, reducing reliance on water exchange and in the case of filter feeding fish, they can reduce the need for commercial feed (191). However, integrating biofloc technology into aquaculture introduces challenges, as high solid densities and minimal water exchange make water quality sensitive to imbalances (192, 193). Accumulated nutrients and solids can disrupt ammonia and nitrite levels, highlighting the importance of managing microbial community composition for stable nitrogen cycling and system health (194).

One design factor that significantly influences the microbial dynamics of biofloc systems, but remains underexplored in aquaponics, is light exposure in fish tanks. Traditional biofloc technology (BFT) setups operate in low-light or dark conditions to favor heterotrophic bacteria, which assimilate nitrogen into microbial biomass when provided with an external carbon source (195, 196). Likewise, guidance on aquaponics system design often discourages allowing sunlight into fish tanks because algal growth is presumed to deprive downstream plants of nutrients (75, 76). However, our past research has shown little to no impact of fish tank light penetration on production of cherry tomatoes over four growing seasons (120).

Nevertheless, exposure to natural light can stimulate the proliferation of photoautotrophic microorganisms, including green algae (e.g., Chlorophyta) and cyanobacteria, and has a multifaceted impact on system function (197). Photoautotrophic biofloc and biofilm communities offer potential nutritional benefits by enriching these materials with algal biomass which can

elevate protein and lipid content, along with a more complete fatty acid profile. This composition potentially enhances the biofloc's value as a supplemental feed source, providing fish with additional nutrients between scheduled feedings (20, 198). Moreover, green algae like *Chlorella* not only take up inorganic nutrients but also produce bioactive compounds that can inhibit pathogens. For example, *Chlorella* cultures have demonstrated antibacterial activity against common fish pathogens, including *Aeromonas hydrophila*, *Vibrio anguillarum*, and *Pseudomonas aeruginosa* (199, 200).

Nevertheless, light exposure can promote the growth of geosmin- and 2-methylisoborneol (201) producing bacteria, such as cyanobacteria (27, 28). These terpenoid compounds are responsible for earthy off-flavors in fish flesh and can accumulate in tissue even at sub-threshold concentrations, diminishing product quality and consumer acceptance (202). The influence of light on nitrification also remains unclear. Effective nitrification is essential in aquaculture and aquaponics systems. While photoautotrophs can enhance ammonia assimilation in some aquaculture and wastewater systems (203-205), other studies report that excessive light may suppress nitrifier populations or impair their activity (206). To address these uncertainties, and in light of the complex algae–bacteria interactions and the inherent variability of aquaculture environments, long-term, system-level studies under realistic operating conditions are essential. Of specific interest is how light exposure influences microbial community dynamics, nitrogen cycling, and fish performance in biofloc aquaponics (62) over long-term production cycles.

In addition to fish tank illumination, system configuration, particularly the distinction between coupled and decoupled aquaponics, plays a key role in shaping microbial community structure and fish health (16). Coupled systems continuously recirculate water between fish tanks and hydroponic beds, whereas decoupled systems maintain separate loops, allowing independent

control of water quality in each component (207). These configurations differ in waste retention, nutrient concentrations, and hydraulic regimes, all of which can influence the microbial colonization and solids levels in different compartments (9, 208). For example, recent findings by Rezaei et al. (2025) indicate that decoupled biofloc systems foster significantly higher populations of nitrifying bacteria in the fish tanks than coupled systems, likely due to higher solid retention time. Moreover, denser biofloc in decoupled systems may also provide more nutritional biomass for fish, but elevated total suspended solids (TSS) can stress fish if not properly managed (113). These variations may directly or indirectly affect fish growth, stress responses, and disease resistance. Thus, understanding how coupling configuration interacts with microbial ecology is critical for optimizing both fish and plant productivity in biofloc aquaponics.

No study to date has reported on the impacts of fish tank illumination under coupled or decoupled aquaponics configurations on the quality of biofloc and biofilms and downstream effects on tilapia. This study was conducted over two full production cycles across two years in a greenhouse setting, offering a novel long-term perspective on how system design influences system performance and yield. We examined the interactive effects of fish tank illumination and system configuration (coupled vs. decoupled) on microbial community structure, biofloc characteristics, nitrification performance, and fish growth. In contrast to previous studies, often limited to short durations or small-scale trials, our extended trial allowed us to capture seasonal variability, biofloc succession, and sustained system responses over time. Particular emphasis was placed on functional microbial groups linked to fish performance, including communities involved in nitrification, off-flavor compounds, and potential pathogens, while plant-related outcomes were reported previously (120). We initially hypothesized that light exposure would stimulate algae growth, providing more nutritious bioflocs and biofilms than dark systems, and translate into more

omega3 and omega6 fats in the fish fillets. We also hypothesized that light systems would result in higher levels of cyanobacteria, resulting in more off-flavor in fish fillets. These findings provide system-level insights for the design and management of biofloc-based aquaponic systems under realistic production conditions.

5.2 Materials and Methods

5.2.1 Experimental design

This study explored the combined effects of water flow configuration and light availability on microbial community dynamics in biofloc-based aquaponics, with an emphasis on microbial groups relevant to fish health and production. A two-factor factorial design was implemented, testing (1) system configuration (coupled vs. decoupled water loops) and (2) fish tank light exposure (light-permissive vs. light-restricted). These treatments yielded four experimental conditions as shown in Figure S5.1: (1) dark-coupled (DC), (2) light-coupled (LC), (3) dark-decoupled (DD), and (4) light-decoupled (LD), each replicated in triplicate using a randomized complete block layout. The experimental unit was an independent aquaponics system, which is described in section 5.2.2.

The experiment was carried out inside a 268 m^2 climate-controlled greenhouse (Atlas Greenhouse, USA) at Auburn University's E.W. Shell Fisheries Center (Alabama, USA). For light-restricted (dark) treatments, tanks were covered with black landscape fabric and painted to block external light, while tanks in the light-exposed treatments remained uncovered, with translucent plastic walls enabling solar radiation to reach the water column. Seasonal variation in photoperiod ranged from 10 to 14 hours between March and December. Additional information on greenhouse climate conditions and operation is available in earlier publications (113, 120).

The study spanned two years (2023–2024), encompassing one full tilapia grow-out cycle and two cherry tomato production trials per year. In 2023, tanks (700 L) were stocked with 40 all-male Nile tilapia fingerlings (~20 g), resulting in an initial stocking density of ~1.2 kg m^{-3}. Fish were cultured to market size (~450 g) over eight months, reaching a final density near 28 kg m^{-3}. In the second year, the initial stocking weight was higher (~130 g per fish; ~8 kg m^{-3}), and final harvest weight averaged ~450 g per fish (~17 kg m^{-3}). To maintain optimal rearing conditions and prevent biomass overload, partial harvesting was conducted in September 2024 to reduce tank density back ~14 kg m^{-3}, in accordance with published recommendations for biofloc aquaponics and in response to a fish mortality event observed in LD systems at the end of the first year (Rezaei et al., 2026). In this manner, maximum fish densities were kept below 20 kg m^{-3} in year 2.

All experimental protocols were approved by the Auburn University Institutional Animal Care and Use Committee (IACUC #22-4099). Before stocking, tanks were inoculated with active biofloc harvested from an established tilapia raceway to ensure early development of nitrifying microbial communities. Concurrent with fish production, tomato (Favorita F1) trials were conducted in the spring and fall of each year using five plants per grow bed. Complete horticultural methods and plant production results are described in Rezaei et al. (2025).

5.2.2 System setup

The operational characteristics of each treatment configuration have been detailed previously (113, 120); briefly, the coupled systems (DC and LC) employed a continuous recirculating design, where water flowed from the fish tanks to the hydroponic beds at a rate of 9 L·min^{-1}. This design maintained hydraulic retention times (HRT) of approximately 80 minutes in Year 1 and 155 minutes in Year 2 within the 700-L fish tanks. The increase in HRT in year 2 was made to improve the ebb and flow irrigation cycle for tomato production. The hydroponic beds were media-filled

and functioned dually as solids traps and biological filters, facilitating nitrification and organic matter breakdown. Intermittent irrigation was achieved via bell siphons in Year 1, promoting oxygenation in the plant root zone. In Year 2, intermittent irrigation in the coupled systems was automated using 30-minute pump on/off cycles, replacing the siphon system, which had become inconsistent due to media clogging from accumulated solids. Water lost through evaporation and sludge removal was replenished twice per week using dechlorinated municipal water. This freshwater was held in open reservoirs for 24 hours to allow chlorine dissipation and verified chlorine-free with onsite test strips before system input. Dissolved oxygen (DO) was maintained near 7 $mg \cdot L^{-1}$ in the fish tanks using aerators with a flow capacity of 40 $L \cdot min^{-1}$.

In contrast, the decoupled systems (DD and LD) operated semi-continuously with discrete water transfers from the fish tanks to the hydroponic beds. Water was pumped twice daily in 3-minute intervals, delivering approximately 25 L per cycle and achieving an overall HRT of around 14 days in the fish tanks. This prolonged retention supported dense biofloc accumulation, enabling active microbial mineralization and nitrification while also providing nutritional benefits to the tilapia. Freshwater inputs of approximately 50 L per day were required to maintain system volume. To meet oxygen demands in the absence of water circulation, aerators with double the capacity (80 $L \cdot min^{-1}$) were used to maintain DO levels at around 7 $mg \cdot L^{-1}$ in decoupled fish tanks.

Solids management strategies evolved between the two study years. In Year 1, solid waste was partially removed by dual-layer foam filtration (coarse and fine) prior to water entering the hydroponic beds. In Year 2, the solids removal process was enhanced by incorporating a 110-L radial flow settler (RFS) before the foam filters. Further technical details on system layout and equipment upgrades are available in our previous publications (113, 120).

5.2.3 System operation

Fish were fed twice daily, once in the early morning (7–8 a.m.) and again in the early afternoon (1–2 p.m.). Juvenile tilapia weighing less than 100 g received Cargill Triton-4512 feed, formulated with 45% crude protein, 12% crude fat, 3% crude fiber, and 1% phosphorus. As fish surpassed the 100 g threshold, their diet was transitioned to Cargill Triton-3606, containing 36% crude protein, 6% crude fat, 4% crude fiber, and 1% phosphorus (52). Feeding rates were adjusted according to fish size, beginning at 3% of body weight for fingerlings and gradually tapering to approximately 1.5% as the fish matured. Feed quantities were adjusted monthly based on fish mass sampling data, temperature, and observed feeding behavior (53). In some tanks, lower feeding activity was noted, which led to a reduction in feed input.

Water chemistry was managed to maintain optimal conditions for fish and microbial health. pH was stabilized near 7.0 through daily dosing of either 3 M hydrochloric acid or calcium carbonate, as needed (Rezaei et al., 2026). Potassium, a commonly limiting nutrient in aquaculture systems, was supplemented via the make-up water to achieve a target concentration of 100 mg L^{-1} in the fish tanks. Mechanical maintenance included twice-daily cleaning of foam filters and biweekly discharge of accumulated sludge from the radial flow settler (RFS) through its bottom outlet.

5.2.4 Fish growth measurements

Fish growth was monitored monthly by randomly sampling and weighing 10 fish per system in their wet state to determine average body mass. At the end of each grow-out cycle, the total biomass of harvested fish from each tank was recorded. In addition to biomass measurements,

growth performance was evaluated using two standard metrics: the apparent feed conversion ratio (FCRa, Eq. 1) and the specific growth rate (SGR, Eq. 2), calculated as follows:

FCRa = feed offered (g, dry basis) / biomass increase (g, wet basis) Eq. 1

SGR (%/day) = (ln final fish weight – ln initial fish weight) × 100 / days Eq. 2

5.2.5 Water quality monitoring

Total suspended solids (TSS) in fish tanks were monitored every other day by measuring optical density (OD) at 550 nm. To establish a TSS–OD calibration curve, suspended solids were centrifuged (4696 × g, 10 min), oven-dried, and weighed, following the method of Bertrand-Krajewski (56). pH levels were recorded daily using a Bluelab Metcombo meter and adjusted as needed to 6.5. Dissolved oxygen (DO) and water temperature were measured every other day using a Milwaukee MW600 portable DO meter. To evaluate nitrification dynamics over time, water samples were collected from each fish tank every other day, filtered through 0.2 µm nylon microfiber filters (VWR, USA), and stored at –20 °C until analysis. Concentrations of nitrate and nitrite were determined by high-performance liquid chromatography (HPLC) using a Prominence LC system (Shimadzu, Japan) equipped with an anion exchange column (Dionex AS22, ThermoFisher Scientific, USA) and an ion suppressor (Dionex AERS 500). Ammonium concentrations were measured using cation chromatography with a Dionex CS16 column and a CERS 500 ion suppressor (ThermoFisher Scientific, USA) (209).

5.2.6 Microbial analyses

Microbial community profiling was conducted using biofloc and biofilm samples collected from the fish tanks at two key time points: May (spring trial) and October (fall trial), during both years

of operation. Suspended biofloc was sampled by collecting 13 mL of tank water, followed by centrifugation at 4696 × g for 10 minutes to concentrate microbial biomass. Biofilm samples were obtained by scraping all four interior tank walls. The supernatant was discarded, and the biomass pellets were stored at –20 °C until further processing.

Genomic DNA was extracted from the biomass pellets using the FastDNA Spin Kit (MP Biomedicals, USA), and DNA concentrations were quantified using the QuantiFluor dsDNA Quantification Kit (Promega, USA) to confirm sufficient input for sequencing. Samples were sent to the Molecular Research Laboratory (MRDNA Lab, Texas, USA) for high-throughput sequencing of the bacterial 16S rRNA gene (primers 515F–806R) and eukaryotic 18S rRNA gene (primers 1391F and EukBr) using the Illumina MiSeq platform. Sequence data were processed via the external laboratory's in-house bioinformatics pipeline, including demultiplexing, denoising, and taxonomic classification into zero-radius operational taxonomic units (ZOTUs) using a custom-curated reference database. All raw sequence data have been deposited in the NCBI Sequence Read Archive (SRA) under BioProject accession numbers BioProject PRJNA1193631, PRJNA1426748, PRJNA1333965, and PRJNA1335545.

5.2.7 Fish and biofloc composition

Protein, lipid, and fatty acid profiles were analyzed in in biofloc and fish tissue samples. Soluble protein concentration in aqueous samples was determined using the Pierce BCA Protein Assay Kit (Thermo Scientific, Waltham, MA, USA). Crude protein content was estimated by measuring total nitrogen using the HACH Total Nitrogen Kit, applying a standard conversion factor of 6.25 to calculate protein content from nitrogen values. Lipid extraction followed the Folch method. Approximately 20 mg of freeze-dried fish fillet or biofloc biomass was placed into 1.5 mL screw-

cap tubes along with zirconia microbeads. Each sample was mixed with 1.5 mL of Folch reagent (chloroform:methanol, 2:1 v/v) and homogenized by bead disruption. Subsequently, 1.2 mL of 0.9% NaCl was added to promote phase separation, and samples were centrifuged to isolate the organic (chloroform) layer. The 2 mL of lipid-rich chloroform phase was transferred into amber vials and evaporated to dryness for gravimetric quantification of crude lipid content.

Fatty acid profiling was conducted using gas chromatography–mass spectrometry (GC-MS) with an Agilent 8890 GC coupled to a 5977 MS detector. A 500 µL aliquot of the chloroform extract was combined with 50 µL of internal standard (1 µg/µL nonadecanoic acid in chloroform), evaporated under nitrogen, and derivatized with 3 mL of 1 M methanolic HCl after resuspension in 1 mL of hexane. Samples were heated at 100 °C for 1 hour to complete transesterification, cooled, and neutralized with 3 mL of 6% Na_2CO_3 solution. After phase separation, the upper hexane layer containing fatty acid methyl esters (FAMEs) was transferred to GC autosampler vials. FAMEs were analyzed using a DB-23 capillary column (Agilent J&W) under splitless injection mode. Helium was used as the carrier gas at a flow rate of 1.0 mL/min. A 1 µL injection volume was applied with oven temperature programmed to ramp from 120 °C at 1.5 °C/min to 198 °C, holding for 8 minutes. Chromatographic peaks were identified based on mass spectra, with emphasis on omega-3 fatty acid content.

Additionally, 50 mL of homogenized wet tilapia tissue was submitted to the Analytical Environmental Laboratory (210) for quantification of geosmin and 2-methylisoborneol (201), compounds known to influence fillet flavor quality.

5.2.8 Statistical analyses

All treatments were independently replicated across three aquaponic systems (n = 3), yielding a total of 12 systems. Statistical analyses were performed in R (v4.3.1), applying multiple regression

models to assess the effects of system configuration (coupled vs. decoupled) and fish tank light exposure (light vs. dark) as fixed factors. Sampling time was included as a random factor for time-series data. Time-course analyses of variance (ANOVA) were conducted using the "car" package, followed by Tukey's Honest Significant Difference (HSD) post hoc test via the "agricolae" package to determine significant differences ($p < 0.05$) in fish growth performance, microbial abundance, and biofloc nutritional composition (lipid, protein, and fatty acid content). Descriptive statistics, including means and standard deviations, were computed using Microsoft Excel.

5.3 Results and Discussion

5.3.1 Light and coupling interactions supported higher fish yield

In Year 1, both light exposure and system coupling enhanced fish growth (Figure 5.1; Table 5.1). The light-coupled (LC) and light-decoupled (LD) systems produced higher fish yields (551 and 434 g, respectively) compared with the dark-coupled (DC; 434 g) and dark-decoupled (DD; 376 g) systems. Mortality rates in year 1 were <2% in all systems from March to October. However, in November, two mass mortality events occurred in two LD systems (other systems had no fish deaths). The cause of these events was not definitively established despite significant investigative effort, as reported previously (Rezaei et al., 2026). Water quality and disease were unlikely causes based on high frequency monitoring and pathological assessment; however, it was determined that fish in these systems were eating trailing tomato vines overhanging their tanks, and this issue was later corrected.

Overall, coupled systems supported greater fish growth than decoupled systems, likely due to improved water clarity, which facilitated more stable feeding conditions and reduced physiological stress on fish. While biofloc can provide nutritional benefits for tilapia, excessive TSS may impair growth. Previous studies observed reduced performance and lower carcass quality

in biofloc systems with elevated settleable solids (>75 mg L^{-1}), particularly under high stocking densities (113, 201, 211). TSS levels in the LC, LD, DC, and DD systems averaged 66, 395, 18, and 206 mg L^{-1} in year 1 and 69, 351, 45, and 310 mg L^{-1} in year 2. This highlights the importance of managing TSS to strike a balance between the dietary value of biofloc and its potential negative physiological impacts.

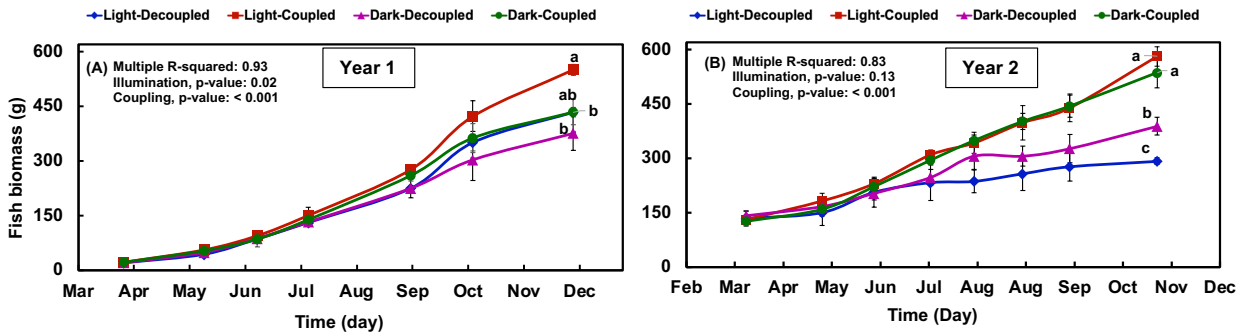

Figure 5.1 Fish biomass accumulation over time in (A) Year 1 and (B) Year 2 across the four aquaponic system treatments: light-coupled (LC), light-decoupled (LD), dark-coupled (DC), and dark-decoupled (DD). Values represent average individual fish mass (g) measured monthly. Error bars denote standard deviation (n = 3). Lowercase letters (a, b, c, etc.) indicate statistically significant differences between treatments at the final sampling point ($p < 0.05$). Figures without letters did not show significant differences.

Table 5.1 Summary of final fish biomass (g), specific growth rate (SGR), feed conversion ratio (FCR), and total feed given (Kg) for each aquaponic treatment over two production years. Values are expressed as mean ± standard deviation (n = 3). Treatments sharing the same letter within a column are not significantly different ($p < 0.05$) based on Tukey's HSD test.

	Year 2023				Year 2024			
	LD	**LC**	**DD**	**DC**	**LD**	**LC**	**DD**	**DC**
Fish yield (g)	433.89 ± 13.44 b	550.69 ± 14.87 a	376.22 ± 47.23 b	434.25 ± 35.46 b	292 ± 26.23 c	581.33 ± 42.16 a	388.67 ± 25.01 b	536.67 ± 9.45 a
Specific growth rate (%/day)	1.23 ± 0.02	1.32 ± 0.05	1.18 ± 0.07	1.21 ± 0.02	0.33 ± 0.08	0.62 ± 0.04	0.42 ± 0.02	0.61 ± 0.08
Feed conversion ratio	1.28 ± 0.1	1.18 ± 0.03	1.38 ± 0.04	1.41 ± 0.07	2.55 ± 0.27	1.69 ± 0.12	2.1 ± 0.08	1.79 ± 0.28
Feed given (Kg)	20.05 ± 0.65	25.02 ± 1.04	19.37 ± 3.25	22.43 ± 0.93	15.87 ± 2.02	26.2 ± 1.21	19.6 ± 0.53	26.55 ± 3.46

The positive effect of light on fish growth could be attributed to both direct and indirect mechanisms. Light can directly influence fish physiology and behavior, while also fostering a shift in the microbial community toward a more photoautotrophic composition. This transition, driven by sunlight exposure, enhances algal proliferation within the biofloc, increasing its nutritional

value and availability as a supplemental food source for tilapia (61, 62, 113). Additionally, natural photoperiod and elevated light intensity have been shown to regulate metabolic rhythms and feeding activity in fish, further contributing to the growth advantages observed in illuminated systems (78, 79).

In the light systems, fish were frequently observed grazing on suspended green biofloc and biofilm formed on the tank walls. It was hypothesized that this green biofloc provided an additional lipid- and protein-rich food source for fish (see Section 5.3.2). Consistent with this hypothesis, fish in the light systems exhibited higher SGR and lower FCR, indicating faster growth and greater biomass gain per unit of feed supplied (Table 5.1). These metrics suggest that fish in the light systems benefited from supplementary nutritional inputs beyond formulated feed. However, more efficient feed utilization in these systems due to physiological changes is also a likely driver.

In Year 2, fish growth patterns partially differed from those observed in Year 1, although system coupling continued to play a clear beneficial role. Coupling increased fish yield by approximately 64%, compared with a 22% increase in the first year. The LC system once again produced the highest fish biomass (581 g), benefiting from the combined advantages of light exposure and system coupling. In contrast, the LD system yielded the lowest fish production (292 g), marking around a 33% decline compared to Year 1. Mortality rates of <1% were observed across all systems in year 2.

The noticeable reduction in performance in the decoupled systems was associated with unstable nitrification and elevated ammonia concentrations between June and September which are peak production months for tilapia (Table S5.1). Ammonia was monitored daily using in-tank ammonia indicator disks before feeding. As shown in Table S5.1, average ammonium concentrations reached 15.34 and 19.43 mg L^{-1} in the LD and DD systems, respectively, with an

average pH of 6.7, a range that allowed partial conversion of ammonium to toxic unionized ammonia. To prevent ammonia accumulation and fish mortality, feed inputs were intentionally reduced in these systems as an operational control strategy. No corrective measures, such as bioaugmentation or targeted microbial manipulation, were applied during this period, as the objective was to initially observe system behavior under natural recovery conditions. The concurrent reduction in nitrifier populations and TSS during this period was also reported in our previous study (120). To restore nitrification capacity, a one-time re-inoculation was performed in mid-September using fresh sludge collected from clarifiers, following principles commonly applied in activated sludge wastewater treatment. This intervention increased nitrifier abundance, particularly *Nitrospira*, and effectively reduced ammonia concentrations (Table S5.1, Figure 5.2) (120). However, the upshot of this period of prolonged feed reduction was lower fish growth in LD systems in year 2. DD systems also experienced elevated ammonia-N levels (Table S5.1), similar to the LD systems but pH remained lower in these systems, likely due to a lack of algal photosynthetic activity. Photosynthesis removes CO_2 and raises water pH, thereby increasing the level of unionized ammonia. In contrast, the closed-loop configuration of the coupled systems facilitated stable nitrification by utilizing the grow beds as biofilters. During the summer months, average ammonia-N concentrations in the LC and DC systems remained relatively low at 8.1 and 7.4 mg L^{-1}, respectively, approximately 60% lower than those in the decoupled systems.

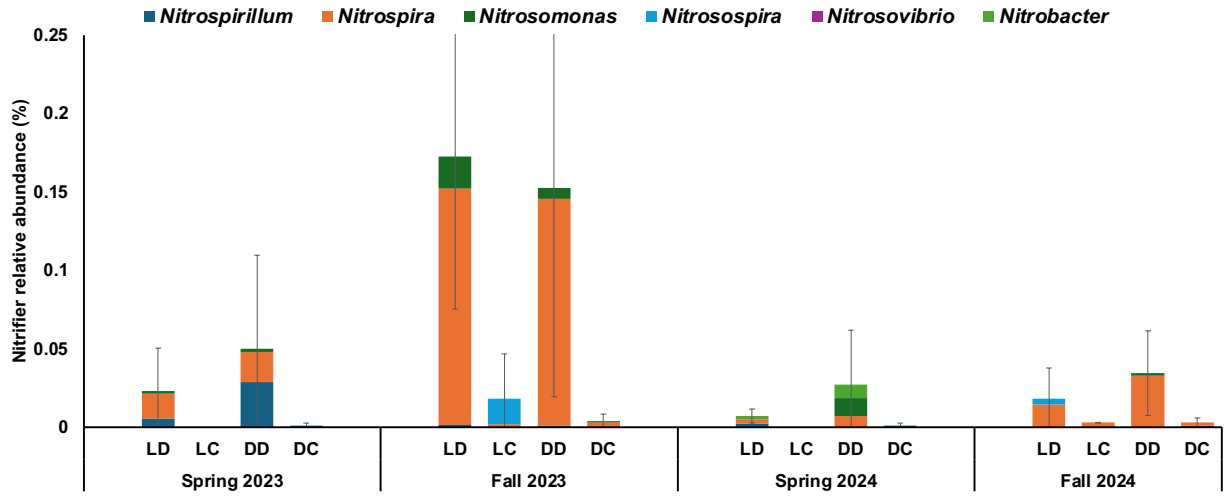

Figure 5.2 Relative abundance of key nitrifying genera across treatments during the spring and fall trials of Year 1 (2023) and Year 2 (2024). Error bars represent standard deviation (n = 3). Lowercase letters (a, b, c, etc.) indicate statistically significant differences between treatments ($p < 0.05$). Figures without letters did not have treatments that were statistically different from each other.

Interestingly, as shown in Figure 5.2, nitrifier abundance in Year 1 was higher, particularly in the decoupled systems, reaching approximately 0.04% and 0.15% during the spring and fall, respectively. In contrast, nitrifier abundance in Year 2 was significantly lower, at 0.02% and 0.04% during the spring and fall. This reduction possibly resulted in the unstable nitrification and ammonia accumulation in the second year, which was more pronounced in the decoupled systems because these systems relied solely on fish-tank biofloc for nitrification. This highlights the limitations of relying solely on suspended biofloc for ammonia removal, as seen in the decoupled systems, and demonstrates the advantage of attached-growth microbial communities in the gravel-based grow plant beds in sustaining more stable nitrification.

Fish continuously excrete ammonia, which must be rapidly converted into nitrate to avoid the accumulation of toxic un-ionized ammonia (NH_3), a form nearly 300 times more harmful to fish than ammonium (NH_4^+), contributing to oxidative stress, tissue damage, and impaired growth (212). Nitrifying bacteria, ammonia and nitrite oxidizers, typically colonize biofilters and root

zones, converting ammonia into nitrate while enhancing water quality and plant nutrition (95). However, these microbes are highly sensitive to environmental factors such as temperature, pH, light, and organic load, making them vulnerable to seasonal fluctuations (95, 213). Together, these challenges illustrate the importance of establishing a resilient nitrifier community to maintain water quality and support optimal fish growth in aquaponic systems.

Despite concerns raised in previous studies regarding potential inhibitory effects of light exposure and algal proliferation on nitrification, over two years of operation, there was no significant effect of light exposure on nitrifier abundance or nitrification performance (Figure 5.2). While earlier experimental work suggested light and microalgae may suppress ammonia-oxidizing activity (206), those findings were based on short-term trials using pure cultures of specific nitrifiers under tightly controlled conditions. In contrast, our systems developed organically, supporting complex and dynamic microbial consortia more representative of real-world aquaponics. This ecological complexity may confer greater functional resilience, reinforcing the relevance of our findings for practical system design and management.

5.3.2 Light-Induced chlorophyta dominance promoted superior protein and fatty acid profiles in bioflocs

Exposing fish tanks to natural sunlight shifted the microbial community toward a photoautotrophic structure and resulted in a significantly higher abundance of Chlorophyta (green algae) in both experimental years (Figures 5.3B and 5.3D). For example, in Year 2, Chlorophyta accounted for 63% and 53% of the microbial community in the LD and LC systems, respectively, whereas their abundance in the DD and DC systems was only 0.005% and 0.29% (Table 5.2, Figure 5.3D). Biofilm was detected exclusively on the tank walls in the light systems, whereas no biofilm developed in the dark systems. Analysis of the tank wall biofilm in Year 2 showed a similar pattern,

with Chlorophyta dominating the LD system biofilm at 78% relative abundance (Table 5.2, Figure 5.3D). Although Chlorophyta were not the most abundant taxon in the LC system biofilm, they remained among the dominant groups, with a relatively consistent abundance of approximately 16% across seasons. Green water systems have been associated with enhanced feed efficiency, lower FCR, and greater biomass yields in tilapia and shrimp, primarily due to the improved nutritional quality, namely higher protein and lipid content, and increased availability of natural feed sources (77, 113, 214).

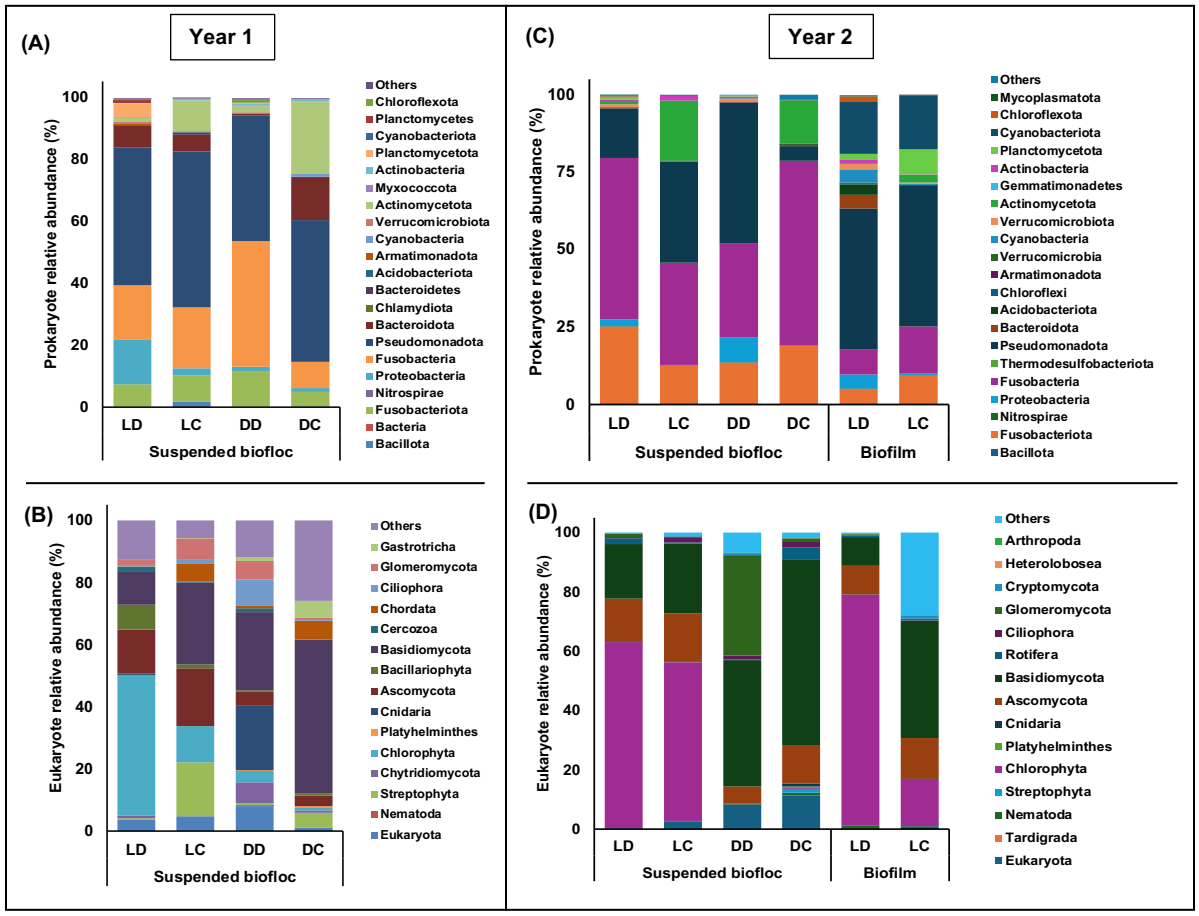

Figure 5.3 Microbial community composition at the phylum level in suspended biofloc and fish tank wall biofilm across treatments during Year 1 and Year 2. Panels show relative abundance of dominant microbial taxa based on (A) 16S rRNA and (B) 18S rRNA gene sequencing for Year 1, and (C) 16S rRNA and (D) 18S rRNA datasets for Year 2. Taxa representing less than 1% relative abundance are grouped under "Others." Biofilm developed only in the light-exposed systems and was sampled exclusively in Year 2.

Table 5.2 Relative abundance (%) of Chlorophyta, Cyanobacteria, and Actinobacteria (off-flavor producing bacteria) in suspended biofloc and tank wall biofilm across treatments during Year 1 and Year 2. Biofilm samples were collected only in Year 2. Values represent means ± standard deviation (n = 3).

	Year 1				**Year 2**				**Year 2**	
	Suspended biofloc				**Suspended biofloc**				**Biofilm**	
	LD	**LC**	**DD**	**DC**	**LD**	**LC**	**DD**	**DC**	**LD**	**LC**
Chlorophyta	45.27 ± 32.05	11.6 ± 1.98	3.7 ± 5.77	1.05 ± 0.92	62.74 ± 23.79	53.42 ± 44.67	0.005 ± 0.005	0.29 ± 0.35	77.67 ± 13.91	16.02 ± 6.7
Cyanobacteria	0.03 ± 0.06	0 ± 0	0 ± 0	1.01 ± 1.75	0.03 ± 0.03	0 ± 0	0 ± 0	0 ± 0	4.29 ± 6.79	0.25 ± 0.4
Actinobacteria	0.15 ± 0.04	0.45 ± 0.69	0.61 ± 0.54	0.88 ± 0.77	0.71 ± 0.41	1.59 ± 1.38	0.58 ± 0.22	0.24 ± 0.11	1.1 ± 1.25	0.13 ± 0.03

Table 5.3 summarizes the soluble protein, crude protein, and crude fat content of suspended biofloc and tank wall biofilm. Because TSS concentrations in the coupled systems were very low, these compositional parameters were not measurable in those systems; therefore, analyses were conducted only for the decoupled systems. In both years, green biofloc in the light systems exhibited significantly higher soluble protein and crude protein content compared with the brown biofloc in the dark systems. Soluble protein and crude protein reached 14.4% and 27%, respectively, in the green biofloc, whereas corresponding values in the brown biofloc were lower at 10.5% and 21.4% ($p = 0.017$ and 0.016). In addition, crude fat content was higher in the green biofloc (9.2%) than in the brown biofloc (5.4%) ($p < 0.001$).

Table 5.3 Soluble protein, crude protein, and crude fat content (% dry biomass) of suspended biofloc and biofilm biomass in Year 1 and Year 2. Biofilm samples were collected only from light-exposed systems (LD and LC) in Year 2. Due to low total suspended solids (TSS) concentrations in the coupled systems, these compositional parameters were not measurable in those treatments. Different lowercase letters within each row indicate statistically significant differences between treatments ($p < 0.05$).

	Year 1		**Year 2**			
	Suspended biofloc		**Suspended biofloc**		**Biofilm**	
	LD	**DD**	**LD**	**DD**	**LD**	**LC**
Soluble protein (% dry biomass)	17.26 a	12.95 b	11.51 a	8.14 b	10.61 a	11.14 a
Crude protein (% dry biomass)	31.11 a	25.48 b	22.94 a	17.23 b	25.77 a	26.17 a

Crude fat (% dry biomass)	8.94 a	3.87 b	9.51 a	6.91 b	11.83 a	10.86 a

Biofilm samples were collected only in Year 2 and showed higher crude protein and crude fat contents compared with suspended biofloc (Table 5.3). In the LD system, crude protein and crude fat in the biofilm reached 25.8% and 11.8%, respectively, whereas the corresponding values in the suspended biofloc were 22.9% and 9.5%. The elevated protein and lipid content of the green biofloc, along with the greater availability of nutritionally rich biomass from tank wall biofilms in the light-exposed systems, may have contributed to enhanced fish yield. However, these differences did not translate into changes in fish fillet lipid or protein composition, as no significant differences were observed among treatments in either year (Table S5.2).

Fatty acid profile analysis further showed that green biofloc in the light systems contained higher total fatty acid methyl esters (FAME) than brown biofloc in the dark systems in both years ($p = 0.04$)(Table 5.4). Total FAME content in the green biofloc was 3.7% and 3.3% in Years 1 and 2, respectively, compared with 2.77% and 2.63% in the brown biofloc. Green biofloc also exhibited higher levels of unsaturated fatty acids, including both monounsaturated fatty acids (MUFAs) and polyunsaturated fatty acids (PUFAs). In Year 1, MUFA and PUFA contents were 0.64% and 0.97% in the green biofloc, compared with 0.44% and 0.38% in the brown biofloc ($p = 0.02$ and 0.03). Similarly, omega-3 fatty acids and essential fatty acids such as 18:2n-6 and 18:3n-3 were significantly higher in the green biofloc than in the brown biofloc in both years ($p < 0.05$). In Year 2, 18:2, 18:3, and total omega-3 fatty acids accounted for 0.32%, 0.29%, and 0.37% in the green biofloc, respectively, whereas corresponding values in the brown biofloc were 0.18%, 0.09%, and 0.11% ($p < 0.001$). These findings were consistent with our initial hypothesis that light exposure in fish tanks would enhance the nutritional quality of biofloc.

The elevated protein and lipid content observed in green biofloc aligns with previously reported values for microbial floc biomass, which typically ranges between 30–40% crude protein and 2–15% lipid. The lipid content of green biofloc in this study falls well within the optimal dietary lipid range for tilapia (approximately 5–12%), supporting its potential as a nutritionally appropriate feed supplement. Previous studies have also demonstrated that exposure to light or balanced photoperiods can significantly enhance the nutritional quality of biofloc. Hu et al. reported that a 12L:12D photoperiod produced biofloc with the highest crude protein content (~41.8%) in an algal-bacterial system, suggesting that photoautotrophic activity plays a key role in enriching biofloc composition (198). Similarly, Khanjani et al. found that biofloc produced under the same photoperiod contained 11% more crude protein and 9% more lipid than biofloc maintained under continuous darkness (20).

Table 5.4 Fatty acid profiles (% of dry biomass) of suspended biofloc and tank wall biofilm across light (LD) and dark (DD) systems in Year 1 (2023) and Year 2 (2024). Biofilm samples were only collected from light-exposed systems (LD and LC) in Year 2. Fatty acids are reported individually and grouped as saturated (SFA), monounsaturated (MUFA), and polyunsaturated (PUFA), with key omega-3 and omega-6 precursors (18:3n-3 and 18:2n-6) highlighted. Total fatty acid methyl esters (FAME) represent the sum of all measured fatty acids. Due to low total suspended solids (TSS) in coupled systems, suspended biofloc composition was not measured for LC and DC. Different lowercase letters within each row indicate statistically significant differences between treatments ($p < 0.05$).

	Year 1		**Year 2**		**Year 2**	
	LD	**DD**	**LD**	**DD**	**LD**	**LC**
Fatty acids	**Suspended biofloc**		**Suspended biofloc**		**Biofilm**	
C14:0	0.07 ± 0.03	0.05 ± 0.01	0.06 ± 0.01	0.05 ± 0.01	0.14 ± 0.03	0.1 ± 0.04
C14:0	0.12 ± 0.01	0.08 ± 0	0.09 ± 0.03	0.12 ± 0.07	0.1 ± 0.02	0.12 ± 0.02
C16:0	1.02 ± 0.09	0.76 ± 0.02	0.9 ± 0.17	0.71 ± 0.08	1.26 ± 0.07	1.3 ± 0.05
C16:1	0.06 ± 0.02	0.02 ± 0	0.04 ± 0.01	0.02 ± 0	0.09 ± 0.04	0.08 ± 0.02
C16:1	0.18 ± 0.03	0.11 ± 0.02	0.12 ± 0.07	0.12 ± 0.04	0.37 ± 0.22	0.28 ± 0.14
C16:2	0.09 ± 0.03	0.04 ± 0.01	0.08 ± 0.02	0.04 ± 0.01	0.09 ± 0.03	0.14 ± 0.09
C16:3	0.02 ± 0.01	0 ± 0	0.04 ± 0.01	0 ± 0	0.06 ± 0.04	0.06 ± 0.04
C16:4	0.04 ± 0.02	0 ± 0	0.04 ± 0.02	0 ± 0	0.11 ± 0.08	0.08 ± 0.03
C18:0	0.86 ± 0.04	1.07 ± 0.04	0.77 ± 0.15	0.86 ± 0.17	0.66 ± 0.05	0.64 ± 0.05

C18:1	0.3 ± 0.04	0.21 ± 0.04	0.28 ± 0.06	0.21 ± 0.04	0.19 ± 0.04	0.15 ± 0.04
C18:1	0.1 ± 0	0.1 ± 0.01	0.11 ± 0.05	0.13 ± 0.03	0.11 ± 0.03	0.15 ± 0.05
C18:2	0.35 ± 0.09	0.18 ± 0.04	0.32 ± 0.07	0.18 ± 0.03	0.3 ± 0.03	0.27 ± 0.06
C18:3	0.02 ± 0.01	0 ± 0	0.02 ± 0.01	0.01 ± 0	0.03 ± 0.01	0.03 ± 0.03
C18:3	0.35 ± 0.13	0.1 ± 0.03	0.27 ± 0.09	0.08 ± 0.03	0.53 ± 0.32	0.66 ± 0.23
C20:4	0.02 ± 0.02	0 ± 0	0.02 ± 0.01	0.01 ± 0.01	0.04 ± 0.02	0.04 ± 0.01
C20:4	0.05 ± 0.01	0.04 ± 0.01	0.06 ± 0.02	0.08 ± 0.03	0.08 ± 0.07	0.06 ± 0.05
C20:5	0.02 ± 0	0.02 ± 0	0.03 ± 0.01	0.03 ± 0.01	0.05 ± 0.02	0.06 ± 0.03
Total FAME	3.68 ± 0.49 a	2.77 ± 0.12 b	3.25 ± 0.6 a	2.63 ± 0.33 a	4.22 ± 0.42 a	4.22 ± 0.49 a
Sum SFAs	2.07 ± 0.15 a	1.95 ± 0.04 a	1.82 ± 0.33 a	1.74 ± 0.22 a	2.16 ± 0.14 a	2.16 ± 0.11 a
Sum MUFAs	0.64 ± 0.07 a	0.44 ± 0.07 b	0.55 ± 0.11 a	0.47 ± 0.08 a	0.77 ± 0.26 a	0.66 ± 0.16 a
Sum PUFAs	0.97 ± 0.31 a	0.38 ± 0.04 b	0.87 ± 0.21 a	0.42 ± 0.11 b	1.29 ± 0.42 a	1.4 ± 0.39 a
Sum 18:2n-6	0.35 ± 0.09 a	0.18 ± 0.04 b	0.32 ± 0.07 a	0.18 ± 0.03 b	0.3 ± 0.03 a	0.27 ± 0.06 a
Sum 18:3n-3	0.35 ± 0.13 a	0.1 ± 0.03 b	0.27 ± 0.09 a	0.08 ± 0.03 b	0.53 ± 0.32 a	0.66 ± 0.23 a
Omega 3	0.43 ± 0.16 a	0.12 ± 0.02 b	0.37 ± 0.12 a	0.11 ± 0.04 b	0.74 ± 0.43 a	0.86 ± 0.29 a
Omega 6	0.42 ± 0.11 a	0.23 ± 0.05 a	0.4 ± 0.08 a	0.26 ± 0.06 b	0.42 ± 0.07 a	0.36 ± 0.09 a

The enriched fatty acid profile of green biofloc observed in this study is also consistent with findings from Hu et al., who demonstrated that moderate light exposure (12L:12D photoperiod) promoted the accumulation of essential unsaturated fatty acids in algal-bacterial bioflocs (198). Their analysis showed that bioflocs produced under this balanced light regime contained a more diverse and complete spectrum of PUFAs and MUFAs, including critical essential fatty acids such as linoleic (18:2) and linolenic acid (18:3), which are vital for fish growth and physiological function (198). Although our study did not manipulate photoperiod length, the natural light exposure in our system appeared to promote similar trends, with green biofloc exhibiting elevated levels of both total and unsaturated FAMEs relative to dark-grown floc.

The presence of essential fatty acids, particularly linoleic (18:2n-6) and α-linolenic acid (18:3n-3), in the green biofloc is nutritionally significant, as tilapia and other freshwater fish are unable to

synthesize these PUFAs de novo. These fatty acids serve critical roles in cell membrane integrity and eicosanoid production, and dietary requirements for linoleic acid in tilapia are estimated at ~0.5–1.0% of total intake. Although the precise requirement for α-linolenic acid is less defined, its inclusion is known to support growth and enhance tissue fatty acid profiles. Importantly, tilapia possess the enzymatic machinery to bioconvert these C18 precursors into long-chain n-3 and n-6 polyunsaturated fatty acids such as EPA, DHA, and arachidonic acid. Prior research by Chen et al. showed efficient conversion of dietary ALA into DHA in Nile tilapia, confirming the utility of precursor-based fatty acid supplementation (118). Thus, the elevated levels of 18:2 and 18:3 in green biofloc not only fulfill tilapia's essential fatty acid requirements but also supply substrates for in vivo synthesis of higher-value PUFA. Despite this promise, the increased levels of essential fatty acids in the light-exposed biofloc and biofilms did not affect the fish fillet fatty acid profile significantly (Table S5.3). The rearing densities in these systems were high, and as a result, the majority of fish nutrition was supplied by pelletized feed. At only 700 L of volume, the fish tank had limited capacity to produce significant quantities of algal biomass. Algal production rates were not measured and in fact were not possible to measure as tilapia kept eating the material. Consequently, future studies should be designed to explore the specific production and consumption rates of green biofloc and biofilms in aquaculture systems. Prior studies in which the algae *Schizochytrium* was incorporated into pelletized feeds at an inclusion rate of 8.77% resulted in a nearly 3-fold increase in tilapia omega-3 fat contents (215). This is a fairly high rate of incorporation and *Schizochytrium* is particularly high in omega-3 fats among algae (~27% of total fatty acids). Thus, high levels of feed displacement with particularly nutritious algae are likely required to improve the fat profile in tilapia fillets.

5.3.3 Light exposure did not compromise fish flavor quality

Although light exposure confers numerous benefits in aquaculture systems, it raises potential concerns regarding the stimulation of microbial taxa implicated in off-flavor compound production. In particular, photosynthetic bacteria such as cyanobacteria are well-documented producers of geosmin and 2-methylisoborneol (201), volatile organic compounds responsible for earthy and musty off-flavors in aquaculture species, including tilapia (27, 28).

Across all treatments, cyanobacterial abundance remained consistently low. In suspended biofloc, cyanobacteria comprised <0.03% of the community in light-exposed systems and <1% in dark treatments, with slightly elevated levels in the latter (Figure 5.3A, C, and Table 5.2). In biofilms, relative abundance reached 4% in the LD treatment and 0.25% in the LC treatment (Table 5.2; Figure 5.3C). Actinobacteria and Myxobacteria are not photosynthetic bacteria but they are also known to produce 2-MIB and geosmin in aquaculture systems (216). Actinobacteria were detected at low levels (< 0.6% on average) with no significant differences among treatments, while Myxobacteria were not detected in any condition, indicating that light exposure did not facilitate the proliferation of canonical geosmin- or MIB-producing taxa. The dominance of photoautotrophic algae in illuminated systems likely imposed competitive exclusion on these microbes. Despite the capacity of over 70 cyanobacterial species to synthesize geosmin (27), environmental filtering and interspecific interactions may have constrained their establishment.

To further assess the potential for off-flavor compound production, we examined the relative abundances of key taxa with members known to produce geosmin- and 2-MIB (Figure S5.2). Within this group, *Oscillatoria* and *Haliangium* were the most prominent in year 1. In Year 2, *Streptomyces* dominated the suspended biofloc community. In biofilm samples, *Oscillatoria* and *Phormidium* were the most abundant genera associated with off-flavor potential. However, these

genera remained at low relative abundances across all treatments, and no statistically significant differences were observed between light and dark systems. These results reinforce our earlier conclusion that light exposure and photoautotrophic dominance did not promote the proliferation of microbial taxa known to generate geosmin or MIB.

Quantification of off-flavor compounds further proved that phototrophic community development did not negatively impact fish sensory quality (Figure 5.4). Average geosmin and 2-MIB concentrations in tilapia fillets remained low across all treatments and consistently below human sensory thresholds. Owing to their high lipophilicity, both compounds bioaccumulate readily in fish muscle via gill, skin, and gastrointestinal uptake (217, 218). However, concentrations remained well below the widely accepted consumer rejection threshold of 200 ng/kg (219), indicating that light exposure did not induce microbial pathways leading to off-flavor accumulation. Reported sensory thresholds for these compounds vary by species and matrix. For instance, geosmin thresholds range from 250 ng/kg to 900 ng/kg in rainbow trout, while 2-MIB thresholds are typically near 700 ng/kg (220, 221).

In Year 1, 2-MIB concentrations in fish fillets from the DC system were elevated (172 ng/kg), although not statistically significant, compared to other systems, which remained below 32 ng/kg. This high level was driven by one system (out of three replicates) that had fish with 299 ng/kg of 2-MIB while another DC system had 123 ng/kg of 2-MIB. Redundancy analysis (RDA) revealed that higher 2-MIB concentrations in DC were associated with the genera *Actinomyces* and *Streptomyces* (Figure 5.5). In contrast, Year 2 showed elevated geosmin concentrations in several replicates from the LD system, with RDA analysis indicating a positive correlation with *Oscillatoria*. Overall, in Year 1, 2-MIB levels were positively correlated with *Actinomyces* (p = 0.01) and *Streptomyces* (p = 0.02), while geosmin levels correlated with *Nocardia* (p = 0.02) and

Rhodococcus (p = 0.04). In Year 2, 2-MIB was strongly associated with *Pseudonocardia* (p = 0.001), and geosmin again showed correlation with *Oscillatoria* (p = 0.01). No significant correlations were found between geosmin/MIB and any putative eukaryotic off-flavor-producing microbes (Figure S5.3).

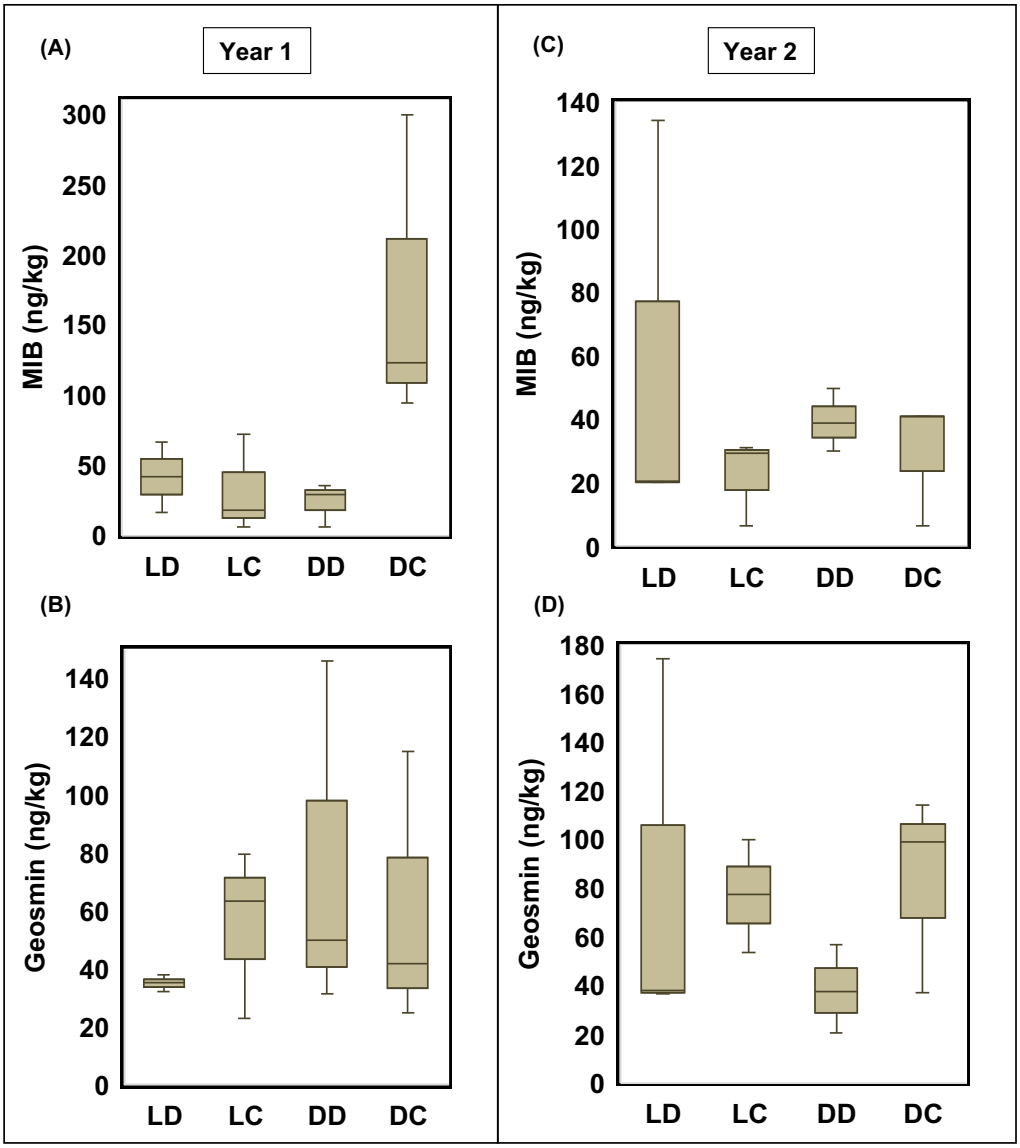

Figure 5.4 Concentrations of off-flavor compounds 2-methylisoborneol (201) (A, C) and geosmin (B, D) in fish fillets across treatments Year 1 (2023) and Year 2 (2024). Data are presented as boxplots showing median, interquartile range, and whiskers for the full range (n = 3). No significant differences were found among treatments ($p > 0.05$) based on Tukey's HSD test, and measurements remained below commonly reported human sensory detection thresholds (≈1 ng/g).

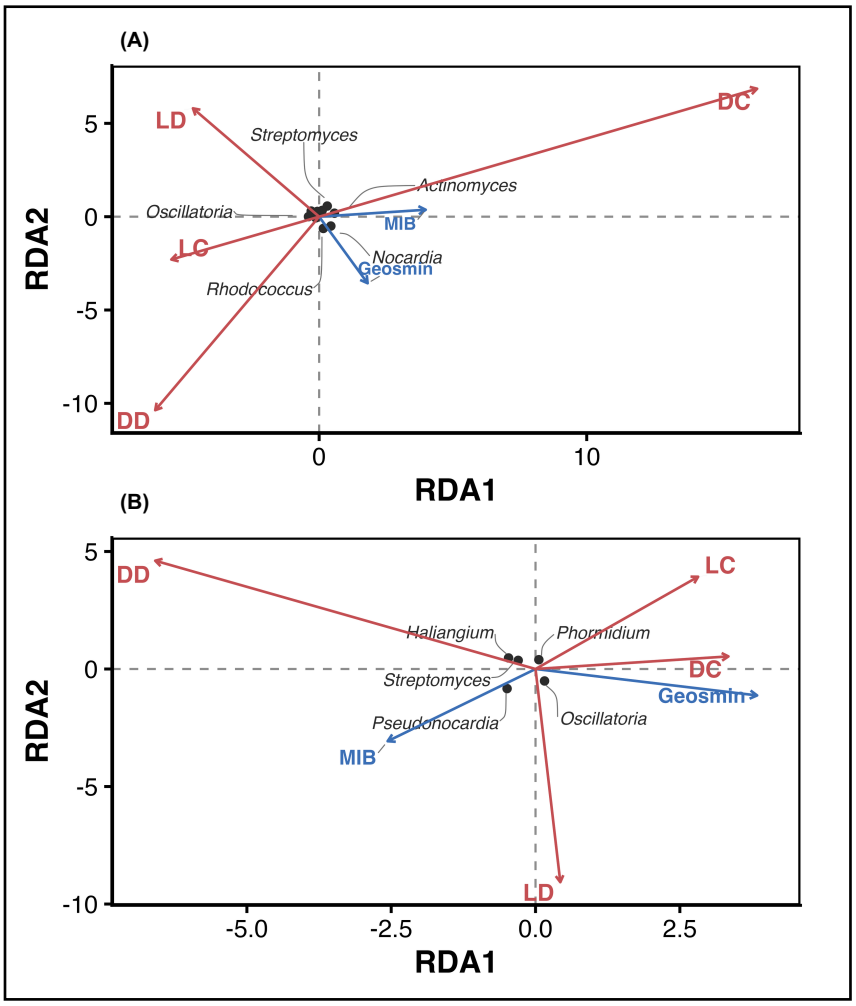

Figure 5.5 Redundancy analysis (RDA) ordination showing the relationships between candidate microbial taxa (prokaryotic community) and fish-flesh off-flavor compounds (MIB and geosmin) under different treatment conditions in (A) Year 1 (2023) and (B) Year 2 (2024). Blue arrows represent the outcome variables (MIB and geosmin), while red arrows indicate the treatment group centroids. Black points represent microbial taxa, with labels shown for those exhibiting significant associations with the response variables.

5.3.4 Putative fish pathogen effects

Bacterial fish pathogens vary depending on fish species, environmental conditions, and system characteristics. In this study, analysis was limited to the genus level for commonly reported pathogen-associated groups, including *Aeromonas, Pseudomonas, Flavobacterium, Streptococcus, Vibrio, and Edwardsiella* (222). Overall, Year 1 exhibited higher relative

abundances of *Aeromonas, Pseudomonas, and Flavobacterium* compared with Year 2 (Figure 5.6). *Vibrio* and *Edwardsiella* were not detected in either year, possibly due to the consistently high dissolved oxygen concentrations maintained throughout the experiment (approximately 7 mg/L).

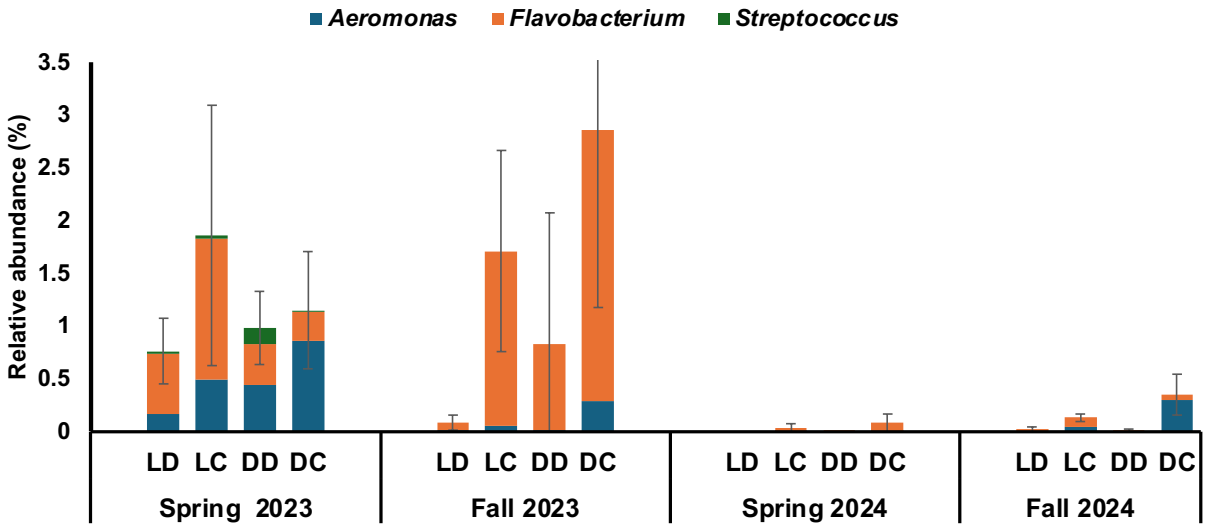

Figure 5.6 Relative abundance of putative fish pathogen genera across treatments during the spring and fall trials of Year 1 (2023) and Year 2 (2024) based on 16S sequencing. Error bars represent standard deviation (n = 3). Lowercase letters (a, b, c, etc.) indicate statistically significant differences between treatments ($p < 0.05$). Figures without letters did not have treatments that were statistically different from each other.

Although not all species within these genera are pathogenic, they were selected based on their established associations with fish disease in aquaculture systems. Specifically, approximately 17–30% of described *Aeromonas* species, 3–11% of *Flavobacterium* species, and 5–6% of *Streptococcus* species are recognized fish pathogens (223-227). Notably, well-characterized pathogenic species such as *A. hydrophila*, *F. columnare*, and *S. iniae* are responsible for frequent and economically significant outbreaks. As such, these genera remain important targets for genus-level monitoring of potential pathogen dynamics in intensive aquaculture environments (226, 228, 229).

Across both years and all seasons, pathogen abundance trended lower in illuminated systems with active photoautotrophic communities, although the regression model did not show a

statistically significant difference from dark systems ($p = 0.3$). Coupled systems showed higher relative abundances of these potential pathogen-associated genera compared with decoupled systems ($p < 0.01$). However, this pattern did not negatively affect fish growth, as coupled systems consistently achieved higher fish yields. In addition, the fish mortality event observed in the LD system during Year 1, reported previously, was not associated with observable disease symptoms, and these systems exhibited lower abundances of potential pathogenic bacteria compared with the coupled systems which had mortality rates <1%.

In addition to sequencing-based analyses, culture-based enumeration of potential bacterial pathogens was conducted throughout Year 2 to provide a complementary perspective on microbial dynamics (Figure S5.4). Samples from the fish tank suspension, tank wall biofilm, and grow bed sludge were collected biweekly during spring and fall, and plated for *Aeromonas*, *Vibrio*, and coliforms. Across all treatments and system compartments, *Vibrio* CFU counts remained consistently low and often near the detection limit, suggesting limited presence or viability under the environmental conditions of the study. This is likely why *Vibrio* was not detected in the sequencing datasets.

In contrast, *Aeromonas* and coliforms displayed consistently detectable and relatively high CFU counts throughout the monitoring period. No statistically significant differences were observed among treatments, and bacterial loads did not follow clear patterns associated with light exposure or coupling configuration. Instead, the dominant patterns were temporal. Both *Aeromonas* and coliform counts were highest during the early months of the experiment (spring), declined during mid-summer, and rose again during the fall sampling period. This U-shaped temporal trajectory paralleled fluctuations in water temperature, which were lowest in early spring,

increased through the summer, and decreased again in the fall. The correlation with water temperature was not statistically significant, however ($p = 0.14$).

The similarity between the bacterial abundance trends and temperature profiles suggests that seasonal thermal shifts may have exerted a stronger influence on pathogen proliferation than experimental treatment effects. The initial high counts in cooler spring temperatures may reflect optimal growth conditions for mesophilic bacteria, followed by heat-induced suppression during the summer peak, and a resurgence as temperatures fell back into a favorable range for these microorganisms. These observations highlight the importance of considering seasonal dynamics, particularly temperature, in pathogen risk assessments within recirculating aquaculture systems.

5.4 Conclusion

This study highlights the potential of integrating natural light exposure and system configuration as critical design levers to enhance the performance and resilience of biofloc-based aquaponics. Light exposure consistently fostered photoautotrophic biofloc communities rich in protein, lipid, and essential fatty acids, and supported higher fish growth and feed efficiency without compromising flesh quality or introducing off-flavor risks. At the same time, system coupling provided microbial stability, particularly in nitrification, by leveraging plant beds as biofilters, enabling more consistent water quality under variable seasonal conditions. While green bioflocs proved nutritious, their benefits did not translate to improved fatty acid profiles in tilapia, likely due to low levels of pelletized feed displacement. Importantly, fish tank light penetration did not lead to high levels of cyanobacteria or measurable increase in off flavor compounds in tilapia fillets. These findings underscore the importance of system-level integration in aquaponics design and suggest that coupling and illumination, when thoughtfully combined, can jointly improve fish performance while minimizing environmental and sensory trade-offs.

Chapter 6: System Design Shapes Nutrient Fate in Biofloc Aquaponics: Nitrogen and Phosphorus Mass Balances Under Different Microbial Regimes and Hydraulic Configurations

System Design Shapes Nutrient Fate in Biofloc Aquaponics: Nitrogen and Phosphorus Mass Balances Under Different Microbial Regimes and Hydraulic Configurations

Authors: Shima Rezaei[1], Qichen Wang[1], Madeline Spoor[1], Sarah Hensless[1], Kelly Sullivan[1], Mary Beth Hall[1], Ellie Malkemus[1], Grace Hohn[1], Sushil Adhikari[1], David Cline[2], Brendan Higgins[1]*

[1]Biosystems Engineering, Auburn University, Auburn, AL 36849, USA

[2]School of Fisheries, Aquaculture and Aquatic Sciences, Auburn University, Auburn, AL 36849, USA

*Corresponding author:

Brendan T. Higgins

Department of Biosystems Engineering, 203 Corley Building, Auburn, AL 36849, USA

Phone: 334-844-3532

e-mail: bth0023@auburn.edu

Abstract

Aquaponics is widely promoted as a circular food production system, yet the whole-system fate of feed-derived nutrients is rarely quantified as a function of system design. This study evaluated nitrogen (N) and phosphorus (P) mass balances in replicated aquaponic systems operated under two key design factors: biofloc metabolic regime and hydraulic configuration. Four treatments were assessed across two production batches representing different fish growth stages: photoautotrophic–coupled (PC), heterotrophic–coupled (HC), photoautotrophic–decoupled (PD), and heterotrophic–decoupled (HD). Nitrogen and phosphorus partitioning were strongly influenced by fish growth stage. In the 2025 batch, when smaller fish were cultured, 30.0–34.4% of feed N was recovered in fish biomass, compared with 10.2–15.6% in 2024 when larger fish were raised. Apparent N loss was approximately 50% lower in 2025 than in 2024. Across both years, photoautotrophic biofloc and hydraulic coupling improved nutrient recovery in fish biomass. The PC treatment consistently showed the highest N and P recovery in fish (34.4% N and 30.8% P in 2025; 15.6% N and 14.5% P in 2024). Photoautotrophic systems also retained a greater fraction of nitrogen in measurable pools (solids and dissolved water) and exhibited lower fish-tank N loss than heterotrophic systems, indicating enhanced internal nitrogen recycling. In contrast to nitrogen, phosphorus lacks a gaseous loss pathway, and most feed P was accumulated in water and solids, accounting for 55.5–66.2% of feed P in 2025 and 69.5–85.6% in 2024. Photoautotrophic systems increased solids-associated P but did not reduce dissolved phosphorus availability. The fish growth stage had minimal influence on plant nutrient recovery, which remained relatively stable across years. Plant uptake accounted for approximately 6–11% of feed N and 7–12% of feed P, with the HC treatment showing the highest nutrient recovery in plants.

Highlights

- Smaller fish had greater N and P recovery in biomass
- Photoautotrophic biofloc promoted internal N recycling and lowered apparent N losses
- Coupled operation improved nitrification and nutrient recovery in fish biomass
- Phosphorus was retained mainly in water and solids rather than plant uptake
- Greater plant bed capacity and improved solids management improve nutrient use

6.1 Introduction

Aquaponics is often described as a circular, nutrient-efficient food production technology; however, the fate of feed-derived nutrients within aquaponic systems is rarely quantified at the whole-system level (38). Feed-derived nutrients enter the system in both dissolved excretions and particulate wastes, and a substantial portion is embedded in solids that must undergo microbial mineralization before becoming available for plant uptake (8).

A central challenge in aquaponic nutrient management is that nitrogen (N) and phosphorus (P) follow fundamentally different pathways, creating distinct constraints on nutrient recovery efficiency. Nitrogen is highly dynamic and can be permanently removed from the system through microbial processes such as nitrification followed by denitrification (39, 40). In contrast, phosphorus lacks a significant gaseous loss pathway under typical aquaponic conditions. Instead, phosphorus often accumulates in solids or becomes chemically immobilized through precipitation reactions with cations such as calcium or magnesium (41). These processes can reduce the availability of soluble phosphate for plant uptake even when total phosphorus inputs are high (42).

System design and associated microbial communities strongly influences these nutrient pathways. Biofloc-based aquaculture systems rely on dense microbial aggregates that assimilate dissolved nutrients and convert them into microbial biomass that can be consumed by fish. Traditionally, biofloc systems operate under low-light conditions that favor heterotrophic bacterial communities capable of rapidly assimilating inorganic nitrogen into microbial biomass (230, 231). However, when natural light penetrates fish tanks, photoautotrophic microorganisms such as Chlorophyta and cyanobacteria can become dominant components of the biofloc community (232). These photoautotrophic organisms can influence nutrient cycling through assimilation of dissolved nitrogen into algal biomass and through oxygen production during photosynthesis,

which may enhance nitrification and reduce the formation of anoxic microzones that promote denitrification (233). Algal–bacterial consortia have been shown to stabilize nitrogen transformations in aquaculture and wastewater systems, potentially increasing nutrient retention in biomass while reducing gaseous nitrogen losses (234, 235).

Photoautotrophic biofloc communities may also influence phosphorus cycling. Microalgae are capable of storing phosphorus through "luxury uptake," accumulating excess phosphate as intracellular polyphosphate granules when phosphorus availability is high, and altering the partitioning of phosphorus among dissolved, particulate, and retained pools within aquaponic systems (236, 237).

In addition to the microbial metabolic regime, the system hydraulic configuration represents another key design factor shaping nutrient fate. Aquaponic systems are commonly operated in either coupled or decoupled configurations. In coupled systems, water continuously recirculates between fish tanks and hydroponic beds, forming a single-loop system. In contrast, decoupled systems operate as multi-loop systems with one-way flow from the aquaculture unit to the hydroponic unit (207). This configuration often results in higher solids retention times in biofloc fish tanks, which can influence microbial community composition and nutrient transformation processes, particularly nitrification and denitrification (120). Hydraulic configuration can also influence calcium and magnesium concentrations, which may affect phosphorus precipitation dynamics (113). Moreover, in decoupled systems, water discharge from the aquaculture loop may represent a pathway for nutrient removal. However, when this water is reused or further processed for nutrient recovery, it may not represent a permanent loss from the overall production system (14).

While many studies have examined microbial communities, nutrient concentrations, and production performance in aquaponic systems, most rely on water chemistry measurements and yield outcomes rather than comprehensive nutrient accounting. Such measurements cannot determine whether nutrients are incorporated into harvestable biomass, retained in solids, discharged, or transformed into gaseous products. Mass-balance analysis provides a more complete framework for evaluating nutrient use efficiency by quantifying nutrient distribution across system compartments. Previous mass balance studies on aquaponics have shown significant N losses via denitrification and P removal in sludge solids (238-240). However, two key gaps remain: no prior studies have evaluated how different biofloc metabolic regimes (photoautotrophic vs. heterotrophic) influence nitrogen and phosphorus partitioning and loss. Moreover, comparisons of coupled versus decoupled aquaponic systems have rarely examined how hydraulic configuration affects whole-system nutrient allocation and recovery efficiency.

This study addresses these gaps by conducting replicated nitrogen and phosphorus mass balances in aquaponic systems operated under two key design factors: fish-tank illumination, which promotes photoautotrophic biofloc communities, and hydraulic configuration (coupled versus decoupled). The systems were operated over two production cycles to capture long-term system behavior under two different tilapia stocking densities. The objective of this study was to quantify how biofloc metabolic regime and hydraulic configuration influence the fate of feed-derived nitrogen and phosphorus within aquaponic systems, including recovery into fish biomass, plant biomass, dissolved pools, and particulate solids. By linking system design to nutrient allocation pathways, this work provides insights into how aquaponic systems can be engineered to improve nutrient recovery efficiency and overall system sustainability.

6.2 Materials and Methods

6.2.1 Experimental design

The experiment was designed to evaluate how microbial metabolic regime and hydraulic configuration influence nitrogen (N) and phosphorus (P) partitioning in biofloc-based aquaponic systems using a system-scale mass balance approach. A two-factor experimental design was used, with the factors consisting of (1) fish tank illumination and (2) system hydraulic configuration (coupled versus decoupled water loops). Fish tank illumination determined the dominant microbial regime by promoting photoautotrophic biofloc under sunlight conditions or heterotrophic biofloc under dark conditions. Combining these two factors produced four treatments: photoautotrophic–coupled (PC), heterotrophic–coupled (HC), photoautotrophic–decoupled (PD), and heterotrophic–decoupled (HD). Each treatment was replicated three times and arranged in a randomized complete block design. Each aquaponic unit operated as an independent experimental system.

All systems were operated in a 268 m² climate-controlled greenhouse (Atlas Greenhouse, USA) at the E.W. Shell Fisheries Center, Auburn University (Alabama, USA). Detailed descriptions of greenhouse operation and environmental control are available in previous publications (Rezaei et al., 2025; Rezaei et al., 2026). In the photoautotrophic treatments (PC and PD), fish tanks were left uncovered so that sunlight could reach the water column from above and through translucent tank walls. In the heterotrophic treatments (HC and HD), tanks were shielded from light using black landscape fabric and surface coatings to minimize algal growth. During the study period, natural photoperiod in the greenhouse ranged from approximately 10 to 14 hours.

The mass balance study consisted of two fall tomato production cycles to capture nutrient dynamics at different fish growth stages. The first batch was conducted from July 28 to November 18, 2024, and involved larger Nile tilapia (Oreochromis niloticus), representing a late grow-out

stage. Fish averaged ~300 g (17 kg/m3 density) at the beginning of the 2024 trial and ~430 g at the end (17 kg/m3 density). Partial harvesting was conducted in September 2024 to reduce tank density to ~14 kg m^{-3}, maintaining optimal conditions and minimizing health risks from elevated biomass and solids (43, 120). The second batch was conducted from August 8 to November 20, 2025, and used smaller fish representing an earlier growth stage. Here, fish averaged ~50 g (3 kg/m3 density) at the beginning of the 2025 trial and ~300 g at the end (17 kg/m3 density). Each batch lasted approximately four months, allowing sufficient time to quantify cumulative nutrient flows and biomass production within the systems. Prior to stocking, fish tanks were inoculated with active biofloc collected from a mature tilapia raceway to accelerate the establishment of microbial communities responsible for nutrient transformation. Fish culture was integrated with hydroponic tomato production. Tomato plants (Favorita F1) were grown concurrently in the hydroponic beds, with five plants maintained in each bed during each cycle. Fish and plant biomass were monitored throughout the trials to quantify nutrient recovery in harvested biomass. All fish handling procedures followed protocols approved by the Auburn University Institutional Animal Care and Use Committee (IACUC #22-4099).

6.2.2 System setup and operation

The general design and operation of the aquaponic systems have been described previously (113, 120). Briefly, the coupled systems (PC and HC) operated as closed recirculating loops in which water continuously circulated between fish tanks and hydroponic beds at a flow rate of approximately 9 L min^{-1} (Figure 6.1). The hydroponic beds were filled with pea gravel media and served both as plant production units and as biofilters for solids retention and nitrification. The fish tanks had a working volume of 700 L, corresponding to a hydraulic retention time (HRT) of 155 minutes. Water lost through evaporation and sludge removal was replenished periodically

using dechlorinated municipal water. A 110-L radial flow settler (RFS) was installed downstream of the fish tank, with settled sludge removed (and quantified) twice per week. Dissolved oxygen in the fish tanks was maintained near 7 mg L^{-1} through continuous aeration. In contrast, the decoupled systems (PD and HD) operated as multi-loop systems with discrete water transfers from the aquaculture unit to the hydroponic unit. Water was pumped from the fish tanks to the plant beds twice daily in short intervals, resulting in a substantially longer fish-tank hydraulic retention time of approximately 14 days. Additional aeration was provided to maintain dissolved oxygen levels comparable to those in the coupled systems. Additional details on system configuration and equipment specifications are provided in prior publications (113, 120).

Fish were fed twice daily, once in the morning (7–8 a.m.) and again in the early afternoon (1–2 p.m.). Juvenile Nile tilapia weighing less than 100 g were fed a commercial diet containing approximately 45% crude protein, 12% crude fat, and 1% phosphorus (Cargill Triton-4512). Once fish exceeded 100 g, the feed was switched to a grow-out formulation containing approximately 36% crude protein, 6% crude fat, and 1% phosphorus (Cargill Triton-3606) (52). Feeding rates were adjusted according to fish size, beginning at approximately 3% of body weight for smaller fish and gradually decreasing to about 1.5% as fish approached market size (53). Feed input was periodically adjusted based on fish biomass measurements, water temperature, and observed feeding activity. Water quality was managed to maintain suitable conditions for fish and microbial processes. System pH was maintained near 7.0 through periodic additions of hydrochloric acid or calcium carbonate as required. Potassium, which can become limiting in aquaponic systems, was supplemented through make-up water to maintain concentrations near 100 mg L^{-1} in the fish tanks.

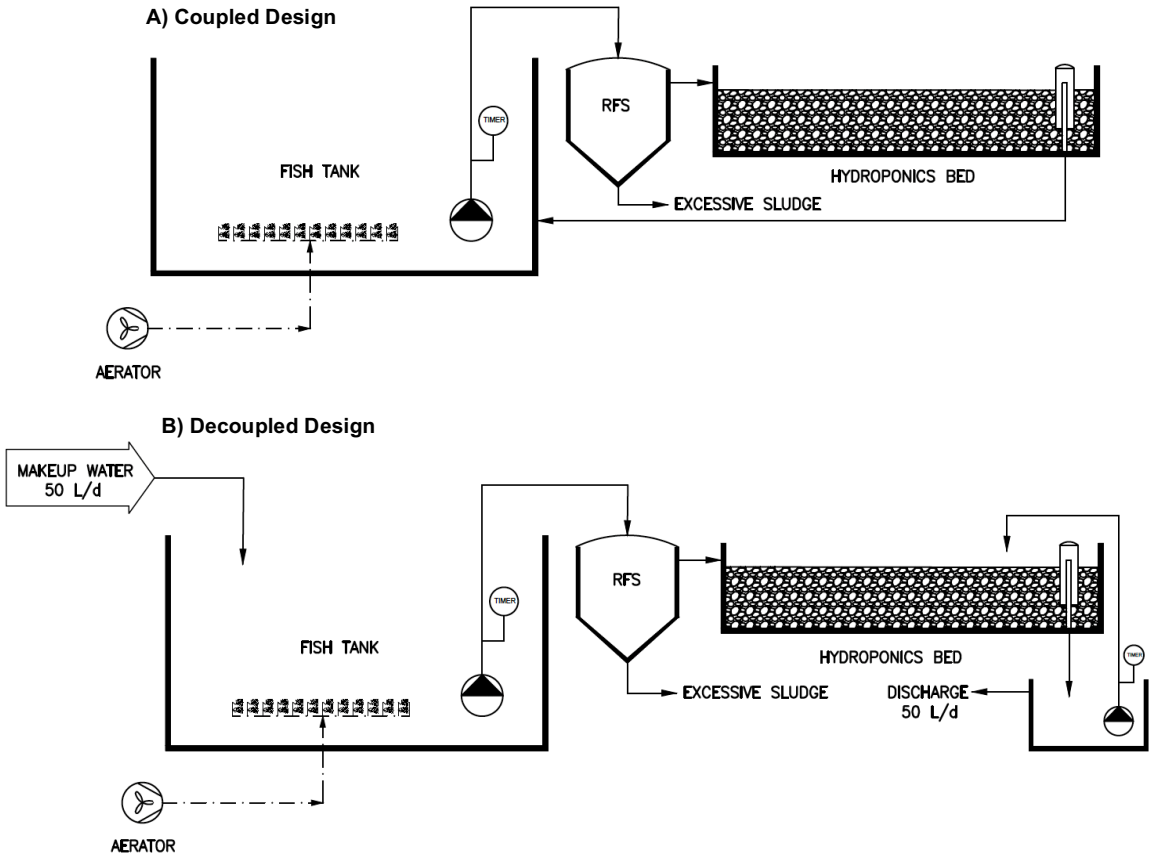

Figure 6.1 Process flow diagram of A) coupled and B) decoupled biofloc aquaponics operation.

6.2.3 Fish and plant growth measurements

Fish growth was monitored throughout each production cycle to quantify biomass production and nutrient recovery in fish tissue. Each month, ten fish were randomly sampled from each system and weighed (wet weight) to estimate average body mass and track growth over time. At the end of each grow-out cycle, all fish were harvested, and the total biomass from each tank was recorded. For elemental composition analysis, three representative fish from each system were collected. Whole fish samples were homogenized using a Ninja food blender, freeze-dried, and then processed for elemental analysis (described later).

Tomato production was monitored during each trial by regularly harvesting ripe fruits. The weight of harvested tomatoes was recorded throughout the production period to determine cumulative fruit yield for each growing season. Each hydroponic grow bed contained five tomato plants and was treated as an experimental unit, with three replicate beds per treatment. At the end of each trial, all tomato plants were removed from the grow beds, and their aboveground biomass (shoots) was measured as fresh mass. Plant samples were then oven-dried at 60 °C until a constant weight was reached to determine dry biomass. The dried plant material was subsequently ground using a hammer mill, followed by a Wiley mill to obtain a homogeneous powder suitable for elemental analysis.

6.2.4 Water and solids sampling

Total suspended solids (TSS) in the fish tanks were monitored every other day by measuring optical density (OD) at 550 nm. Sludge accumulated in the radial flow settlers (RFS) was discharged twice per week from the bottom outlet. The discharge volume was recorded on site, and representative sludge samples were collected after thorough mixing to ensure homogeneity. TSS concentrations in both fish tank water and RFS sludge were estimated from OD_{550} measurements using a system-specific calibration curve. To establish the relationship between optical density and suspended solids concentration, representative samples were centrifuged (4696 × g for 10 min), and the resulting pellets were oven-dried and weighed following the procedure described by Bertrand-Krajewski (56). The resulting calibration was subsequently used to estimate TSS concentrations from routine OD measurements throughout the experiment. Solid biomass samples for nutrient analysis were collected once during each production cycle from multiple system compartments, including suspended biofloc in the fish tanks, biofilm attached to tank walls, sludge accumulated in the radial flow settlers, and solids retained in the hydroponic grow beds.

Water samples were collected every other day from each fish tank and from the decoupled system sumps. Samples were filtered through 0.2 µm nylon microfiber filters (VWR, USA) and stored at −20 °C until chemical analysis.

6.2.5 Nutrient analyses

Filtered water samples were analyzed for dissolved inorganic nitrogen and phosphorus species. Concentrations of nitrate (NO_3^--N), nitrite (NO_2^--N), and phosphate (PO_4^{3-}-P) were determined using high-performance liquid chromatography (HPLC) with a Prominence LC system (Shimadzu, Japan) equipped with an anion exchange column (Dionex AS22, Thermo Fisher Scientific, USA) and an ion suppressor (Dionex AERS 500). Ammonium (NH_4^+-N) concentrations were measured using ion chromatography with a Dionex CS16 cation exchange column and a CERS 500 ion suppressor (Thermo Fisher Scientific, USA). Total nitrogen in water samples was determined using a Shimadzu TOC/TN analyzer. Total phosphorus (TP) concentrations in water were measured using HACH colorimetric assays following the manufacturer's protocols. Solid samples, including fish tissue, plant biomass (shoots and fruit), and organic solids (biofloc, sludge, and biofilm), were digested in nitric acid and analyzed for phosphorus content using inductively coupled plasma optical emission spectroscopy (ICP-OES) at the University of Georgia Soil, Plant, and Water Laboratory. Total nitrogen in solid samples was measured at the same laboratory using an Elementar Vario Max combustion analyzer.

6.2.6 Nitrogen and phosphorus mass balance

Nitrogen and phosphorus mass balances were developed to quantify nutrient inputs, internal partitioning, and outputs in the four aquaponic system configurations. The analyses were conducted independently for each treatment to capture differences in nutrient recovery associated with biofloc metabolic regime and hydraulic configuration. Mass balances were developed for

both production batches using measurements collected from water, fish, plants, and solid-associated organic matter.

Water samples were analyzed for the main dissolved nutrient forms relevant to nitrogen and phosphorus cycling, including ammonium (NH_4-N), nitrite (NO_2-N), nitrate (NO_3-N), total nitrogen (120), phosphate (PO_4-P), and total phosphorus (TP). Concentrations were measured at two-day intervals, linearly interpolated to daily values, and used to estimate cumulative dissolved nutrient transport through the systems over each batch. Because of their different hydraulic structures, coupled and decoupled systems were treated differently in the mass-balance analysis. In the decoupled systems, nutrient transport was evaluated sequentially across compartments because water moved in one direction from the fish tank to downstream units. The fish tank, radial flow settler (RFS), and the hydroponic loop were included in the compartment-level mass balance. The grow bed and decoupled sump were treated as a single compartment because they recirculated frequently and maintained similar water quality. In contrast, the coupled systems were treated as a single integrated unit because rapid recirculation among the fish tank, RFS, and grow bed minimized spatial differences in dissolved nutrient concentrations, and therefore whole-system input–output balances were used.

The cumulative dissolved mass of each nutrient species in the effluent of each compartment was calculated by numerical integration over time:

$$M_{n,c,\text{effluent}} = \sum_{t=0}^{T} C_{n,c,t}\ Q_{c,t}\ \Delta t \qquad (1)$$

where $M_{n,c,\text{effluent}}$is the cumulative mass of nutrient species n leaving the compartment c, $C_{n,c,t}$is the concentration of nutrient species n in the effluent of the compartment c at time t, $Q_{c,t}$ is the

corresponding flow rate, and Δt is the time interval (1 d). For nitrogen, this equation was applied to NH_4-N, NO_2-N, NO_3-N, and TN. For phosphorus, it was applied to PO_4-P and TP.

Nutrients retained in fish biomass, fruit, plant biomass, and solids-associated organic matter were calculated from dry mass and elemental composition. Solid-associated pools included biofloc, biofilm, clarifier sludge, and sludge retained in the grow beds. Nutrient mass in each solid or biomass pool was calculated as:

$$M_{\text{pool}} = DM \times E \qquad (2)$$

where DM is the dry mass of the pool at the end of the study, and E is the elemental concentration of nitrogen or phosphorus in that material. Nutrient accumulation in water and solid residues over the batch was estimated as the difference between the final and initial measured masses.

The total nutrient output from each compartment or system was then calculated as the sum of dissolved effluent loads and the nutrient masses retained in solids, fish, and plants:

$$M_{c,\text{output}} = \sum M_{n,c,\text{effluent}} + M_{\text{solids}} + M_{\text{fish}} + M_{\text{plant}} \qquad (3)$$

For the decoupled systems, nutrient loss within each compartment was estimated as the difference between nutrient input and nutrient output in that compartment:

$$M_{c,\text{input}} - M_{c,\text{output}} = M_{c,\text{loss}} \qquad (4)$$

For the coupled systems, the same framework was applied at the whole-system level rather than at the compartment level. The cumulative nutrient flows calculated from Equations (1)–(4) were used to construct Sankey diagrams for nitrogen and phosphorus partitioning.

Daily water addition and clarifier discharge were recorded for each system and incorporated into the water balance. In the decoupled systems, clarifier effluent flow rate was estimated from the

difference between water added to the system and water discharged from the clarifier. Effluent from the hydroponic loop was estimated from clarifier discharge and evapotranspiration (ET). In the coupled systems, no routine process discharge occurred; therefore, water added to the system was assumed to equal ET.

The following assumptions were used in the mass-balance calculations:
(1) The fish tank was assumed to be completely mixed because of continuous aeration and circulation.
(2) In the coupled and decoupled counterparts of the same light treatment, evapotranspiration was assumed to be similar; thus, ET was taken as equal for PD and PC, and for HD and HC, within each cycle.
(3) A constant elemental composition was assumed for each biomass category within a cycle, including fish, fruit, shoot, and organic solids.

6.2.7 Statistical analyses

All treatments were independently replicated across three aquaponic systems (n = 3), resulting in a total of 12 experimental units. Statistical analyses were conducted in R (v4.3.1). Linear models were used to evaluate the effects of system configuration (coupled vs. decoupled) and microbial regime (photoautotrophic vs. heterotrophic), which were treated as fixed factors. For time-series datasets, sampling time was included as a random effect to account for repeated measurements over the experimental period. When significant treatment effects were detected, pairwise comparisons were performed using Tukey's Honest Significant Difference (HSD) test implemented through the *agricolae* package. Statistical significance was evaluated at $\alpha = 0.05$ for fish mass, plant biomass, solids, water, and nitrogen loss and their nutrient partitioning. Descriptive statistics, including means and standard deviations, were calculated using Microsoft Excel.

6.3 Results and Discussion

6.3.1 Fish growth stage and nitrogen loading shaped nitrogen partitioning

Nitrogen mass balances showed clear differences in nutrient partitioning among the four aquaponic system configurations and between the two production batches (Figure 6.2). Across both years, input nitrogen was distributed among fish biomass, plant biomass, solids, dissolved nitrogen remaining in the water, and apparent nitrogen loss. A key difference between the two batches was the fish growth stage, with larger fish in 2024 and smaller fish in 2025. However, the resulting nitrogen loading differed among system configurations. In the coupled systems (PC and HC), larger fish in 2024 received higher feed inputs, resulting in greater nitrogen loading than in 2025. In contrast, in the decoupled systems (PD and HD), unstable nitrification during the 2024 batch required temporary reductions in feeding, resulting in lower feed input compared with 2025 despite the larger fish size (Figure S6.1).

Nitrogen recovery in fish biomass reflected these differences in both growth stage and feeding regime, with smaller fish having higher nitrogen recovery ($p < 0.001$). In 2025, the proportion of input nitrogen recovered in fish ranged from 30.0 to 34.4% across treatments. In contrast, in 2024, only 10.2 to 15.6% of input nitrogen was recovered in fish (Figure 6.2A, B). This reduction occurred even though feeding increased in the coupled systems, indicating that the fish growth stage strongly influenced nitrogen retention efficiency. Smaller fish generally allocate a larger proportion of nutrients to tissue accretion, whereas larger fish direct more nitrogen toward maintenance metabolism and excretion (50). As a result, a smaller fraction of dietary nitrogen was incorporated into biomass during the later grow-out stage, while a greater fraction entered dissolved or particulate nitrogen pools within the system.

The Sankey diagrams further support this interpretation (Figure 6.3). In the decoupled systems, the amount of nitrogen leaving the fish tank in the effluent was substantially higher in 2024 than in 2025 (p <0.01). For example, total nitrogen leaving the fish tank in the decoupled systems was 79.2 g in 2024 compared with 45.7 g in 2025, indicating that a larger fraction of feed nitrogen entered the water column rather than being incorporated into fish biomass (Figure 6.3A, C). However, this additional nitrogen did not translate into greater recovery in plants or measurable water pools. Instead, the main response to elevated nitrogen throughput was an increase in solids-associated nitrogen and apparent nitrogen loss. In 2025, solids-associated nitrogen accounted for 7.9–17.5% of feed nitrogen, and apparent nitrogen loss ranged from 31.1–46.9% across treatments. In contrast, in 2024, solids-associated nitrogen ranged from 10.6–19.6%, while apparent nitrogen loss increased substantially to 50.2–62.6% of feed nitrogen.

Apparent nitrogen loss in aquaponic systems can arise through several pathways, most notably microbial conversion of nitrate to gaseous forms through denitrification, as well as other unmeasured gaseous or dissolved losses (241, 242). Denitrification is especially likely in solids-rich and oxygen-limited microenvironments such as sludge layers, clarifiers, and dense biofloc aggregates, where nitrate can be reduced to N_2 or N_2O gas (95, 243). The Sankey diagrams of the decoupled systems provide further evidence for this mechanism, showing a marked reduction in nitrate between the fish tank and the RFS in both years. This pattern suggests that the clarifier served as an important site of nitrate consumption. Oxygen measurements support this interpretation: the average dissolved oxygen concentration in the RFS during 2025 was approximately 4 mg L^{-1}, compared with 7.6 mg L^{-1} in the fish tanks, indicating more oxygen-limited conditions within the clarifier that could promote microbial nitrate reduction.

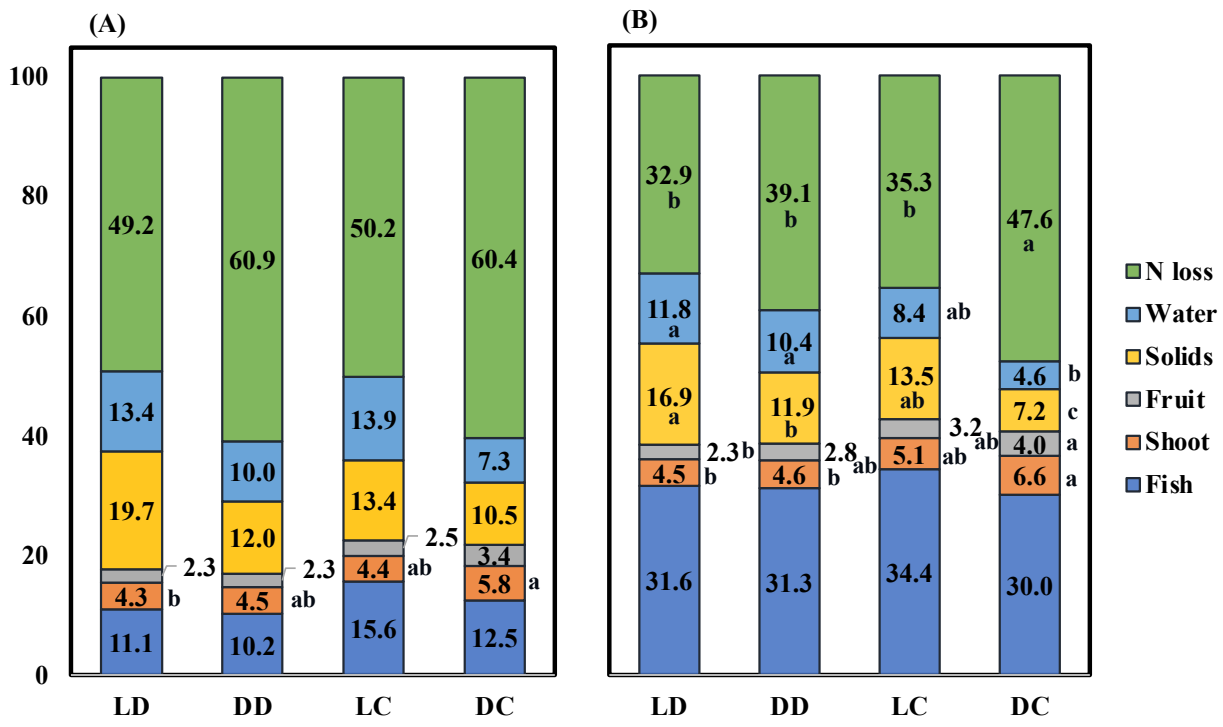

Figure 6.2 Partitioning of feed-derived nitrogen across major system compartments in aquaponic treatments during (A) the 2024 batch and (B) the 2025 batch. Treatments include photoautotrophic–decoupled (PD), heterotrophic–decoupled (HD), photoautotrophic–coupled (PC), and heterotrophic–coupled (HC) systems. Values represent the percentage of feed nitrogen recovered in fish biomass, plant biomass (shoot and fruit), accumulated solids, and dissolved nitrogen in water. Lowercase letters (a, b, c, etc.) indicate statistically significant differences between treatments ($p < 0.05$). Figures without letters were not statistically different from the others.

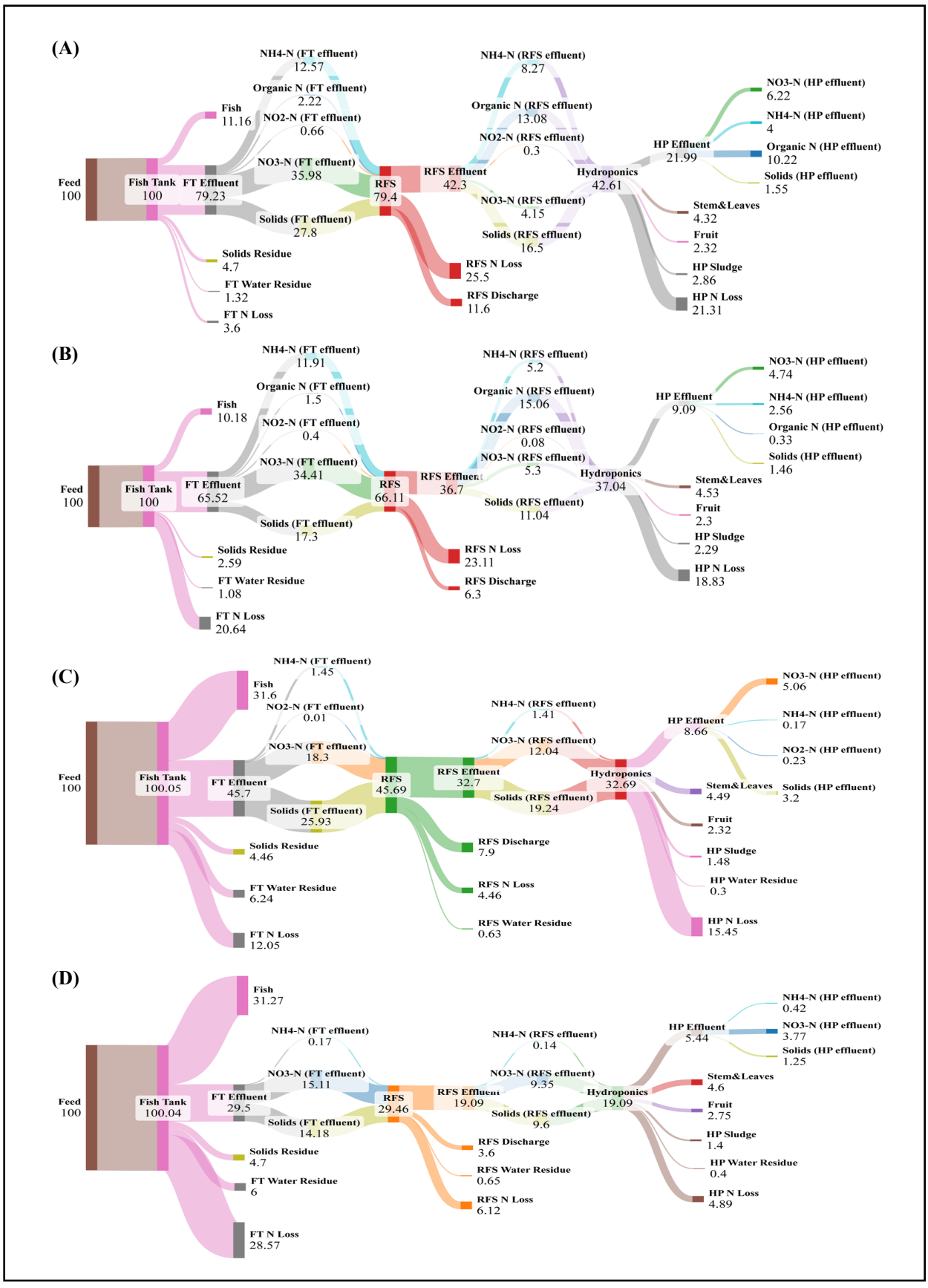
(A)
Feed 100
Fish Tank 100
FT Effluent 79.23
Fish 11.16
NH4-N (FT effluent) 12.57
Organic N (FT effluent) 2.22
NO2-N (FT effluent) 0.66
NO3-N (FT effluent) 35.98
Solids (FT effluent) 27.8
Solids Residue 4.7
FT Water Residue 1.32
FT N Loss 3.6
RFS 79.4
RFS Effluent 42.3
RFS N Loss 25.5
RFS Discharge 11.6
NH4-N (RFS effluent) 8.27
Organic N (RFS effluent) 13.08
NO2-N (RFS effluent) 0.3
NO3-N (RFS effluent) 4.15
Solids (RFS effluent) 16.5
Hydroponics 42.61
HP Effluent 21.99
NO3-N (HP effluent) 6.22
NH4-N (HP effluent) 4
Organic N (HP effluent) 10.22
Solids (HP effluent) 1.55
Stem&Leaves 4.32
Fruit 2.32
HP Sludge 2.86
HP N Loss 21.31
(B)
Feed 100
Fish Tank 100
FT Effluent 65.52
Fish 10.18
NH4-N (FT effluent) 11.91
Organic N (FT effluent) 1.5
NO2-N (FT effluent) 0.4
NO3-N (FT effluent) 34.41
Solids (FT effluent) 17.3
Solids Residue 2.59
FT Water Residue 1.08
FT N Loss 20.64
RFS 66.11
RFS Effluent 36.7
RFS N Loss 23.11
RFS Discharge 6.3
NH4-N (RFS effluent) 5.2
Organic N (RFS effluent) 15.06
NO2-N (RFS effluent) 0.08
NO3-N (RFS effluent) 5.3
Solids (RFS effluent) 11.04
Hydroponics 37.04
HP Effluent 9.09
NO3-N (HP effluent) 4.74
NH4-N (HP effluent) 2.56
Organic N (HP effluent) 0.33
Solids (HP effluent) 1.46
Stem&Leaves 4.53
Fruit 2.3
HP Sludge 2.29
HP N Loss 18.83
(C)
Feed 100
Fish Tank 100.05
FT Effluent 45.7
Fish 31.6
NH4-N (FT effluent) 1.45
NO2-N (FT effluent) 0.01
NO3-N (FT effluent) 18.3
Solids (FT effluent) 25.93
Solids Residue 4.46
FT Water Residue 6.24
FT N Loss 12.05
RFS 45.69
RFS Effluent 32.7
RFS Discharge 7.9
RFS N Loss 4.46
RFS Water Residue 0.63
NH4-N (RFS effluent) 1.41
NO3-N (RFS effluent) 12.04
Solids (RFS effluent) 19.24
Hydroponics 32.69
HP Effluent 8.66
NO3-N (HP effluent) 5.06
NH4-N (HP effluent) 0.17
NO2-N (HP effluent) 0.23
Solids (HP effluent) 3.2
Stem&Leaves 4.49
Fruit 2.32
HP Sludge 1.48
HP Water Residue 0.3
HP N Loss 15.45
(D)
Feed 100
Fish Tank 100.04
FT Effluent 29.5
Fish 31.27
NH4-N (FT effluent) 0.17
NO3-N (FT effluent) 15.11
Solids (FT effluent) 14.18
Solids Residue 4.7
FT Water Residue 6
FT N Loss 28.57
RFS 29.46
RFS Effluent 19.09
RFS Discharge 3.6
RFS Water Residue 0.65
RFS N Loss 6.12
NH4-N (RFS effluent) 0.14
NO3-N (RFS effluent) 9.35
Solids (RFS effluent) 9.6
Hydroponics 19.09
HP Effluent 5.44
NH4-N (HP effluent) 0.42
NO3-N (HP effluent) 3.77
Solids (HP effluent) 1.25
Stem&Leaves 4.6
Fruit 2.75
HP Sludge 1.4
HP Water Residue 0.4
HP N Loss 4.89

Figure 6.3 Sankey diagrams illustrating the distribution of feed-derived nitrogen across major system compartments in the decoupled aquaponic systems. (A) Photoautotrophic–decoupled (PD) system in the 2024 batch, (B) heterotrophic–decoupled (HD) system in the 2024 batch, (C) photoautotrophic–decoupled (PD) system in the 2025 batch, and (D) heterotrophic–decoupled (HD) system in the 2025 batch. Flows represent the percentage of feed nitrogen recovered in fish biomass, plant biomass (shoot and fruit), solids, dissolved nitrogen in water, and apparent nitrogen loss. Dissolved nitrogen is further separated into inorganic nitrogen species (NH_4^+–N, NO_2^-–N, and NO_3^-–N). The width of each flow is proportional to the magnitude of nitrogen partitioned into each pool.

6.3.2 Impact of system configuration and algal biofloc on nitrogen partitioning

Although the fish growth stage strongly influenced whole-system nitrogen partitioning, system design effects were also evident. Overall, the photoautotrophic community had a positive impact on fish growth ($p = 0.02$), with PC treatment consistently showing the highest nitrogen recovery in fish biomass in both years (not statistically significant). In 2025, PC recovered 34.4% of input nitrogen in fish, compared with 31.6%, 31.3%, and 30.0% in PD, HD, and HC, respectively. In 2024, PC again had the highest fish nitrogen recovery (15.6%), followed by HC (12.5%), HD (11.1%), and HD (10.2%) (Figure 6.2A, B). These patterns are consistent with previous observations that fish growth can be enhanced in light-exposed systems, partially because algal biofloc provides a supplemental nutritional source. Meanwhile, coupled configurations maintained more stable water quality through continuous recirculation and filtration, enabling higher rates of fish growth and lower feed conversion ratios (Table 6.1)(113).

Exposure of fish tanks to light promoted the development of algal biofloc communities, which also influenced nitrogen partitioning beyond fish growth alone. Across treatments, light-exposed systems retained a larger fraction of nitrogen in measurable pools (solids and dissolved water) than the dark systems ($p < 0.01$)(Figure 6.2A, B). Sankey diagrams of the decoupled systems showed that nitrogen fractions in fish tank effluent were higher in the phototrophic treatments than in the heterotrophic treatments, by 21% in 2024 and 55% in 2025 (Figure 6.3). At the same time, nitrogen losses from the fish tanks were markedly lower under illumination, decreasing by 83% in

2024 and 57% in 2025 relative to the corresponding dark systems ($p < 0.001$). This is significant because lost nitrogen is no longer recoverable for downstream plant production. Algal growth in aquaponics has been criticized for competing with plants for nutrients; however, this study indicates that the algae-containing systems had lower total N losses. This could be the mitigating factor that partially explains our previous report that phototrophic systems suffered no loss in tomato yield compared to the heterotrophic systems, while enjoying higher levels of fish production (120). That said, phototrophic systems did have lower overall plant yields than heterotrophic systems (Table 6.1) while diverting more N into sludge.

The higher recovery of nitrogen in solids and water pools in the light treatments further indicates that photoautotrophic biofloc did not reduce measurable system nitrogen; rather, illumination promoted a more retentive internal nitrogen cycle in which a larger fraction of nitrogen remained in quantifiable compartments instead of being diverted to loss pathways. Microalgae can assimilate multiple dissolved inorganic nitrogen forms (NH_4^+, NO_2^-, and NO_3^-) and incorporate them into cellular biomass (233). Once assimilated, this nitrogen becomes part of particulate biofloc biomass that can contribute to microbial protein and serve as a supplemental food source for fish, thereby recycling dissolved inorganic nitrogen into productive biomass within the system (244). Nitrogen in the sludge is not lost and could also benefit soil-based plant production (which falls outside the scope of this analysis).

Illumination can also shift the balance between aerobic and anoxic processes that control nitrogen fate. Photosynthetic oxygen production increases local dissolved oxygen concentrations and reduces the extent of oxygen-limited zones where denitrification is favored, while simultaneously supporting more stable nitrification. These micro-zones of oxygen limitation within flocs are distinct from the bulk dissolved oxygen in the fish tank water, which was stable

and close to 7 mg L^{-1} in all treatments due to intensive aeration. Similar patterns have been reported in bacterial–algae biofilm reactors used in recirculating aquaculture systems, where light exposure enhanced ammonia removal, stabilized nitrification, and reshaped microbial community structure (234). Because algal biomass is not permanently removed unless harvested, part of the assimilated nitrogen can later re-enter the dissolved pool through grazing, microbial turnover, cell lysis, or decomposition. This creates a recycling loop that increases nitrogen retention within measurable pools (232). Consistent with this interpretation, studies of algal–bacterial consortia have shown that algal assimilation can account for a substantial share of nitrogen transformation (e.g., 28–41% of total nitrogen removal in controlled systems) while also mitigating nitrous oxide emissions, indicating that algal uptake and photosynthesis can shift nitrogen away from nitrification–denitrification pathways that lead to gaseous losses (235).

In the decoupled systems, especially in the high-loading batch, Sankey diagrams showed substantially greater ammonium fractions in the fish tank effluent, indicating less stable nitrification. In our previous work, we showed that decoupled biofoc systems were more susceptible to ammonia accumulation, that poor nitrification forced temporary reductions in feeding, and that this ultimately reduced nitrogen availability to plants and lowered productivity. In contrast, coupled systems benefited from distributed nitrification across both the fish tank and grow bed loop, which supported a more stable nitrogen cycle and lower ammonia fraction in the water, as shown in the Sankey diagrams of coupled systems in both years (Figure S6.2).

Nitrogen partitioning to plant biomass was comparatively stable across years (Figure 6.2A, B). In 2025, the proportion of nitrogen recovered in plants ranged from 6.8 to 10.6%, with the HC treatment showing the highest value, the PC treatment an intermediate value, and both decoupled treatments exhibiting the lowest values. In 2024, however, plant nitrogen recovery ranged from

6.7 to 9.3% and did not differ significantly among treatments. The consistently higher plant nitrogen fraction in the HC is in line with the higher fruit yield and plant biomass (Table 6.1). At the same time, the treatment effect on plant nitrogen recovery was much more apparent under the lower-loading 2025 conditions than in the higher-loading 2024 batch. This suggests that when nitrogen loading becomes excessive, a large portion of the additional nitrogen is diverted to loss pathways rather than to plants, thereby masking differences among treatments. In other words, treatment effects on plant nitrogen uptake became easier to detect when the systems were operating closer to their assimilative capacity. These results show that nitrogen use efficiency in aquaponics depends not only on total nitrogen input, but also on how system configuration influences nitrification stability, solids retention, and microbial processing of nitrogen. Specifically, smaller fish, coupled operation, and fish tank lighting all increased nitrogen retention in the systems.

Table 6.1 Fish biomass gain and tomato biomass production (fruit and shoot) across aquaponic treatments during the 2024 and 2025 production batches. Values represent mean ± standard deviation (n = 3). Different lowercase letters within each row and year indicate statistically significant differences among treatments (Tukey's HSD test, $p < 0.05$).

	Year 2024				**Year 2025**			
	PD	**HD**	**PC**	**HC**	**PD**	**HD**	**PC**	**HC**
Fish mass gain (kg)	2.51 ± 0.8 c	2.33 ± 1.1 b	6.12 ± 1.02 a	5.16 ± 2.11 a	10.15 ± 0.5 ab	9.22 ± 0.81 b	11.01 ± 0.72 a	9.7 ± 0.8 ab
Fruit biomass (kg)	6.27 ± 3.81 b	7.72 ± 1.92 b	11.2 ± 2.06 ab	17.36 ± 2.55 a	7.2 ± 1.16 b	10.62 ± 3.63 ab	11.06 ± 0.97 ab	14.54 ± 3.41 a
Shoot mass (kg)	0.9 ± 0.15 b	1.12 ± 0.07 b	1.27 ± 0.18 b	1.92 ± 0.14 a	1.62 ± 0.15 a	1.7 ± 0.3 a	1.82 ± 0.38 a	2.23 ± 0.33 a

6.3.3 Fish growth stage shifted phosphorus away from fish and toward water and solids

Across both production batches, feed phosphorus (P) was partitioned primarily into dissolved P remaining in the water column and solids-associated P, while smaller fractions were recovered in

fish biomass and plant biomass (stems, leaves, and fruit). In the 2025 batch, dissolved P in the water accounted for 35.4–48.62% of feed P, and solids-associated P accounted for 12.5–27.5%. In contrast, 26.1–32.5% of feed P was recovered in fish biomass and 8.45–12.34% in plant biomass (Figure 6.4). In the 2024 batch, phosphorus distribution shifted further away from biological sinks. The water pool accounted for 39.7–60.3% of feed P, and solids accounted for 21.9–30.8%, whereas only 8.33–14.48% of feed P was recovered in fish biomass and 6.64–10.57% in plant biomass (Figure 6.5).

This behavior contrasts with nitrogen cycling in aquaponic systems, where a substantial fraction of nitrogen can be removed through gaseous pathways such as denitrification. Phosphorus, in contrast, lacks a significant gaseous loss pathway under typical aquaponic conditions. Instead, phosphorus tends to be redistributed among dissolved pools, particulate solids, and biological biomass. Previous studies of aquaponic nutrient cycling similarly report that a large proportion of feed phosphorus accumulates in solid wastes, where it remains unavailable to plants unless it is re-mineralized or recovered through sludge management processes (245).

The most pronounced difference between the two batches was associated with the fish growth stage. In 2025, when smaller and rapidly growing fish were cultured, phosphorus recovery in fish biomass ranged from 26.1 to 32.5% of feed P across treatments. In contrast, when larger fish were raised in 2024, phosphorus recovery in fish tissue declined sharply to 8.33–14.48%, similar to the findings with nitrogen. This indicates that a smaller fraction of dietary phosphorus was incorporated into new biomass during the later grow-out stage, similar to the nitrogen recovery.

As fish increase in size, the marginal requirement for phosphorus incorporation into new tissue decreases, and a larger fraction of dietary phosphorus is excreted or retained in non-biological compartments. Phase-feeding studies demonstrate that diets for larger fish can contain

lower available phosphorus without compromising performance, indicating reduced phosphorus retention efficiency during later growth stages (246). Similarly, studies on tilapia have shown that phosphorus requirements vary substantially across life stages and environmental conditions (50). The mass balance distributions observed here support this biological interpretation. In 2024, the system consistently shifted toward higher phosphorus fractions in the water and solids pools, reflecting reduced conversion of dietary phosphorus into fish biomass. For example, in the PC treatment, the fraction of phosphorus recovered in water decreased to 40.93% in 2025 versus 47.16% in 2024. Phosphorus in solids declined from 30.2% in 2024 to 25.28% in 2025, while phosphorus recovery in fish biomass increased from 14.48% to 32.51% (Figures 6.4 and 6.5).

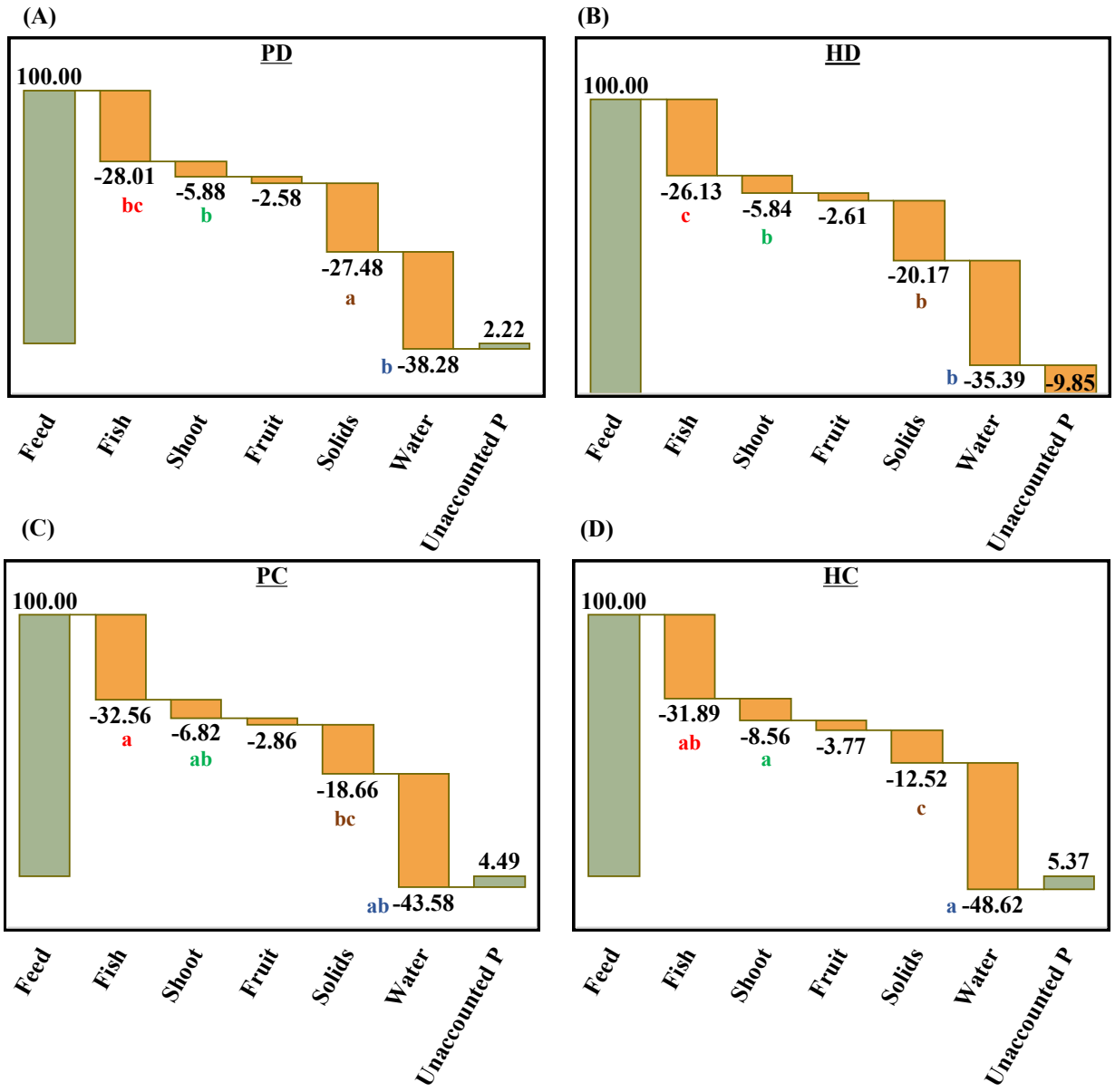

Figure 6.4 Waterfall diagrams illustrating the partitioning of feed-derived phosphorus in aquaponic treatments during the 2025 production batch. Panels represent (A) photoautotrophic–decoupled (PD), (B) heterotrophic–decoupled (HD), (C) photoautotrophic–coupled (PC), and (D) heterotrophic–coupled (HC) systems. Bars show the percentage of feed phosphorus allocated to fish biomass, plant biomass (shoot and fruit), accumulated solids, and dissolved phosphorus in water, with the final bar representing the unaccounted phosphorus fraction.

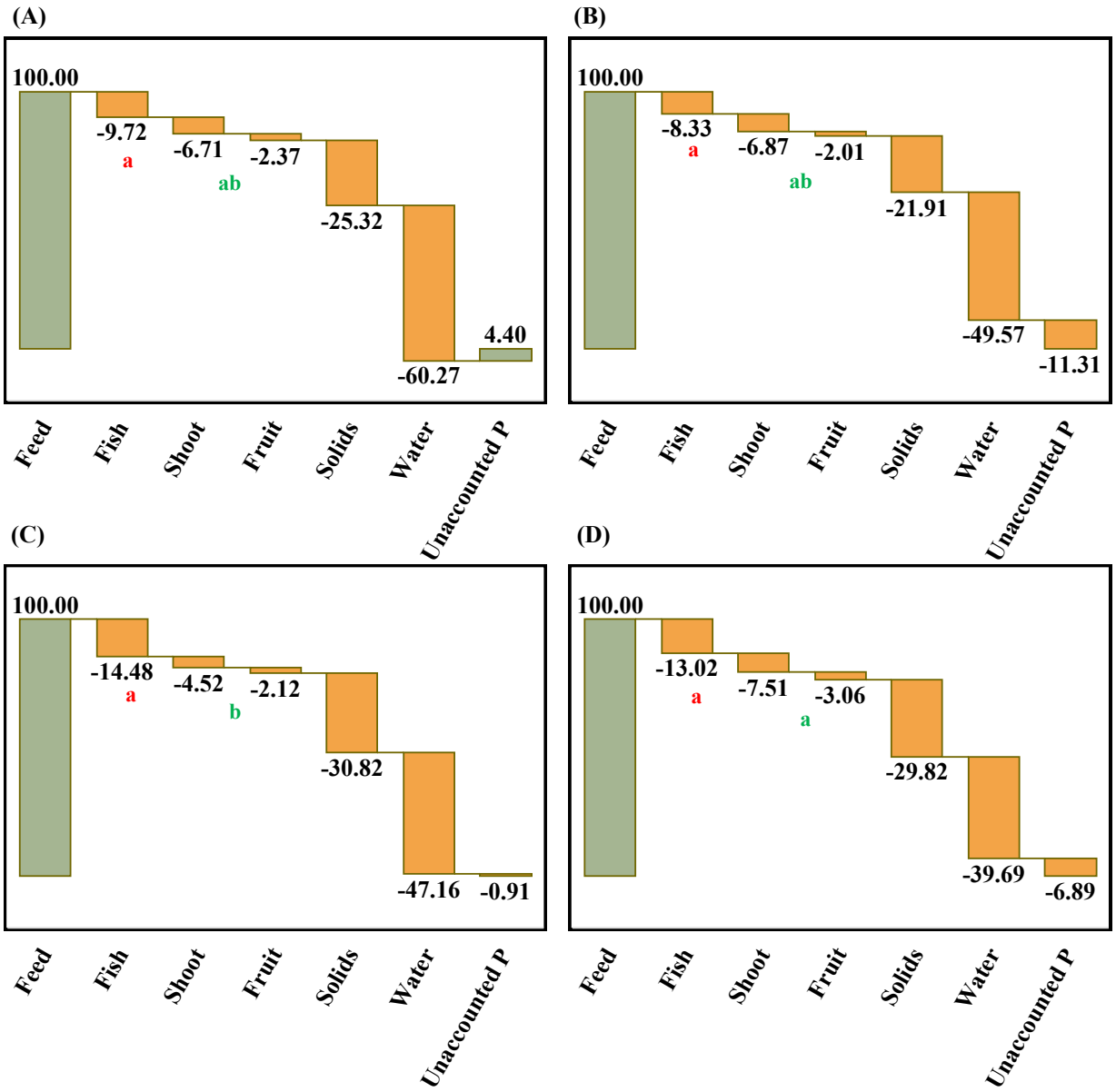

Figure 6.5 Waterfall diagrams illustrating the partitioning of feed-derived phosphorus in aquaponic treatments during the 2024 production batch. Panels represent (A) photoautotrophic–decoupled (PD), (B) heterotrophic–decoupled (HD), (C) photoautotrophic–coupled (PC), and (D) heterotrophic–coupled (HC) systems. Bars show the percentage of feed phosphorus allocated to fish biomass, plant biomass (shoot and fruit), accumulated solids, and dissolved phosphorus in water, with the final bar representing the unaccounted phosphorus fraction.

6.3.4 System configuration impact on fish–plant phosphorus tradeoff

System configuration influenced how phosphorus was partitioned between fish and plant biomass. In 2025, coupling had a positive impact on phosphorus recovery in fish (p = 0.003). The PC systems exhibited the highest phosphorus recovery in fish tissue (32.56% a), followed by HC (31.89% ab), PD (28.01% bc), and HD (26.13% c) (Figure 6.4). A similar ranking occurred in 2024, although overall recovery in fish was lower due to the larger fish cohort in that batch. PC again showed the highest fish P recovery (14.48%), followed by HC (13.02%), while the decoupled systems had substantially lower values (PD 9.72% and HD 8.33%) (Figure 6.5). Consistent with these patterns, PC also produced the greatest fish mass gain in both years, with growth approximately 17% higher than HC in 2024 and 14% higher in 2025 (Table 6.1) [3]. These results indicate that the combination of tank illumination and hydraulic coupling favored phosphorus assimilation into fish biomass.

In contrast, the HC systems consistently directed the largest fraction of phosphorus toward plant biomass, with 12.34% of feed P recovered in plants in 2025 and 10.57% in 2024. This pattern was accompanied by relatively high phosphate concentrations in the coupled systems. In 2024, average soluble PO_4-P concentrations were much higher in PC and HC (38.95 and 38.09 mg L^{-1}, respectively) than in PD and HD (7.94 and 9.11 mg L^{-1}) (Figure S6.3A). In 2025, HC exhibited the highest phosphate concentrations during the main accumulation period (mean after October 8: 16.09 mg L^{-1}), compared with 12.51, 8.70, and 6.48 mg L^{-1} in PC, HD, and PD, respectively (Figure S6.3B). However, phosphate concentration alone did not fully explain plant phosphorus recovery, since PC also maintained relatively high phosphate levels but did not consistently direct as much phosphorus to plants as HC. Instead, the higher plant P fraction in HC likely reflected a combination of adequate phosphorus availability and stronger plant growth performance, as

evidenced by the greater tomato biomass and fruit yield observed in this treatment. This higher plant yield was not driven by greater P availability but rather by other biotic and abiotic factors as described in a previous article (113).

A useful system-level metric is the recovery of phosphorus in harvested biomass (fish + plants). In 2025, harvested biomass accounted for 34.6–44.3% of feed phosphorus, with the lowest recovery observed in HD and the highest in HC. In 2024, harvested biomass recovery was substantially lower, ranging from 17.2–23.6%, again with the highest values in HC. These recoveries are lower than those reported by Cerozi and Fitzsimmons (2017), who found that fish and plants together assimilated approximately 71.7% of feed phosphorus in a small-scale coupled aquaponic system stocked with 20 g tilapia juveniles and planted with lettuce over a 28-day period (239). Their system was intentionally sized so that lettuce uptake would remove nearly all dissolved phosphorus, and their model assumed no phosphorus precipitation. The higher recovery reported in that study likely reflects the use of rapidly growing juvenile fish, a short-cycle leafy crop, and a short experimental duration, all of which favor recovery of phosphorus in harvested biomass rather than accumulation in water, solids, or precipitated pools. In contrast, the lower recovery observed here indicates that a larger fraction of phosphorus remained in non-harvested pools, such as dissolved water phosphorus, solids, or precipitated forms. This pattern suggests that increasing plant growing area or improving solids remineralization could enhance phosphorus utilization efficiency by transferring more phosphorus into harvestable biomass.

6.3.5 Light exposure increased solids-associated phosphorus without reducing dissolved phosphorus

One objective of comparing illuminated and dark fish tanks was to evaluate whether photoautotrophic biofloc communities, dominated by algae, would compete with plants for

available nutrients and thereby reduce phosphorus availability within the system. The phosphorus mass balances did not support a nutrient-depletion effect in the illuminated treatments.

Across both years, illumination consistently increased the fraction of phosphorus associated with solids within comparable system configurations (Figures 6.4 and 6.5). In the decoupled systems, the solids-associated phosphorus fraction was higher in PD than in HD in both batches (27.48% vs. 20.17% in 2025 ($p = 0.015$) and 25.32% vs. 21.91% in 2024). A similar pattern was observed in the coupled systems, where PC retained a larger fraction of phosphorus in solids than HC (18.66% vs. 12.52% in 2025 ($p = 0.015$) and 30.82% vs. 29.82% in 2024). Microorganisms, particularly microalgae, can assimilate phosphate into biomass and store it intracellularly as polyphosphate (polyP) under "luxury uptake" conditions, which can increase cellular phosphorus content (236). This mechanism may have contributed to the higher phosphorus fraction associated with solids in the illuminated systems. In addition, light exposure can promote greater microbial biomass development dominated by Chlorophyta (120). Consistent with this, Figure S6.4 shows that the light-coupled systems had higher TSS compared with the dark-coupled systems. The greater abundance of algal biomass likely enhanced phosphorus retention in the particulate fraction through both direct assimilation and incorporation into biofloc aggregates.

Importantly, the increased retention of phosphorus in solids did not correspond to a reduction in the dissolved phosphorus pool. In most paired comparisons, the illuminated systems maintained equal or higher phosphorus fractions in the water phase (Figures 6.4 and 6.5). For example, in the decoupled systems, the water-associated phosphorus fraction was consistently higher in PD than in HD (38.28% a vs. 35.39% b in 2025 and 60.27% vs. 49.57% in 2024). A similar pattern occurred in the coupled systems in 2024, where PC had a higher water phosphorus fraction than HC (47.16% vs. 39.69%). The only exception occurred in the 2025 coupled systems, where HC exhibited a

higher water phosphorus fraction (48.62%) than PC (43.58%). Overall, these results indicate that illumination and algal biofloc did not deplete measurable dissolved phosphorus within the system and, in most comparisons, resulted in a larger proportion of phosphorus being retained in the water phase.

Algal communities might primarily alter the internal storage and cycling of phosphorus rather than removing it from the system. Phosphorus assimilated into algal biomass remains within the system unless the biomass is harvested externally. Through processes such as microbial turnover, grazing, and organic matter decomposition, particulate phosphorus can subsequently be remineralized and returned to dissolved pools. Polyphosphate dynamics in microbial communities are known to be highly dynamic, with accumulation and release occurring in response to changes in growth conditions and cellular metabolism (247). Consequently, algal biofloc may enhance internal phosphorus retention and cycling without reducing overall phosphorus availability for plant uptake.

6.3.6 Mass-Balance residuals and sources of unaccounted phosphorus

Across treatments, the residual phosphorus term ranged from −8.41% to 11.31% of feed phosphorus. Because phosphorus is not expected to leave aquaponic systems through gaseous pathways, this term should be interpreted as a mass-balance residual (i.e., unaccounted phosphorus) rather than a true loss from the system.

One likely explanation for this residual is the precipitation and sequestration of phosphorus in mineral forms that were not fully captured during sampling. In aquaponic nutrient solutions, phosphate solubility decreases as pH increases because phosphate can bind with divalent cations such as calcium and magnesium, forming insoluble phosphate minerals. Modeling and experimental studies show that precipitation of calcium phosphate species can substantially reduce

the concentration of dissolved phosphate in solution (41, 248). In the present systems, lime addition for pH control may have promoted precipitation of calcium–phosphate minerals. Even under near-neutral bulk pH, localized microenvironments, such as biofilms, sludge layers, or regions with elevated calcium, can favor precipitation and retention. These precipitates likely accumulated in poorly sampled locations, including tank bottoms, sumps, clarifiers, and deeper grow-bed layers. In addition, spatial heterogeneity in solids and precipitate distribution may have contributed to the observed mass-balance residuals, as composite sampling may not fully capture phosphorus accumulation over the production cycle.

6.4 Conclusion

This study demonstrated that nutrient fate in aquaponic systems is strongly influenced by both microbial metabolic regime and hydraulic configuration. Photoautotrophic biofloc promoted greater nitrogen retention in fish, solids, and water while reducing apparent nitrogen losses, suggesting enhanced internal nutrient recycling. Coupled systems supported more stable nitrification and greater recovery of nitrogen in fish biomass. For phosphorus, photoautotrophic systems also increased phosphorus recovery in fish and solids, but resulted in lower phosphorus uptake in plants. This occurred despite similar soluble P levels in phototrophic and hetertrophic systems, suggesting other mechanisms influenced plant growth and upatek. The fish growth stage emerged as a major driver of nutrient partitioning. Systems stocked with smaller fish incorporated a larger fraction of feed nutrients into fish biomass and exhibited lower nitrogen losses, whereas later growth stages shifted nutrient partitioning toward water, solids, and loss pathways. These results indicate that nutrient assimilation efficiency declines as fish approach market size, increasing the importance of system design and nutrient management during later production stages. The mass-balance results also suggest that the plant systems were undersized relative to

the nutrient loading during the high-biomass batch, leading to excess nitrogen accumulation and eventual loss rather than recovery in plants. For phosphorus, strategies that promote remineralization of solids, such as improved sludge management or digestion processes, may help mobilize retained phosphorus into plant-available forms.

Chapter 7: Conclusions and Recommendations

7.1 Summary

Section 1.2 outlined five research objectives aimed at understanding how system configuration and fish-tank illumination influence productivity, microbial dynamics, nutrient cycling, and long-term reliability in biofloc aquaponics systems. These objectives were addressed through long-term replicated greenhouse experiments evaluating fish growth, tomato productivity, microbial community structure, root-zone health, and whole-system nutrient mass balances. The results provide new insight into how hydraulic design and microbial metabolic regimes shape aquaponic performance and nutrient recovery.

Objective 1: Evaluate the effects of fish tank illumination and hydraulic configuration on aquaponic productivity, including fish growth, plant yield, nutrient availability, and nitrification dynamics.

This study demonstrated that both fish-tank illumination and hydraulic coupling significantly improved tilapia production. Illumination increased fish yield by approximately 21%, while coupled systems increased fish yield by 22%. These improvements were attributed to the development of algal biofloc under illuminated conditions, which served as an additional food source for tilapia, and to improved water clarity and filtration in coupled systems. Tomato productivity responded differently depending on system conditions and production stage. During the spring trial, coupled systems produced approximately 44.5% greater tomato yield due to higher nutrient concentrations and more frequent irrigation. However, during the fall trial, decoupled systems outperformed coupled systems by approximately 26%, producing up to 1711 g of fruit per plant. This shift was linked to excessive sludge accumulation and poor drainage in coupled systems

under higher feeding rates. Nitrifying bacteria were also influenced by system configuration, with decoupled systems supporting higher nitrifier abundance in fish tanks due to longer hydraulic retention times and greater solids retention.

Objective 2: Determine how fish tank illumination and hydraulic configuration shape microbial communities involved in nutrient cycling, plant growth promotion, and disease risk in aquaponics systems.

Microbial community analysis revealed that system configuration strongly influenced microbiome composition and function. Coupled systems retained higher nutrient concentrations and produced higher tomato yields in some production periods, while decoupled systems supported greater microbial diversity and higher abundance of plant growth-promoting bacteria. Genera associated with plant growth promotion, including Bradyrhizobium, Ensifer, and Streptomyces, were enriched in decoupled systems. Streptomyces abundance in particular was associated with increased siderophore production and improved iron uptake in tomato leaves. Despite the greater abundance of beneficial taxa, decoupled systems exhibited unstable nitrification and elevated ammonia concentrations, which contributed to nutrient imbalances and reduced plant productivity. Microbial analysis also identified potential pathogens, including Pythium graminicola and plant-parasitic nematodes such as Xiphinema rivesi, demonstrating that system design can influence both beneficial and harmful microbial populations within aquaponic environments.

Objective 3: Investigate the causes of root rot and plant wilt in media-based biofloc aquaponics and evaluate how system design and solids management affect long-term system reliability.

Long-term operation revealed that root-zone conditions were a critical determinant of plant productivity and system stability. During the first year of operation, plant wilt observed in coupled

systems was primarily associated with sludge accumulation and poor drainage within the gravel grow beds. These conditions created hypoxic root zones and reduced tomato yield by approximately 21% compared with decoupled systems. In the second year, system modifications including radial flow settlers and timer-controlled pumping improved solids removal and root-zone oxygenation, resulting in improved plant performance. However, some wilting plants still occurred, indicating that physical design changes alone were insufficient to eliminate system failures. Microbial analysis of root zones revealed that wilted plants were associated with lower dissolved oxygen and greater abundance of pathogenic organisms, including Pythium species and plant-parasitic nematodes, whereas healthy plants were associated with beneficial microbes such as Bacillus and Streptomyces. These findings highlight the importance of both physical design and microbial balance in maintaining long-term aquaponic system reliability.

Objective 4: Assess the role of fish-tank illumination in shaping biofloc composition and evaluate its effects on tilapia growth performance and product quality.

Fish-tank illumination promoted the development of photoautotrophic biofloc communities dominated by green algae (Chlorophyta), which accounted for up to 78% of biofilm biomass and more than 60% of suspended biofloc. Tilapia were observed actively consuming these bioflocs in addition to pelletized feed. Green bioflocs contained higher protein and lipid concentrations compared with brown heterotrophic flocs and were enriched in unsaturated fatty acids and essential omega-3 and omega-6 precursors. These nutritional differences contributed to improved fish performance, with illuminated systems achieving the highest fish biomass and the lowest feed conversion ratios across both production cycles. Importantly, illumination did not promote undesirable cyanobacterial blooms or off-flavor accumulation. Cyanobacteria remained below 0.03% of microbial communities, and geosmin and 2-methylisoborneol concentrations in fish

fillets remained below human sensory detection thresholds. These results demonstrate that controlled light exposure can enhance fish productivity by promoting nutritionally beneficial biofloc communities without compromising product quality.

Objective 5: Quantify the whole-system fate of feed-derived nitrogen and phosphorus and determine how microbial regime and hydraulic configuration affect nutrient recovery and losses.

Whole-system nutrient mass balance analysis revealed that nitrogen and phosphorus partitioning in aquaponics systems is strongly influenced by fish growth stage, microbial metabolic regime, and hydraulic configuration. Nitrogen recovery in fish biomass ranged from 10.2–15.6% during the first production year to 30.0–34.4% in the second year when smaller fish were cultured. Photoautotrophic-coupled systems consistently achieved the highest nitrogen and phosphorus recovery in fish biomass, reaching up to 34.4% nitrogen and 30.8% phosphorus in the 2025 production cycle. Photoautotrophic conditions also reduced nitrogen loss and increased nitrogen retention in measurable pools such as water and solids, suggesting improved internal recycling. In contrast to nitrogen, phosphorus was largely retained in solids and dissolved water fractions because it lacks a gaseous loss pathway. Across both years, plant uptake accounted for approximately 6–11% of feed nitrogen and 7–12% of feed phosphorus. These findings demonstrate that system design significantly influences nutrient recovery pathways and highlight opportunities to improve resource efficiency in aquaponic systems.

7.2 Recommendations for future research

Although this dissertation provides new insight into how design decisions impact biofloc aquaponics performance, several important questions remain that warrant further investigation.

1. Grow-bed and hydroponic platform engineering.

Future research should focus on the development of improved grow-bed substrates and hydroponic platform designs that minimize clogging while maintaining favorable conditions for beneficial microbial communities. In media-based systems, long-term accumulation of solids can reduce drainage, create hypoxic conditions, and promote the development of root diseases. Designing lightweight, low-cost, and easily replaceable substrates or hydroponic support structures could help maintain long-term system performance. These materials should provide sufficient surface area for microbial colonization while avoiding physical and chemical conditions that favor pathogenic organisms. Engineering grow-bed structures that balance hydraulic performance, microbial habitat, and root-zone aeration may significantly improve system reliability.

2. Microbiome management using probiotics and prebiotics.

Another promising area for future work is the intentional manipulation of microbial communities in aquaponics systems. The results of this dissertation suggest that microbial composition plays a major role in plant health and disease development. Future studies should evaluate the use of probiotic microbial inoculants and prebiotic substrates to promote beneficial microorganisms and suppress pathogens. In addition to identifying effective microbial strains, research should investigate environmental conditions that support their long-term persistence, including nutrient availability, dissolved oxygen levels, and hydraulic conditions within hydroponic beds.

3. Life cycle and techno-economic assessment of biofloc aquaponics.

While this research evaluated biological performance and nutrient recovery, additional work is needed to assess the environmental and economic sustainability of biofloc aquaponics systems.

Life cycle assessment (LCA) and techno-economic analysis (TEA) could be used to quantify energy use, resource efficiency, greenhouse gas emissions, and production costs associated with different system configurations. Such analyses would help determine the feasibility of scaling these systems for commercial production and identify design strategies that improve economic viability and environmental performance.

4. Comparative microbiome analysis across aquaponic systems.

Further research should also examine microbial communities across multiple aquaponics facilities, including both research and commercial systems. Collecting water and biofilm samples from diverse systems and analyzing their functional microbiomes could help identify key microbial taxa associated with high system productivity and stability. Identifying potential keystone species and understanding their ecological roles may provide insight into how microbial interactions influence nutrient cycling, plant health, and fish performance in aquaponics systems.

5. Optimization of fish–plant production balance.

Determining the optimal ratio between fish production and plant production remains an important challenge in aquaponics design. Future research should investigate system sizing strategies that balance fish feed input with plant nutrient demand. Experiments evaluating different fish stocking densities, feed inputs, and hydroponic growing areas could help establish design guidelines for optimizing plant bed size or plant density relative to fish biomass and feeding rates.

6. Integration of advanced monitoring technologies.

Finally, integrating advanced monitoring technologies may improve system management and long-term stability. The use of real-time water quality sensors, automated control systems, and

data-driven monitoring platforms could enable more precise control of key parameters such as dissolved oxygen, nutrient concentrations, and solids accumulation. Combining these monitoring tools with predictive models or machine learning approaches may allow early detection of system imbalances and improve overall aquaponic system performance.

References

1. Goddek S, Joyce A, Kotzen B, Burnell GM. Aquaponics food production systems: combined aquaculture and hydroponic production technologies for the future: Springer Nature; 2019.
2. Liao C-P, Chu Y-T, Hu Y-F, Lee M-C, Nan F-H, Lu Y-H. From Feeding to Flourishing: Aquaponics Strategies and their Impact on Taiwan. Circular Economy and Sustainability. 2025.
3. Pattillo DA, Cline DJ, Hager JV, Roy LA, Hanson TR. Challenges Experienced by Aquaponic Hobbyists, Producers, and Educators. Journal of Extension. 2022;60(4):13.
4. Turnsek M, Joly A, Thorarinsdottir R, Junge R. Challenges of Commercial Aquaponics in Europe: Beyond the Hype. Water. 2020;12(1):306.
5. Goddek S, Delaide B, Mankasingh U, Ragnarsdottir KV, Jijakli H, Thorarinsdottir R. Challenges of Sustainable and Commercial Aquaponics. Sustainability. 2015;7(4):4199–224.
6. Yep B, Zheng Y. Aquaponic trends and challenges – A review. Journal of Cleaner Production. 2019;228:1586–99.
7. Kasozi N, Abraham B, Kaiser H, Wilhelmi B. The complex microbiome in aquaponics: significance of the bacterial ecosystem. Annals of Microbiology. 2021;71(1):1.
8. Eck M, Körner O, Jijakli MH. Nutrient Cycling in Aquaponics Systems. In: Goddek S, Joyce A, Kotzen B, Burnell GM, editors. Aquaponics Food Production Systems: Combined Aquaculture and Hydroponic Production Technologies for the Future. Cham: Springer International Publishing; 2019. p. 231–46.
9. Ruiz A, Scicchitano D, Palladino G, Nanetti E, Candela M, Furones D, et al. Microbiome study of a coupled aquaponic system: unveiling the independency of bacterial communities and their beneficial influences among different compartments. Scientific Reports. 2023;13(1):19704.
10. Eck M, Sare AR, Massart S, Schmautz Z, Junge R, Smits THM, et al. Exploring Bacterial Communities in Aquaponic Systems. Water. 2019;11(2):260.
11. Joyce A, Timmons M, Goddek S, Pentz T. Bacterial relationships in aquaponics: new research directions. Aquaponics food production systems: Combined aquaculture and hydroponic production technologies for the future. 2019:145–61.
12. Coskuner G, Jassim MS. Development of a correlation to study parameters affecting nitrification in a domestic wastewater treatment plant. Journal of Chemical Technology & Biotechnology. 2008;83(3):299–308.
13. Sun C, Zhang B, Chen Z, Qin W, Wen X. Sludge retention time affects the microbial community structure: A large-scale sampling of aeration tanks throughout China. Environmental Pollution. 2020;261:114140.
14. Goddek S, Keesman KJ. Improving nutrient and water use efficiencies in multi-loop aquaponics systems. Aquaculture International. 2020;28(6):2481–90.
15. Palm HW, Knaus U, Appelbaum S, Strauch SM, Kotzen B. Coupled aquaponics systems. 2019.
16. Aslanidou M, Elvanidi A, Mourantian A, Levizou E, Mente E, Katsoulas N. Nutrients Use Efficiency in Coupled and Decoupled Aquaponic Systems. Horticulturae. 2023;9(10):1077.
17. Goddek S, Joyce A, Wuertz S, Körner O, Bläser I, Reuter M, et al. Decoupled aquaponics systems. Aquaponics food production systems. 2019;10:978–3.
18. Liang J-Y, Chien Y-H. Effects of feeding frequency and photoperiod on water quality and crop production in a tilapia–water spinach raft aquaponics system. International Biodeterioration & Biodegradation. 2013;85:693–700.

19. Jiang W, Ren W, Li L, Dong S, Tian X. Light and carbon sources addition alter microbial community in biofloc-based Litopenaeus vannamei culture systems. Aquaculture. 2020;515:734572.
20. Khanjani MH, Sharifinia M. Production of Nile tilapia Oreochromis niloticus reared in a limited water exchange system: The effect of different light levels. Aquaculture. 2021;542:736912.
21. Baloi M, Arantes R, Schveitzer R, Magnotti C, Vinatea L. Performance of Pacific white shrimp Litopenaeus vannamei raised in biofloc systems with varying levels of light exposure. Aquacultural Engineering. 2013;52:39–44.
22. Zimmermann S, Kiessling A, Zhang J. The future of intensive tilapia production and the circular bioeconomy without effluents: Biofloc technology, recirculation aquaculture systems, bio-RAS, partitioned aquaculture systems and integrated multitrophic aquaculture. Reviews in Aquaculture. 2023;15(S1):22–31.
23. Bankston EM, Wang Q, Higgins B. Algae support populations of heterotrophic, nitrifying, and phosphate-accumulating bacteria in the treatment of poultry litter anaerobic digestate. Chem Eng J. 2020;398:125550.
24. Wang Q, Childree E, Box J, López-Vela M, Sprague D, Cherones J, et al. Microalgae Can Promote Nitrification in Poultry-Processing Wastewater in the Presence and Absence of Antimicrobial Agents. ACS ES&T Engineering. 2023.
25. El Arroussi H, Benhima R, Elbaouchi A, Sijilmassi B, El Mernissi N, Aafsar A, et al. Dunaliella salina exopolysaccharides: a promising biostimulant for salt stress tolerance in tomato (Solanum lycopersicum). Journal of Applied Phycology. 2018;30:2929–41.
26. Renuka N, Guldhe A, Prasanna R, Singh P, Bux F. Microalgae as multi-functional options in modern agriculture: current trends, prospects and challenges. Biotechnology advances. 2018;36(4):1255–73.
27. Devi A, Chiu Y-T, Hsueh H-T, Lin T-F. Quantitative PCR based detection system for cyanobacterial geosmin/2-methylisoborneol (2-MIB) events in drinking water sources: Current status and challenges. Water Research. 2021;188:116478.
28. Jüttner F, Watson SB. Biochemical and ecological control of geosmin and 2-methylisoborneol in source waters. Appl Environ Microbiol. 2007;73(14):4395–406.
29. Morard P, Silvestre J. Plant injury due to oxygen deficiency in the root environment of soilless culture: A review. Plant and Soil. 1996;184(2):243–54.
30. Rakocy JE, Masser M, Losordo T. Recirculating aquaculture tank production systems: Aquaponics-Integrating fish and plant culture. SRAC Publication. 2006;454.
31. García P, Singh S, Graciet E. New Insights into the Connections between Flooding/Hypoxia Response and Plant Defenses against Pathogens. Plants. 2024;13(16):2176.
32. Stouvenakers G, Massart S, Jijakli MH. First Study Case of Microbial Biocontrol Agents Isolated from Aquaponics Through the Mining of High-Throughput Sequencing Data to Control Pythium aphanidermatum on Lettuce. Microbial Ecology. 2023;86(2):1107–19.
33. You MP, Rensing K, Renton M, Barbetti MJ. Modeling effects of temperature, soil, moisture, nutrition and variety as determinants of severity of Pythium damping-off and root disease in subterranean clover. Frontiers in Microbiology. 2017;8:2223.
34. Kilany M, Ibrahim EH, Al Amry S, Al Roman S, Siddiqi S. Microbial suppressiveness of Pythium damping-off diseases. Organic amendments and soil suppressiveness in plant disease management: Springer; 2015. p. 187–206.

35. Dubey MK, Zehra A, Aamir M, Yadav M, Samal S, Upadhyay RS. Isolation, identification, carbon utilization profile and control of Pythium graminicola, the causal agent of chilli damping-off. Journal of Phytopathology. 2020;168(2):88–102.
36. Al-Sadi AM, Al-Masoudi RS, Al-Habsi N, Al-Said FA, Al-Rawahy SA, Ahmed M, et al. Effect of salinity on pythium damping-off of cucumber and on the tolerance of Pythium aphanidermatum. Plant Pathology. 2010;59(1):112–20.
37. Laevens GCS, Dolson WC, Drapeau MM, Telhig S, Ruffell SE, Rose DM, et al. The Good, the Bad, and the Fungus: Insights into the Relationship Between Plants, Fungi, and Oomycetes in Hydroponics. Biology. 2024;13(12):1014.
38. Joyce A, Goddek S, Kotzen B, Wuertz S. Aquaponics: Closing the Cycle on Limited Water, Land and Nutrient Resources. In: Goddek S, Joyce A, Kotzen B, Burnell GM, editors. Aquaponics Food Production Systems: Combined Aquaculture and Hydroponic Production Technologies for the Future. Cham: Springer International Publishing; 2019. p. 19–34.
39. Wongkiew S, Popp BN, Khanal SK. Nitrogen recovery and nitrous oxide (N2O) emissions from aquaponic systems: Influence of plant species and dissolved oxygen. International Biodeterioration & Biodegradation. 2018;134:117–26.
40. Yang T, Kim H-J. Comparisons of nitrogen and phosphorus mass balance for tomato-, basil-, and lettuce-based aquaponic and hydroponic systems. Journal of Cleaner Production. 2020;274:122619.
41. Cerozi BdS, Fitzsimmons K. The effect of pH on phosphorus availability and speciation in an aquaponics nutrient solution. Bioresource Technology. 2016;219:778–81.
42. Yang T, Kim H-J. Characterizing Nutrient Composition and Concentration in Tomato-, Basil-, and Lettuce-Based Aquaponic and Hydroponic Systems. Water. 2020;12(5):1259.
43. Manduca LG, da Silva MA, Alvarenga ÉRd, Alves GFdO, Fernandes AFdA, Assumpção AF, et al. Effects of a zero exchange biofloc system on the growth performance and health of Nile tilapia at different stocking densities. Aquaculture. 2020;521:735064.
44. Zou Y, Hu Z, Zhang J, Xie H, Guimbaud C, Fang Y. Effects of pH on nitrogen transformations in media-based aquaponics. Bioresource Technology. 2016;210:81–7.
45. Pinho SM, Lima JP, David LH, Oliveira MS, Goddek S, Carneiro DJ, et al. Decoupled FLOCponics systems as an alternative approach to reduce the protein level of tilapia juveniles' diet in integrated agri-aquaculture production. Aquaculture. 2021;543:736932.
46. Deng M, Dai Z, Senbati Y, Li L, Song K, He X. Aerobic denitrification microbial community in biofloc-based aquaculture system: influence of the carbon-to-nitrogen ratio. Frontiers in Microbiology. 2020;11:1760.
47. Derikvand P, Sauter B, Stein LY. Development of an aquaponics microbial inoculum for efficient nitrification at acidic pH. Applied microbiology and biotechnology. 2021;105(18):7009–21.
48. Cassán F, Coniglio A, López G, Molina R, Nievas S, de Carlan CLN, et al. Everything you must know about Azospirillum and its impact on agriculture and beyond. Biology and Fertility of Soils. 2020;56:461–79.
49. Hamid SHA, Lananan F, Noor NAM, Endut A. Physical filtration of nutrients utilizing gravel-based and lightweight expanded clay aggregate (LECA) as growing media in aquaponic recirculation system (ARS). Aquacultural Engineering. 2022;98:102261.
50. Carvalho PLPF, Koch JFA, Cintra FT, Fernandes Júnior AC, Sartori MMP, Barros MM, et al. Available phosphorus as a reproductive performance enhancer for female Nile tilapia. Aquaculture. 2018;486:202–9.

51. Chandramenon P, Aggoun A, Tchuenbou-Magaia F. Smart approaches to Aquaponics 4.0 with focus on water quality − Comprehensive review. Computers and Electronics in Agriculture. 2024;225:109256.
52. Siddiqui AQ, Howlader MS, Adam AA. Effects of dietary protein levels on growth, feed conversion and protein utilization in fry and young Nile tilapia, Oreochromis niloticus. Aquaculture. 1988;70(1):63–73.
53. Riche M, Garling D. Feeding tilapia in intensive recirculating systems. 2003.
54. Rakocy JE. Aquaponics—integrating fish and plant culture. Aquaculture production systems. 2012:344–86.
55. Wenzel LC, Strauch SM, Eding E, Presas-Basalo FX, Wasenitz B, Palm HW. Effects of Dissolved Potassium on Growth Performance, Body Composition, and Welfare of Juvenile African Catfish (Clarias gariepinus). Fishes. 2021;6(2):11.
56. Bertrand-Krajewski J-L. TSS concentration in sewers estimated from turbidity measurements by means of linear regression accounting for uncertainties in both variables. Water Science and Technology. 2004;50(11):81–8.
57. (NASA) NAaSA. NASA Power database 2023 [Available from: https://power.larc.nasa.gov/data-access-viewer/.
58. Chaump K, Preisser M, Shanmugam SR, Prasad R, Adhikari S, Higgins BT. Leaching and anaerobic digestion of poultry litter for biogas production and nutrient transformation. Waste Manage. 2018;84:413–22.
59. Bryson GM, Mills HA, Sasseville DN, Jones JB, Barker AV. Plant analysis handbook III : a guide to sampling, preparation, analysis, interpretation and use of results of agronomic and horticultural crop plant tissue. Athens, Georgia: Micro-Macro Publishing, Inc. Athens, Georgia; 2014.
60. Reis WG, Wasielesky W, Abreu PC, Brandão H, Krummenauer D. Rearing of the Pacific white shrimp Litopenaeus vannamei (Boone, 1931) in BFT system with different photoperiods: Effects on the microbial community, water quality and zootechnical performance. Aquaculture. 2019;508:19–29.
61. Hossain S, Debi D, Chowdhury M, Waiho K, Minhaz TM, Islam Z, et al. Bibliographic insight of biofloc technology (BFT): Global trend, research hotspots and prospects. Aquaculture. 2025;600:742251.
62. Raza B, Ramzan MN, Yang W. A review: Improving aquaculture rearing water quality by removal of nutrients using microalgae, challenges and future prospects. Aquaculture. 2025;598:741959.
63. Luquet P. Tilapia, Oreochromis spp. Handbook of Nutrient Requirements of Finfish (1991): CRC Press; 2017. p. 169–80.
64. Karaca M, Erbas O. Solanine Poisoning: Effects, Risks, and Management Strategies. Journao of Experimental and Basic Medicinal Sciences. 2024;5(2):189–93.
65. Crawford L, Kocan RM. Steroidal alkaloid toxicity to fish embryos. Toxicology Letters. 1993;66(2):175–81.
66. Tyson RV, Simonne EH, White JM, Lamb EM, editors. Reconciling water quality parameters impacting nitrification in aquaponics: the pH levels. Proceedings of the Florida State Horticultural Society; 2004.
67. Boyd CE. Water quality management for pond fish culture1982.

68. Dey BK, Verdegem MCJ, Nederlof MAJ, Masagounder K, Mas-Muñoz J, Schrama JW. Effect of temperature on the energy utilization efficiencies of digested protein, fat, and carbohydrates in Nile tilapia (Oreochromis niloticus). Aquaculture. 2023;576:739876.
69. Hochmuth G, Hochmuth R. Nutrient Solution Formulation for Hydroponic (Perlite, Rockwool, NFT) Tomatoes in Florida: HS796/CV216, rev. 9/2018. EDIS. 2018;2018.
70. Patil S, Kadam U, Mane M, Mahale D, Dhekale J. Hydroponic growth media (substrate): a review. International Research Journal of Pure and Applied Chemistry. 2020;21(23):106–13.
71. Khanjani MH, Mozanzadeh MT, Sharifinia M, Emerenciano MGC. Biofloc: A sustainable dietary supplement, nutritional value and functional properties. Aquaculture. 2023;562:738757.
72. Helal AM, Zaher MM, Meshhal DT, Ashour M, Younis EM, Abdelwarith AA, et al. Biofloc supplementation improves growth performances, nutrient utilization, and histological status of Nile tilapia (Oreochromis niloticus) while enhancing zooplankton diversity, community, and abundance. Aquaculture. 2024;585:740711.
73. Nunes LJL, da Silva Campos CVF, da Silva SMBC, Gálvez AO, Brito LO, dos Santos JF. The culture of Nile tilapia (Oreochromis niloticus) juvenile at different culture technologies: autotrophic, bioflocs and synbiotic. Aquaculture. 2024;588:740912.
74. Khanjani MH, Sharifinia M, Hajirezaee S. Recent progress towards the application of biofloc technology for tilapia farming. Aquaculture. 2022;552:738021.
75. Yergeau S, Zemeckis D, VanVranken R. Introduction to Aquaponics Systems. New Brunswick, NJ: Rutgers University; 2025.
76. Underwood J, Dunn B. Aquaponics. Stillwater, OK: Oklahoma State University; 2017.
77. Suarez-Puerto B, Delgadillo-Díaz M, Sánchez-Solís MJ, Gullian-Klanian M. Analysis of the cost-effectiveness and growth of Nile tilapia (Oreochromis niloticus) in biofloc and green water technologies during two seasons. Aquaculture. 2021;538:736534.
78. Elsbaay AM. Effects of photoperiod and different artificial light colors on Nile tilapia growth rate. Journal of Agriculture and Veterinary Science. 2013;3(3):05–12.
79. de Alba G, Conti F, Sanchez J, Godoy LM, Sánchez-Vázquez FJ, López-Olmeda JF, et al. Effect of light and feeding regimes on the daily rhythm of thermal preference in Nile tilapia (Oreochromis niloticus). Aquaculture. 2024;578:740122.
80. Nguyen HYN, Trinh TL, Baruah K, Lundh T, Kiessling A. Growth and feed utilisation of Nile tilapia (Oreochromis niloticus) fed different protein levels in a clear-water or biofloc-RAS system. Aquaculture. 2021;536:736404.
81. Long L, Yang J, Li Y, Guan C, Wu F. Effect of biofloc technology on growth, digestive enzyme activity, hematology, and immune response of genetically improved farmed tilapia (Oreochromis niloticus). Aquaculture. 2015;448:135–41.
82. Cavatti Neto A, Alvarenga ÉRd, Toral FLB, Leite NR, da Costa FFB, Goulart LQ, et al. Impact of selection for growth and stocking density on Nile tilapia production in the biofloc system. Aquaculture. 2023;577:739908.
83. Pai M, Verma AK, Krishnani KK, Varghese T, Hittinahalli CM, John VC, et al. Effects on the productivity, haematological indices, and carcass quality of Nile tilapia reared at different stocking densities in a hybrid biofloc-RAS. Aquaculture. 2025;596:741756.
84. Ekasari J, Napitupulu AD, Djurstedt M, Wiyoto W, Baruah K, Kiessling A. Production performance, fillet quality and cost effectiveness of red Tilapia (Oreochromis sp.) culture in different biofloc systems. Aquaculture. 2023;563:738956.

85. Dunn B, Hendrickson T. Algae Control for Greenhouse Production. Stillwater, OK: Oklahoma State University; 2021.
86. Maynard DN, Barker AV, Minotti PL, Peck NH. Nitrate Accumulation in Vegetables. In: Brady NC, editor. Advances in Agronomy. 28: Academic Press; 1976. p. 71–118.
87. Zhang J, Wang X, Zhou Q. Co-cultivation of Chlorella spp and tomato in a hydroponic system. Biomass and Bioenergy. 2017;97:132–8.
88. Chiaiese P, Corrado G, Colla G, Kyriacou MC, Rouphael Y. Renewable sources of plant biostimulation: microalgae as a sustainable means to improve crop performance. Frontiers in plant science. 2018;9:430391.
89. Sun W, Shahrajabian MH, Kuang Y, Wang N. Amino Acids Biostimulants and Protein Hydrolysates in Agricultural Sciences. Plants. 2024;13(2):210.
90. Barone V, Puglisi I, Fragalà F, Lo Piero AR, Giuffrida F, Baglieri A. Novel bioprocess for the cultivation of microalgae in hydroponic growing system of tomato plants. Journal of Applied Phycology. 2019;31(1):465–70.
91. Martins VB, Dartora A, de Lima Lasala M, Morais KF, de Andrade JIA, Jatobá A. Cultivation of vegetables in an integrated biofloc system with nile tilapia. Aquaculture. 2025;596:741818.
92. Nebauer SG, Sánchez M, Martínez L, Lluch Y, Renau-Morata B, Molina RV. Differences in photosynthetic performance and its correlation with growth among tomato cultivars in response to different salts. Plant Physiology and Biochemistry. 2013;63:61–9.
93. Cantore V, Pace B, Todorović M, De Palma E, Boari F. Influence of salinity and water regime on tomato for processing. Italian Journal of Agronomy. 2012;7(1):e10–e.
94. Rakocy J, Masser M, Losordo T. Recirculating aquaculture tank production systems: aquaponics-integrating fish and plant culture. 2016. SRAC Publication-Southern Regional Aquaculture Center (454). 2006.
95. Schmautz Z, Espinal CA, Smits THM, Frossard E, Junge R. Nitrogen transformations across compartments of an aquaponic system. Aquacultural Engineering. 2021;92:102145.
96. Tzortzakis N, Pitsikoulaki G, Stamatakis A, Chrysargyris A. Ammonium to Total Nitrogen Ratio Interactive Effects with Salinity Application on Solanum lycopersicum Growth, Physiology, and Fruit Storage in a Closed Hydroponic System. Agronomy [Internet]. 2022; 12(2).
97. Risgaard-Petersen N, Nicolaisen MH, Revsbech NP, Lomstein BA. Competition between Ammonia-Oxidizing Bacteria and Benthic Microalgae. Appl Environ Microbiol. 2004;70(9):5528.
98. Fang Y, Hu Z, Zou Y, Fan J, Wang Q, Zhu Z. Increasing economic and environmental benefits of media-based aquaponics through optimizing aeration pattern. Journal of Cleaner Production. 2017;162:1111–7.
99. Liu G, Wang J. Role of solids retention time on complete nitrification: mechanistic understanding and modeling. Journal of Environmental Engineering. 2014;140(1):48–56.
100. Daims H, Lebedeva EV, Pjevac P, Han P, Herbold C, Albertsen M, et al. Complete nitrification by Nitrospira bacteria. Nature. 2015;528(7583):504–9.
101. González-Tineo P, Aguilar A, Reynoso A, Durán U, Garzón-Zúñiga M, Meza-Escalante E, et al. Organic matter removal in a simultaneous nitrification–denitrification process using fixed-film system. Scientific Reports. 2022;12(1):1882.

102. Arthur W, Morgan Z, Reina Antillon M, Drabold E, Wells DE, Bourassa DV, et al. Pilot-Scale Evaluation of Poultryponics: Insights into Nitrogen Utilization and Food Pathogen Dynamics. ACS ES&T Water. 2024;4(9):3964–75.
103. Kasozi N, Abraham B, Kaiser H, Wilhelmi B. The complex microbiome in aquaponics: significance of the bacterial ecosystem. Annals of Microbiology. 2021;71.
104. Ajijah N, Apriyana AY, Sriwuryandari L, Priantoro EA, Janetasari SA, Pertiwi TYR, et al. Beneficiary of nitrifying bacteria for enhancing lettuce (Lactuca sativa) and vetiver grass (Chrysopogon zizanioides L.) growths align with carp (Cyprinus carpio) cultivation in an aquaponic system. Environmental Science and Pollution Research. 2021;28(1):880–9.
105. Patel M, Islam S, Glick BR, Vimal SR, Bhor SA, Bernardi M, et al. Elaborating the multifarious role of PGPB for sustainable food security under changing climate conditions. Microbiological Research. 2024;289:127895.
106. Singh VK, Singh AK, Kumar A. Disease management of tomato through PGPB: current trends and future perspective. 3 Biotech. 2017;7(4):255.
107. Rilling JI, Acuña JJ, Nannipieri P, Cassan F, Maruyama F, Jorquera MA. Current opinion and perspectives on the methods for tracking and monitoring plant growth–promoting bacteria. Soil Biology and Biochemistry. 2019;130:205–19.
108. Thijs S, Sillen W, Rineau F, Weyens N, Vangronsveld J. Towards an enhanced understanding of plant–microbiome interactions to improve phytoremediation: engineering the metaorganism. Frontiers in Microbiology. 2016;7:341.
109. Cammies C, Prior T, Lawson R, Gilarte P, Crichton R. An exploration of nematode assemblages in the hydroponic media beds of a commercial aquaponics system. Nematology. 2023;25(5):495–508.
110. Suárez-Cáceres GP, Pérez-Urrestarazu L, Avilés M, Borrero C, Lobillo Eguíbar JR, Fernández-Cabanás VM. Susceptibility to water-borne plant diseases of hydroponic vs. aquaponics systems. Aquaculture. 2021;544:737093.
111. Khalil S, Panda P, Ghadamgahi F, Rosberg A, Vetukuri RR. Comparison of two commercial recirculated aquacultural systems and their microbial potential in plant disease suppression. BMC microbiology. 2021;21:1–19.
112. Mori J, Smith R. Transmission of waterborne fish and plant pathogens in aquaponics and their control with physical disinfection and filtration: A systematized review. Aquaculture. 2019;504:380–95.
113. Rezaei S, Spoor M, Hohn G, Schorer R, Bender G, Cline D, et al. Enhancing yields: The role of fish tank illumination and coupling/decoupling in biofloc aquaponics performance. Aquaculture. 2026;613:743286.
114. Schmautz Z, Graber A, Jaenicke S, Goesmann A, Junge R, Smits THM. Microbial diversity in different compartments of an aquaponics system. Archives of Microbiology. 2017;199(4):613–20.
115. Kalvakaalva R, Prior SA, Smith M, Runion GB, Ayipio E, Blanchard C, et al. Direct greenhouse gas emissions from a pilot-scale aquaponics system. Journal of the ASABE. 2022;In Press.
116. Bertrand-Krajewski JL. TSS concentration in sewers estimated from turbidity measurements by means of linear regression accounting for uncertainties in both variables. Water Sci Technol. 2004;50(11):81–8.

117. Keck H, Strubbe L, Magyar PM, Joss A, Froemelt A, Kupferschmid A, et al. Continuous analysis of N2O isotopic composition during biological nitrogen removal in wastewater treatment to disentangle production and reduction processes. EGUsphere. 2026;2026:1–29.
118. Chen C, Guan W, Xie Q, Chen G, He X, Zhang H, et al. n-3 essential fatty acids in Nile tilapia, Oreochromis niloticus: Bioconverting LNA to DHA is relatively efficient and the LC-PUFA biosynthetic pathway is substrate limited in juvenile fish. Aquaculture. 2018;495:513–22.
119. Beach N, Young M. Rethinking Aeration: Enhancing Efficiency and Biological Nutrient Removal with Low Dissolved Oxygen Operations. The Splash. 2026:25–8, no.
120. Rezaei S, Otto M, Hohn G, Wang Q, Arthur W, Hall MB, et al. Coupling, decoupling, and fish tank illumination shape the functional microbiome and nutrient cycling in aquaponics. Bioresource Technology Reports. 2025;32:102439.
121. Bryson GM, Mills HA, Sasseville DN, Jones JB, Barker AV. Plant analysis handbook III: A guide to sampling, preparation, analysis, interpretation and use of results of agronomic and horticultural crop plant tissue: Micro-Macro Publishing, Incorporated; 2014.
122. Schwyn B, Neilands J. Universal chemical assay for the detection and determination of siderophores. Analytical biochemistry. 1987;160(1):47–56.
123. Patz S, Gautam A, Becker M, Ruppel S, Rodríguez-Palenzuela P, Huson D. PLaBAse: A comprehensive web resource for analyzing the plant growth-promoting potential of plant-associated bacteria. bioRxiv. 2021:2021.12.13.472471.
124. Kloepper J. Plant growth promoting rhizobacteria (PGPR) for plant health, nutrient uptake, and disease & pest control library. Department of Entomology and Plant Pathology: Auburn University; 2025.
125. Schober I, Koblitz J, Sardà Carbasse J, Ebeling C, Schmidt ML, Podstawka A, et al. BacDive in 2025: the core database for prokaryotic strain data. Nucleic Acids Research. 2024;53(D1):D748–D56.
126. Pedro H, Maheswari U, Urban M, Irvine AG, Cuzick A, McDowall MD, et al. PhytoPath: an integrative resource for plant pathogen genomics. Nucleic Acids Research. 2015;44(D1):D688–D93.
127. Urban M, Cuzick A, Seager J, Nonavinakere N, Sahoo J, Sahu P, et al. PHI-base – the multi-species pathogen–host interaction database in 2025. Nucleic Acids Research. 2024;53(D1):D826–D38.
128. InnoTech HH. Healthy Hydroponics Pathogen, Plant Pathogens 2021 [Available from: https://www.healthyhydroponics.ca/pathogens-we-detect/.
129. Ferris H. Nemaplex.UCDavis.edu: Revision Date: 10/20/2025; Accessed (04/30/2025). In: Ferris H, editor. Department of Entomology and Nematology: University of California; 2025.
130. EPPO EaMPPO. EPPO Global Database. In: (EPPO) EaMPPO, editor. 2025.
131. Rout GR, Sahoo S. Role of iron in plant growth and metabolism. Reviews in Agricultural Science. 2015;3:1–24.
132. Magalhaes JR, Wilcox G. Ammonium toxicity development in tomato plants relative to nitrogen form and light intensity. Journal of Plant Nutrition. 1984;7(10):1477–96.
133. Seleiman MF, Santanen A, Mäkelä PSA. Recycling sludge on cropland as fertilizer – Advantages and risks. Resources, Conservation and Recycling. 2020;155:104647.
134. Ru D, Liu J, Hu Z, Zou Y, Jiang L, Cheng X, et al. Improvement of aquaponic performance through micro- and macro-nutrient addition. Environmental Science and Pollution Research. 2017;24(19):16328–35.

135. Chen T-Y, Zheng Y-Y, Wang Y-H, Yeh C-C, Liao C-H, Lee T-M. A zero-waste approach to Sarcodia suiae valorization: Recycling aquaculture wastes and carbon dioxide for biostimulant, biofertilizer, and bioenergy production. Bioresource Technology. 2025;418:131929.
136. Sallam NM, Eraky AM, Sallam A. Effect of Trichoderma spp. on Fusarium wilt disease of tomato. Molecular Biology Reports. 2019;46:4463–70.
137. Stouvenakers G, Dapprich P, Massart S, Jijakli MH. Plant pathogens and control strategies in aquaponics. Aquaponics food production systems. 2019;14:353–78.
138. He Y, Liu J, Shen C, Yi X, Li X, Huang X, et al. Innovative method of culturing bdelloid rotifers for the application of wastewater biological treatment. Frontiers of Environmental Science & Engineering. 2022;16:1–9.
139. Kirke J, Jin X-L, Zhang X-H. Expression of a Tardigrade Dsup Gene Enhances Genome Protection in Plants. Molecular Biotechnology. 2020;62(11):563–71.
140. Ahlawat OP, Yadav D, Walia N, Kashyap PL, Sharma P, Tiwari R. Root Exudates and Their Significance in Abiotic Stress Amelioration in Plants: A Review. Journal of Plant Growth Regulation. 2024;43(6):1736–61.
141. Timofeeva AM, Galyamova MR, Sedykh SE. Bacterial Siderophores: Classification, Biosynthesis, Perspectives of Use in Agriculture. Plants (Basel). 2022;11(22).
142. Singh VK, Singh AK, Singh PP, Kumar A. Interaction of plant growth promoting bacteria with tomato under abiotic stress: A review. Agriculture, Ecosystems & Environment. 2018;267:129–40.
143. Han JW, Oh M, Choi GJ, Kim H. Genome Sequence of Delftia acidovorans HK171, a Nematicidal Bacterium Isolated from Tomato Roots. Genome Announcements. 2017;5(9):10.1128/genomea.01746–16.
144. Reimann S, Hauschild R, Hildebrandt U, Sikora R. Interrelationships between Rhizobium etti G12 and Glomus intraradices and multitrophic effects in the biological control of the root-knot nematode Meloidogyne incognita on tomato/Interaktionen zwischen Rhizobium etli G12 und Glomus intraradices und multitrophische Effekte bei der biologischen Bekämpfung von Meloidogyne incognita an Tomaten. Journal of Plant Diseases and Protection. 2008:108–13.
145. Dey R, Devi S, Dube SP, Raghuwanshi R. Potentials of endophytic bacteria Pseudomonas gessardii RRBHU-1 in promoting tomato growth under biotic stress. Plant Disease Research. 2023;38(2):306–.
146. Ahmed W, Wang Y, Ji W, Liu S, Zhou S, Pan J, et al. Unraveling the mechanism of the endophytic bacterial strain pseudomonas oryzihabitans GDW1 in enhancing tomato plant growth through modulation of the host transcriptome and bacteriome. International Journal of Molecular Sciences. 2025;26(5):1922.
147. Corral R, Leach J, Verdier V, Vera Cruz C. Recovery plan for Xanthomonas oryzae causing bacterial blight and bacterial leaf streak of rice. Bulletin, NPDRS. 2013;22.
148. KarmelReetha A, Muthukumar A. Occurrence, virulence and pathogenicity of Pythium aphanidermatum causing tomato damping off. Plant Arch. 2019;19(2):2476–80.
149. Baaji Z, Farrokhinejad R, Mehrabi-Koushki M. New host and record of Didymella prosopidis from Iran. Mycologia Iranica. 2022;9(1):117–21.
150. Auger J, Leal G, Magunacelaya JC, Esterio M. Xiphinema rivesi from Chile Transmits Tomato ringspot virus to Cucumber. Plant Dis. 2009;93(9):971.
151. Jones MGK, Fosu-Nyarko J. Molecular biology of root lesion nematodes (Pratylenchus spp.) and their interaction with host plants. Annals of Applied Biology. 2014;164(2):163–81.

152. Martin H. California Pest Rating Profile for Xiphinema rivesi Dalmasso 1969 Dagger nematode California Department of Food and Agriculture; 2024.
153. Szekely I, Jijakli MH. Bioponics as a Promising Approach to Sustainable Agriculture: A Review of the Main Methods for Producing Organic Nutrient Solution for Hydroponics. Water [Internet]. 2022; 14(23).
154. Giménez A, Fernández JA, Pascual JA, Ros M, Egea-Gilabert C. Application of Directly Brewed Compost Extract Improves Yield and Quality in Baby Leaf Lettuce Grown Hydroponically. Agronomy [Internet]. 2020; 10(3).
155. Arthur W, Morgan Z, Reina Antillon M, Drabold E, Wells DE, Bourassa DV, et al. Pilot-Scale Evaluation of Poultryponics: Insights into Nitrogen Utilization and Food Pathogen Dynamics. ACS ES&T Water. 2024.
156. Palm HW, Knaus U, Appelbaum S, Goddek S, Strauch SM, Vermeulen T, et al. Towards commercial aquaponics: a review of systems, designs, scales and nomenclature. Aquaculture International. 2018;26(3):813–42.
157. Lennard WA, Leonard BV. A comparison of three different hydroponic sub-systems (gravel bed, floating and nutrient film technique) in an aquaponic test system. Aquaculture International. 2006;14(6):539–50.
158. Chung H, Lee Y-H. Hypoxia: A Double-Edged Sword During Fungal Pathogenesis? Frontiers in Microbiology. 2020;11.
159. Sirakov I, Lutz M, Graber A, Mathis A, Staykov Y, Smits THM, et al. Potential for Combined Biocontrol Activity against Fungal Fish and Plant Pathogens by Bacterial Isolates from a Model Aquaponic System. Water. 2016;8(11):518.
160. Love DC, Fry JP, Li X, Hill ES, Genello L, Semmens K, et al. Commercial aquaponics production and profitability: Findings from an international survey. Aquaculture. 2015;435:67–74.
161. Villarroel M, Junge R, Komives T, König B, Plaza I, Bittsánszky A, et al. Survey of aquaponics in Europe. Water. 2016;8(10):468.
162. Nazari MT, Schommer VA, Braun JCA, dos Santos LF, Lopes ST, Simon V, et al. Using Streptomyces spp. as plant growth promoters and biocontrol agents. Rhizosphere. 2023;27:100741.
163. Chandramenon P, Aggoun A, Tchuenbou-Magaia F. Smart approaches to Aquaponics 4.0 with focus on water quality− Comprehensive review. Computers and Electronics in Agriculture. 2024;225:109256.
164. Kalvakaalva R, Prior SA, Smith M, Runion GB, Ayipio E, Blanchard C, et al. Direct greenhouse gas emissions from a pilot-scale aquaponics system. Journal of the ASABE. 2022;65(6):1211–23.
165. Nelson RL. Aquaponics. Tilapia in Intensive Co-culture2017. p. 246–60.
166. Love DC, Fry JP, Genello L, Hill ES, Frederick JA, Li X, et al. An International Survey of Aquaponics Practitioners. PloS one. 2014;9(7):e102662.
167. Sojka RE, Oosterhuis DM, Scott HD. Root oxygen deprivation and the reduction of leaf stomatal aperture and gas exchange. 2005.
168. Else MA, Janowiak F, Atkinson CJ, Jackson MB. Root signals and stomatal closure in relation to photosynthesis, chlorophyll a fluorescence and adventitious rooting of flooded tomato plants. Annals of botany. 2009;103(2):313–23.
169. van de Vossenberg BT, Prodhomme C, Vossen JH, van der Lee TA. Synchytrium endobioticum, the potato wart disease pathogen. Molecular Plant Pathology. 2022;23(4):461–74.

170. CABI C. Synchytrium endobioticum (wart disease of potato). CABI Compendium. 2022a.
171. CABI C. Pythium graminicola (seedling blight of grasses). CABI Compendium. 2022b.
172. Wu W, Ogawa F, Ochiai M, Yamada K, Fukui H. Common strategies to control pythium disease. Reviews in Agricultural Science. 2020;8:58–69.
173. van der Plaats-Niterink AJ. Monograph of the genus Pythium: Centraalbureau voor Schimmelcultures Baarn; 1981.
174. Shivas RG. Fungal and bacterial diseases of plants in Western Australia. Journal of the Royal Society of Western Australia (Australia). 1989;72(12).
175. Huang J-S, Peng Y-H, Chung K-R, Huang J-W. Suppressive efficacy of volatile compounds produced by Bacillus mycoides on damping-off pathogens of cabbage seedlings. The Journal of Agricultural Science. 2018;156(6):795–809.
176. Wu J-J, Huang J-W, Deng W-L. Phenylacetic acid and methylphenyl acetate from the biocontrol bacterium Bacillus mycoides BM02 suppress spore germination in Fusarium oxysporum f. sp. lycopersici. Frontiers in microbiology. 2020;11:569263.
177. Paul B, Charles R, Bhatnagar T. Biological control of Pythium mamillatum causing damping-off of cucumber seedlings by a soil bacterium, Bacillus mycoides. Microbiological Research. 1995;150(1):71–5.
178. Khan S, Srivastava S, Karnwal A, Malik T. Streptomyces as a promising biological control agents for plant pathogens. Front Microbiol. 2023;14:1285543.
179. Múnera JDC, Hausbeck MK. Integrating Host Resistance and Plant Protectants to Manage Pythium Root Rot on Geranium and Snapdragon. HortScience. 2015;50(9):1319–26.
180. Heather.Martin. California Pest Rating Proposal for Pratylenchus crenatus Loof 1960 Root lesion nematode. California Department of Food and Agriculture; 2023.
181. Abrantes IMdO, Esteves I. Pratylenchus penetrans (northern root lesion nematode). CABI Compendium. 2022.
182. Mountain W, Fisher J. Stunting of tomato associated with Pratylenchus penetrans, an apparent migrant from an adjoining peach orchard. 1954.
183. Potter J, Olthof TH. Analysis of crop losses in tomato due to Pratylenchus penetrans. Journal of Nematology. 1977;9(4):290.
184. Handbooks PNPM. Cherry (Prunus spp.)-Nematode, Dagger2025.
185. Akinbade S, Mojtahedi H, Guerra L, Eastwell K, Villamor D, Handoo Z, et al. First report of Xiphinema rivesi (Nematoda, Longidoridae) in Washington state. Plant disease. 2014;98(7):1018–.
186. Migunova VD, Sasanelli N. Bacteria as Biocontrol Tool against Phytoparasitic Nematodes. Plants. 2021;10(2):389.
187. Bélair G, Dauphinais N, Jobin G. Soil amendments with Streptomyces lydicus WYEC108 and chitin against the northern rootknot nematode, Meloidogyne hapla Chitwood, on tomato. Russian Journal of Nematology. 2011;19(1):93–.
188. CABI C. Burkholderia andropogonis (bacterial leaf stripe of sorghum and corn). CABI Compendium. 2022c.
189. Sun J, Li Y, Zheng L, Chen D, Zhou X, Li P. The first complete genome of Robbsia andropogonis reveals its arsenal of virulence system causing leaf spot disease of areca palm. Phytopathology Research. 2024;6(1):51.

190. Okomoda VT, Oladimeji SA, Solomon SG, Olufeagba SO, Ogah SI, Ikhwanuddin M. Aquaponics production system: A review of historical perspective, opportunities, and challenges of its adoption. Food Science & Nutrition. 2023;11(3):1157–65.
191. Martinez-Cordova LR, Emerenciano MGC, Miranda-Baeza A, Pinho SM, Garibay-Valdez E, Martínez-Porchas M. Advancing toward a more integrated aquaculture with polyculture > aquaponics > biofloc technology > FLOCponics. Aquaculture International. 2023;31(2):1057–76.
192. Li C, Ge Z, Dai L, Chen Y. Integrated application of biofloc technology in aquaculture: a review. Water. 2025;17(14):2107.
193. Khanjani MH, Mohammadi A, Emerenciano MGC. Water quality in biofloc technology (BFT): an applied review for an evolving aquaculture. Aquaculture International. 2024;32(7):9321–74.
194. Pinho SM, de Lima JP, David LH, Emerenciano MG, Goddek S, Verdegem MC, et al. FLOCponics: The integration of biofloc technology with plant production. Reviews in Aquaculture. 2022;14(2):647–75.
195. Yu Y-B, Choi J-H, Lee J-H, Jo A-H, Han SW, Han S-H, et al. Biofloc Application Using Aquaponics and Vertical Aquaculture Technology in Aquaculture: Review. Fishes. 2023;8(11):543.
196. Chen S, Sun X, Tian X, Jiang W, Dong X, Li L. Influence of ammonia nitrogen management strategies on microbial communities in biofloc-based aquaculture systems. Science of The Total Environment. 2023;903:166159.
197. Raza B, Zheng Z, Yang W. A Review on Biofloc System Technology, History, Types, and Future Economical Perceptions in Aquaculture. Animals. 2024;14(10):1489.
198. Hu F, Cang S, Zhu Q, Li Y, Sun D, Tan H. Extended photoperiods enhance the production and water treatment performance of algal-bacterial bioflocs from aquaculture wastewater. Journal of Water Process Engineering. 2024;67:106258.
199. Little SM, Senhorinho GN, Saleh M, Basiliko N, Scott JA, Shannon ML, et al. Antibacterial compounds in green microalgae from extreme environments: a review. Algae. 2021;36(1):61–72.
200. Aly SM, ElBanna NI, Fathi M. Chlorella in aquaculture: challenges, opportunities, and disease prevention for sustainable development. Aquaculture International. 2024;32(2):1559–86.
201. Neto AC, de Alvarenga ÉR, Toral FLB, Leite NR, da Costa FFB, Goulart LQ, et al. Impact of selection for growth and stocking density on Nile tilapia production in the biofloc system. Aquaculture. 2023;577:739908.
202. Zheng D, Wilén BM, Öberg O, Wik T, Modin O. "Metagenomics reveal the potential for geosmin and 2-methylisoborneol production across multiple bacterial phyla in recirculating aquaculture systems". Environ Microbiol. 2024;26(10):e16696.
203. Wang Q, Childree E, Box J, López-Vela M, Sprague D, Cherones J, et al. Microalgae Can Promote Nitrification in Poultry-Processing Wastewater in the Presence and Absence of Antimicrobial Agents. ACS ES&T Engineering. 2023;3(4):568–79.
204. Mirzaei M, Jazini M, Aminiershad G, Refardt D. Biodesalination of saline aquaculture wastewater with simultaneous nutrient removal and biomass production using the microalgae Arthrospira and Dunaliella in a circular economy approach. Desalination. 2024;581:117564.
205. Geng B, Li Y, Liu X, Ye J, Guo W. Effective treatment of aquaculture wastewater with mussel/microalgae/bacteria complex ecosystem: a pilot study. Scientific Reports. 2022;12(1):2263.

206. Wu D, Cheng M, Zhao S, Peng N, Hu R, Hu J, et al. Algal Growth Enhances Light-Mediated Limitation of Bacterial Nitrification in an Aquaculture System. Water, Air, & Soil Pollution. 2020;231(2):73.
207. Goddek S, Joyce A, Wuertz S, Körner O, Bläser I, Reuter M, et al. Decoupled Aquaponics Systems. In: Goddek S, Joyce A, Kotzen B, Burnell GM, editors. Aquaponics Food Production Systems: Combined Aquaculture and Hydroponic Production Technologies for the Future. Cham: Springer International Publishing; 2019. p. 201–29.
208. Schmautz Z, Walser J-C, Espinal CA, Gartmann F, Scott B, Pothier JF, et al. Microbial diversity across compartments in an aquaponic system and its connection to the nitrogen cycle. Science of The Total Environment. 2022;852:158426.
209. Wang Q, Cherones J, Higgins B. Acclimation of an algal consortium to sequester nutrients from anaerobic digestate. Bioresource technology. 2021;342:125921.
210. Gruber W, Magyar PM, Mitrovic I, Zeyer K, Vogel M, von Känel L, et al. Tracing N2O formation in full-scale wastewater treatment with natural abundance isotopes indicates control by organic substrate and process settings. Water Research X. 2022;15:100130.
211. Manduca LG, da Silva MA, de Alvarenga ER, de Oliveira Alves GF, de Araújo Fernandes AF, Assumpcao AF, et al. Effects of a zero exchange biofloc system on the growth performance and health of Nile tilapia at different stocking densities. Aquaculture. 2020;521:735064.
212. Xu Z, Cao J, Qin X, Qiu W, Mei J, Xie J. Toxic effects on bioaccumulation, hematological parameters, oxidative stress, immune responses and tissue structure in fish exposed to ammonia nitrogen: a review. Animals. 2021;11(11):3304.
213. Kushwaha J, Priyadarsini M, Rani J, Pandey KP, Dhoble AS. Aquaponic trends, configurations, operational parameters, and microbial dynamics: a concise review. Environment, Development and Sustainability. 2025;27(1):213–46.
214. Reis WG, Wasielesky Jr W, Abreu PC, Brandão H, Krummenauer D. Rearing of the Pacific white shrimp Litopenaeus vannamei (Boone, 1931) in BFT system with different photoperiods: Effects on the microbial community, water quality and zootechnical performance. Aquaculture. 2019;508:19–29.
215. Stoneham TR, Kuhn DD, Taylor DP, Neilson AP, Smith SA, Gatlin DM, et al. Production of omega-3 enriched tilapia through the dietary use of algae meal or fish oil: Improved nutrient value of fillet and offal. PloS one. 2018;13(4):e0194241.
216. Abd El-Hack ME, El-Saadony MT, Elbestawy AR, Ellakany HF, Abaza SS, Geneedy AM, et al. Undesirable odour substances (geosmin and 2-methylisoborneol) in water environment: Sources, impacts and removal strategies. Marine Pollution Bulletin. 2022;178:113579.
217. From J, Hørlyck V. Sites of uptake of geosmin, a cause of earthy-flavor, in rainbow trout (Salmo gairdneri). Canadian Journal of Fisheries and Aquatic Sciences. 1984;41(8):1224–6.
218. Lindholm-Lehto P, Vielma J, Pakkanen H, Alén R. Depuration of geosmin-and 2-methylisoborneol-induced off-flavors in recirculating aquaculture system (RAS) farmed European whitefish Coregonus lavaretus. Journal of food science and technology. 2019;56(10):4585–94.
219. Grimm CC, Lloyd SW, Zimba PV. Instrumental versus sensory detection of off-flavors in farm-raised channel catfish. Aquaculture. 2004;236(1-4):309–19.
220. Petersen MA, Hyldig G, Strobel BW, Henriksen NH, Jørgensen NO. Chemical and sensory quantification of geosmin and 2-methylisoborneol in rainbow trout (Oncorhynchus

mykiss) from recirculated aquacultures in relation to concentrations in basin water. Journal of Agricultural and Food Chemistry. 2011;59(23):12561–8.
221. Robertson R, Jauncey K, Beveridge M, Lawton L. Depuration rates and the sensory threshold concentration of geosmin responsible for earthy-musty taint in rainbow trout, Onchorhynchus mykiss. Aquaculture. 2005;245(1-4):89–99.
222. Austin B, Austin DA. Bacterial Fish Pathogens. 2012. p. 229–78.
223. Nokhwal A, Vaid RK, Anand T, Verma R, Gulati R. Aeromonas Species Diversity, Virulence Characteristics, and Antimicrobial Susceptibility Patterns in Village Freshwater Aquaculture Ponds in North India. Antibiotics (Basel). 2025;14(3).
224. Lee B-H, Nicolas P, satıcıoğlu I, Fradet B, Bernardet J-F, Rigaudeau D, et al. Investigation of the Genus Flavobacterium as a Reservoir for Fish-Pathogenic Bacterial Species: the Case of Flavobacterium collinsii. Applied and environmental microbiology. 2023;89:e0216222.
225. Agnew W, Barnes AC. Streptococcus iniae: An aquatic pathogen of global veterinary significance and a challenging candidate for reliable vaccination. Veterinary Microbiology. 2007;122(1):1–15.
226. Fernández-Bravo A, Figueras MJ. An Update on the Genus Aeromonas: Taxonomy, Epidemiology, and Pathogenicity. Microorganisms. 2020;8(1).
227. Loch TP, Faisal M. Emerging flavobacterial infections in fish: A review. J Adv Res. 2015;6(3):283–300.
228. Van Doan H, Soltani M, Leitão A, Shafiei S, Asadi S, Lymbery AJ, et al. Streptococcosis a Re-Emerging Disease in Aquaculture: Significance and Phytotherapy. Animals (Basel). 2022;12(18).
229. Lee BH, Nicolas P, Saticioglu IB, Fradet B, Bernardet JF, Rigaudeau D, et al. Investigation of the Genus Flavobacterium as a Reservoir for Fish-Pathogenic Bacterial Species: the Case of Flavobacterium collinsii. Appl Environ Microbiol. 2023;89(4):e0216222.
230. De Schryver P, Crab R, Defoirdt T, Boon N, Verstraete W. The basics of bio-flocs technology: The added value for aquaculture. Aquaculture. 2008;277(3):125–37.
231. Ahmad I, Babitha Rani AM, Verma AK, Maqsood M. Biofloc technology: an emerging avenue in aquatic animal healthcare and nutrition. Aquaculture International. 2017;25(3):1215–26.
232. Yadav NK, Paul S, Patel AB, Mahanand SS, Biswas P, Choudhury TG, et al. The role of biofloc technology in sustainable aquaculture: nutritional insights and system efficiency. Blue Biotechnology. 2025;2(1):7.
233. Addy MM, Kabir F, Zhang R, Lu Q, Deng X, Current D, et al. Co-cultivation of microalgae in aquaponic systems. Bioresource Technology. 2017;245:27–34.
234. Jiang W, Li Q, Jiang L, Huang Q, Liang J, Zhou Y, et al. Red Light Enhanced Nitrogen Removal Efficiency by Bacterial–Algae Biofilm Reactor in Recirculating Aquaculture Systems. Processes. 2025;13(11):3594.
235. Li Q, Xu Y, Liang C, Peng L, Zhou Y. Nitrogen removal by algal-bacterial consortium during mainstream wastewater treatment: Transformation mechanisms and potential N(2)O mitigation. Water Res. 2023;235:119890.
236. Bossa R, Di Colandrea M, Salbitani G, Carfagna S. Phosphorous Utilization in Microalgae: Physiological Aspects and Applied Implications. Plants. 2024;13(15):2127.

237. Raj S, Sreenikethanam A, Gobi M, Sakate D, Jayakumar T, Rakesh S, et al. Effect of phosphate availability on the dynamics of polyphosphate accumulation in microalgae. Scientific Reports. 2025;15(1):39069.
238. Kalvakaalva R, Smith M, Ayipio E, Blanchard C, Prior SA, Runion GB, et al. Mass-Balance Process Model of a Decoupled Aquaponics System. Journal of the ASABE. 2023;66(4):955–67.
239. Cerozi BS, Fitzsimmons K. Phosphorus dynamics modeling and mass balance in an aquaponics system. Agricultural Systems. 2017;153:94–100.
240. Yogev U, Barnes A, Gross A. Nutrients and Energy Balance Analysis for a Conceptual Model of a Three Loops off Grid, Aquaponics. Water. 2016;8(12):589.
241. Deng M, Li L, Dai Z, Senbati Y, Song K, He X. Aerobic denitrification affects gaseous nitrogen loss in biofloc-based recirculating aquaculture system. Aquaculture. 2020;529:735686.
242. Van Rijn J, Tal Y, Schreier HJ. Denitrification in recirculating systems: theory and applications. Aquacultural engineering. 2006;34(3):364–76.
243. Nootong K, Pavasant P, Powtongsook S. Effects of organic carbon addition in controlling inorganic nitrogen concentrations in a biofloc system. Journal of the World Aquaculture Society. 2011;42(3):339–46.
244. Fang Y, Hu Z, Zou Y, Zhang J, Zhu Z, Zhang J, et al. Improving nitrogen utilization efficiency of aquaponics by introducing algal-bacterial consortia. Bioresource Technology. 2017;245:358–64.
245. Nishanth D, Somanathan Nair C, Manoharan R, Subramanian R, Salim I, Maqsood S, et al. Current technologies for nutrient recovery in aquaponic systems: a review. Frontiers in Sustainable Food Systems. 2025;Volume 9 - 2025.
246. Lellis WA, Barrows FT, Hardy RW. Effects of phase-feeding dietary phosphorus on survival, growth, and processing characteristics of rainbow trout Oncorhynchus mykiss. Aquaculture. 2004;242(1-4):607–16.
247. Powell N, Shilton AN, Pratt S, Chisti Y. Factors Influencing Luxury Uptake of Phosphorus by Microalgae in Waste Stabilization Ponds. Environmental Science & Technology. 2008;42(16):5958–62.
248. Li Z, Ren X, Zuo J, Liu Y, Duan E, Yang J, et al. Struvite Precipitation for Ammonia Nitrogen Removal in 7-Aminocephalosporanic Acid Wastewater. Molecules. 2012;17(2):2126–39.

Appendix: Supplementary Information

Chapter 2: Enhancing Yields: The Role of Fish Tank Illumination and Coupling/Decoupling in Aquaponics Performance

Table S2.1. Survival rates of fish (A) and specific growth rate (B) across the four treatments.

Survival rate	Mar-27 to Jun-1	Jun-1 to Aug-1	Aug-1 to Oct-1	Oct-1 to Nov-28
Light-Decoupled	100%	99%	100%	0.33% (*60%)
Light-Coupled	100%	100%	100%	100%
Dark-Decoupled	100%	100%	99%	100%
Dark-Coupled	100%	98%	98%	100%

*This value was calculated based on the total number of fish stocked in this treatment, which amounted to 200 fish. Following each mass mortality event, the tanks were re-stocked to maintain this total.

Table S2.2. Thermal growth coefficient (TGC) for tilapia over an 8-month grow-out

	Light-Decoupled	Light-Coupled	Dark-Decoupled	Dark-Coupled
Thermal growth coefficient	1.64 ± 0.04	1.83 ± 0.03	1.52 ± 0.11	1.61 ± 0.05

Figure S2.1. Setup of twelve aquaponics systems (four treatments with three replicates each) at the E.W. Shell Fisheries Station, Auburn University, Alabama, USA.

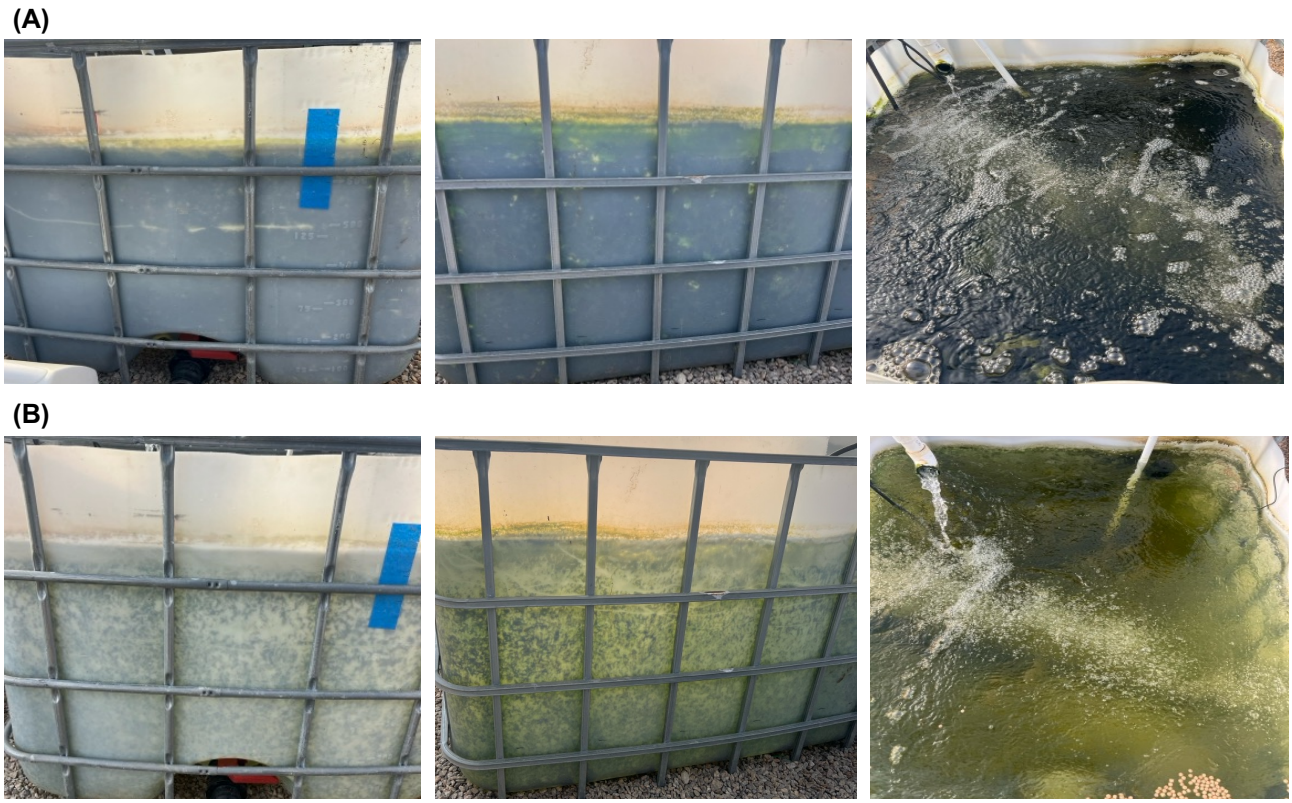

Figure S2.2. Biofilm patterns on the fish tank wall observed before (A) and after (B) the introduction of fish in a representative system.

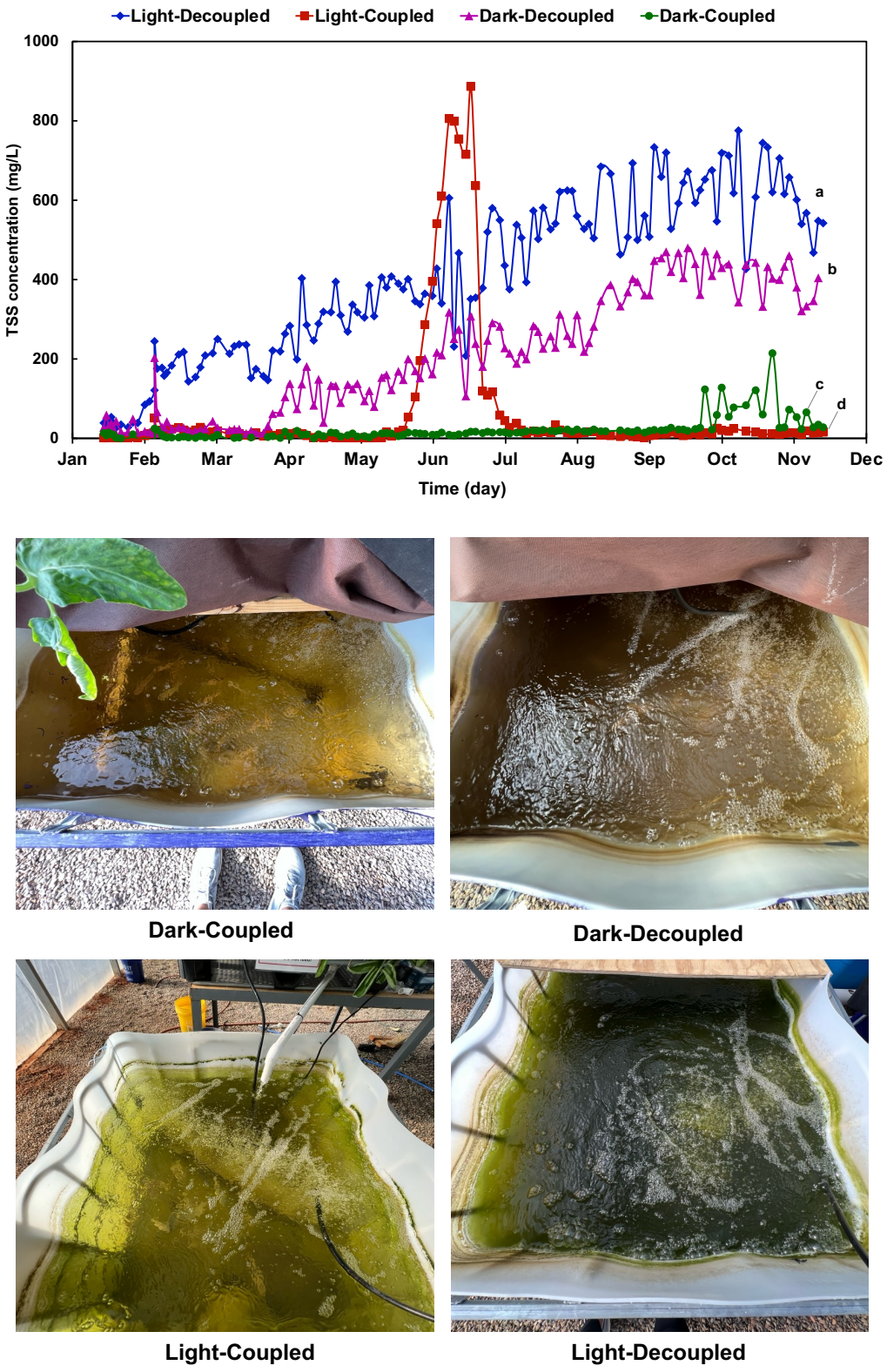

Figure S2.3. (A) Total suspended solids (TSS) in the fish tanks measured over the 10-month experimental period across the four treatments. Treatments with the same letter are not significantly different (alpha > 0.05) based on Tukey's HSD test using time-course ANOVA. (B) Comparison of water clarity across the four treatments.

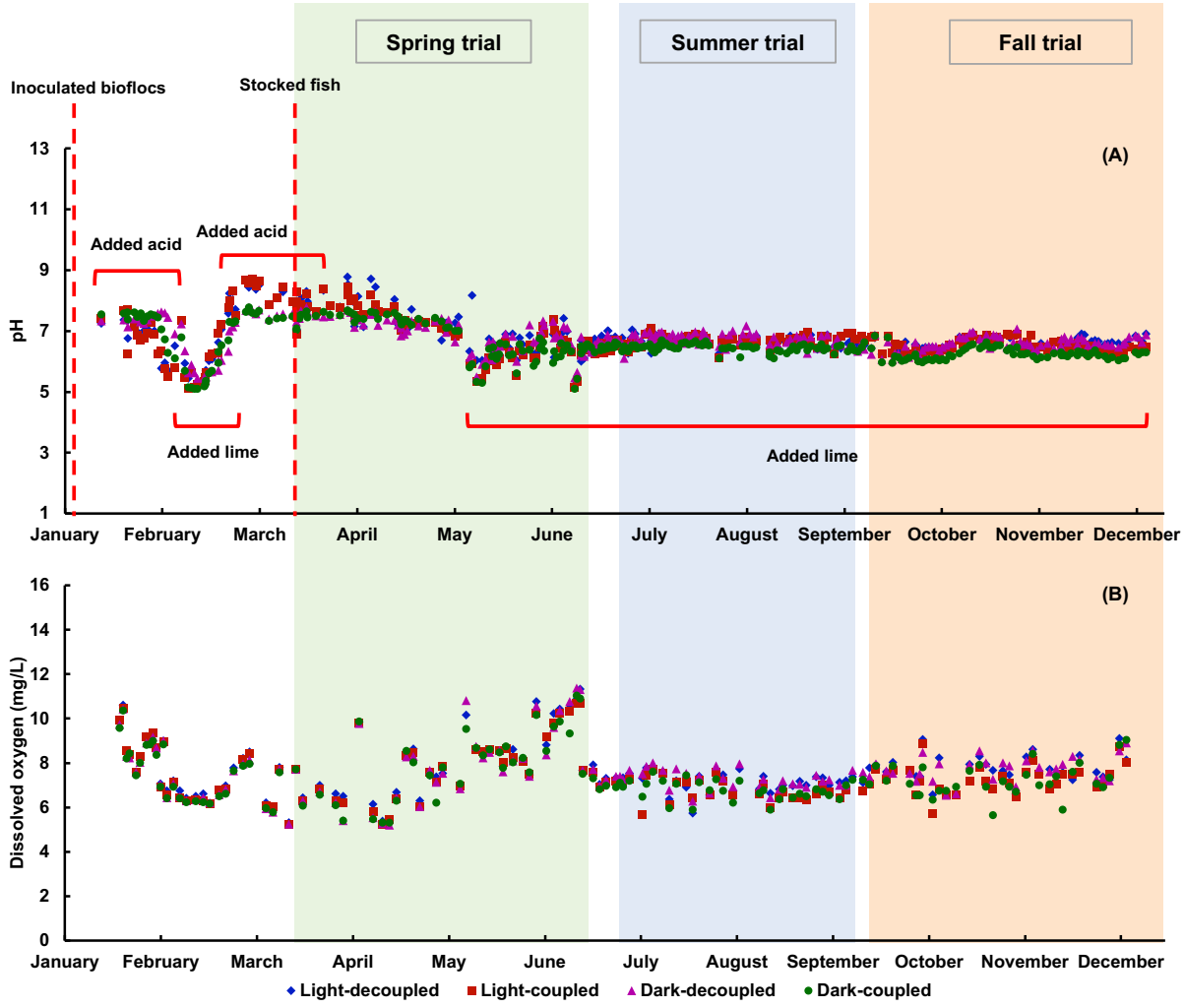

Figure S2.4. Time-course plots of (A) pH, and (B) dissolved oxygen (DO) measured in the fish tanks across the four treatments.

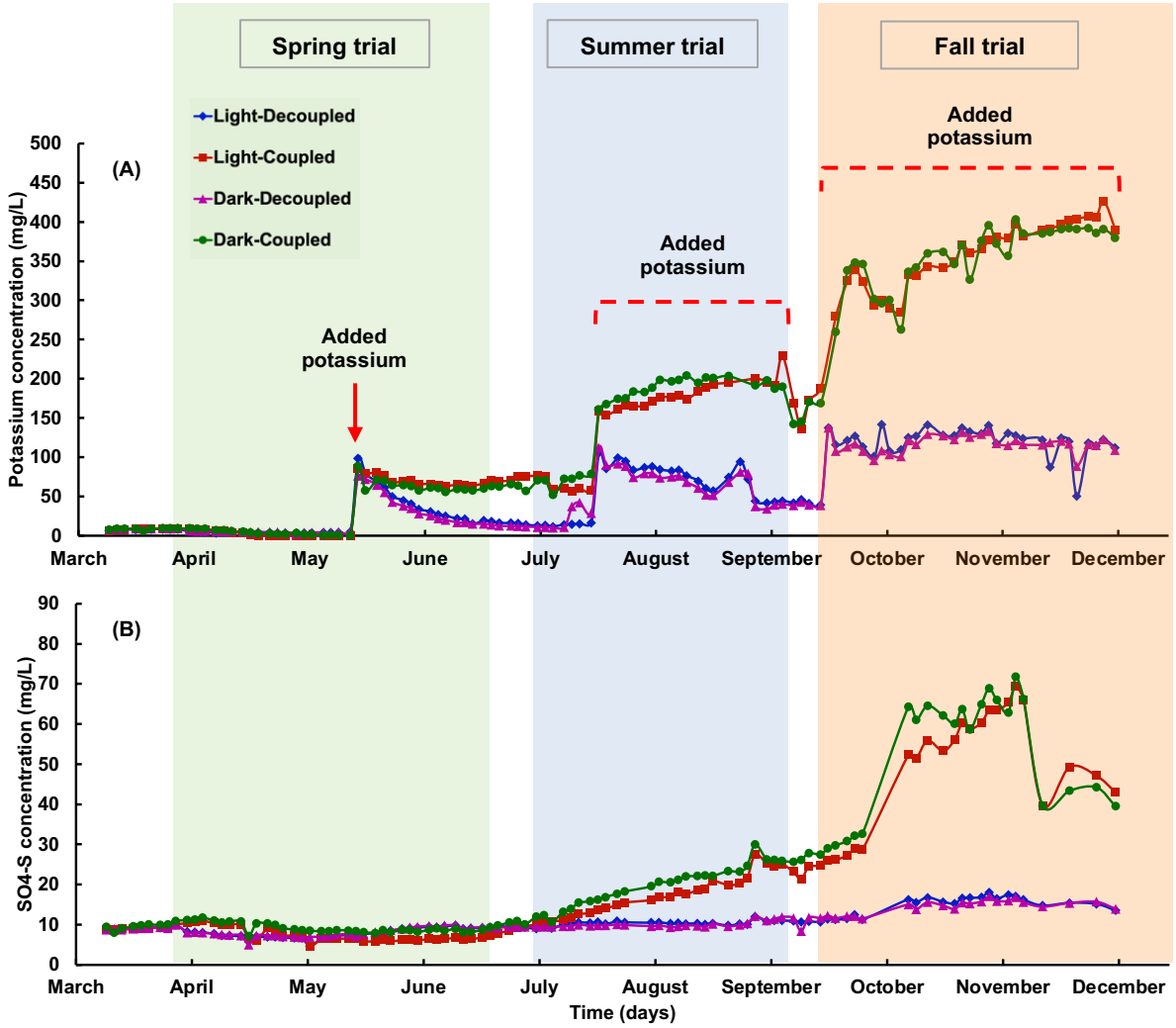

Figure S2.5. Time-course plots of (A) potassium and (B) sulfate (SO4-S) concentrations in the fish tanks across the four treatments. Potassium was added at single time points to the fish tanks at the beginning of each experiment. In decoupled systems, it was also added to the make-up water tank starting in the summer trial.

Figure S2.6. Visual indicators of root asphyxiation observed in the coupled systems.

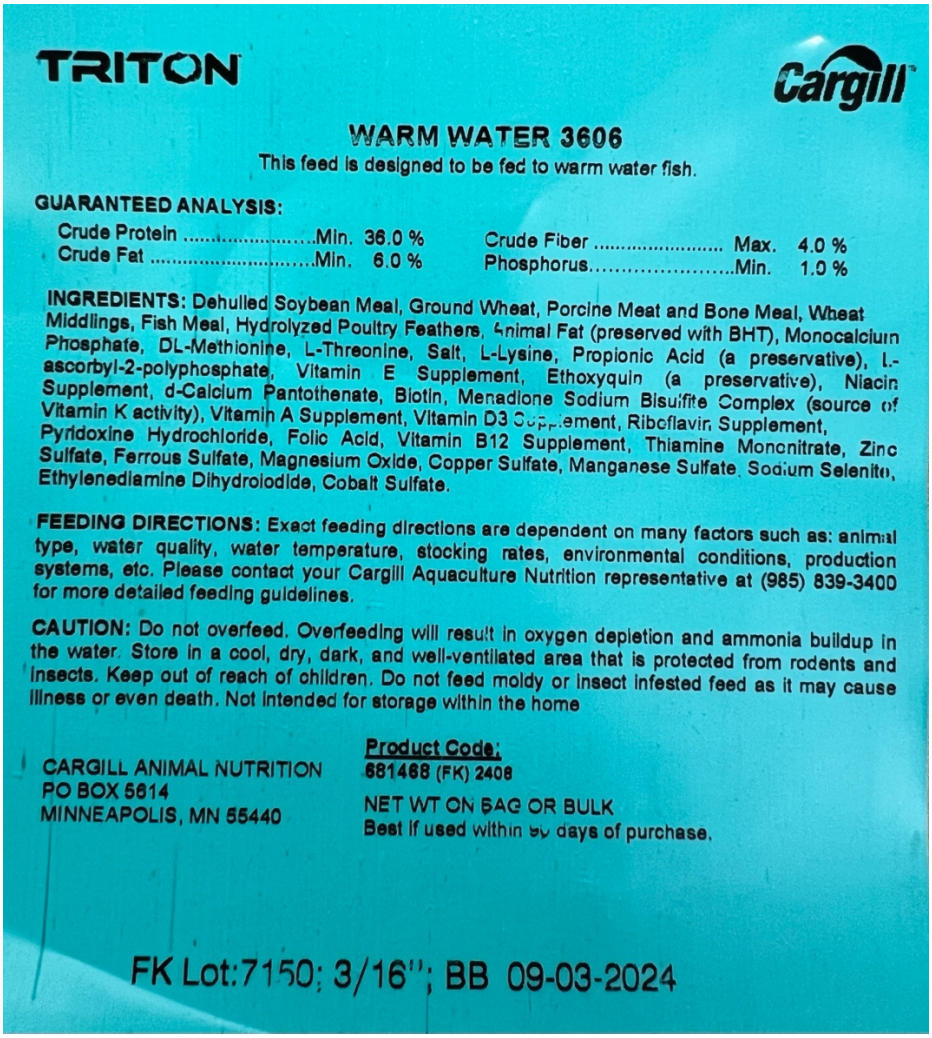

Figure S2.7. Fish feed ingredients

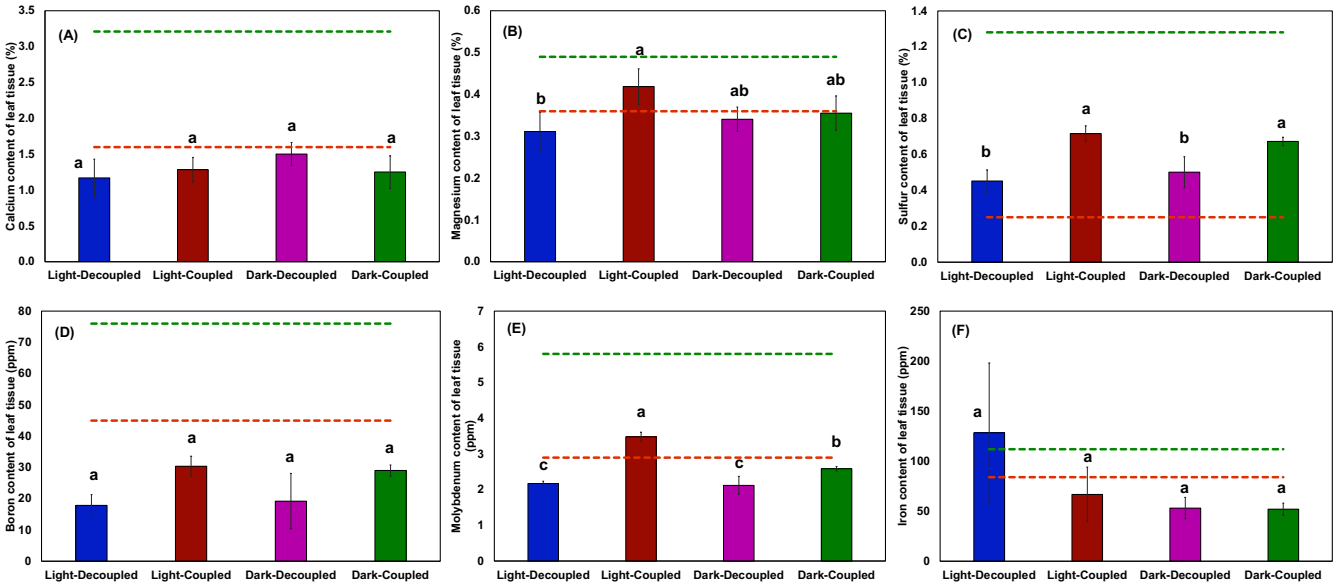

Figure S2.8. Nutrient contents of leaf tissue measured during the second trial across the four treatments: (A) calcium, (B) magnesium, (C) sulfur, (D) boron, (E) molybdenum, and (F) iron. The orange and green lines represent the minimum and maximum thresholds of the sufficiency range, respectively.

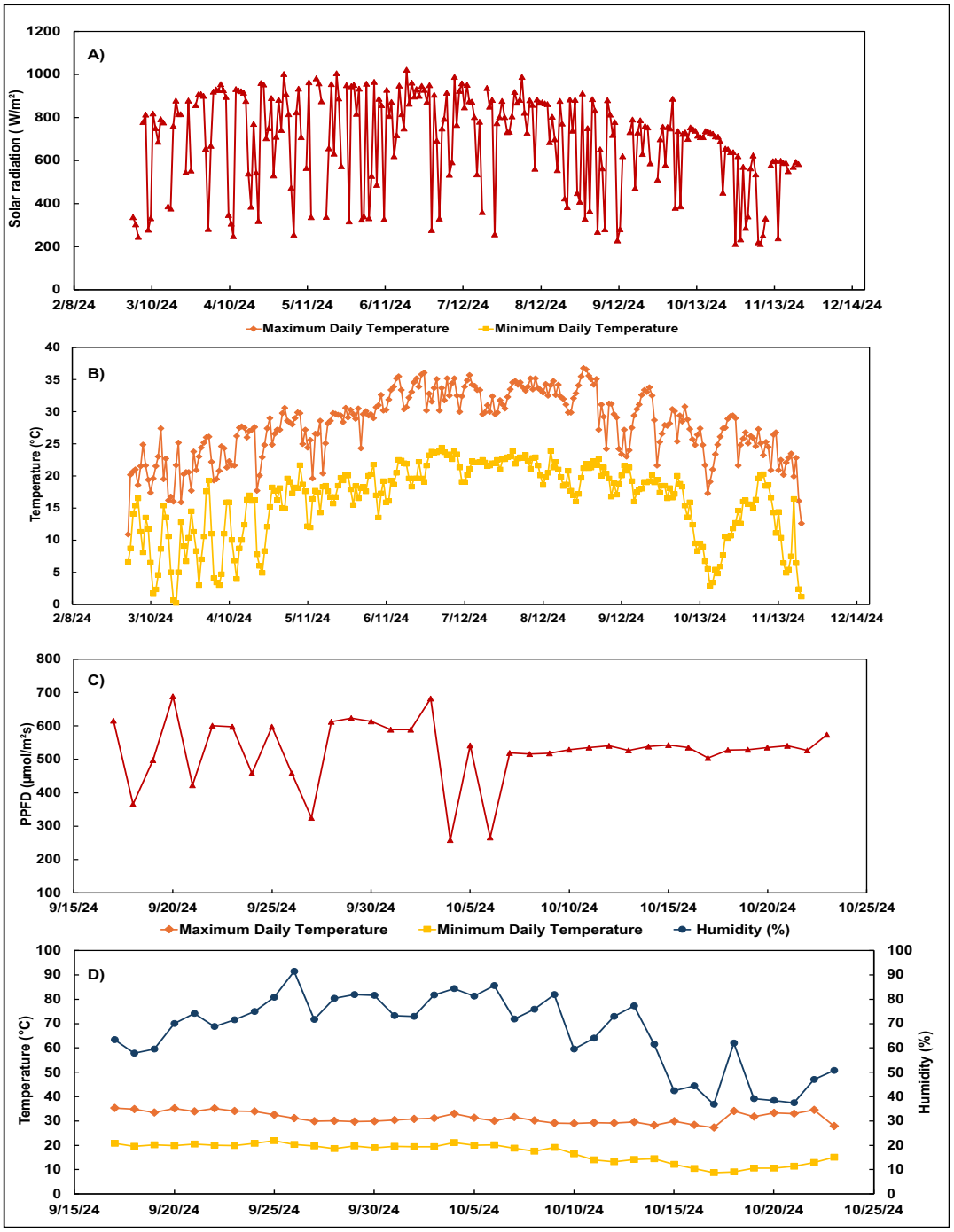

Figure S3.1. (A) Solar radiation (W/m²) and (B) maximum and minimum outdoor temperature (°C) data during the trial period as measured by a Zentra z6-25229 weather station located adjacent to the aquaponics greenhouse. (C) Temporal variation of Photosynthetic Photon Flux Density (PPFD, µmol m^{-2} s^{-1}) at noon (D), temperature (°C), and

relative humidity (%) inside the greenhouse as measured by an Apogee SM-600 during the fall trial. This unit was acquired after the spring trial concluded, which is why the data is not shown.

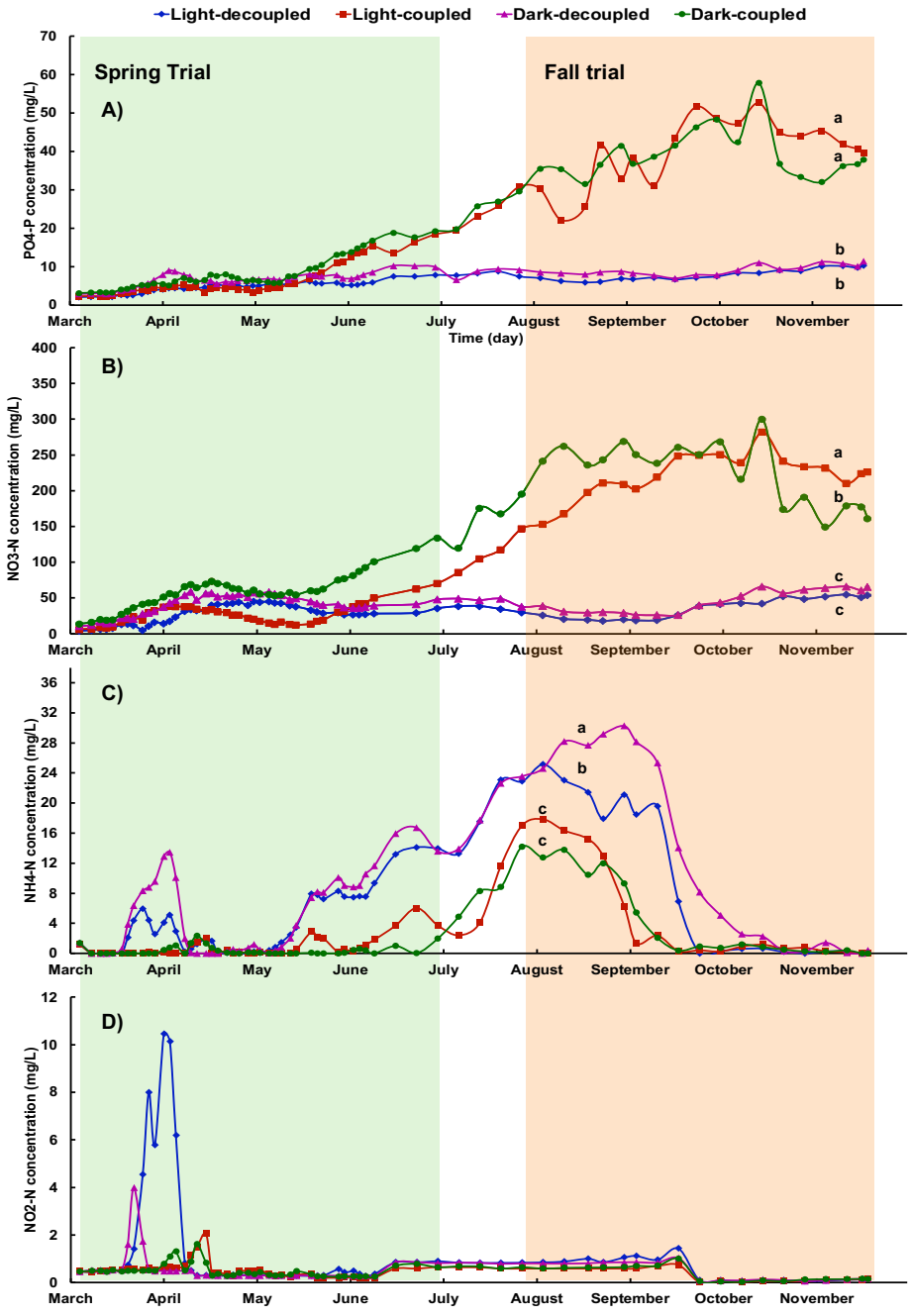

Figure S3.2. Time-course plots of nutrient concentrations in the fish tanks across the four treatments (light-decoupled (LD), light-coupled (LC), dark-decoupled (DD), and dark-coupled (DC)): (A)PO4-P, (B) NO3-N, (C) NH4-N, and (D) NO2-N

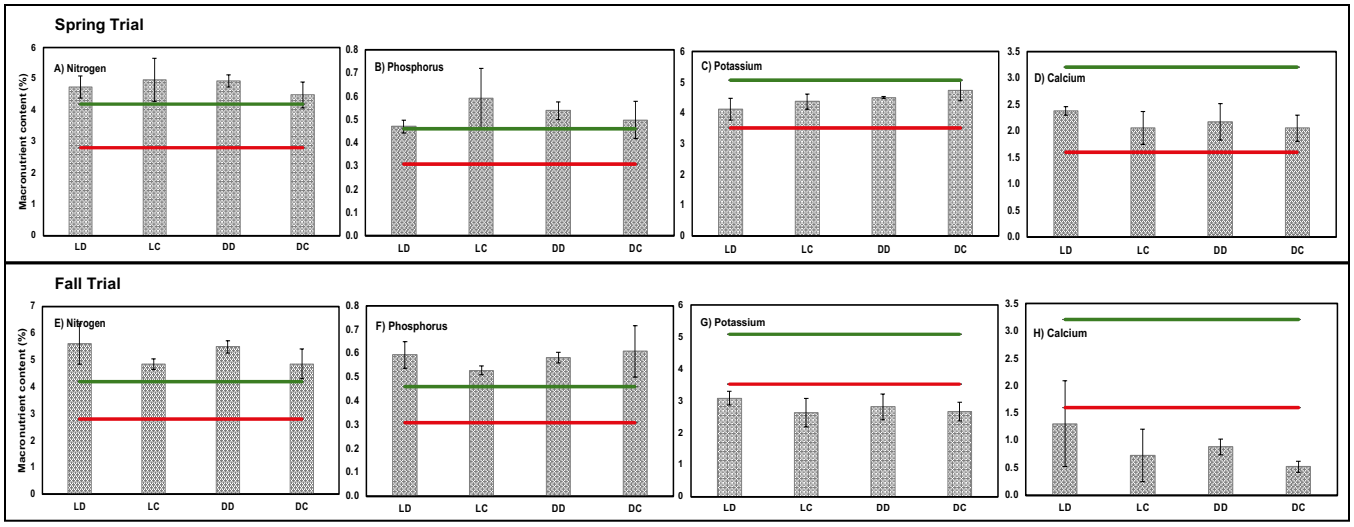

Figure S3.3. Micronutrient contents of leaf tissue measured during the spring and fall trial across the four treatments: (A), (E) Nitrogen, (B), (F) Phosphorus, (C), (G) Potassium, and (D), (H) Calcium. The red and green lines represent the minimum and maximum thresholds of the sufficiency range, respectively.

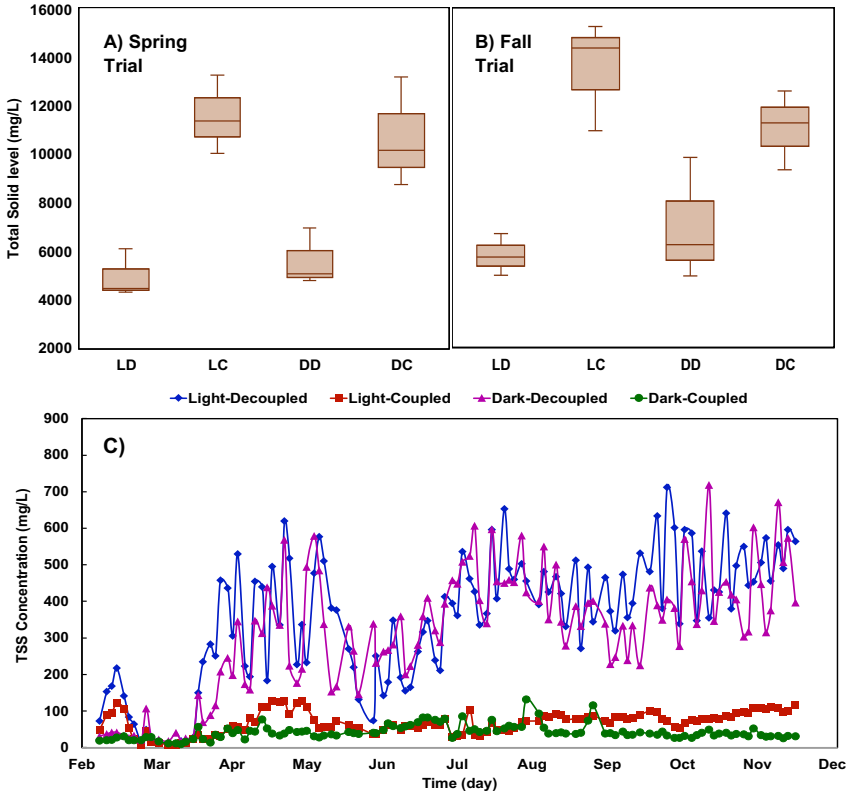

Figure S3.4. Total solid levels in the grow beds during the A) spring and B) fall trials, and C) in the fish tanks across the four treatments.

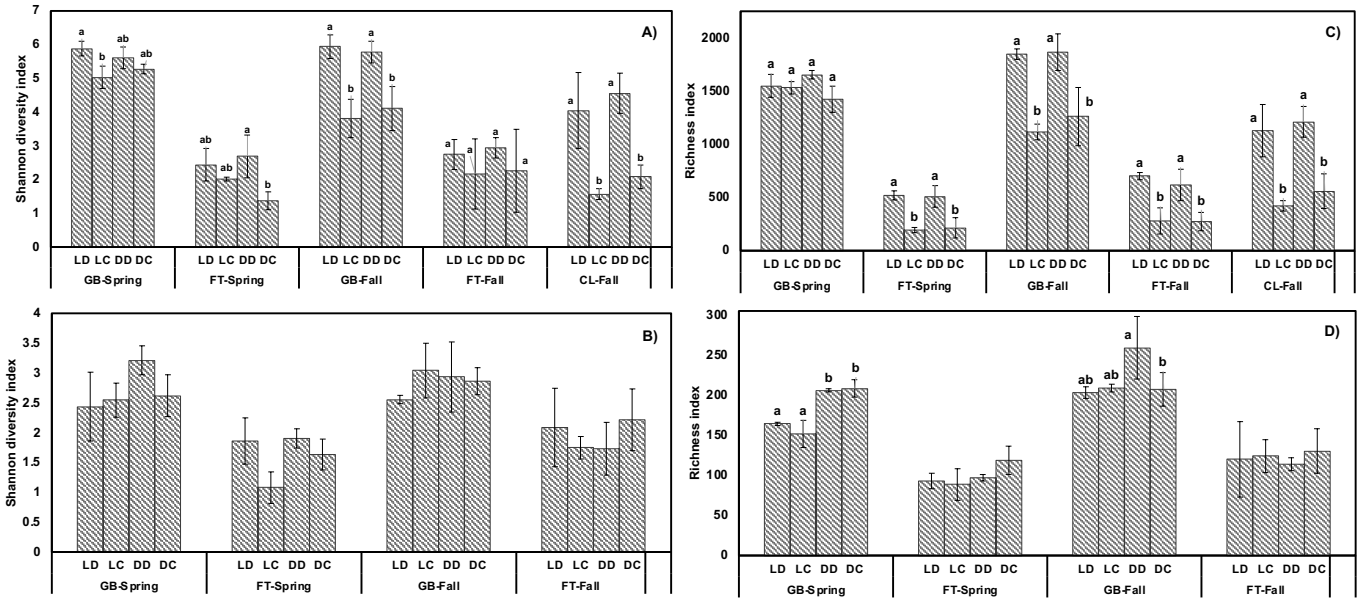

Figure S3.5. Shannon diversity index for (A) 16S and (B) 18S rRNA gene sequences, and species richness for (C) 16S and (D) 18S rRNA gene sequences across treatments and compartments.

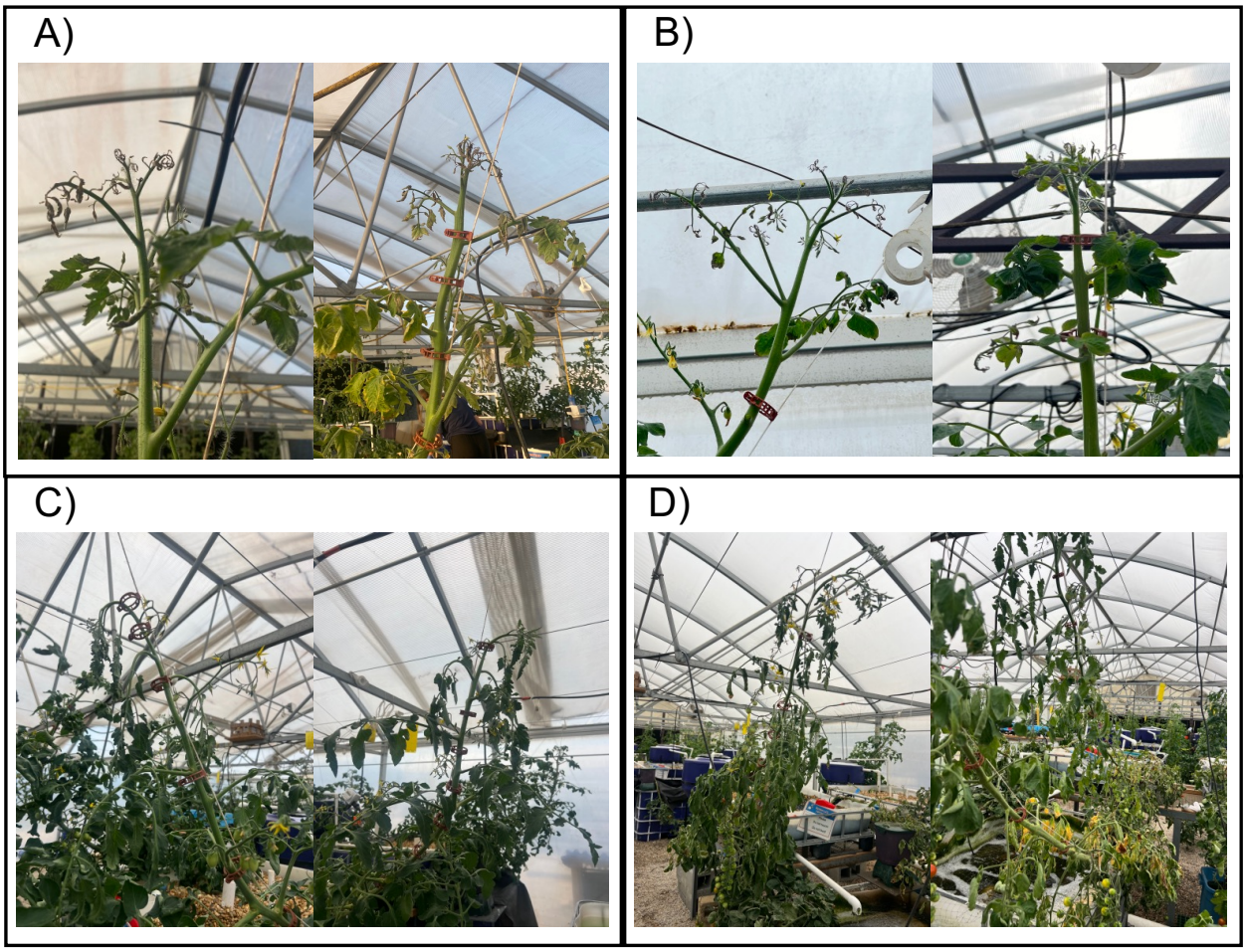

Figure S3.6. Apical bud necrosis in (A) two replicates of the light-decoupled system and (B) one replicate of the dark-decoupled system, and wilted and stunted plants in (C) the dark-decoupled and (C) the light-coupled systems.

Chapter 4: Physical and Microbial Root-Zone Factors Underlying Tomato Wilt in Long-Term Biofloc Aquaponic Systems

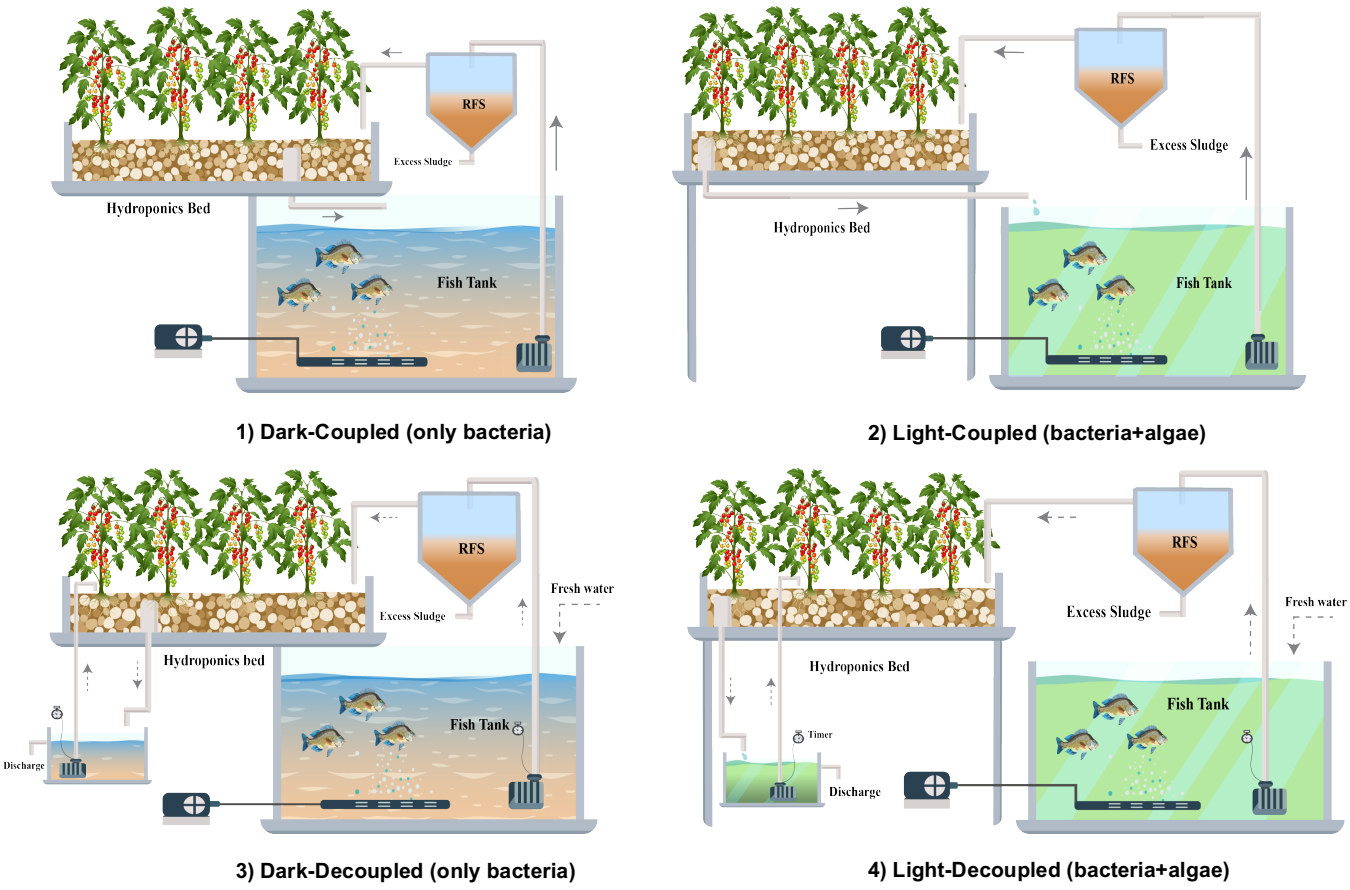

Figure S4.1. Schematic representation of the four aquaponic system types operated over ten months, encompassing fish growth from fingerlings to marketable size and two tomato production trials. The four system types include: (1) Dark-coupled (bacteria-dominant community), (2) Light-coupled (algae-dominant community), (3) Dark-decoupled (bacteria-dominant community), and (4) Light-decoupled (algae-dominant community).

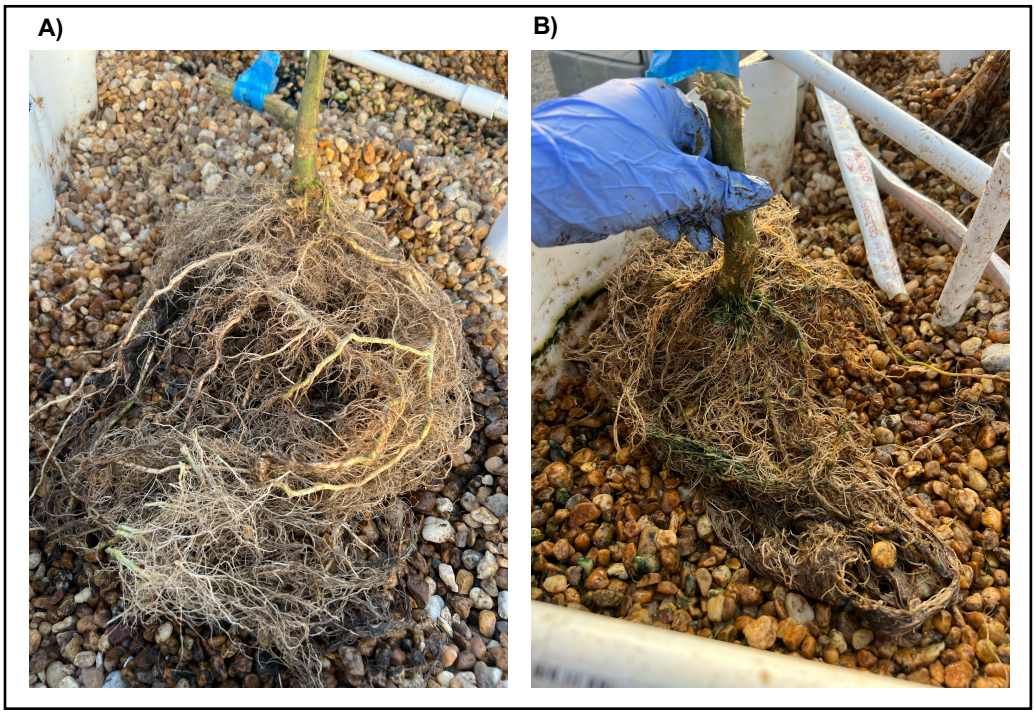

Figure S4.2. An example of (A) healthy and intact roots versus (B) rotten and brown roots.

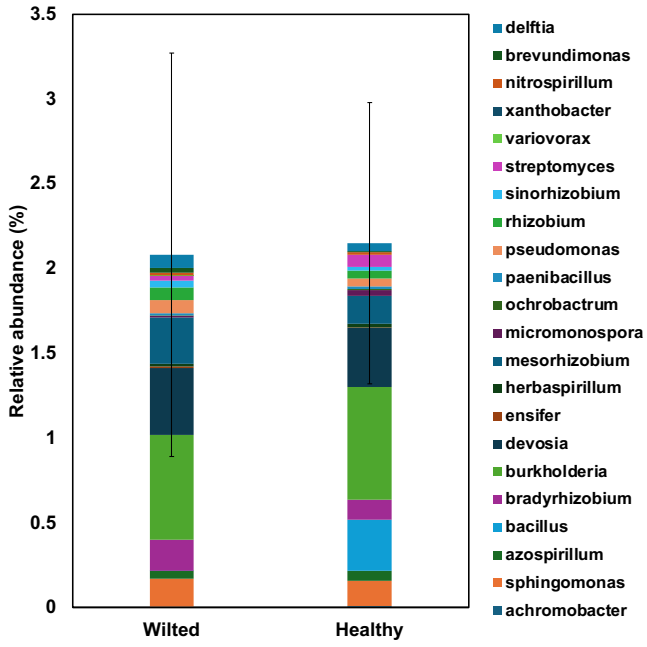

Figure S4.3. Relative abundance of putative plant growth-promoting bacteria at the genus level across the root zones of healthy and wilted plants.

Chapter 5: Photoautotrophic Conditions and Coupled Configuration Improve Aquaponics Productivity Without Increased Off-Flavor

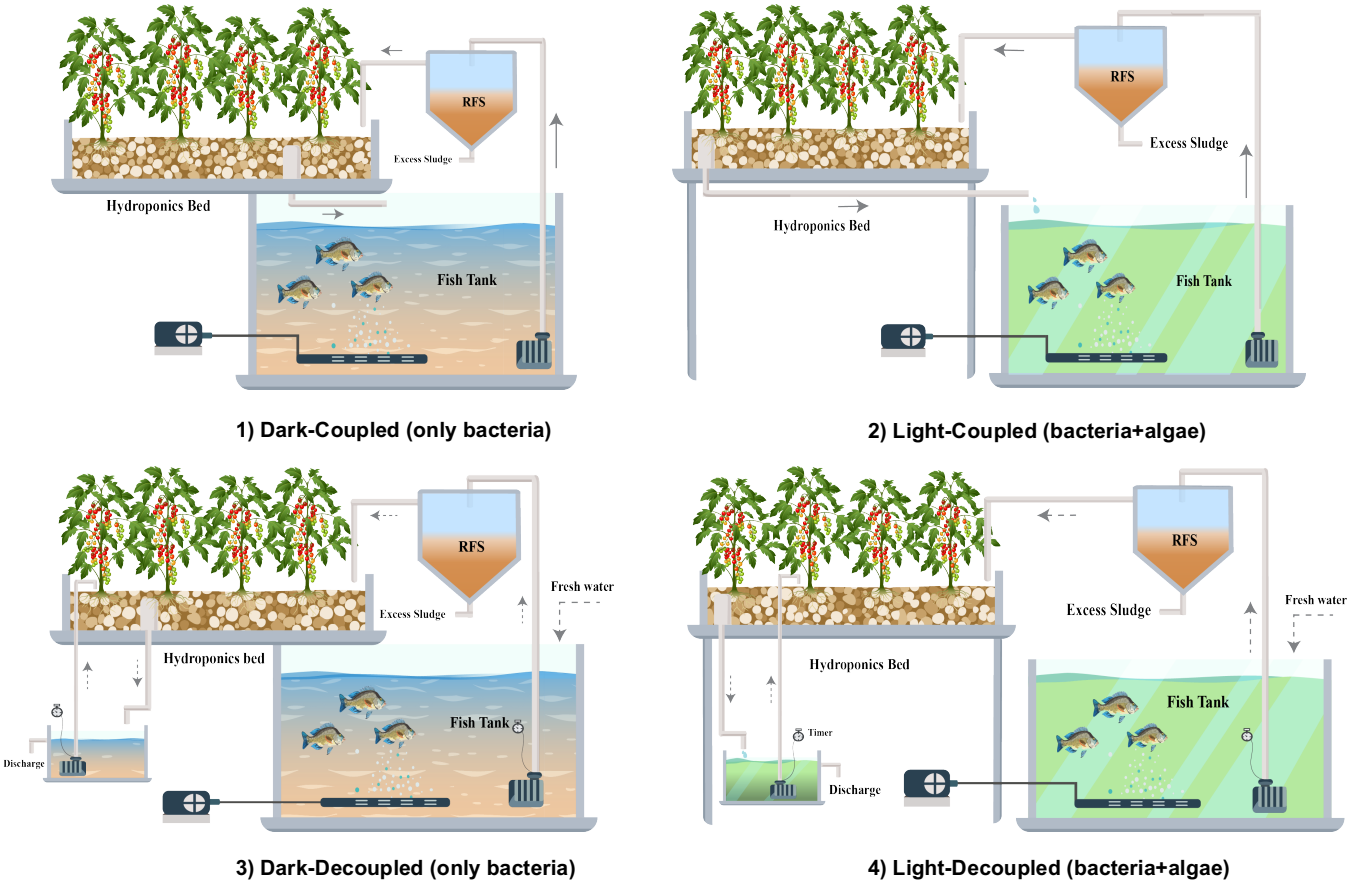

Figure S5.1. (A) Schematic of the four aquaponic system types: (1) Dark-coupled (bacteria-dominant community), (2) Light-coupled (algae-dominant community), (3) Dark-decoupled (bacteria-dominant community), and (4) Light-decoupled (algae-dominant community).

Table S5.1. Water quality parameters (mean ± SD, n = 3) in each treatment across four seasonal sampling periods (April–May, June–July, August–September, October–November) over two production years (2023 and 2024). Parameters include (A) total ammonium nitrogen (NH_4-N), (B) nitrite nitrogen (NO_2-N), (C) nitrate nitrogen (NO_3-N), and (D) pH. Treatments include light–decoupled (LD), light–coupled (LC), dark–decoupled (DD), and dark–coupled (DC) systems.

	Year 1				Year 2			
	LD	**LC**	**DD**	**DC**	**LD**	**LC**	**DD**	**DC**
				NH4-N				
April-May	0.85 ± 0.56	0.2 ± 0.1	1.47 ± 0.72	0.34 ± 0.37	2.81 ± 0.87	0.5 ± 0.75	4.23 ± 0.39	0.32 ± 0.04
June-July	1.1 ± 0.93	2.06 ± 1.85	2.79 ± 1.82	0.29 ± 0.07	13.63 ± 1.57	4.78 ± 1.91	14.91 ± 1.83	3.7 ± 2.45
August-September	0.26 ± 0.28	2.43 ± 1.35	0.64 ± 0.49	3.62 ± 3.33	17.05 ± 3	8.12 ± 2.9	23.94 ± 3.11	7.44 ± 10.21
October-November	1.83 ± 1.06	3.35 ± 1.35	1.31 ± 0.83	5.53 ± 4.65	0.27 ± 0.15	0.48 ± 0.18	1.36 ± 0.88	0.46 ± 0.18
				NO2-N				
April-May	0.55 ± 0.16	0.01 ± 0.01	0.58 ± 0.14	0.01 ± 0	1.89 ± 1.11	0.54 ± 0.16	0.39 ± 0.07	0.52 ± 0.11
June-July	0.01 ± 0.02	0.19 ± 0.02	0.01 ± 0.01	0.08 ± 0.01	0.68 ± 0.05	0.47 ± 0.03	0.62 ± 0.01	0.52 ± 0.03
August-September	0.65 ± 0.9	0.37 ± 0.3	0.27 ± 0.24	0.26 ± 0.16	0.92 ± 0.06	0.56 ± 0.01	0.77 ± 0.02	0.62 ± 0.06
October-November	0.1 ± 0.04	0.31 ± 0.16	0.15 ± 0.09	0.13 ± 0.07	0.1 ± 0.01	0.09 ± 0.03	0.11 ± 0	0.1 ± 0.02
				NO3-N				
April-May	11.67 ± 5.43	35.95 ± 6.99	19.48 ± 2.54	55.87 ± 6.11	32.49 ± 4.79	25.96 ± 6.3	47.79 ± 3.36	60.11 ± 5.56
June-July	34.29 ± 12.93	95.05 ± 11.58	31 ± 10.72	146.57 ± 24.72	31.35 ± 16.59	74.48 ± 32.23	42.11 ± 7.41	126.68 ± 56.75
August-September	64.35 ± 8.79	160.51 ± 37.43	58.33 ± 19.23	330.53 ± 48.82	22.82 ± 13.94	206.41 ± 91.23	30.71 ± 4.54	250.24 ± 99.84
October-November	72.46 ± 16.52	300.38 ± 48.51	67.75 ± 12.74	510.31 ± 122.16	48.66 ± 4.15	237.74 ± 66.43	59.64 ± 9.93	201.75 ± 125.68
				pH				
April-May	7.37 ± 0.11	7.18 ± 0.11	7.06 ± 0.06	7.03 ± 0.09	6.68 ± 0.06	6.78 ± 0.03	6.6 ± 0.04	6.9 ± 0.52
June-July	6.63 ± 0.15	6.56 ± 0.08	6.69 ± 0.25	6.53 ± 0.24	6.72 ± 0.17	6.52 ± 0.09	6.6 ± 0.06	6.45 ± 0.09
August-September	6.58 ± 0.02	6.62 ± 0.05	6.56 ± 0.11	6.35 ± 0.12	6.86 ± 0.11	6.43 ± 0.02	6.81 ± 0.02	6.55 ± 0.2
October-November	6.61 ± 0.13	6.79 ± 0.37	6.78 ± 0.2	7.28 ± 1.71	6.34 ± 0.04	6.29 ± 0.07	6.3 ± 0.03	6.35 ± 0.2

Table S5.2. Crude fat content (% dry biomass) of fish muscle tissue across treatments in Year 1 (2023) and Year 2 (2024). Values are presented as mean ± standard deviation (n = 3). No statistically significant differences were observed among treatments ($p > 0.05$).

	Year 1				Year 2			
	LD	**LC**	**DD**	**DC**	**LD**	**LC**	**DD**	**DC**
Crude fat (% dry biomass)	6.35 ± 1.02 a	8.26 ± 2.48 a	7.89 ± 1.68 a	9.65 ± 1.63 a	6.72 ± 2.24 a	5.41 ± 0.43 a	7.05 ± 1.43 a	10.04 ± 8.53 a

Table S5.3. Fatty acid methyl ester (FAME) profiles of fish muscle tissue from different treatments during Year 1 (2023) and Year 2 (2024). Data represent mean ± standard deviation (n = 3). Fatty acids are presented as % of dry biomass. No significant differences were found among treatments ($p > 0.05$), as indicated by shared letters (a).

	Year 1				Year 2			
Fatty acids	**LD**	**LC**	**DD**	**DC**	**LD**	**LC**	**DD**	**DC**
C16:0	1.76 ± 0.47	2.14 ± 0.06	2.27 ± 0.24	2.69 ± 0.42	2 ± 0.73	1.95 ± 0.18	2.08 ± 0.26	2.32 ± 1.32
C16:1	0.12 ± 0.04	0.13 ± 0.03	0.16 ± 0.05	0.24 ± 0.08	0.14 ± 0.06	0.14 ± 0.02	0.16 ± 0.03	0.31 ± 0.34
C16:1	0.33 ± 0.27	0.54 ± 0.07	0.66 ± 0.26	1.04 ± 0.39	0.55 ± 0.53	0.43 ± 0.1	0.57 ± 0.19	1.22 ± 1.69
C18:0	1.28 ± 0.15	1.34 ± 0.05	1.47 ± 0.03	1.56 ± 0.15	1.36 ± 0.17	1.35 ± 0.06	1.4 ± 0.08	1.44 ± 0.3

C18:1	1.89 ± 1.23	2.56 ± 0.06	2.83 ± 0.46	3.64 ± 0.82	2.28 ± 1.12	2.16 ± 0.3	2.58 ± 0.48	2.74 ± 2.14
C18:1	0.37 ± 0.26	0.53 ± 0.05	0.65 ± 0.2	0.96 ± 0.39	0.51 ± 0.42	0.46 ± 0.1	0.55 ± 0.2	1.06 ± 1.31
C18:2	1.08 ± 0.66	1.43 ± 0.07	1.17 ± 0.96	1.84 ± 0.4	1.27 ± 0.78	1.05 ± 0.22	1.19 ± 0.36	1.65 ± 1.63
C18:3	0.08 ± 0.07	0.09 ± 0.05	0.12 ± 0.05	0.21 ± 0.1	0.1 ± 0.08	0.1 ± 0.04	0.11 ± 0.05	0.32 ± 0.47
C18:3	0.09 ± 0.07	0.11 ± 0.04	0.12 ± 0.04	0.16 ± 0.06	0.1 ± 0.08	0.08 ± 0.03	0.09 ± 0.04	0.22 ± 0.28
C20:1	0.03 ± 0.03	0.02 ± 0.02	0.02 ± 0.01	0.05 ± 0.04	0.02 ± 0.01	0.03 ± 0.02	0.04 ± 0.02	0.12 ± 0.12
C20:3	0.04 ± 0.03	0.03 ± 0.03	0.04 ± 0.02	0.08 ± 0.06	0.04 ± 0.01	0.05 ± 0.03	0.07 ± 0.03	0.14 ± 0.16
C20:2	0.07 ± 0.06	0.07 ± 0.04	0.07 ± 0.02	0.11 ± 0.05	0.07 ± 0.05	0.07 ± 0.02	0.08 ± 0.04	0.13 ± 0.17
C20:3	0.13 ± 0.08	0.13 ± 0.07	0.14 ± 0.04	0.22 ± 0.07	0.14 ± 0.06	0.14 ± 0.03	0.15 ± 0.06	0.24 ± 0.23
C20:4	0.39 ± 0.05	0.38 ± 0.12	0.42 ± 0.08	0.53 ± 0.1	0.43 ± 0.04	0.48 ± 0.08	0.46 ± 0.08	0.61 ± 0.26
C20:5	0.05 ± 0.05	0.04 ± 0.04	0.03 ± 0.03	0.07 ± 0.03	0.05 ± 0.05	0.03 ± 0.02	0.03 ± 0.03	0.06 ± 0.07
C22:4	0.14 ± 0.09	0.12 ± 0.08	0.17 ± 0.1	0.2 ± 0.07	0.14 ± 0.03	0.17 ± 0.04	0.17 ± 0.06	0.29 ± 0.28
C22:5	0.22 ± 0.09	0.2 ± 0.12	0.19 ± 0.06	0.29 ± 0.02	0.22 ± 0.04	0.3 ± 0.06	0.31 ± 0.04	0.36 ± 0.17
C22:5	0.12 ± 0.09	0.13 ± 0.07	0.18 ± 0.13	0.26 ± 0.2	0.13 ± 0.1	0.1 ± 0.04	0.11 ± 0.05	0.17 ± 0.18
C22:6	0.36 ± 0.16	0.36 ± 0.2	0.4 ± 0.13	0.51 ± 0.1	0.38 ± 0.17	0.35 ± 0.07	0.36 ± 0.07	0.45 ± 0.24
Total FAME	8.55 ± 3.94 a	10.36 ± 1.25 a	11.11 ± 2.82 a	14.67 ± 3.41 a	9.93 ± 4.47 a	9.44 ± 1.3 a	10.52 ± 2.1 a	13.84 ± 11.33 a
Sum SFAs	3.04 ± 0.62 a	3.48 ± 0.12 a	3.74 ± 0.27 a	4.25 ± 0.57 a	3.36 ± 0.9 a	3.3 ± 0.22 a	3.48 ± 0.34 a	3.76 ± 1.61 a
Sum MUFAs	2.74 ± 1.83 a	3.78 ± 0.22 a	4.32 ± 0.97 a	5.94 ± 1.7 a	3.51 ± 2.15 a	3.23 ± 0.53 a	3.89 ± 0.91 a	5.45 ± 5.59 a
Sum PUFAs	2.77 ± 1.49 a	3.1 ± 0.93 a	3.04 ± 1.57 a	4.48 ± 1.21 a	3.06 ± 1.42 a	2.92 ± 0.65 a	3.14 ± 0.88 a	4.64 ± 4.12 a
Sum18:2	1.08 ± 0.66 a	1.43 ± 0.07 a	1.17 ± 0.96 a	1.84 ± 0.4 a	1.27 ± 0.78 a	1.05 ± 0.22 a	1.19 ± 0.36 a	1.65 ± 1.63 a
Sum18:3	0.17 ± 0.14 a	0.2 ± 0.09 a	0.24 ± 0.09 a	0.36 ± 0.16 a	0.2 ± 0.15 a	0.17 ± 0.07 a	0.21 ± 0.09 a	0.54 ± 0.75 a
Omega 3	0.58 ± 0.35 a	0.6 ± 0.33 a	0.67 ± 0.23 a	0.95 ± 0.28 a	0.63 ± 0.37 a	0.55 ± 0.14 a	0.6 ± 0.19 a	1.04 ± 1.06 a

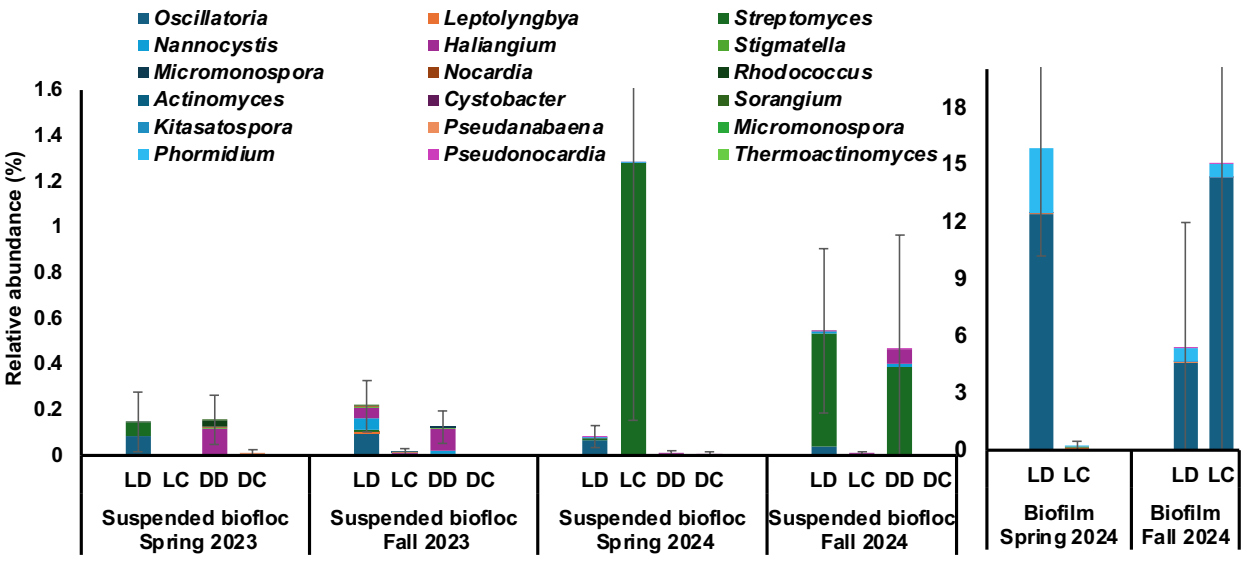

Figure S5.2. Relative abundance of key geosmin- and 2-methylisoborneol (2-MIB)-producing taxa in the suspended biofloc and biofilm compartments during Years 1 and 2. Data indicate a low overall abundance of these taxa across both years and system compartments, suggesting limited potential for accumulation of off-flavor compounds under the experimental conditions.

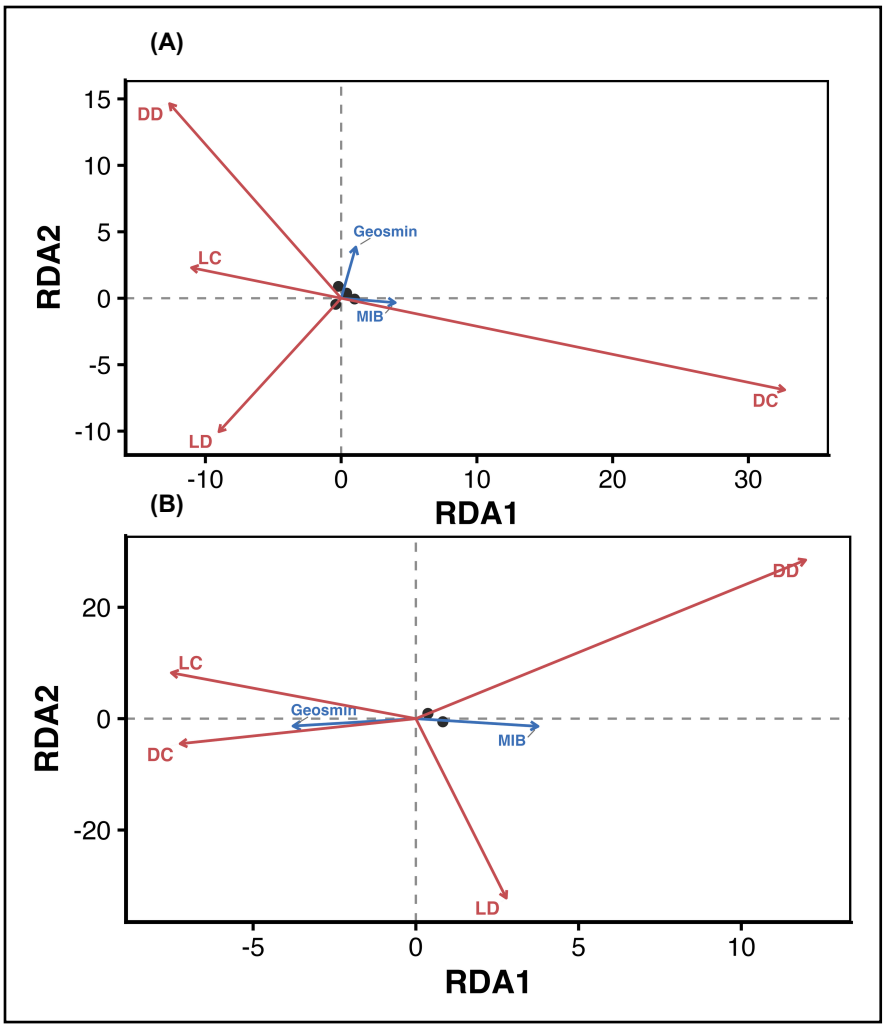

Figure S5.3. Redundancy analysis (RDA) ordination showing the relationships between candidate microbial taxa (eukaryotic community) and fish-flesh off-flavor compounds (MIB and geosmin) under different treatment conditions in (A) Year 1 (2023) and (B) Year 2 (2024). Blue arrows represent the outcome variables (MIB and geosmin), while red arrows indicate the treatment group centroids. Black points represent microbial taxa, with labels shown for those exhibiting significant associations with the response variables.

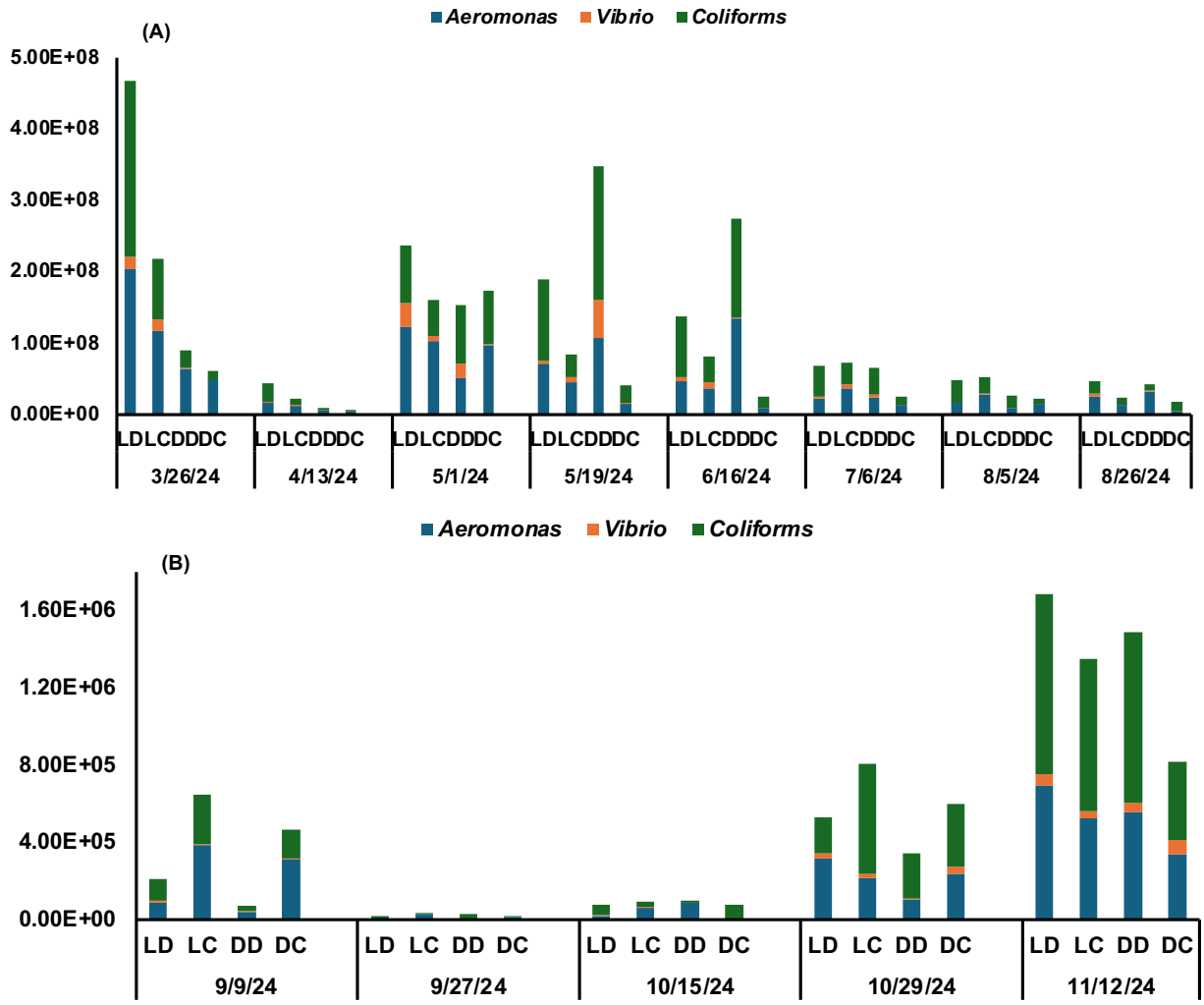

Figure S5.4. Culture-based quantification of Aeromonas, Vibrio, and coliform bacteria during Year 2 of the experiment. Samples were collected biweekly during spring and fall from fish tank suspension, tank wall biofilm, and grow bed sludge, and plated on selective media for bacterial enumeration. (A) Spring sampling; (B) Fall sampling. Bars represent total CFU/mL in the three compartments. Aeromonas and coliforms were consistently detected at higher concentrations than Vibrio, which was often near or below detection limits. Temporal variation, rather than treatment or compartment, was the primary driver of changes in bacterial abundance.

Chapter 6: System Design Shapes Nutrient Fate in Biofloc Aquaponics: Nitrogen and Phosphorus Mass Balances Under Different Microbial Regimes and Hydraulic Configurations

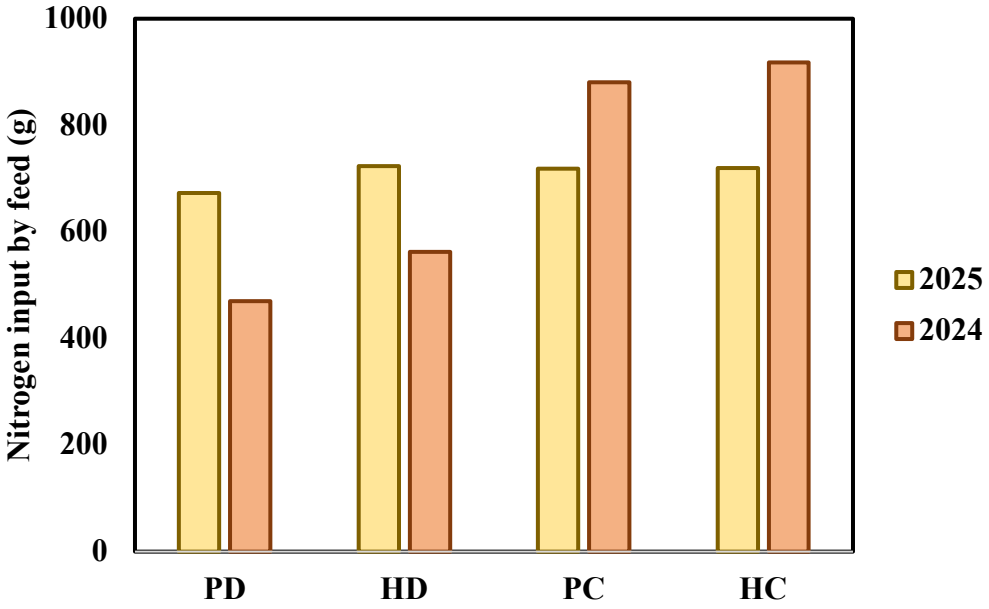

Figure S6.1. Total nitrogen input from feed across aquaponic treatments during the 2024 and 2025 production batches.

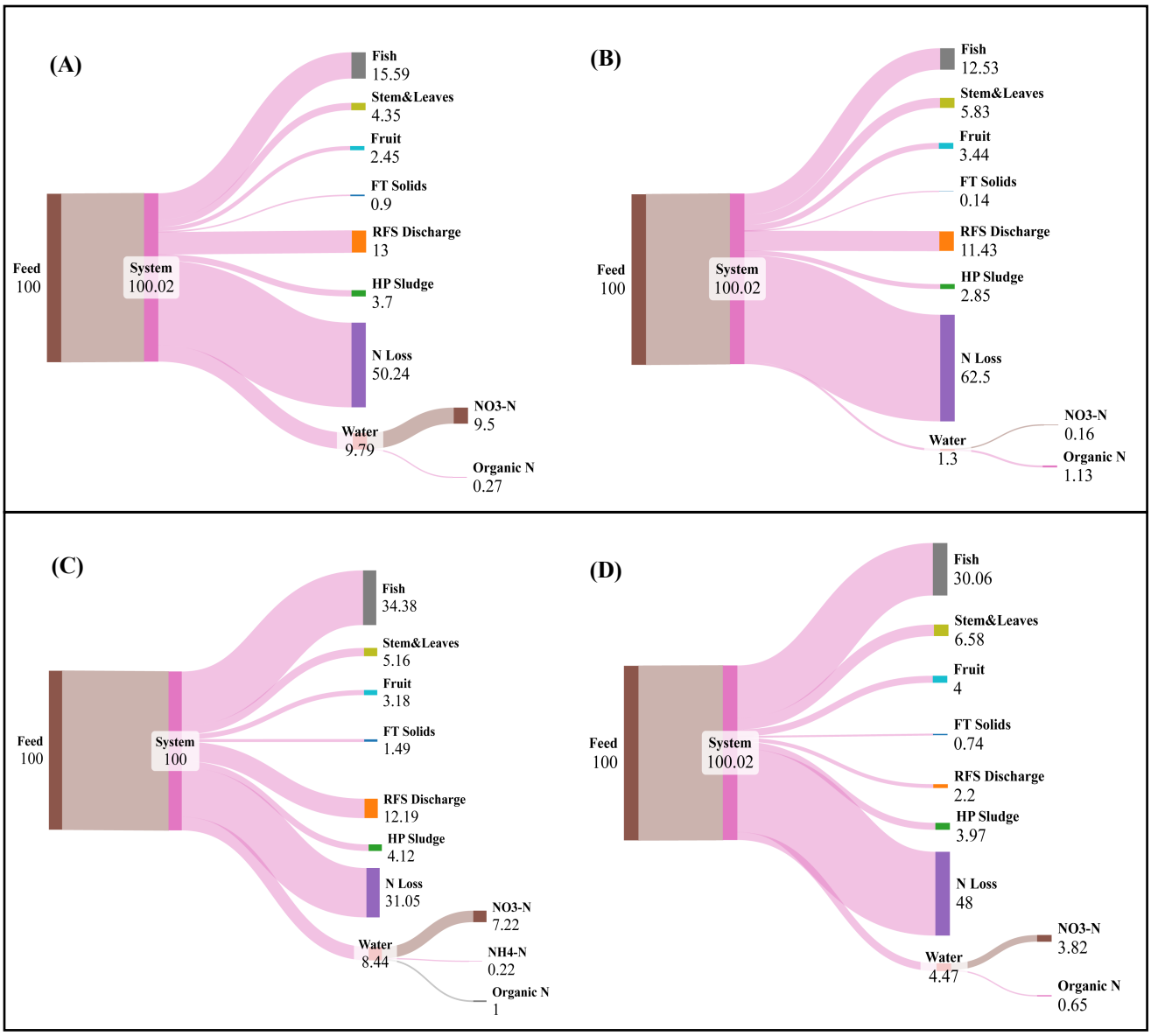

Figure S6.2. Sankey diagrams illustrating the distribution of feed-derived nitrogen across major system compartments in the coupled aquaponic systems. Panels correspond to the same treatment and year order as Figure 3: (A) photoautotrophic–coupled (PC) in 2024, (B) heterotrophic–coupled (HC) in 2024, (C) photoautotrophic–coupled (PC) in 2025, and (D) heterotrophic–coupled (HC) in 2025. Flows represent the percentage of feed nitrogen recovered in fish biomass, plant biomass (shoot and fruit), accumulated solids, dissolved nitrogen in water, and apparent nitrogen loss. The width of each flow is proportional to the magnitude of nitrogen partitioned into each pool.

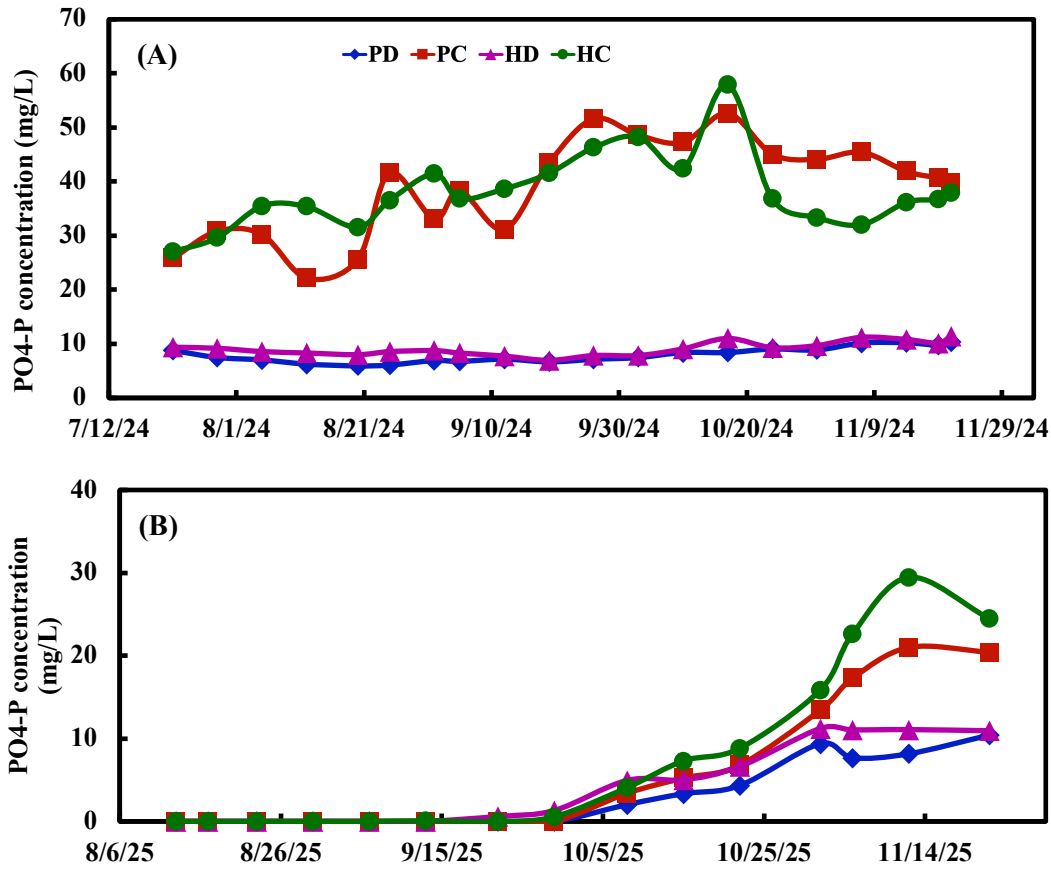

Figure S6.3. Temporal dynamics of dissolved phosphate (PO_4–P) concentrations in the aquaponic systems during the 2024 (A) and 2025 (B) production batches. Lines represent treatment means for the photoautotrophic–decoupled (PD), heterotrophic–decoupled (HD), photoautotrophic–coupled (PC), and heterotrophic–coupled (HC) systems measured throughout the experimental period.

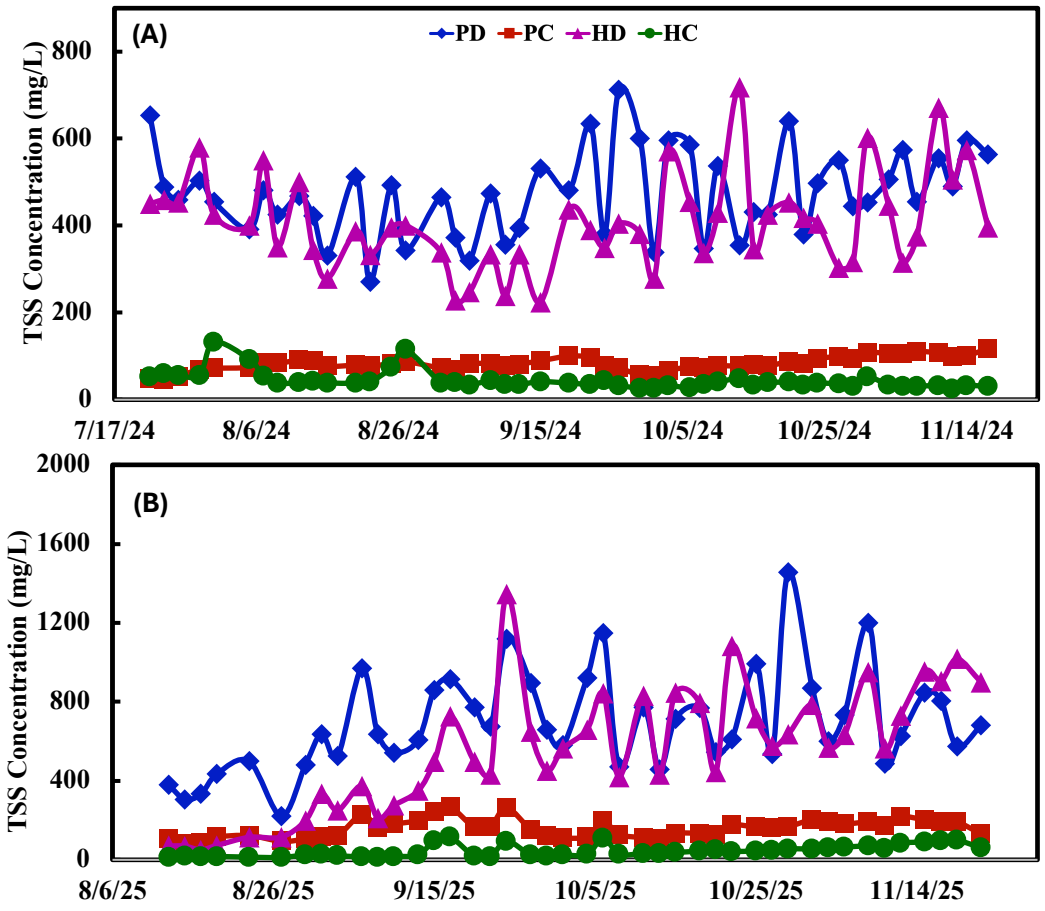

Figure S6.4. Temporal variation of total suspended solids (TSS) concentrations in fish tanks across aquaponic treatments during the 2024 (A) and 2025 (B) production batches.